ADSORPTION OF SIMULATED AND REAL EFFLUENTS ONTO ACTIVATED CARBON SURFACES

By

OCHOLI, ODIKE JOTHAM

DEPARTMENT OF CHEMISTRY,

FACULTY OF SCIENCE,

AHMADU BELLO UNIVERSITY,

ZARIA, NIGERIA

NOVEMBER, 2012

ADSORPTION OF SIMULATED AND REAL EFFLUENTS ONTO ACTIVATED CARBON SURFACES

By

OCHOLI, ODIKE JOTHAM

B.Sc.(Hons) Chemistry(A.B.U), M.Sc.Chemistry(A.B.U)

Ph.D/SCIEN/10067/2007-2008

A DISSERTATION SUBMITTED TO THE SCHOOL OF POSTGRADUATE STUDIES, AHMADU BELLO UNIVERSITY,ZARIA IN PARTIAL FULFILMENT OF THE REQUIREMENTS FOR THE AWARD OF THE DEGREE OF DOCTOR OF PHILOSOPY IN ANALYTICAL CHEMISTRY

DEPARTMENT OF CHEMISTRY

AHMADU BELLO UNIVERSITY

ZARIA

NOVEMBER 2012

Declaration

I declare that the work in this Dissertation entitled "**Adsorption of Simulated and Real Effluents onto Activated Carbon Surfaces**," has been performed by me in the Department of Chemistry under the supervision of Prof. Gimba, C.E., Prof. Ndukwe, G.I. and Dr Turoti, M. The information derived from literature has been duly acknowledged within the text and a list of references provided. No part of this thesis was previously presented for another degree or diploma at any university.

_____ _____

OCHOLI, Odike Jotham Date

Certification

This dissertation entitled "**ADSORPTION OF SIMULATED AND REAL EFFLUENTS ONTO ACTIVATED CARBON SURFACES**" by Ocholi, Odike Jotham meets the regulations governing the award of the degree of Doctor of Philosopy (Ph.D.) Chemistry of Ahmadu Bello University, Zaria, and is approved for it's contribution to knowledge and literary presentation.

Prof. Gimba, C. E. (Chairman, Supervisory Committee)	Date
Prof. Ndukwe, G. I. (Member, Supervisory Committee)	Date
Dr. Turoti, M. (Member, Supervisory Committee)	Date
Prof. Gimba, C. E (Head of Department)	Date
Prof. Joshua, A.A. (Dean, School of Postgraduate studies)	Date

Dedication

This work is dedicated to:

i. The *Author* of *Life*

ii. Mum and Dad

Acknowledgements

I wish to express my sincere gratitude to:

i. The Lord God Almighty for His mercies and favours throughout the course of this work.

ii. Prof. Gimba, C.E., Prof. Ndukwe, G.I. and Dr. Turoti, M. for the confidence and trust imposed on me; the liberty granted me to explore and for their interest, counsel and support which has enhanced the quality of this work. Specifically, I thank Prof. Gimba, C.E. for gently and patiently guiding this work. Thank you for being a positive influence and for adding "solid blocks" to my life's progress… May the Lord lift you higher. Amen.

iii. To Prof. Kagbu, J.A.(of Blessed memory) who was part of the work from the start and was desirous to see the work completed on schedule.

iv. To Prof. Ndukwe, G.I. who was instrumental in "pushing" the work to it's completion.

v. My colleagues in the Department of Chemistry, A.B.U. - Zaria (academic and non-academic) for providing a friendly environment to work. I must specifically mention Dr.S.E. Abechi for being faithful ally in sharing materials and useful advice, Mr Silas Ekwuribe (Multi-User Science Research Laboratory, A.B.U. - Zaria), Mr Celestine Ochigbo (Postgraduate Laboratory, Department of Chemistry, A.B.U. - Zaria) and Simon U.(Hydrobiology

vi. Laboratory, Department of Biological Sciences, A.B.U. - Zaria)for all the help and technical advice.

vii. The Hydrobiology Laboratory, Department of Biological sciences, for their contribution to the preliminary stage of the work.

viii. Asabe (NARICT) for the FT-IR analysis

ix. Okpuwhara Rita (Textile Science Department.), for supplying the textile effluent samples.

x. The University Board for Research, A.B.U. - Zaria for partly funding the work.

xi. All my friends too numerous to mention.

xii. Rev. I.G. Baba (Chapel of Redemption. ABU-Zaria) and Pastor Chris Delvan Gwamna (The New Life Assembly. Kaduna) for the prayers and counsel.

xiii. My loving and caring parents Mr and Mrs S.A. Ocholi

xiv. My faithful siblings, Amana, Ene, Obj, Agbenyo(with their families), Okpas and Ebus, I couldn't have gotten better siblings. Thanks for being there.

xv. My fiancée, Faith Yakubu, for being a help and support morally and spiritually. I look forward to that day…

Abstract

Adsorption studies of simulated and real effluents was carried out with an aim to better understand adsorption processes in multi-component dye and heavy metal mixtures. Three (3) different Activated Carbon (AC) matrices were used as adsorbent: Unmodified activated carbon (UMAC), chemically modified activated carbon (CMAC) and physically modified activated carbon (PMAC). Simulated effluent systems were developed from various aqueous combinations of methylene blue (MB), methyl orange (MO), indigo carmine (IG), $Pb(NO_3)_2$ and $Cd(NO_3)_2.4H_2O$. A total of twenty two (22) different simulated effluent systems were developed which were interacted with the AC matrices and three (3) textile effluents samples (TXT 1, TXT 2 and TXT 3) were also collected from a textile industry in Kaduna and used for this study. Adsorption results from single dye rate experiments revealed that the adsorption process was particle-diffusion controlled with chemisorption as the predominant adsorption type. For single dye effluent systems, adsorption results showed that the AC matrices had good performance especially at low concentrations of adsorbates. The order of adsorption for the different dyes was MO > MB > IG, while the efficiency of the matrices was PMAC > UMAC > CMAC. For binary dye effluent systems, adsorption of combinations of MB and MO (MBMO) and MO and IG (MOIG) in aqueous and aqueous $Pb(NO_3)_2$ and $Cd(NO_3)_2.4H_2O$ mixtures onto the AC matrices was observed. Results revealed that for MBMO system, the

component that was preferentially adsorbed was dependent on the heavy metal environment and the AC sample involved. Generally, the adsorption range was 89 – 98%. For the MOIG system, the result showed similar adsorption trends irrespective of the heavy metal environment. MO was preferentially adsorbed than IG while the performance of the matrices was PMAC > UMAC > CMAC. The adsorption range was 54 – 82 %. For MBMOIG in aqueous $Pb(NO_3)_2$ and $Cd(NO_3)_2.4H_2O$ mixture, the components were preferentially adsorbed as follows: MO > MB > IG with an adsorption range of 73 – 97%, while the performance of the matrices was PMAC > UMAC > CMAC. With the real textile effluents, the AC matrices adsorbed components of TXT 2 and TXT 3 appreciably with average adsorption ranges of 72 – 82% and 19 – 68% respectively, while the adsorption range for TXT 1 was wide between 2 – 70% (close to 80% of the results were below 31%). The performance of the matrices was PMAC > UMAC > CMAC, just like most of the simulated effluent cases. Generally, adsorption involving multi-component adsorbate systems is dynamic and is influenced by numerous factors, like pH of AC surface, pH of adsorbate solution, size, shape and orientation of adsorbate species, concentration of adsorbate species and contact time between adsorbate and adsorbent. The resulting adsorption trend for any component is usually an inter-play of all these factors.

Table of Contents

Title Page……...	Page
Declaration…….	i
Certification……	ii
Dedication……..	iii
Acknowledgements……	iv
Abstract……..	vi
Table of Contents……...	viii
List of Tables…….	xvi
List of Figures……	xviii
List of Appendices…….	xxv
Abbreviations…….	xxvi

CHAPTER ONE

Page

1.0 Introduction…… 1

1.1 The multi-component nature of effluents and waste waters…….. 1

1.2.0 Dyes and Heavy metals…… 1

1.2.1 Dyes…….. 1

1.2.2 Heavy metals…… 2

1.3 Treatment of effluents and waste waters……. 3

1.4 Adsorption of dyes and heavy metals from aqueous solution……. 3

1.5 Use of activated carbon in effluent treatment…….. 4

1.5.1 Adsorption…… 6

1.5.2 Preferential Adsorption…… 7

1.6 Availability, Accessibility and use of activated carbon in Nigeria……. 7

1.7 Statement of the research problem…….. 8

1.8 Justification…….. 9

1.9 Aim…….. 10

1.9.1 Objectives…… 10

CHAPTER TWO

2.0 Literature Review……. 11

2.1.0 Adsorption in single adsorbate/adsorbent systems…… 11

2.1.1 Nature of activated carbon…… 12

2.1.2.0 Removal of lead…….. 13

2.1.2.1 Removal of Cadmium from aqueous solution…… 13

2.1.2.2 Adsorptive removal of organics…….. 14

2.3.0 Adsorption Isotherms…… 15

2.3.1 Langmuir Isotherm Equation……. 15

2.3.2 The Freundlich Isotherm Equation……... 17

2.3.3 The Temkin isotherm……. 17

2.4.0 Factors affecting adsorption from binary solutions……... 18

2.4.1 Adsorbate-Adsorbent/Adsorbate-Adsorbate Interaction…… 18

2.4.2 Porosity of adsorbent…… 19

2.4.3 Surface Heterogenity…… 19

2.4.4 Orientation of adsorbed molecules…… 19

2.5.0 Dye (adsorbate) molecules…… 20

2.5.1 Methylene blue (MB)…… 20

2.5.2 Methyl orange (MO)……. 21

2.5.3 Indigo carmine (IG)…… 23

CHAPTER THREE

3.0 Materials and Methods…… 25

3.1Instruments and Reagents……. 25

3.1.0Activated Carbon Sample…….. 25

3.1.1 Sample Modification …… 26

3.1.2 Physical Modification ……... 26

3.1.3 Chemical Modification ……. 27

3.2.0 Preparation of methylene blue, indigo and methyl orange stock solutions …… 27

3.2.1 Preparation of 1M $Pb(NO_3)_2$ and $Cd(NO_3)_2.4H_2O$ solutions …….. 28

3.2.2 Preparation of binary dye mixtures ……. 28

3.2.3 Preparation of binary dye mixtures in heavy metal solution……. 28

3.3 Adsorbate systems.(Simulated Effluents) ……... 28

3.4 Rate of Dye Adsorption ……... 29

3.5 Adsorption Studies …….. 30

CHAPTER FOUR

4.0 Results and Discussion……. 35

4.1.0 Introduction …….. 35

4.1.1 Unmodified and Modified Activated Carbon Samples…… 35

4.1.2 pH of AC samples……. 35

4.1.3.pH of Dyes, Heavy metal solution, Dye/Heavymetal mixtures and Real Textile effluents ……. 36

4.2.0 Behaviour of Dyes and Heavy metals in solution …….. 37

4.2.1 Effect of Time on Adsorption of MB, MO and IG…… 40

4.2.2. Influence of size of dyes on adsorption rates…… 50

4.2.3 Possible inferences from rate experiments …… 53

4.2.4 Statistical Analysis of Rate Experiment Results ……. 53

4.2.5 Effect of Chemical and Physical modification of AC sample……... 54

4.3.0 Adsorption Studies Results. ……. 56

4.3.1 Adsorption Studies for Single Dye Systems ……. 56

4.3.2 Methylene blue adsorption from heavy metal environment…….. 57

4.3.3 Methyl orange adsorption from heavy metal environment ……... 62

4.3.4 Indigo carmine adsorption from heavy metal environment ……. 67

4.3.5 Summary of results of adsorption of single dyes in heavy metal environment. 72

4.4.0 Adsorption of Binary dye mixtures in heavy metal environment…….. 73

4.4.1MBMO Adsorption in Heavy Metal Environment. …….. 74

4.4.1.1 MBMO Adsorption from $Pb(NO_3)_2$ and $Cd(NO_3)_2.4H_2O$ mixture …….. 74

4.4.1.2 MBMO Adsorption from $Pb(NO_3)_2$ solution …… 78

4.4.1.3MBMO Adsorption from $Cd(NO_3)_2.4H_2O$ solution …….. 82

4.4.2 MOIG Adsorption in Heavy Metal Environment. ……... 86

4.4.2.1MOIG Adsorption from [$Pb(NO_3)_2$ + $Cd(NO_3)_2.4H_2O$] mixture……. 87

4.4.2.2MOIG Adsorption from $Pb(NO_3)_2$ ……. 90

4.4.2.3MOIG Adsorption from $Cd(NO_3)_2.4H_2O$ ……... 93

4.4.3 Summary of results of adsorption of binary dyes in heavy metal environment 97

4.5.0 Adsorption of Tertiary Dye Mixture in Heavy Metal Environment …… 98

4.6.0 Adsorption Isotherms ……. 104

4.6.1 Adsorption Isotherms for Aqueous Single Dye Systems …… 105

4.6.1.2 Summary of results of the adsorption isotherms of MO, MB, and IG onto the different AC samples. ……... 111

4.6.2 Adsorption Isotherm of aqueous Binary Dye mixtures.……. 112

4.6.2.1 Adsorption of components of MBMO from aqueous and aqueous $Pb(NO_3)_2$ and $Cd(NO_3)_2.4H_2O$ mixture……... 112

4.6.2.2 Adsorption of components of MOIG from aqueous and aqueous $Pb(NO_3)_2$ and $Cd(NO_3)_2.4H_2O$ mixture……. 119

4.7.0 Adsorption of components of MBMOIG from aqueous and aqueous $Pb(NO_3)_2$ and $Cd(NO_3)_2.4H_2O$ mixture…….. 125

4.8.0 Freundlich, Langmuir and Temkin constants…… 131

4.9.0 Adsorption of Real Textile Effluents onto AC sample …… 132

CHAPTER FIVE

5.0. Summary, Conclusion and Recommendations. …….. 139

5.1 Summary……... 139

5.2 Conclusion. ……. 142

5.3 Recommendations ……... 143

References…… 145

Appendices…….. 152

List of Tables

Table 3.1: Factory Specifications of AC sample……. 26

Table 4.1: pH of AC samples…….. 35

Table 4.2: pH ranges of Dyes, Heavy metal solution, Dye/Heavy metal mixtures and Real Textile effluents…… 37

Table 4.3: Interaction of dyes with high concentrations of heavy metal solution.. 39

Table 4.3(i): Percentage yield and pH of Modified AC samples…… 55

Table 4.4 Average percentage from summary graphs for MB……... 61

Table 4.5 Average percentage from summary graphs for MO…… 66

Table 4.6 Average percentage from summary graphs for IG……. 72

Table 4.7: Table of percentage averages of components of MBMO adsorbed from different heavy metal environment onto different AC samples…… 86

Table 4.8: Table of percentage average of components of MBMO adsorbed from different heavy metal environment onto different AC samples…….. 96

Table 4.9: Table of percentage average of components of MBMOIG adsorbed from $Pb(NO_3)_2$ and $Cd(NO_3)_2.4H_2O$ mixture onto different AC samples……. 102

Table 4.10: Average percentage of components of MBMO adsorbed from both aqueous and aqueous $Pb(NO_3)_2$ and $Cd(NO_3)_2.4H_2O$ mixture……. 115

Table 4.11: Average percentage of components of MOIG adsorbed from both aqueous and aqueous $Pb(NO_3)_2$ and $Cd(NO_3)_2.4H_2O$ mixture…….. 121

Table 4.12: Average percentage of components of aqueous tertiary dye mixture (MBMOIG) adsorbed onto UMAC,CMAC and PMAC……. 128

Table 4.13: Average percentage of components of aqueous tertiary dye mixture (MBMOIG) adsorbed onto UMAC,CMAC and PMAC……. 131

Table 4.14: Colour and pH of textile effluent samples…… 132

Table 4.15: Wavelength of maximum absorption of effluents…….. 135

Table 4.16: Table of percentage of effluents adsorbed onto UMAC,CMAC and PMAC…… 135

Table 5.2: Order of component adsorbed and ranking of AC sample in tertiary dye mixtures…… 141

List of Figures

Figure 2.1(a): Structural formular of Methylene blue……... 20

Figure 2.1(b): 3D- structural formular of Methylene blue…… 20

Figure 2.2(a): Structural formular of Methyl orange…… 22

Figure 2.2(b): Structure of Methyl orange in acid solution…….. 22

Figure 2.2(c): Structure of Methyl orange in basic solution……. 22

Figure 2.2(d): 3D- structural formular of Methyl orange…….. 23

Figure 2.3: Structure of Indigo carmine…… 24

Figure 2.4: 3D- structural formular of indigo……... 24

Figure 4.1(a): Effect of time on the amount of MB, MO and IG adsorbed onto 20mg UMAC……. 43

Figure 4.1(b): Curve of effect of time on the amount of MB, MO and IG adsorbed onto 20mg UMAC……. 44

Figure 4.1(c): Trend line of effect of time on the amount of MB, MO and IG adsorbed onto 20mg UMAC……. 44

Figure 4.2(a): Effect of time on the amount of MB, MO and IG adsorbed onto 10mg UMAC……. 45

Figure 4.2(b): Curve of effect of time on the amount of MB, MO and IG adsorbed onto 10mg UMAC……. 45

Figure 4.2(c): Trend line of the amount of MB, MO and IG adsorbed onto 10mg UMAC……. 46

Figure 4.3: Bar graph of effect of time on the amount of MB, MO and IG adsorbed onto 20mg of UMAC……. 46

Figure 4.4: Bar graph of effect of time on the amount of MB, MO and IG adsorbed onto 10mg UMAC……. 47

Figure 4.5: Cumulative percentage average of amount of MB, MO and IG adsorbed onto UMAC……... 47

Figure 4.6: Plot of ln(1-*f*) versus time(t)……... 48

Figure 4.7: plot of *f* against Time (*t*)……. 49

Figure 4.8(a): Percentage of MB adsorbed from aqueous $Pb(NO_3)_2$…… 58

Figure 4.8(b): Cumulative percentage average of MB adsorbed from aqueous $Pb(NO_3)_2$…… 59

Figure 4.9(a): Percentage of MB adsorbed from aqueous $Cd(NO_3)_2.4H_2O$…… 59

Fig 4.9(b): Cumulative Percentage average of MB adsorbed from aqueous $Cd(NO_3)_2.4H_2O$…… 60

Figure 4.10(a): Percentage of MB adsorbed from aqueous $Pb(NO_3)_2$ and $Cd(NO_3)_2.4H_2O$ mixture…… 60

Figure 4.10(b): Cumulative percentage average of MB adsorbed from aqueous $Pb(NO_3)_2$ and $Cd(NO_3)_2.4H_2O$ mixture……..... 61

Figure 4.11(a): Percentage of MO adsorbed from aqueous $Pb(NO_3)_2$……... 63

Figure 4.11(b): Cumulative Percentage of MO adsorbed from aqueous $Pb(NO_3)_2$…… 64

Figure 4.12(a): Percentage of MO adsorbed from aqueous $Cd(NO_3)_2.4H_2O$…. 64

Figure 4.12(b): Cumulative Percentage of MO adsorbed from aqueous $Cd(NO_3)_2.4H_2O$…… 65

Figure 4.13(a): Percentage of MO adsorbed from aqueous $Pb(NO_3)_2$ and $Cd(NO_3)_2.4H_2O$ mixture…… 65

Figure 4.13(b): Cumulative percentage average of MO adsorbed from aqueous $Pb(NO_3)_2$ and $Cd(NO_3)_2.4H_2O$ mixture……..... 66

Figure 4.14(a) : Percentage of IG adsorbed from aqueous $Pb(NO_3)_2$……... 68

Figure 4.14(b): Cumulative percentage average of IG adsorbed from aqueous $Pb(NO_3)_2$…… 68

Figure 4.15(a): Percentage of IG adsorbed from aqueous $Cd(NO_3)_2.4H_2O$…. 69

Fig 4.15(b) : Cumulative percentage average of IG adsorbed from aqueous $Cd(NO_3)_2.4H_2O$…… 69

Figure 4.16(a): Percentage of IG adsorbed from aqueous $Pb(NO_3)_2$ and $Cd(NO_3)_2.4H_2O$ mixture…… 70

Figure 4.16(b): Cumulative percentage average of IG adsorbed from aqueous $Pb(NO_3)_2$ and $Cd(NO_3)_2.4H_2O$ mixture…… 70

Figure 4.17(a): Percentage of components of MBMO adsorbed from aqueous $Pb(NO_3)_2$ and $Cd(NO_3)_2.4H_2O$ mixture onto UMAC……..... 74

Figure 4.17(b): Percentage of components of MBMO adsorbed from aqueous $Pb(NO_3)_2$ and $Cd(NO_3)_2.4H_2O$ mixture onto CMAC……..... 75

Figure 4.17(c): Percentage of components of MBMO adsorbed from aqueous $Pb(NO_3)_2$ and $Cd(NO_3)_2.4H_2O$ mixture onto PMAC…….. 75

Figure 4.17(d): Cumulative percentage average of components of MBMO adsorbed from aqueous $Pb(NO_3)_2$ and $Cd(NO_3)_2.4H_2O$ mixture……..... 76

Figure 4.18(b): Percentage of components of MBMO adsorbed from aqueous $Pb(NO_3)_2$onto CMAC…… 79

Figure 4.18(c): Percentage of components of MBMO adsorbed from aqueous $Pb(NO_3)_2$ onto PMAC……... 80

Figure 4.18(d): Cumulative percentage average of components of MBMO adsorbed from aqueous $Pb(NO_3)_2$…….. 80

Figure 4.19(a): Percentage of components of MBMO adsorbed from aqueous $Cd(NO_3)_2.4H_2O$ onto UMAC…….. 82

Figure 4.19(b): Percentage of components of MBMO adsorbed from aqueous $Cd(NO_3)_2.4H_2O$ onto CMAC…… 82

Figure 4.19(c): Percentage of components of MBMO adsorbed from aqueous $Cd(NO_3)_2.4H_2O$ onto PMAC ……... 83

Figure 4.19(d): Cumulative percentage average of components of MBMO adsorbed from aqueous $Cd(NO_3)_2.4H_2O$……... 83

Figure 4.20(a): Percentage of components of MOIG adsorbed from aqueous $Pb(NO_3)_2$ and $Cd(NO_3)_2.4H_2O$ mixture onto UMAC……..... 87

Figure 4.20(b): Percentage of components of MOIG adsorbed from aqueous $Pb(NO_3)_2$ and $Cd(NO_3)_2.4H_2O$ mixture onto CMAC…… 88

Figure 4.20(c): Percentage of components of MOIG adsorbed from aqueous $Pb(NO_3)_2$ and $Cd(NO_3)_2.4H_2O$ mixture onto PMAC……. 88

Figure 4.20(d): Cumulative percentage average of components of MOIG adsorbed from aqueous $Pb(NO_3)_2$ and $Cd(NO_3)_2.4H_2O$ mixture……... 89

Figure 4.21(a): Percentage of components of MOIG adsorbed from aqueous $Pb(NO_3)_2$ onto UMAC…….. 90

Figure 4.21(b): Percentage of components of MOIG adsorbed from aqueous $Pb(NO_3)_2$ onto CMAC……..... 91

Figure 4.21(c): Percentage of components of MOIG adsorbed from aqueous $Pb(NO_3)_2$ onto PMAC……... 91

Figure 4.21(d): Cumulative percentage average of components of MOIG adsorbed from aqueous $Pb(NO_3)_2$..... 92

Figure 4.22(a): Percentage of Components of MOIG adsorbed from $Cd(NO_3)_2.4H_2O$ onto UMAC…… 94

Figure 4.22(b): Percentage of components of MOIG adsorbed from aqueous $Cd(NO_3)_2.4H_2O$ onto CMAC……. 94

Figure 4.22(c): Percentage of components of MOIG adsorbed from aqueous $Cd(NO_3)_2.4H_2O$ onto PMAC……. 95

Figure 4.22(d): Cumulative percentage average of components of MOIG adsorbed from aqueous $Cd(NO_3)_2.4H_2O$ onto UMAC…….. 95

Figure 4.23(a): Percentage of components of MBMOIG adsorbed from aqueous $Pb(NO_3)_2$ and $Cd(NO_3)_2.4H_2O$ mixture onto UMAC…… 99

Figure 4.23(b): Cumulative percentage average of components of MBMOIG from aqueous $Pb(NO_3)_2$ and $Cd(NO_3)_2.4H_2O$ mixture onto UMAC……. 99

Figure 4.24(a): Percentage of components of MBMOIG adsorbed from aqueous $Pb(NO_3)_2$ and $Cd(NO_3)_2.4H_2O$ mixture onto CMAC…… 100

Figure 4.24(b) : Cumulative percentage average of components of MBMOIG adsorbed from aqueous $Pb(NO_3)_2$ and $Cd(NO_3)_2.4H_2O$ mixture onto CMAC…. 100

Figure 4.25(a): Percentage of components of MBMOIG adsorbed from aqueous $Pb(NO_3)_2$ and $Cd(NO_3)_2.4H_2O$ mixture onto PMAC……. 101

Figure 4.25(b): Cumulative percentage average of components of MBMOIG adsorbed from aqueous $Pb(NO_3)_2$ and $Cd(NO_3)_2.4H_2O$ mixture onto PMAC….. 101

Figure 4.26(a): Adsorption isotherm of aqueous MO adsorbed onto UMAC,CMAC & PMAC…….. 105

Figure 4.26(b): Adsorption isotherm of MO adsorbed from aqueous $Pb(NO_3)_2$ and $Cd(NO_3)_2.4H_2O$ mixture onto UMAC and PMAC……. 107

Figure 4.27(a): Adsorption isotherm of aqueous MB adsorbed onto UMAC, CMAC, & PMAC…….. 108

Figure 4.27(b): Adsorption isotherm of MB adsorbed from aqueous $Pb(NO_3)_2$ and $Cd(NO_3)_2.4H_2O$ mixture onto UMAC and PMAC……. 109

Figure 4.28(a): Adsorption isotherm of aqueous IG onto UMAC,CMAC and PMAC…… 110

Figure 4.28(b): Adsorption isotherm of IG adsorbed from aqueous $Pb(NO_3)_2$ and $Cd(NO_3)_2.4H_2O$ mixture onto UMAC and PMAC…… 111

Figure 4.29(a): Adsorption isotherm of components of aqueous MBMO onto UMAC…… 113

Figure 4.29(b): Adsorption isotherm of components of MBMO from aqueous $Pb(NO_3)_2$ and $Cd(NO_3)_2.4H_2O$ mixture onto UMAC…… 114

Figure 4.30(a): Adsorption isotherm of components of aqueous MBMO onto CMAC…… 115

Figure 4.30(b): Adsorption isotherm of components of MBMO from aqueous $Pb(NO_3)_2$ and $Cd(NO_3)_2.4H_2O$ mixture unto CMAC…… 116

Figure 4.31(a): Adsorption isotherm of components of aqueous MBMO mixture onto PMAC……... 118

Figure 4.31(b) : Adsorption isotherm of components of MBMO in aqueous $Pb(NO_3)_2$ and $Cd(NO_3)_2.4H_2O$ mixture unto PMAC……. 118

Figure 4.32(a): Adsorption isotherm of components of aqueous MOIG onto UMAC…… 120

Figure 4.32(b): Adsorption isotherm of components of MOIG from aqueous $Pb(NO_3)_2$ and $Cd(NO_3)_2.4H_2O$ mixture onto UMAC…… 120

Figure 4.33(a): Adsorption Isotherm for components of Aqueous MOIG mixture onto CMAC…….. 122

Figure 4.33(b): Adsorption Isotherm for components of MOIG from aqueous $Pb(NO_3)_2$ and $Cd(NO_3)_2.4H_2O$ mixture onto CMAC…… 123

Figure 4.34(a): Adsorption isotherm of components of aqueous MOIG mixture onto PMAC…… 124

Figure 4.35(a): Adsorption isotherm of components of aqueous MBMOIG mixture onto UMAC……. 125

Figure 4.35(b): Adsorption isotherm of components of aqueous MBMOIG mixture onto CMAC…….. 126

Figure 4.35(c): Adsorption isotherm of components of aqueous MBMOIG mixture onto PMAC……... 126

Figure 4.36(a): Adsorption isotherm of components of MBMOIG from aqueous $Pb(NO_3)_2$ and $Cd(NO_3)_2.4H_2O$ mixture onto UMAC ……... 129

Figure 4.36(b): Adsorption isotherm of components of MBMOIG from aqueous $Pb(NO_3)_2$ and $Cd(NO_3)_2.4H_2O$ mixture onto UMAC …… 130

Figure 4.36(c): Adsorption isotherm of components of MBMOIG from aqueous $Pb(NO_3)_2$ and $Cd(NO_3)_2.4H_2O$ mixture onto PMAC……. 130

Figure 4.37: Visible spectra of TXT 1……... 133

Figure 4.38: Visible Spectra of TXT 2…….. 134

Figure 4.39: Visible Spectra of TXT 3…….. 134

Figure 4.40: Percentage of components of TXT 1 adsorbed onto UMAC, CMAC and PMAC……. 136

Figure 4.41: Percentage of components of TXT 2 adsorbed onto UMAC, CMAC and PMAC ……..……. 136

Figure 4.42: Percentage of components of TXT 3 adsorbed onto UMAC, CMAC and PMAC …… 137

List of Appendices

Appendix I(a): Table of pH measurements of dyes and heavy metal solutions…… 151

Appendix I(b): pH of Textile Effluent Samples……. 153

Appendix II: Table of Absorbances of dyes in aqueous $Pb(NO_3)_2$ and $Cd(NO_3)_2.4H_2O$…….. 154

Appendix III(a): Table of Absorbances of dyes in aqueous $Pb(NO_3)_2$ and $Cd(NO_3)_2.4H_2O$…….. 157

Appendix III(b): Table of Absorbances of MBMO in aqueous $Pb(NO_3)_2$ and $Cd(NO_3)_2.4H_2O$……. 158

Appendix IV: Table of effect of Time on amount of MB, MO and IG adsorbed onto UMAC……..... 159

Appendix IV(a): One Way Anova for rate experiment……. 160

Appendix IV(b): One-Sample t-test for rate experiment……... 161

Appendix V: Table of performance (%) of UMAC,CMAC and PMAC after interaction with components of MBMOIG in aqueous $Pb(NO_3)_2$ and $Cd(NO_3)_2.4H_2O$ mixture…… 161

Appendix VI(a): Data for MBMO adsorption from aqueous $Pb(NO_3)_2$ and $Cd(NO_3)_2.4H_2O$ mixture……..... 162

Appendix VI(b): Data for adsorption of aqueous MOMB mixture…….. 163

Appendix VII(a): Data for MOIG adsorption from aqueous $Pb(NO_3)_2$ and $Cd(NO_3)_2.4H_2O$ mixture …… 163

Appendix VII(b): Data for adsorption of aqueous MOIG mixture…… 164

Appendix VIII(a): Data for adsorption of aqueous MO, MB and IG …….. 165

Appendix VIII(b): Data for adsorption of MO, MB and IG from aqueous $Pb(NO_3)_2$ and $Cd(NO_3)_2.4H_2O$ mixture ……..... 166

Appendix IX: Data for adsorption of components of aqueous MBMOIG mixture onto different AC matrices …… 167

Appendix X: Data for adsorption of components of MBMOIG from aqueous $Pb(NO_3)_2$ and $Cd(NO_3)_2.4H_2O$ mixture onto different AC matrices……. 168

Appendix XI: Absorbances of textile effluents (TXT 1, TXT 2 & TXT 3)…….. 170

Appendix XII: Freundlich, Langmuir and Temkin isotherms constants…… 172

Appendix XIII: Freundlich, Langmuir and Temkin isotherms…….. 174

Appendix XIV : FTIR analysis result (CM)…….. 221

Appendix XV : FTIR analysis result (UM)…… 222

Appendix XVI : FTIR analysis result (PM)…….. 223

Appendix XVII : General types of adsorption isotherms…….. 224

Appendix XVIII : Giles classification of isotherms for adsorption from solution…….. 225

Abbreviations

MB	Methylene blue
MO	Methyl orange
IG	Indigo carmine
MBMO	Aqueous methylene blue and methyl orange binary dye mixture
MOIG	Aqueous methyl orange and indigo carmine binary dye mixture
MBMOIG	Aqueous methylene blue, methyl orange and indigo carmine binary dye mixture
Cd nitrate	$Cd(NO_3)_2.4H_2O$ solution
Pb nitrate	$Pb(NO_3)_2$ solution
Cd/Pb nitrate	Aqueous $Pb(NO_3)_2$ and $Cd(NO_3)_2.4H_2O$ mixture
% Adsbd	Percentage adsorbed
AC	Activated carbon
UMAC	Unmodified Activated carbon
CMAC	Chemically modified Activated carbon
PMAC	Physically modified Activated carbon

CHAPTER ONE

1.0 Introduction

1.1 The multi-component nature of effluents and waste waters

The chemical constitution of most effluents and waste waters makes them likely culprits of environmental pollution. (Visa *et al.*, 2010). The production processes in most industries utilize various chemicals and chemical processes to get their desired products. Be it textile, tannery, petroleum, agro, pharmaceutical, electronic, mining, chemical, paper or food industries; their effluents are most likely to contain at least two or more pollutant species which may be dyes, heavy metals, pesticides, metal complexes, organic solvents e.t.c, hence making them binary or multi-component mixtures. (Meevasana and Pavasant, 2008; Özacar and Şengil, 2005).

Dyes and heavy metals which are major pollutant species usually exist side by side in effluents and waste waters (Saffaj *et al.,*2004; Hestekin *et al.*, 1998). This gives rise to different mixtures or complexes which makes the treatment of effluents difficult to handle (Visa *et al*., 2010)

1.2.0 Dyes and Heavy metals

1.2.1 Dyes

Dyes can simply be said to be species used to impart colour. This can be to textiles, leather, paper, drugs, drinks, food , petrol etc. (Daintith, 2000). Their chemistries are said to be broad and complex and may pose a difficulty to non-experts. (Griffiths, 1986). However, an understanding of their methods of

production may be of assistance. Approximately 7000 metric tonnes of 10000 different types of dyes and pigments are produced world wide of which up to 30% are wasted in industrial effluents during finishing processes in textile industries (Kannan and Meenakshisundaram, 2002). This leads to pollution of streams and rivers and eventually becomes a health risk to man and other living things. (Leechart *et al*., 2009).

Some dyes are known to be toxic, carcinogenic or mutagenic (e.g. methyl orange). Their molecular structures make them more stable and not easily biodegradable (Yasin *et al.,* 2007). Dyes contain conjugated double bonds. The group producing the colour is the chromophore while other non colored groups that influence or intensify the color are called auxochromes. Dye classification is based on the chemical structure of the dye molecule and mode of application; and on this basis they can be classified as azo dyes, acid dyes, metalized dyes, basic dyes, direct dyes(or substantive dye), vat dyes, sulphur dyes, disperse dyes and reactive dyes (Daintvith 2000)

1.2.2. Heavy metals

This is a term that is usually applied to common transition metals such as copper, lead, zinc *etc*. Heavy metals are generally considered a threat to man and the environment because of their potentially high toxicity (Qin *et* a*l*., 2006). They are a major cause of environmental pollution. They can get into the environment through sources including lead in petrol, industrial effluents and leaching of metal

ions from soils into lakes and rivers by acid rain.(Daintith, 2000; Sarin *et al*., 2006 ; Abdulrasaq and Basiru, 2010)

1.3 Treatment of effluents and waste waters

Indiscriminate discharge of effluents into the environment can have far reaching consequences. (Abdulrasaq and Basiru, 2010; Ong *et al.*, 2010). The degree of damage to the environment depends on the nature and amount of the hazardous species present. There are acceptable standards/levels to which the pollutant load from effluents should be reduced to before discharge into the environment.

Various techniques can be used to regulate the pollutant load of raw effluents. Some of them are precipitation, filtration, biosorption, chemical coagulation and flocculation, oxidation and adsorption. (Kadrivelu *et al*., 2003, Ong *et al.,* 2010). However adsorption using activated carbon is considered efficient for dye removal and is also widely used for heavy metal removal or recovery. This is because the technique is not as cumbersome as others and is also cost effective when compared to other methods such as filtration, precipation, coagulation, precipitation e.t.c.

1.4 Adsorption of dyes and heavy metals from aqueous solution

Dyes and heavy metals are generally classified under organic and inorganic compounds respectively. Works done by Puri (1981), Goyal and Bansal (1997), and Aggarwal (1998) suggests that the adsorption of organic and inorganic compounds using activated carbon as adsorbent is influenced by the

presence of carbon-oxygen surface groups. Goyal and co-workers (2001, 1999, 1989) studied the adsorption of several cationic and anionic dyes where it was observed that their adsorption was not primarily determined by the surface area of the carbon, but was enhanced by the presence of surface oxides. The amount of cationic dyes adsorbed increased as the surface oxides increased. The reverse was the observed trend for anionic dyes. Goyal *et al.,* (1997, 1989) also studied the adsorption of several metals, observing the effect of surface oxides on the activated carbon surface on the adsorption of the metals. It was observed that the adsorption was not solely dependent on the surface area but on the amount of the surface oxides, and more so the presence of acidic oxygen groups. Adsorption of these metals increased on oxidation and reduced on degassing. This trend is based on the premise that the acidic surface groups ionize in water to produce H^+ and are directed towards the liquid phase hence leaving a negatively charged activated carbon surface on which the adsorption of metal cations could take place. On degassing, the negative sites are removed hence a reverse trend is observed.

1.5 Use of Activated carbon for effluent treatment.

Effluents are generally comprised of organic and inorganic species. The versatile nature of activated carbon makes it useable for uptake of various pollutant species from effluents. It has high degree of porosity and an extended inter-particulate surface area. It is mainly produced via combustion, partial combustion or thermal decomposition of a variety of carbonaceous substances and can be in granular or powdered form (Bansal and Goyal, 2005). The characteristics of each end-product is influenced by the starting material, the

method of combustion, the method of activation and the type of activating agent employed. (Abram, 1973).

Activated carbon is used in the adsorption of heavy metals like Pb, Cd, Cr, Hg etc., and also the recovery of certain precious metals like Ag and Au. (Linstedt *et al.*, 1971; Cheremisinoff and Habib, 1972; Argaman and Weddle, 1973). They can take these metals from effluents due to their ion-exchange properties because of the polar nature of the acidic groups found on the activated carbon surfaces (Bansal and Goyal, 2005).

The pH of the medium also plays a role. For organic molecules, the nature and dimensions of the molecules, the porous and chemical structure of the activated carbon surface and pH of the solution will affect the amount of organic molecules adsorbed. Many industries utilize dyes for various purposes. The residual dyes makes most effluents colored (Hameed *et al*., 2006). When dyes and heavy metals are simultaneously resident in effluent samples, their treatment may prove difficult; this is because the competition and interaction between these different chemical species will to a large degree determine the extent to which each species will be adsorbed.

Activated carbon is a preferred choice adsorbent for obvious reasons. It can easily be produced with less complicated procedure. The procedure for it's practical use or application is straight forward, and it can be re-used when spent via regeneration. This makes it relatively easy to use and a less expensive

adsorbent to employ compared to others. e.g. filtration, precipation, coagulation e.t.c.

1.5.1 Adsorption

Adsorption is the accumulation of species unto the surface of another species. It arises as a result of unsaturated and unbalanced molecular forces present at any surface (Bansal and Goyal, 2005). When solid surfaces contact a liquid or gas, there are force field interactions at the surface and that of the liquid or gas where the surface attracts and retains on it's surface molecules, atoms or ions of the gas or liquid; resulting in greater concentration of the liquid or gas near the solid surface. The process by which liquids or gases accumulates on surfaces is called adsorption. It can occur at gas-solid, liquid-solid, gas-liquid and liquid-liquid interfaces (Cheremisinoff and Ellerbusch, 1978). Based on the energy dynamics involved, adsorption can be said to be

(a) physisorption and

(b) chemisorption (Atkins, 1999)

Adsorption studies is usually undertaken using single adsorbate/adsorbent systems where a single adsorbate (usually in a liquid or gas phase) is interacted with an adsorbent. In situations where there is more than one adsorbate to be adsorbed then a different scenario arises which usually is not as straight forward as what is obtained in single adsorbate systems. The adsorption studies in this type of system is usually refered to as "preferential adsorption."(Bansal and Goyal, 2005)

1.5.2 Preferential Adsorption.

Preferential adsorption arises when there is more than one adsorbate in an adsorption system. In this case, the different adsorbates in solution begin to "compete" for the limited available active sites on the adsorbent or the adsorbent may seem to display a "selective" function to a particular adsorbate; hence the names "competitive adsorption" or "selective adsorption" is used inter-changeably with the name preferential adsorption (Bansal and Goyal, 2005). Here, adsorption is influenced by a number of factors e.g the size and nature of the adsobates, the chemical interactions between the adsorbates, the peculiar behaviour/chemistry of the adsorbates in varying media and the functional groups on the activated carbon surface. Kipling and coworkers (1952, 1960) and Kipling(1965) have done works to shed more light on this dimension of adsorption. Their results were presented using composite isotherms.

1.6 Availability, Accessibility and use of activated carbon in Nigeria.

Nigeria is not in lack of precursors that can be used for activated carbon production. Work has been conducted using 'preferred' materials like coconut shell, palm kernel shell, groundnut shell, and sawdust of which the nation has vast amounts of these 'wastes.' (Gimba 2001; Ocholi 2001; Siyaka 2000; Abechi 2006, 2011, Dika 2009). Ongoing work seeks to produce activated carbon using 'alternative' sources like *Khaya senegalensis, Delonix regia* (Ocholi 2006; Okpe, 2010; Bari 2010) and *Canarium schweinforthii* (Yileng, 2008).

The activated carbon produced from these materials have been used to adsorb pollutant species like dyes, heavy metals, pesticides and enzymes. Nigeria also has rich deposits of coal which can be employed for the same purpose. It can be said that the nation has enough material to produce activated carbon to meet both internal and external demands. It can also be said that the nation is not lacking the manpower, technical know how and skill to produce activated carbon on an industrial scale. The sad note is that despite the availability of materials and personel needed to establish plants for large scale activated carbon production, the country at present does not have one industry in this direction.

Most of the products in the Nigerian market are imported and the quality of some is questionable. As regards the use and application of activated carbon, majority of the populace know little about this product and it's use, hence the low demand for it. A lot of work needs to be done by scientists, engineers , technologists and their societies to enlighten the general populace and also suggest and advice the government to see the need to establish activated carbon production plants in the nation.

1.7 Statement of the Research Problem.

Fundamental adsorption studies from solution have been restricted to a solute in a solvent and a single adsorbent (Kipling, 1965). The practical application of adsorption is however for separation of mixtures of solutes present in a common or mixture of solvents. Numerous adsorption studies have been undertaken using single adsorbate/adsorbent systems, of which the adsorbates

were pollutant species like dyes, heavy metals, anionic species and pesticides (Gimba, 2001, 2009; Abechi 2006, 2011; Ocholi 2001, 2006; Yileng 2008). Scarce work has been conducted using binary or multi-component adsorbate/adsorbent systems hence the need to look more into this dimension of adsorption.

1.8 Justification

Environmental pollution is a global challenge with industrial effluents as major contributors (Garg *et al*., 2003; Kadrivelu *et al.,* 2003). These effluents foul streams and rivers, affect marine life and are carcinogenic. They are normally a mixture of at least two or more pollutant species i.e. aqueous binary or multi-component mixtures. (Kadrivelu *et al.,* 2003; Meesavana and pavasant, 2008).

The common laboratory practice is to carry out adsorption studies using single adsorbate systems (Meesavana and Pavasant, 2008). This does not adequately represent the true situation in real effluent samples. The focus of this work is to simulate various effluent sample using dyes and heavy metals and study the adsorption and preferential adsorption trends of the dyes unto unmodified and modified activated carbon matrices.

1.9 Aim

-To study the adsorption of simulated and real effluent systems onto activated carbon surfaces.

1.9.1 Objectives

- To establish working concentration ranges for the different adsorbate systems and their wavelength of maximum absorption.

- To study the adsorption trends of single dye systems in aqueous and heavy metal environment using activated carbon.

- To study the preferential adsorption trends of binary dye systems in aqueous and heavy metal environment using activated carbon.

- To study adsorption trends of tertiary dye mixtures in aqueous and heavy metal environment using activated carbon.

- To study the adsorption of real effluent samples using activated carbon.

CHAPTER TWO

2.0 Literature Review

2.1.0 Adsorption in single adsorbate/adsorbent systems

Single solute systems involve interacting one adsorbate with an adsorbent. This is typically the case when we have gas streams (e.g. O_2, N_2, Cl_2 e.t.c) being adsorbed unto activated carbon. In the aqueous phase the concept is not necessarily single because in most cases, the water molecules also act like an adsorbate and interfere in the adsorption process. This is more pronounced when organics are the solvent media. Hence, it can be said to be a binary adsorbate/adsorbent system where the solute is one component while the solvent is the second component.

In this work, the single solute systems are systems where there is only one solute in the aqueous medium (distilled water) e.g. methylene blue in distilled water or methyl orange in distilled water. And a binary system is where there are two solutes in a solvent e.g. methylene blue and methyl orange in distilled water. Various factors affect the extent of adsorption of adsorbates unto activated carbon. Some of them include:

1. Nature of the activated carbon. (i.e. surface reactivity and porosity)
2. Nature of the adsorbate. (i.e. adsorbate size and orientation)
3. pH of solution
4. Temperature of adsorption

The overall adsorption is an interplay of these factors.

2.1.1 Nature of activated carbon.

The versatility of activated carbon as an adsorbate is usually tied to it's surface chemistry, surface area and internal porous network. (Bansal and Goyal, 2005). These properties are affected primarily by the nature of the starting material and method of preparation (Abram, 1973). A good activated carbon is expected to have a surface area of 800-1500m^2/g. The surface chemistry is tied to the functional groups present on the activated carbon surface which may include >C=O, -COOH, >C=S, -C≡N groups (Bansal and Goyal, 2005).

Activated carbon can be modified to either add or remove these functional groups by surface modification using several methods like nitrogenation, oxidation, halogenation, sulphurization, impregnation and degassing. This makes the activated carbon suitable for specific purposes.

The internal porosity of activated carbon can be classified into three (3) categories:

1. Micropores- with pore size less than 2nm
2. Mesopores- with pore size between 2-50nm
3. Macropores-with pore size greater than 50nm

It is believed that adsorption occurs mainly in the micro and mesopores with the macropores serving as a conduit to the micro and mesopores (Abram, 1973)

2.1.2.0 Removal of lead

Lead is present in both water and air. It can get into water as a result of activities of lead battery factories or industries that use lead compounds for one purpose or the other. It can easily get into the air from emissions from automobiles since lead is used as an anti-knocking agent in the form of lead tetraethyl in gasoline. In the human body, lead tends to form complexes that interfere with several synthetic and metabolic processes. Netzer and Hughes (1984) studied Pb adsorption from aqueous solution with different pH.

The process of adsorption involved both hydrolysis and precipitation depending on the pH of the solution. Corapcioglu and Huang (1987) observed that Pb adsorption was larger at higher pH values and complex formation and precipitation were involved. Cheng *et al*., (1993) studied Pb adsorption unto activated carbon at different pH with regards their >C=O surface groups. Taylor and Kuennen (1994) observed also that pH and surface groups played an important role in Pb adsorption from aqueous media unto activated carbon.

2.1.2.1 Removal of Cadmium from aqueous solution

Huang and Ostovic (1978) are credited with carrying out the first systematic studies of Cd removal from aqueous solutions. They studied the influence of pH , carbon surface, carbon dose, influence of the addition of chelating agents on Cd adsorption. The amount adsorbed increased with increase in pH of solution; small amounts were adsorbed at pH less than 3 and increased until it became constant at pH above 8. The maximum adsorption also depended

on the nature of the activated carbon surface. Basic surfaces adsorbed more than acidic carbons. The amount adsorbed was also a function of the carbon dose, concentration and the presence of chelating agents. Dobrowloski *et al.,*(1986) also studied Cd removal from aqueous solutions unto modified activated carbon samples. The adsorption isotherms obeyed the Langmuir equation. This present work is not focused on the adsorption of Pb or Cd but on how it may hinder or enhance dye uptake from aqueous solutions.

2.1.2.2 Adsorptive removal of organics.

Dyes are generally classified under "organics" of which others include compounds like phenols, pesticides, herbicides, surfactants, ethers, amines, nitro compounds e.t.c. Numerous organic compounds are said to be present in drinking waters derived from industrial and municipal waste water. Natural decomposition of animal and vegetable matter, agricultural practices and leaching of solid industrial waste are also sources of several organic compounds in water.

Activated carbon due to it's surface area and micro porous structure is considered a good adsorbent for removal of organic compounds (Quinlivan, 2001). Graham (1955) studied the adsorption of two dyes of opposite character but of similar molecular dimensions (methylene blue and metanil yellow) from aqueous solutions on a number of activated carbon samples. The methylene blue (a cationic dye) adsorption increased while the metanil yellow (an anionic dye) adsorption decreased with increase in the acidity of the carbon surface. Similar results were obtained by Puri (1981)and Arora (1977) in their studies on the

adsorption of Methylene blue and Rhodamine B. Guzel (1996) studied the effect of carbon surface acidity on Methylene blue and Metanil yellow adsorption .The methylene blue adsorption was larger than metanil yellow. It was suggested that the methylene blue molecules were attracted by the carbon surface while those of metanil yellow were repelled.

2.3.0 Adsorption Isotherms

Adsorption isotherms are a functional expressions of the variation of adsorption relative to the concentration of adsorbate in the bulk solution at constant temperature (Weber, 1972). They are graphical representations of equilibrium states in an adsorption system at constant temperature (Daintith 2000).

Useful information regarding the adsorbate, adsorbent and adsorption process can be derived; other parameters like the surface area of the adsorbent, volume of the pores, their size distributions and relative adsorbability of a given gas or vapour on a given adsorbent can be determined. There are several existent isotherms of which some are Langmuir, Freundlich, Temkin, Brunauer-Emmet-Teller (BET) and Dubinin Equations (Bansal and Goyal, 2005)

2.3.1 Langmuir Isotherm Equation

It is the first theoretically developed adsorption isotherm (Bansal and Goyal, 2005). Many of the other proposed equations which fit with experimental data are either based on it or use it's concept. It was proposed by an American scientist, Langmuir (1918). The equation is derived from assumptions:

1. The adsorbed entities (atoms, molecules or ions) are attached to the surface at definite localized sites.
2. Each site accommodates only one adsorbed entity.
3. The energy state of each adsorbed entity is the same at all sites on the surface independent of the presence or absence of other adsorbed entities at neighbouring sites.

The theory assumes that the surface is perfectly smooth and homogenous, and that lateral interactions between the adsorbed entities are negligible. The Langmuir Isotherm is given as

$$qe = \frac{bCQo}{1+bC} \quad \text{.....(2.1)}$$

where qe is the amount of adsorbate adsorbed per unit weight of carbon, Q^o is a constant relating to the monolayer adsorption capacity, 'b' is a constant which measures the surface energy of the adsorption process and 'C' is the equilibrium concentration in solution. Two convenient linear forms of the equation exists:

$$\frac{C}{qe} = \frac{1}{bQo} + \frac{C}{Qo} \quad \text{..... (2.2)}$$

$$\frac{1}{qe} = \frac{1}{Qo} + \left[\frac{1}{bQo}\right]\left[\frac{1}{C}\right] \quad \text{.....(2.3)}$$

The choice of the equation depends on the range and spread of the data and the particular data emphasized (Weber, 1972).

2.3.2 The Freundlich Isotherm Equation

The Freundlich Isotherm is a limiting form of the Langmuir equation and is applicable only in the middle ranges of vapour pressure i.e when gases are involved (Bansal and Goyal, 2005). The Freundlich Isotherm adsorption equation is a special case for heterogenous surfaces and is mostly used to model adsorption from solution. It has the general form as expressed by Thomas and Crittenden 1998 as

$$qe = K_f C^{1/n} \quad \text{.....(2.4)}$$

where *qe* is the amount of adsorbate adsorbed per unit weight of carbon. 'n' is a constant related to adsorption efficiency and energy of adsorption , K_f is a constant measuring adsorption capacity, The logarithmic form can be written as

$$\log qe = \log Kf + \frac{1}{n} logC \quad \text{.....(2.5)}$$

it's mathematical simplicity usually favours it's use. The equation is empirical and is useful for data description . (Hartman, 1974 and Ribeiro *et al.,* 2001). The equation is adequate to describe non-linear adsorption in a narrow range of adsorbate concentration.

2.3.3 The Temkin isotherm

This is derived from the Langmuir Isotherm by introducing the condition that the heat of adsorption decreases in a linear fashion with surface coverage. Such effects can arise due to repulsive forces on a uniform surface or heterogeneity of the surface (Bansal and Goyal, 2005)

$$qe = \frac{RT}{bln(ACe)} \quad \text{..... (2.6)}$$

$$qe = BlnA + BlnC \quad \text{.....(2.7)}$$

equation 2.7 is a linear expression of equation 2.6. *A* and *B* are the Temkin constants while qe (mg/g) and Ce (mg/l) are the amount of adsorbate adsorbed per unit weight of adsorbent and unadsorbed adsorbate concentration in solution at equilibrium respectively. (Ozacar and Sengil 2005)

2.4.0 Factors affecting adsorption from binary solutions

Adsorption from binary solution is generally referred to as "competitive," "selective," or "preferential" adsorption. It depends on several factors such as:

1. Adsorbate – Adsorbent/Adsorbate-Adsorbate interaction
2. Porosity of Adsorbent
3. Surface Heterogenity
4. Orientation/Size of adsorbed molecules

2.4.1 Adsorbate-Adsorbent/Adsorbate-Adsorbate Interaction

Competitive adsorption between components in solution on the surface of a solid adsorbent depends on the strength of the interaction between the adsorbent and the two components in solution. The polarity of the adsorbates and adsorbent will also contribute to the extent of adsorption so that polar compounds are likely to be more strongly adsorbed on the surface than the non-polar compounds. Thus competitive adsorption becomes more prominent when adsorption is carried out from a solution containing a polar and non-polar component (Quinlivan, 2001).

2.4.2 Porosity of adsorbent

The ability of activated carbon to behave as a molecular sieve is not ruled out due to it's widespread pore sizes. This will be pronounced when the components of the binary solution do not have similar dimensions. This factor will add a degree of preferential adsorption of the components of smaller sized molecules irrespective of other factors.

2.4.3 Surface Heterogenity

Activated carbon surfaces cannot be considered as elementary carbon but as polynuclear hydrocarbons interspersed with different carbon-oxygen types and in some cases other elements such as nitrogen, sulphur, and halogens. The presence of these create a certain degree of surface heterogeneity which leads to preferential adsorption of components when binary solutions with different sizes and varying polarities are used (Bansal and Goyal, 2005).

2.4.4 Orientation of adsorbed molecules

The orientation of the molecules in the adsorbed phase also influences the adsorption of components of binary solutions as it determines the extent of adsorption of a given component (Quinlivan, 2001). An ideal adsorbate is one that is spherical. However, for unsymmetrical adsorbate molecules, the orientation adopted on the surface of the adsorbent is of considerable consequence since it determines the number of molecules that can occupy a unit area of the surface.

2.5.0 Dye (adsorbate) molecules.

Three different dye molecules were used as adsorbates in this work. They are: Methylene blue (MB), Methyl orange (MO) and Indigo carmine (IG).

2.5.1 Methylene blue(MB)

Methylene blue (C.I.52015); Methylthionine chloride; 3,7-bis[Dimethylamino]-Phenazothionium chloride (SIGMA , 1991), is a potent Cationic dye with chemical formular $C_{16}H_{18}ClN_3S$ and formular weight of 319.9 g/mol. Below is the structural formular.

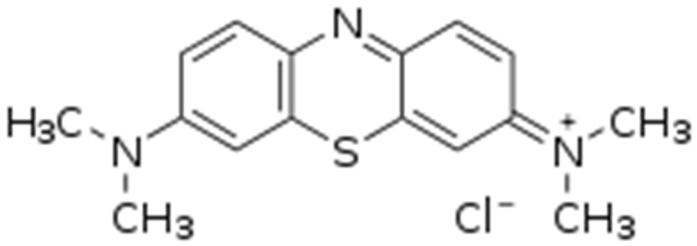


Figure 2.1(a): Structural formular Methylene blue.

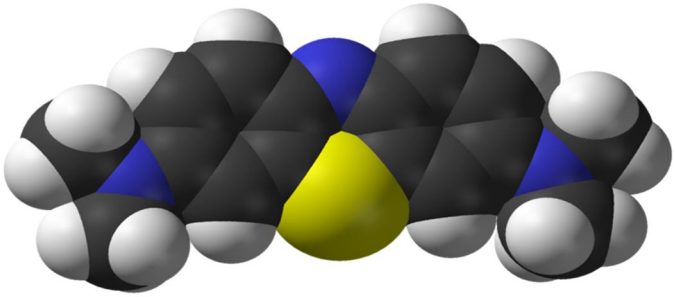


Figure 2.1(b): 3D- structural formular of Methylene blue.

Methylene blue is used in different fields such as Chemistry, Biology and Medicine. At room temperature it is a dark green odourless solid that yields a blue solution when dissolved in water. The hydrated form has 3 molecules of water per molecule of methylene blue. It has a maximum absorption of light around 670nm, though specifics of absorption depend on factors like protonation, adsorption to other materials and metachromasy i.e. the formation of dimmers and higher – order aggregates depending on concentration and other interactions.(Cenens and Schoonheydt(1988). In this work the wavelength of maximum absorption (λ_{max}) was confirmed to be 664 nm which shows a MB^+ species in solution according to Cenens and Schoonheydt (1988).

2.5.2 Methyl orange(MO)

Methyl orange(C.I.13025); Acid Orange 52 (AO 52); [p-(Dimethylamino)-Phenylazo]benzene sulfonic acid, sodium salt; $C_{14}H_{14}N_3O_3SNa$. FW=327.3g/mol. (SIGMA 1991). It is a pH indicator (at pH 3.0 (pink)- pH4.4 (yellow)). It is a pH indicator frequently used in titrations because of it's clear and distinct colour change. It is also known to posses mutagenic properties.

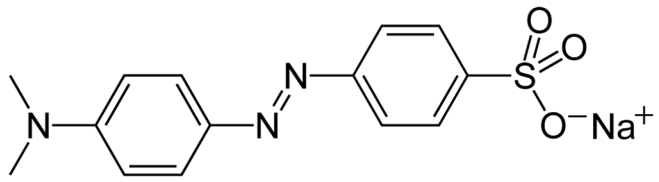


Figure 2.2(a): Structural Formular of Methyl orange

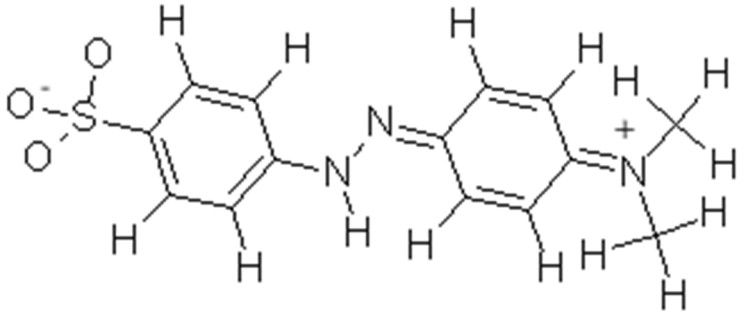


Fig 2.2(b): Structure of Methyl orange in acid solution.

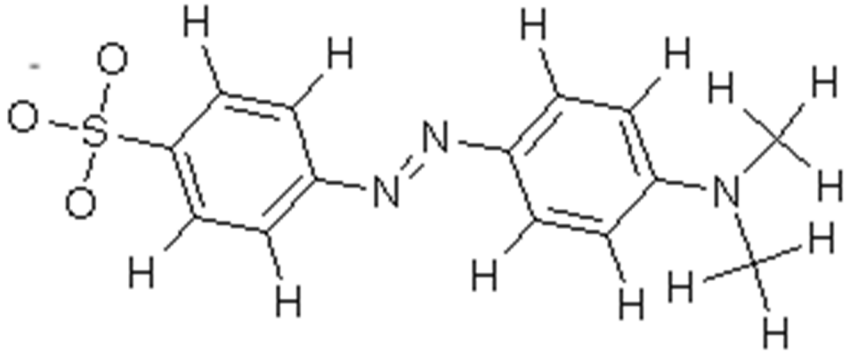


Fig 2.2(c): Structure of Methyl orange in basic solution.

The molecule absorbs blue-green light, which makes it's solution appear red. The nitrogen bearing the positive charge is involved in a double bond.

In the basic form of methyl orange, a hydrogen ion is lost from the azo (–N=N-) bridge between the rings, and the electrons used to bind the hydrogen neutralize the positive charge on the terminal nitrogen so that it is no longer able to π-bond. Solutions of MO appear yellow in alkaline solution. The wavelength of maximum absorption (λ_{max}) of the MO sample used in this work was 464nm.

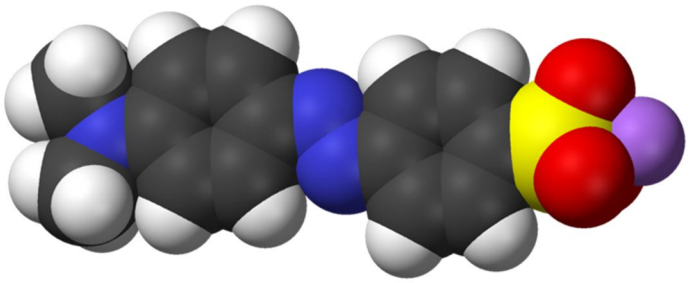


Fig 2.2(d): 3D- structural formular of Methyl orange.

2.5.3 Indigo carmine (IG)

Indigo carmine(C.I. 73015); Acid blue 74 (AB 74); 5,5'-indigosulfonic acid disodium. $C_{16}H_8N_2Na_2O_8S_2$. FW=466.3 g/mol (SIGMA 1991). It is an approved food colourant in America and the European Union. It is used as a pH indicator givin a blue colour at pH below 11.4 and yellow at pH 13. It is also used as a dye in capsule manufacturing and in Obstetrics.

It's IUPAC name is 3,3'-dioxo-2,2'-bis-indolyden-5,5'-disulfonic acid disodium salt. The wavelength of maximum absorption of the IG sample used in this was 602 nm.

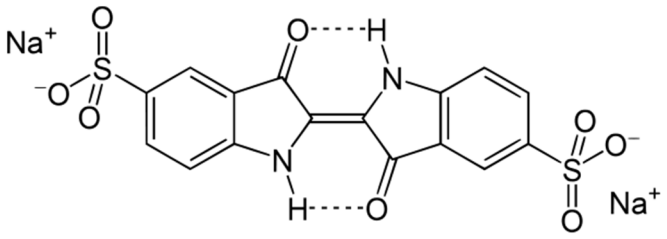


Figure 2.3: Structure of Indigo carmine.

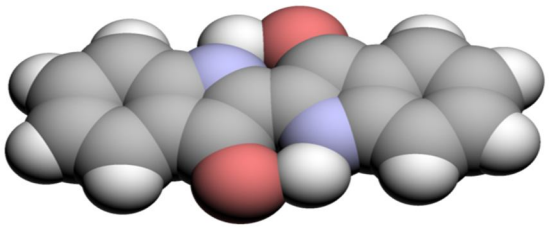


Figure 2.4: 3D- structural formular of indigo.

It's IUPAC name is 3,3'-dioxo-2,2'-bis-indolyden-5,5'-disulfonic acid disodium salt. The wavelength of maximum absorption (λ_{max}) of the IG sample used in this work was 602 nm.

CHAPTER THREE

3.0 Materials and Methods

3.1Instruments and Reagents

The instruments and reagents used in the work include:

1. Micro pH 2000 Crison Digital pH meter
2. Analytical Digital Balance (GR-2000) A & D instruments Ltd.
3. Thermospectronic Hελios γ UV- Visible Spectrophotometer
4. Jenway Digital Spectrophotometer
5. Laboratory Mechanical Shaker
6. Memmert Laboratory Oven
7. FTIR- 8400S Fourier Transform Infrared Spectophotometer-Shimadzu
8. Methylene blue(MB) (Kibran light Laboratories)
9. Methyl Orange(MO) (BDH)
10. Lead nitrate ($Pb(NO_3)_2$) (BDH)
11. Cadmium nitrate tetrahydrate ($Cd(NO_3)_2.4H_2O$) (BDH)
12. Conc Nitric Acid (HNO_3) (BDH)

3.1.0 Activated Carbon Sample

The activated carbon sample used in this work was extra pure food grade granular activated carbon from Merck Darmstadt Germany. Below is the

summary of it's manufacturer's specifications. the sample was pulverized and sieved. Particle size of between 425 μm - 850μm was used for the work.

Table 3.1: Factory Specifications of AC sample

Identity	Conforms
Particle Size	1.5mm
Substances soluble in Nitric acid	≤ 5%
Chlorides	≤500ppm
Cyano compounds	Passes test
Arsenic	≤ 5ppm
Iron	≤ 500ppm
Lead	≤ 20 ppm
Zinc	≤ 100ppm
n-hexane adsorption	≥ 30%
Residue on ignition	≤ 6%
Loss on drying	≤ 10%

3.1.1 Sample Modification

The sample was further modified using simple physical and chemical methods

3.1.2 Physical Modification

This was done by heat treatment. 10g of the sample was introduced into an oven at 200^{o}C and was left for 24hrs after which it was allowed to cool in a

dessicator and the percentage yield was calculated. It was then stored in polyethylene sample bottles.The sample was coded PMAC (Bansal and Goyal, 2005)

3.1.3 Chemical Modification

This was done using the procedure of Vasu (2008) with slight modification in which the ratio of the activated carbon and nitric acid was varied. 10g of the sample was weighed in a beaker. 50cm^3 of Conc HNO_3 was then added and allowed to stand for 24hrs. It was then thoroughly washed with distilled water and dried in an oven at 105^oC for 6hrs, cooled in a dessicator then stored in polyethylene sample bottles. The sample was coded CMAC.

3.2.0 Preparation of methylene blue, methyl orange and indigo carmine stock solutions

For MB and MO, 1000ppm solutions of each dye was prepared by separately weighing 0.5g of each dye and were partially dissolved in a beaker using distilled water . It was then transferred into a 500cm^3 volumetric flask and was made up to the mark using distilled water. They were then stored in amber coloured bottles and kept in a locker. The various needed concentrations of the dyes were prepared via serial dilution. For IG, smaller volumes of stock solution were prepared (i.e. 100cm^3 capacity) when needed. This was because it is not stable on storage. It goes from blue to orange colour, hence the need to freshly prepare it when needed. The various needed concentrations of the dyes were then prepared via serial dilution.

3.2.1 Preparation of 1M $Pb(NO_3)_2$ and 1M $Cd(NO_3)_2.4H_2O$ solutions

33.1g and 30.8g of $Pb(NO_3)_2$ and $Cd(NO_3)_2.4H_2O$ respectively were separately weighed. Each weight was separately dissolved in a beaker, transferred into a $100cm^3$ volumetric flask and made up to the mark with distilled water. They were then stored in separate polyethylene bottles. The needed concentrations of the dyes were prepared via serial dilution.

3.2.2 Preparation of binary dye mixtures

This was prepared by mixing stock solutions of methylene blue and methyl orange dyes in the ratio 1:1 (v/v). subsequent concentrations were prepared by serial dilution.

3.2.3 Preparation of binary dye mixtures in heavy metal solution.

This was prepared by mixing stock solutions of methylene blue and methyl orange dyes in the ratio 1:1 (v/v) and then diluting to various concentrations using the prepared heavy metal salt solutions.

3.3 Adsorbate systems (Simulated Effluents)

The adsorbate systems used in the adsorption studies are given below:

1. Aqueous MB system
2. Aqueous MO system
3. Aqueous IG system
4. Aqueous MBMO system
5. Aqueous MOIG system

6. Aqueous MBMOIG system
7. Aqueous MB in $Pb(NO_3)_2$ system
8. Aqueous MO in $Pb(NO_3)_2$ system
9. Aqueous IG in $Pb(NO_3)_2$ system
10. Aqueous MB in $Cd(NO_3)_2.4H_2O$ system
11. Aqueous MO $Cd(NO_3)_2.4H_2O$ system
12. Aqueous IG $Cd(NO_3)_2.4H_2O$ system
13. Aqueous MB in $Pb(NO_3)2/Cd(NO_3)_2.4H_2O$ system
14. Aqueous MO $Pb(NO_3)_2/ Cd(NO_3)_2.4H_2O$ system
15. Aqueous IG $Pb(NO_3)_2/Cd(NO_3)_2.4H_2O$ system
16. Aqueous MBMO in $Pb(NO_3)_2$ system
17. Aqueous MOIG in $Pb(NO_3)_2$ system
18. Aqueous MBMO in $Cd(NO_3)_2.4H_2O$ system
19. Aqueous MOIG in $Cd(NO_3)_2.4H_2O$ system
20. Aqueous MBMO in $Pb(NO_3)_2$ /$Cd(NO_3)_2.4H_2O$ system
21. Aqueous MOIG $Pb(NO_3)_2$ / $Cd(NO_3)_2.4H_2O$ system
22. Aqueous MBMOIG $Pb(NO_3)_2$ / $Cd(NO_3)_2.4H_2O$ system

3.4 Rate of Dye Adsorption

The rate at which the individual dyes (MB, MO and IG) were adsorbed onto UMAC was monitored using two different experiments involving different time frames, AC dose and Adsorbate concentration.

In the first experiment, 10 cm^3 of 20ppm of the individual dyes were separately interacted with 20mg each of UMAC. Agitation times were for 5, 10, 15, 20, 30, 45, and 60 minutes respectively. The mixtures were allowed to settle and the absorbances of the supernatants were taken using a Spectrophotometer.

In the second experiment, $10cm^3$ of 10ppm of the individual dyes were separately interacted with 10mg each of UMAC. This was to observe the adsorption trend when a lower dose of activated carbon was used. Agitation times were for 15, 30, 45 and 60 minutes respectively. The mixtures were allowed to settle and the absorbances of the supernatants were taken using a Jenway Digital UV-Visible Spectrophotometer.

3.5 Adsorption Studies

Adsorption studies was executed using the Batch Mode of interaction . For each experiment, $10cm^3$ of each adsorbate system was interacted separately with 10mg of the different AC matrix (i.e UMAC,PMAC & CMAC). Shaking was done using a mechanical shaker for 1 hr. The absorbance of the supernatants were then taken using a Jenway Digital UV-Visible Spectrophotometer and the amount of the coloured adsorbate adsorbed was evaluated. (Hameed *et al*., 2006) . A series of procedures were developed for each adsorbate system and are as follows:

Single dye systems

Procedure 1

1. MB adsorption in aqueous medium.

- 10, 20, 30, and 40ppm MB solution was separately interacted with 10mg of AC for 1 hour.

2. MB adsorption in $Pb(NO_3)_2$ solution

- 10ppm MB in 0.005, 0.006, 0.007 and 0.008M $Pb(NO_3)_2$ solution was interacted with 10mg of AC for 1 hour.

3. MB adsorption in $Cd(NO_3)_2.4H_2O$ solution.

- 10ppm MB in 0.005, 0.006, 0.007 and 0.008M $Cd(NO_3)_2.4H_2O$ solution was interactedwith 10mg AC for 1 hour.

- 10, 20, 30 and 40ppm MB in 0.01M $Cd(NO_3)_2.4H_2O$ solution was interacted with 10mg AC for 1 hour.

4. MB in [$Pb(NO_3)_2$ + $Cd(NO_3)_2.4H_2O$] mixture

- 10ppm MB in 0.005, 0.006, 0.007 and 0.008M [$Pb(NO_3)_2$ + $Cd(NO_3)_2.4H_2O$] mixture was interacted with10mg AC for 1 hour.

Procedure 2

1. MO Adsorption in aqueous medium.

- 10, 20, 30 and 40ppm MO solution was interacted with 10mg of AC for 1 hour.

2. MO adsorption in $Pb(NO_3)_2$ solution

- 10ppm MO in 0.005, 0.006, 0.007and 0.008M $Pb(NO_3)_2$ solution was interacted with 10mg AC for 1 hour.

- 10, 20, 30 and 40ppm MO in 0.01M $Pb(NO_3)_2$ solution was interacted with 10mg AC for 1 hour.

3. MO adsorption in $Cd(NO_3)_2.4H_2O$ solution.

- 10ppm MO in 0.005, 0.006, 0.007 and 0.008 $Cd(NO_3)_2.4H_2O$ solution was interacted with 10mg AC for 1 hour.

- 10, 20, 30 and 40ppm MO in 0.01M $Cd(NO_3)_2.4H_2O$ solution was interacted with 10mg AC for 1 hour.

4. MO in [$Pb(NO_3)_2$ + $Cd(NO_3)_2.4H_2O$] mixture

- 10ppm MO in 0.005, 0.006, 0.007 and 0.008 [$Pb(NO_3)_2$ + $Cd(NO_3)_2.4H_2O$] mixture was interacted with 10mg AC for 1 hour.

-10, 20, 30 and 40ppm MO in 0.01M [$Pb(NO_3)_2$ + $Cd(NO_3)_2.4H_2O$] mixture was interacted with 10mg AC for 1 hour.

Procedure 3

1. IG adsorption in aqueous medium.

- 10, 20, 30 and 40ppm IG solution was interacted with 10mg of AC for 1 hour.

2. IG adsorption in $Pb(NO_3)_2$ solution

- 10ppm IG in 0.005, 0.006, 0.007 and 0.008 $Pb(NO_3)_2$ solution was interacted with 10mg AC for 1 hour.

- 10, 20, 30 and 40 ppm IG in 0.01M $Pb(NO_3)_2$ solution was interacted with 10mg AC for 1 hour.

3. IG adsorption in $Cd(NO_3)_2.4H_2O$ solution.

- 10ppm MO in 0.005, 0.006, 0.007 and 0.008M $Cd(NO_3)_2.4H_2O$ solution was interacted with 10mg AC for 1 hour.

- 10, 20, 30 and 40 ppm IG in 0.01M $Cd(NO_3)_2.4H_2O$ solution was interacted with 10mg AC for 1 hour.

4. IG in [$Pb(NO_3)_2$ + $Cd(NO_3)_2.4H_2O$] mixture

- 10ppm IG in 0.005, 0.006, 0.007 and 0.008M [$Pb(NO_3)_2$ + $Cd(NO_3)_2.4H_2O$] mixture was interacted with 10mg AC for 1 hour.

-10, 20, 30 and 40 ppm IG in 0.01M [$Pb(NO_3)_2$ + $Cd(NO_3)_2.4H_2O$] mixture was interacted with 10mg AC for 1 hour.

Binary Dye Systems

Procedure 4

1.[MBMO]adsorption in aqueous medium.

- 10, 20, 30 and 40ppm solution was interacted with 10mg of AC for 1 hour

2. [MBMO] adsorption in $Pb(NO_3)_2$ solution

- 10ppm [MBMO] in 0.005, 0.006, 0.007and 0.008M $Pb(NO_3)_2$ solution was interacted with 10mg AC for 1 hour.

- 10, 20, 30 and 40 ppm [MBMO] in 0.01M $Pb(NO_3)_2$ solution was interacted with 10mg AC for 1 hour.

3. [MBMO] adsorption in $Cd(NO_3)_2.4H_2O$ solution.

- 10ppm [MBMO] in 0.005, 0.006, 0.007 and 0.008M $Cd(NO_3)_2.4H_2O$ solution was interacted with 10mg AC for 1 hour.

- 10, 20, 30 and 40ppm [MBMO] in 0.01M $Cd(NO_3)_2.4H_2O$ solution was interacted with 10mg AC for 1 hour.

4. [MBMO] in [$Pb(NO_3)_2$ + $Cd(NO_3)_2.4H_2O$] mixture

- 10ppm [MBMO] in 0.005, 0.006, 0.007 and 0.008M [$Pb(NO_3)_2$ + $Cd(NO_3)_2.4H_2O$] mixture was interacted with 10mg AC for 1 hour.

-10, 20, 30 and 40ppm [MBMO] in 0.01M [$Pb(NO_3)_2$ + $Cd(NO_3)_2.4H_2O$] mixture was interacted with 10mg AC for 1 hour.

Procedure 5

1.[MOIG]adsorption in aqueous medium.

- 10, 20, 30 and 40 ppm solution was interacted with 10mg of AC for 1 hour.

2. [MOIG] adsorption in $Pb(NO_3)_2$ solution

- 10ppm [MOIG] in 0.005, 0.006, 0.007 and 0.008M $Pb(NO_3)_2$ solution was interacted with 10mg AC for 1 hour.

- 10, 20, 30 and 40 ppm [MOIG] in 0.01M $Pb(NO_3)_2$ solution was interacted with 10mg AC for 1 hour.

3. [MOIG] adsorption in $Cd(NO_3)_2.4H_2O$ solution.

- 10ppm [MOIG] in 0.005, 0.006, 0.007 and 0.008M $Cd(NO_3)_2.4H_2O$ solution was interacted with 10mg AC for 1 hour.

- 10, 20, 30 and 40 ppm[MOIG] in 0.01M $Cd(NO_3)_2.4H_2O$ solution was interacted with 10mg AC for 1 hour.

4. [MOIG] in [$Pb(NO_3)_2$ + $Cd(NO_3)_2.4H_2O$] mixture

- 10ppm [MOIG] in 0.005, 0.006, 0.007 and 0.008M [$Pb(NO_3)_2$ + $Cd(NO_3)_2.4H_2O$] mixture was interacted with 10mg AC for 1 hour.

-10, 20, 30 and 40ppm [MOIG] in 0.01M [$Pb(NO_3)_2$ + $Cd(NO_3)_2.4H_2O$] mixture was interacted with 10mg AC for 1 hour.

Tertiary Dye Mixture

Procedure 6

1.[MBMOIG] adsorption in aqueous medium

-10, 20, 30 and 40 ppm solution was interacted with 10mg of AC for 1 hour.

2. . [MBMOIG] in [$Pb(NO_3)_2$ + $Cd(NO_3)_2.4H_2O$] mixture

-10, 20, 30 and 40ppm [MBIGMO] in 0.01M [$Pb(NO_3)_2$ + $Cd(NO_3)_2.4H_2O$] mixture was interacted with 20mg AC for 1 hour.

CHAPTER FOUR

4.0 Results and Discussion

4.1.0 Introduction

The results obtained from the work were presented using appropriate Tables and Figures while attempts were made to discuss the observations and also state likely inferences based on literature.

4.1.1 Unmodified and Modified Activated Carbon Samples

The manufacturer's specifications of the main AC sample for this work are in Table 3.1.The parameters in the table attest to the quality of the product. This was taken as the control or Unmodified Activated Carbon Sample (UMAC). It was from this product that procedures in articles 3.1.1 and 3.1.2 were applied to give two other "new" products which were named Physically Modified Activated Carbon (PMAC) and Chemically Modified Activated Carbon (CMAC) samples.

4.1.2 pH of AC samples

Table 4.1: pH of AC samples

Sample	pH
UMAC	7.23
CMAC	3.42
PMAC	4.66

The adsorption efficiency of any adsorbate/adsorbent system is pH dependent (Aksu and Donmez, 2003). Changes in pH of solution leads to changes in surface properties of the adsorbent and the extent of ionization of the adsorbate (Gupta *et al*., 2007) which determines to a large extent the affinity an adsorbent's surface may have for different adsorbates in solution. Various organic molecules have optimum pH values in solution which lead to their maximum adsorption onto different surfaces (Kathiresan *et al.,*). The surface charge density of most surfaces increases as pH is lowered due to protonation (*Yasin et al*., 2007) Generally, acidic surfaces will preferentially adsorb adsorbates in alkaline solution and verse versa. This is because electro-static repulsions are more likely to be less in such arrangements (Chiou and Chuang, 2006). However this may not always be the case as other factors may be involved which may over- ride this .

The pH of the AC surfaces are given in Table 4.1 above. The pH for UMAC (7.23) is in the neutral range while the CMAC (3.42) and PMAC (4.66) are acidic. This may suggest that CMAC and PMAC have positively charged surfaces and may not be ideal for uptake of positively charged species in solution.

4.1.3. pH of Dyes, Heavy metal solution, Dye/Heavy metal mixtures and real textile effluents

Table 4.2 is a summary table which shows pH readings of the dyes, heavy metals, their mixtures and real textile effluents. Details of other tables leading to this summary table can be seen in Appendices I(a) and I(b). From the table above, the observed pH for all the samples fell between 4 and 7.Which makes them

acidic. pH readings of the dyes and their mixture were less acidic than the heavy metal salts and their mixture. pH readings for the Dye/Heavy metal mixture was intermediate between the dyes, heavy metal and their mixtures.

This suggests that pH values of aqueous mixtures can be influenced by the individual component solutions that they are comprised of. Based on these results adsorption between these aqueous mixtures and the AC samples for this work may not be favourable; though this is not what is seen as the work progressed. This shows that other factors are involved.

Table 4.2 pH ranges of dyes, heavy metal solution, dye/heavymetal mixtures and real textile effluents

Sample	pH range	Mid point
MB	6.52-6.76	6.64
MO	6.39-6.57	6.48
MBMO	6.26-6.36	6.31
Pb nitrate	5.00-5.33	5.16
Cd nitrate	6.00-6.27	6.13
Cd/Pb nitrate	5.23-5.42	5.32
MBMO/Cd/Pb nitrate	5.35-5.63	5.49
Textile effluents	4.70-6.49	5.91

4.2.0 Behaviour of Dyes and Heavy metals in solution

"The solubility and behaviour of solutes is a complicated subject."(Huheey, 1972).Although Advanced spectroscopic techniques is aiding to further understand this subject, fundamental questions like "what

happens to metal ions in solution?" are still asked(Skanthakumar *et al*.,2007). By extension, questions like, "what happens to dyes in solution?", "What happens to dyes and metal ions when they are present in the same solution?"These questions are valid . Huheey (1972) describes the forces involved in solute-solvent and solvent-solvent interaction as London dispersion forces which are relatively weak.

Part of the preliminaries of this work involved simulating effluent samples by mixing aqueous dyes with aqueous heavy metal mixtures (Section 3.3 of this work). This was based on the premise that effluents and waste waters contain dyes and heavy metals simultaneously (Saffaj *et al.,* (2004). ; Hestekin *et al.* (1998)). The goal was to establish working concentration ranges for the adsorption of the different adsorbate systems and to also observe whether the wavelengths of maximum absorption of the dyes were altered in the presence of the heavy metal solutions. This can be seen in Table 4.3

Table 4.3: Interaction of dyes with 0.005 – 0.008M concentrations of heavy metal solution

Test	Observtion	Inference
MB(aq) + $Pb(NO_3)_2$	Blue precipitate formed	Probably a complex
MB(aq)+$Cd(NO_3)_2.4H_2O$	Gelatinous blue precipitate formed	Probably a complex
MO(aq) + $Pb(NO_3)_2$	No precipitate formed	Clear mixture
MO(aq)+$Cd(NO_3)_2.4H_2O$	No precipitate formed	Clear mixture
MBMO(aq) + $Pb(NO_3)_2$	Gelatinous precipitate formed	Probably a complex due to presence of MB.
MBMO(aq)+$Cd(NO_3)_2.4H_2O$	Gelatinous precipitate formed	Probably a complex due presence of MB.

Precipitates were observed for MB and MBMO in the different heavy metal salt solutions for concentrations above 0.02M. Although no precipitate was observed for MO, the possibility of forming precipitate is not ruled out at higher concentration. The nature of the interaction forming the precipitates is not clear, but it may be attributed to MB serving as a ligand to form a dative bond with the heavy metal ions. It was also observed that the precipitates

dispersed on agitation and formed back after agitation was stopped. The amount of the precipitates also increased in the test tubes as samples were left overnight.

Absorbances of the dyes in the heavy metal mixtures was also taken to see if the wavelength of maximum absorption for the dyes will be affected. It was observed that for MB especially, there were fluctuations in the absorbance readings . Details of this aspect of the work are in Appendix II(a) and II(b). From these, the working concentration ranges for the dyes (i.e.MB, MO) were set at 10 to 50ppm, while a range of 0.005 to 0.01M was set for the heavy metal salts (i.e. $Pb(NO_3)_2$ and $Cd(NO_3)_2.4H_2O$). As a precaution, all the adsorbate systems used in this work were freshly prepared (i.e. at the point of use) to avoid any hint of precipitate forming.

4.2.1 Effect of Time on Adsorption of MB, MO and IG

Contact time and pH are two significant variables that affect dye uptake from solution (Ong *et al.*, 2010). Time is crucial to the success of most chemical processes. For Adsorption processes, the rates of adsorption or the time taken to reach equilibrium is usually monitored; where fast rates are usually desired. Fast adsorption rates are related to high degree of affinity between adsorbate and adsorbent via chemisorptions (Hammed *et al*., in Kathiresan *et al*., 2010).

The rate or kinetics of adsorption processes can give valuable information regarding the "order" of the process. It can help to predict if the process is Physisorption or Chemisorption, and it can also give insight to the sorption process (i.e whether film diffusion or particle diffusion is occuring)

(Horsfall Jnr and Spiff, 2005). For this work, The effect of time on the adsorption of individual dyes(MB, MO and IG) was monitored as part of the preliminaries of this work. Detailed kinetic studies was not embarked upon as this was not a major objective . Hence, the work was limited to the UMAC sample and only the aqueous individual dyes i.e MB, MO and IG and not their binary or tertiary mixtures.

To achieve this, two different experiments were performed seperately. (Details of procedure used are in section 3.5 of this work). The raw data from this aspect of the work can be seen in Appendix III.

Figure 4.1(a), shows the graph for effect of time on the amount of MB, MO and IG individually adsorbed onto 20mgUMAC. Figures 4.1(b), 4.1(c) and 4.3 show the graphs for the adsorption curve, adsorption trendline and bar graphs respectively. Figure 4.1(a) gives an idea of the sorption process, Figure 4.1(b) gives an idea of the movement of the dyes towards adsorption equilibrium states; Figure 4.1(c) can be employed for predictive studies, (extrapolation) while Figure 4.3 gives a general idea of the adsorption trend.

Figures 4.2(a), 4.2(b), 4.3(c) are similar to Figures 4.1(a), 4.1(b) and 4.1(c) respectively. They convey the same information. The difference between the Figures 4.1(a)-(c) series and Figures4.2(a)-(c) series is that the adsorption process of the former was based on the interaction of 20mg of UMAC with $10cm^3$ of 20ppm of the separate dyes and time of 5,10, 15, 20, 30, 45 and 60 minutes while the process of the latter was based on the interaction of 10mg of

UMAC with 10cm^3 of 10ppm of the separate dyes for 15, 30, 45 and 60 minutes respectively. The results from Figures 4.1(a) – (c) series seems to reveal more details compared to Figures 4.2(a) – (c) series results. This suggests that changes in dose of adsorbate, concentration of adsorbates and change in agitation periods amplify or influence results especially when rates are involved.

From Figure 4.3, it can be seen that for all the dyes, the amount adsorbed increased as the time increased. But comparatively, MO was adsorbed more than MB and IG, especially in the first 30minutes. The amount of MB then appreciably increases and becomes comparable with the amount of MO adsorbed at 60minutes. The amount adsorbed for IG was generally lower than the others. This may be attributed to individual qualities of the dyes like (a) Solubility/Mobility of the dyes (b) Film or Particle Diffusion (c) Size and Orientation of the dyes, and also the surface properties of the UMAC sample (Bansal and Goyal, 2005).

Figure 4.5 shows the cumulative average percentage of the amount of the dyes adsorbed onto UMAC. It is a summary of results in Figure 4.3 and Figure 4.4 . This gives a summary of the amount of the individual dyes adsorbed from the two rate experiments performed. The order is MO>MB>IG for both experiments.

Figures 4.1(a) and 4.2(a) are line graphs for the two separate rate experiments conducted showing the effect of time on the amount of individual dyes adsorbed. The graphs show similar trends but Figure 4.1(a) brings more

details. From Figure 4.1(a) two distinct stages (or steps) can be seen for all the dyes. The first stage is from 0 to 20min and the second stage is from 20min to 60min. the first stage can be attributed to film-diffusion of the dyes from the media to the AC surface while the second stage can be attributed to particle-diffusion within the UMAC sample (Horsfall Jnr and Spiff,2005).

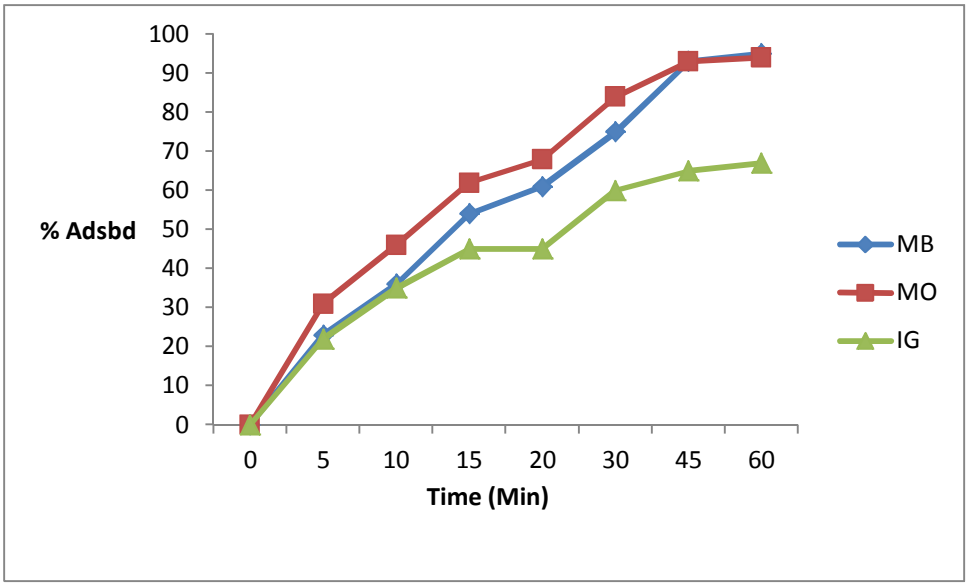


Figure 4.1(a) : Effect of Time on the amount of MB, MO and IG adsorbed onto 20mg UMAC

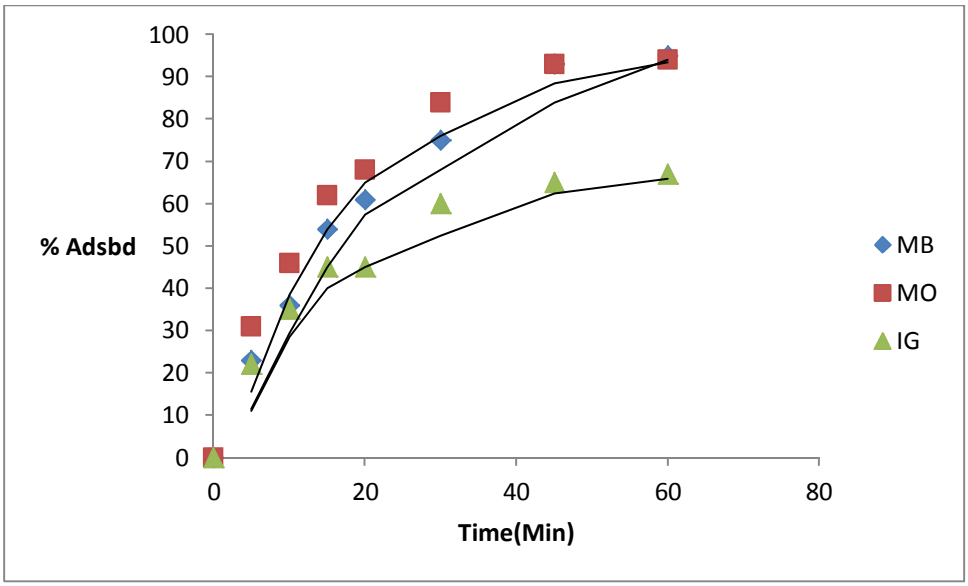


Figure 4.1(b) : Curve of Effect of Time on the amount of MB, MO and IG adsorbed onto 20mg UMAC

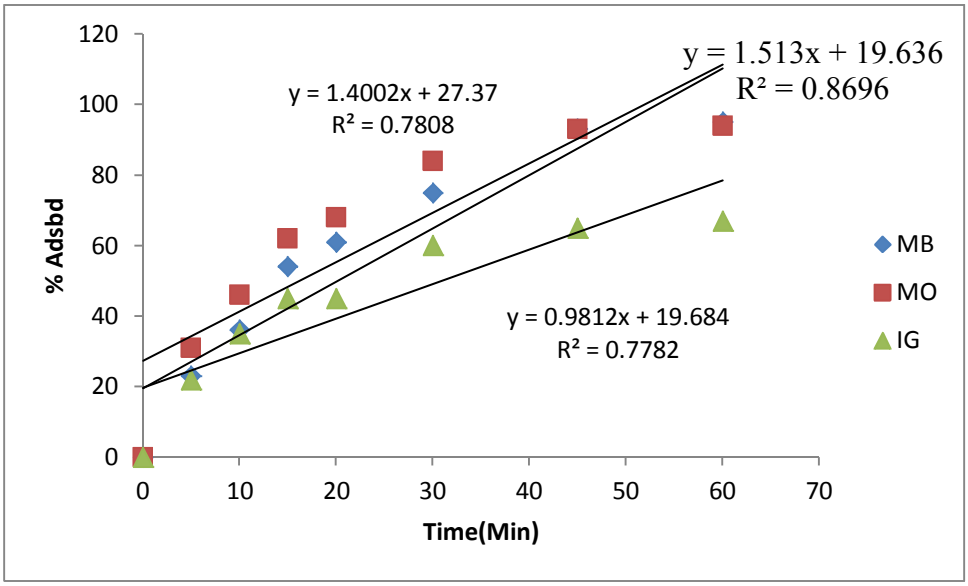


Figure 4.1(c): Trendline of effect of Time on amount of MB, MO and IG adsorbed onto 20mg UMAC

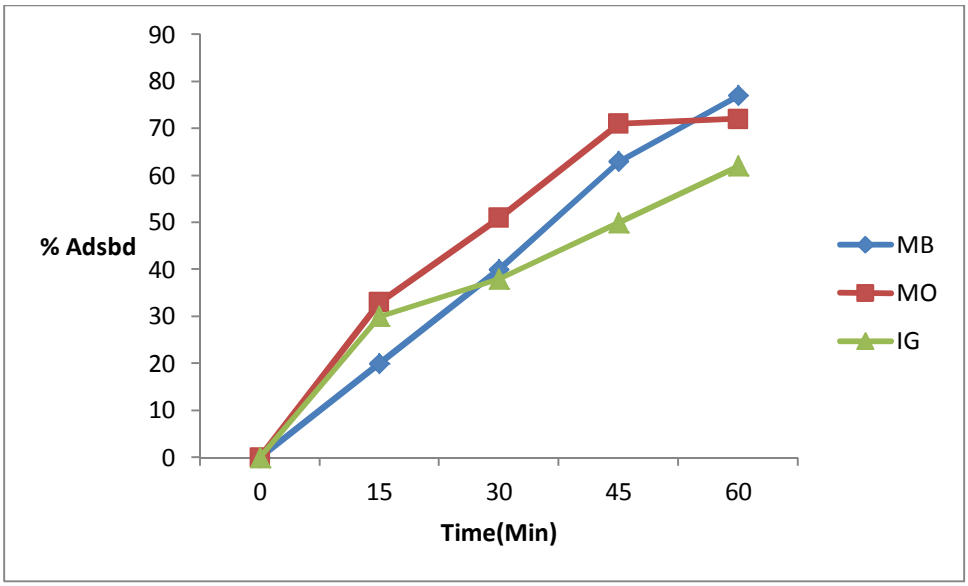


Figure 4.2(a): Effect of time on the amount of MB, MO and IG adsorbed onto 10mg UMAC

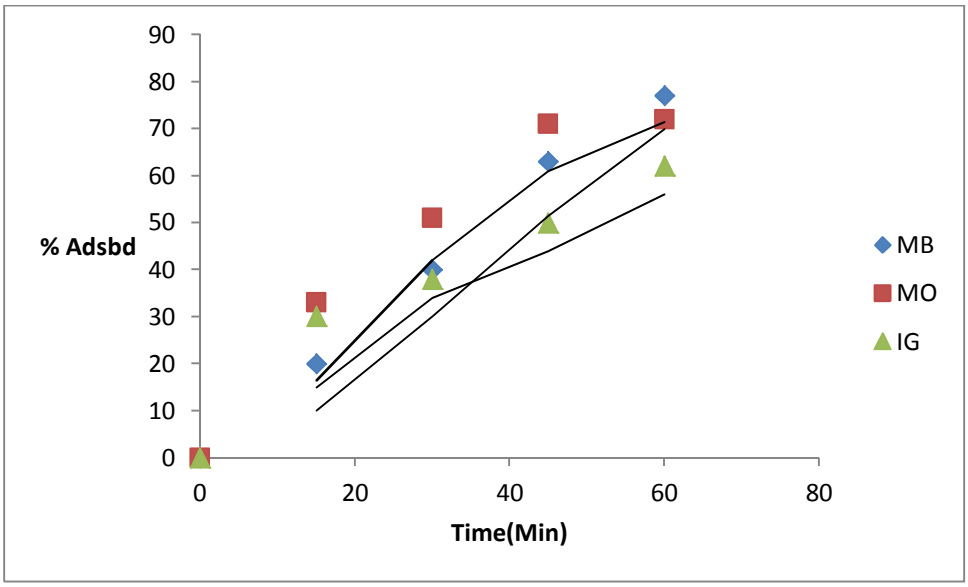


Figure 4.2(b) : Curve of MB, MB and IG adsorbed onto 10mg UMAC

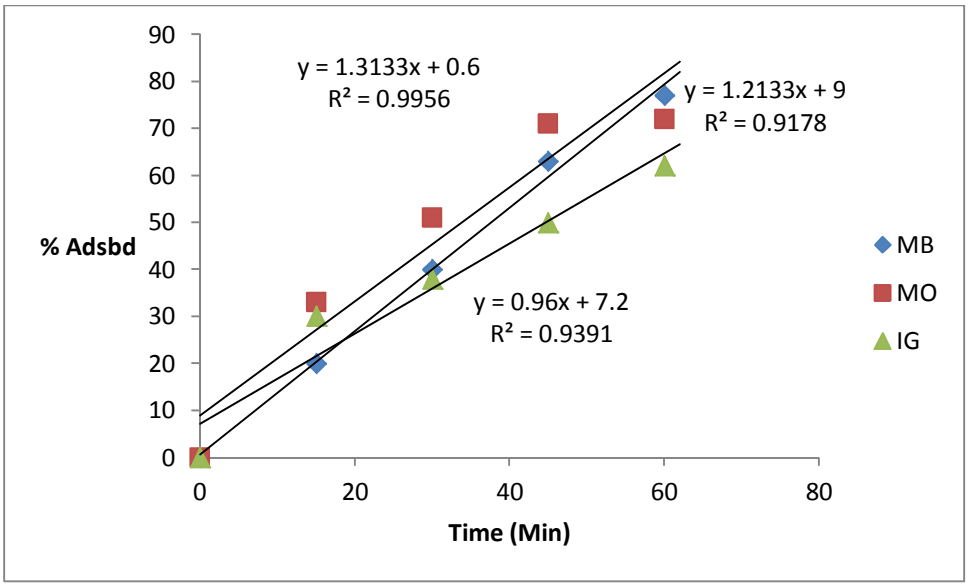


Figure 4.2(c) : Trendline of amount of MB, MO and IG adsorbed onto 10mg UMAC

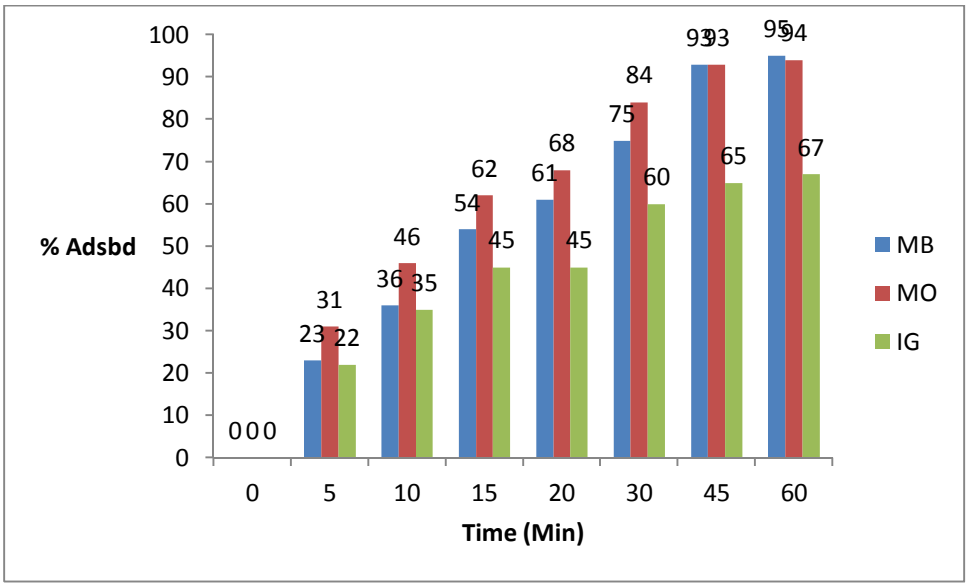


Figure 4.3: Bar graph of effect of Time on the amount of MB, MO and IG adsorbed onto 20mg of UMAC.

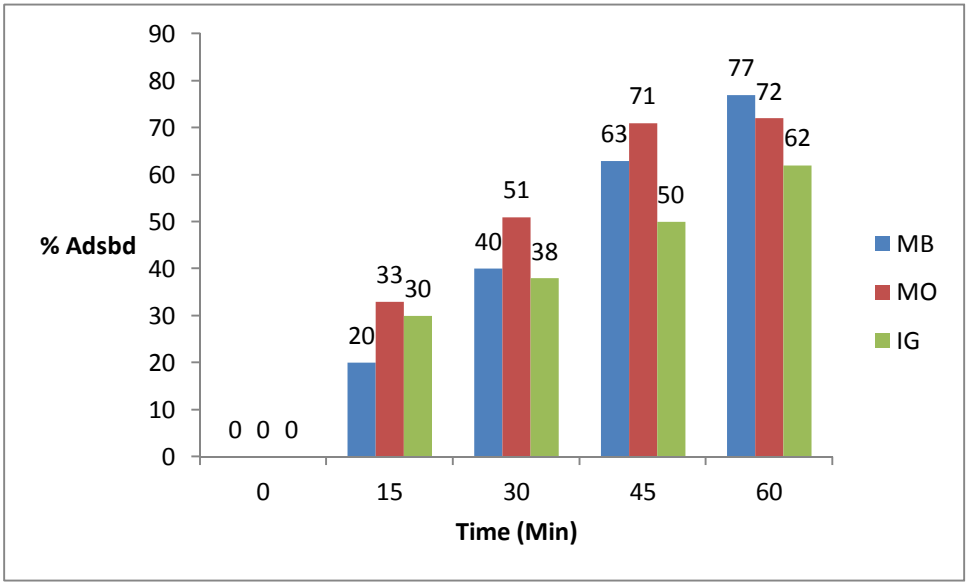


Figure 4.4: Bar graph of effect of Time on the amount of MB, MO and IG adsorbed onto 10mg UMAC

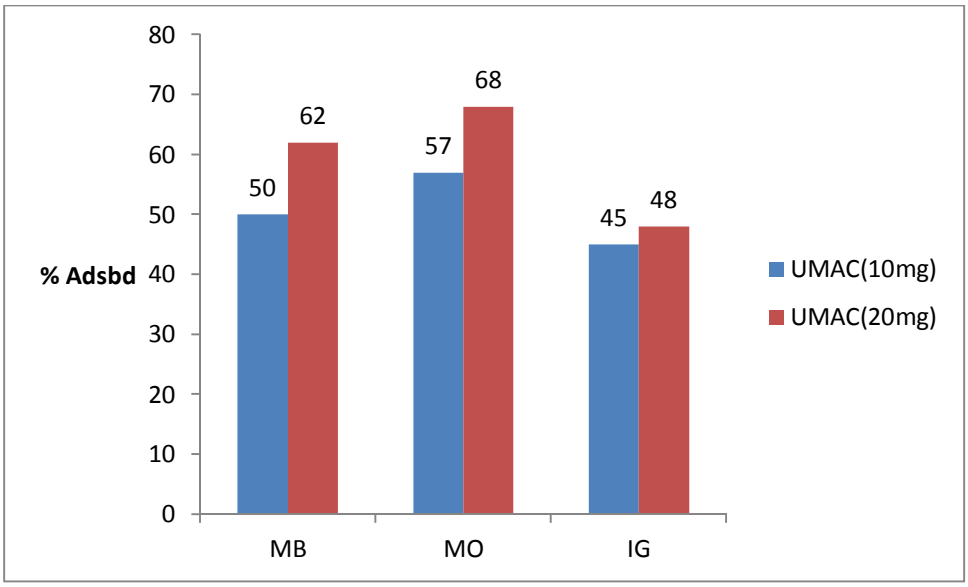


Figure 4.5: Cumulative average percentage of amount of MB, MO and IG adsorbed onto UMAC

Figure 4.6 is diffusivity plot of ln(1-*f*) against time(*t*), where *f* is the fractional attainment of equilibrium which is the ratio of the amount of adsorbates removed from solution after time(*t*) to that removed when sorption equilibrium is attained. The theory behind the plot above is that it can be used to explain whether the sorption process is film-diffusion controlled or particle-diffuson controlled (Ho *et al.,* 1995). If the ln(1-*f*) against *t* gives a linear relationship then adsorption is particle-diffusion controlled and the diffusivity of the adsorbate onto the surface is independent of the extent of sorption. However a non-linear plot indicates that the diffusivity of the ions onto the adsorbent surface is controlled by film diffusion(Vinod and Anirudhan, 2001). The plots for the dyes above are all linear with high R^2 values. This suggests that for all the dyes involved, the sorption process is particule-diffusion controlled.

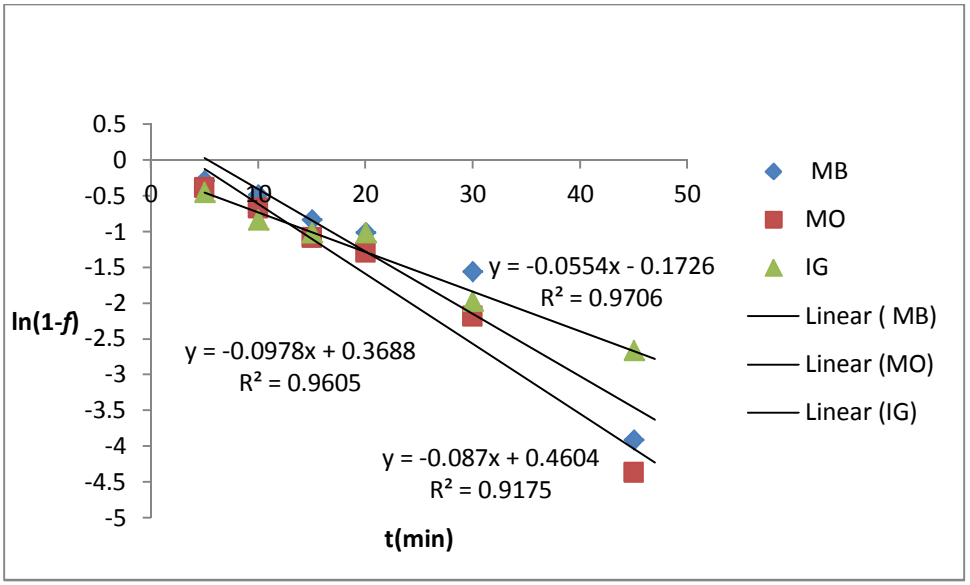


Fig 4.6: Plot of ln(1-*f*) versus time(t)

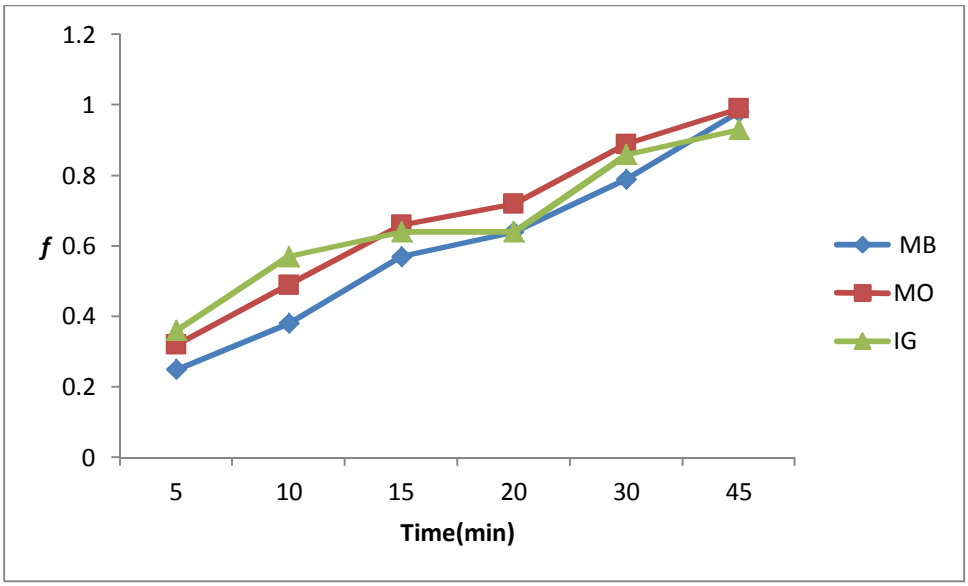


Figure 4.7: plot of *f* against Time (t)

Fig 4.7 is a plot of *f* against time(*t*). it shows an increase(though not linear) in the f values as contact time(t). This indicates that increasing the contact time may still lead to adsorption. Although, most of the dyes are predominantly taken up the first 30minutes. This is evident from Fig 4.1(b) which shows how the graphs for the dyes curve to attain equilibrium after 30 minutes.

The time taken for adsorbates to reach maximum adsorption is indicative of the type of adsorption occurring. When a long constsant time is needed to attain equilibrium, physisorption may be responsible. A relatively short contact time indicates chemisorptions (Ho *et al* in Horsfall Jnr and Spiff;2005). Hence , for the two rate experiments performed, chemsorption may be predominant even though physisorption may also be occurring alongside.

Figures 4.1(c) and 4.2(c) are the trendlines for the two rate experiments. The slope and R^2 values for MB are higher than the MO and IG. This suggests that MB is the most dependent on time for it's adsorption process onto UMAC.

4.2.2 Influence of size of dyes on adsorption rates.

For atoms, ions and simple molecules, it is easy to determine parameters like the atomic and ionic radii which give information about their size. For large molecules like dyes, this is not the case. The size or shape of a molecule to an extent will determine the film-diffusion in the medium and particle diffusion within the pore network of the adsorbent (Horsfall Jnr and Spiff, 2005). where the predominant pore size of the adsorbent corresponds with the size of an adsorbate molecule, the adsorption process will be easier and faster; provided all other factors remain constant. For the rate experiments conducted, the adsorbent was constant i.e. UMAC,with a pH of 7, the medium was constant i.e aqueous media, the pH of the aqueous dyes are relatively the same i.e. between(6.39 – 6.76), this leaves two factors which can influence the adsorption rates. They are (a) the functional groups of the dyes and (b) the size of the dyes. The functional groups of the dyes can be seen from their structures in Figures 2.1(a), 2.2(a) and 2.3. two of the dyes (MO and IG) have similar functional groups, which is the sulphonate group(SO_3^-). If the rates where determined by the functional groups then MO and IG should have been expected to have close rates, yet this is not the case. These narrows the adsorption rates to one factor i.e. the individual sizes of the dye molecules.

Considering the formular weights of the dyes

MB = 319.9 g/mol

MO = 327.3 g/mol and

IG = 466.3 g/mol.

MB with the smallest weight would have had better rates than MO and IG. The order of the rate of Adsorption on the grounds of their formular weights would have been MB > MO > IG, but the experimental data shows MO > MB > IG. However , on looking closely at the dye structures with regards their ring structures and orientation, MO has one ring(benzene) on both sides of the azo group giving a total of two rings. It's structure is symmetrical and linear compared to MB and IG structures. It will also be more flexible than the others.

MB on the other hand has three rings i.e. two benzene rings and one heterocyclic compound. The molecule is symmetrical around the heterocyclic ring. This will restrict the flexibility of the molecule. The molecule is more bulky or compact than MO .

IG has four rings. Two benzene rings and two heterocyclic rings which are bridged by a C=C bond and two supporting Hydrogen bonds. The molecule is symmetrical around the conjoined heterocyclics. This will make this molecule the bulkiest of the three and the least flexible or the most restricted in space. From this discussion a trend has evolved which shows a similarity between the dye molecules. The similarity is that :

i. all the molecules are symmetrical in a way.

ii. all the molecules have “a unique bridge.”

iii. all the molecules have one benzene ring on both sides of the bridge.

From the above observation and discussion, it can also be seen that the dye molecules also differ with respect to the number of cyclic compounds they are comprised of.

i. MO has two(2) cyclic compounds(i.e. 2 benzene rings),

ii. MB has three (3) cyclic compounds(2 benzene rings and 1 heterocyclic)

iii. IG has four (4) cyclic compounds (2 benzene rings and 2 heterocyclics).

. Based on the number of cyclic compounds, the order of the dyes sizes is represented as: MO < MB < IG

It can be said for the rate experiment in question, that there is an inverse relationship between the size of the dye molecules and their adsorption rates from aqueous media. The number of cyclic compounds determine the size and bulkiness of the molecules and this is strongly perceived to be the main reason for the differences in the adsorption rates of each dye onto UMAC. Where MO being the smallest has the greatest advantage while IG being the bulkiest has the least. The 3-D structures of each dye also buttresses these observations (see Figures 2.1(b), 2.2(d) and 2.4). although Fig 2.4 is the 3-D structure of indigo

and not indigo carmine(IG) it is still appropriate since IG is a derivative of indigo.

4.2.3 Possible inferences from rate experiments

From results and discussion of the experiments conducted to monitor the effect of time on the amount of MB, MO and IG adsorbed onto UMAC, the following inferences can be drawn

i. The order for the rate of the amount of the separate dyes adsorbed onto UMAC is: MO > MB > IG.

ii. The factor that is strongly responsible for the order in (i) above is strongly attributed to steric factors i.e. size (i.e. bulkiness and orientation) of the individual dye molecules.

iii. the sorption process of the dyes is predominantly Chemisorption

iv. the adsorption process is particle-diffusion controlled

v. MB is the most dependent on time to attain adsorption equilibrium.

4.2.4 Statistical Analysis of Rate Experiment Results

Statistical Analysis of the results was done using Sigma Plot 11.0 statistical package; where the % of the dyes adsorbed as contact time increased was used. These gave three different groups which were subjected to a One way anova test. This gave the mean and standard deviations for each group as follows:

$$MB = 62.143 \pm 27.65$$

$$MO = 68.286 \pm 23.963 \text{ and}$$

$$IG = 48.429 \pm 16.612.$$

Even though the standard deviations were quite large for each group, the difference in the mean values are not great enough to exclude the possibility that the difference is due to random sampling and that there is no statistically significant difference. The full table can be viewed in Appendix IV(a).

The mean values obtained from the test above were then subjected to a One-Sample t-test. The result showed that there is a statistically significant difference between the sampled population and the hypothesized population mean ($p=0.010$) at 95% confidence interval. The full table can be viewed in Appendix IV(b).

4.2.5 Effect of Chemical and Physical modification of AC sample.

Two simple methods were used to modify the AC sample obtained for this work which was high quality AC sample of food grade(see section 3.1 and Table 3.2). The two methods were meant to produce AC of opposing surface qualities. The use of concentrated nitric acid was the chemical used for chemical method while "long term low temperature" heating was used for physical modification. In chemical modification process the nitric is expected to oxidize the AC and increase the –COOH group on it's surface and produce an acidic surfaced product while physical modification was meant to reduce the acidic

functional groups by expelling them as CO_2 and then produce a basic surface sample. This were done by modifying existing methods (see sections 3.11 and 3.1.2). Below is a summary of the two products of the processes

Table 4.3(i): Percentage yield and pH of Modified AC samples

Sample	% yield	pH
CMAC	88	3.42
PMAC	82	4.66

Their yields were comparable while their pH were seen to be acidic. This shows that the physical modification process did not achieve it's intended purpose of producing a basic surface. An FT-IR scan for the samples was done using a SHIMADZU FTIR – 8400S Spectrophotometer. (See Appendices XIV, XV and XVI). The spectra showed that the UMAC and PMAC samples had similar number of peaks (nine peaks) with similar assignments. CMAC had seven peaks. This suggests that the chemical modification process may have removed some species or functional groups from the original product. While the physical modification may not have added or removed any species or functional group from the original material, the degassing may have adequately removed trapped gases within it's matrix and also modify the electronic arrangement of the system such that more active sites were formed (Ishizaki *et al*., 1983)

4.3.0 Adsorption Studies Results.

Adsorption Studies were conducted for three (3) broad categories of Simulated Effluent Systems(adsorbate systems) which are

i. Single Dye Systems

ii. Binary Dye Systems and

iii. Tertiary Dye Systems

Three (3) Real textile effluent samples (TXT 1, TXT 2 and TXT 3), using three (3) different Activated Carbon matrices (UMAC, CMAC and PMAC) as adsorbents. Procedure for adsorption processes can be seen in article 3.4.

Results from the studies was presented using graphs and figures like bar graphs, adsorption isotherms, Freundlich Isotherms, Langmuir Isotherms and Temkin Isotherms while attempt was made to discuss the results using literature and also drawing appropriate conclusions

4.3.1 Adsorption Studies for Single Dye Systems

The single dye systems were aqueous MB, MO and IG only ; MB, MO and IG separately in different concentrations of $Pb(NO_3)_2$ and $Cd(NO_3)_2$. 4H2O respectively and MB, MO and IG in different concentrations of aqueous $Pb(NO_3)_2$ and $Cd(NO_3)_2$. $4H_2O$ mixture. The experiments done in $Pb(NO_3)_2$ and $Cd(NO_3)_2$. $4H_2O$ aqueous solutions and their mixtures was to observe if the presence of these heavy metal salts will decrease or increase the amount of the individual dyes from solution.

Below are some bar graphs showing the % of each of the separate dyes adsorbed onto the different AC matrices i.e UMAC, CMAC and PMAC. It shows the efficiency or performance of the different AC matrices and which dye will be adsorbed more from the different aqueous heavy metal environment. Pb^{2+} and Cd^{2+} are either expected to adsorb onto the AC surfaces and block active sites for adsorption of the dyes or affect adsorption by their charge contributions hence, influencing electrostatic attraction or rejection of the dyes onto the surface (Saffaj *et al*., 2004). They can also form complexes or chelates with the dyes in which case the whole adsorption process will be altered (Visa *et al.,* 2010). The ionic radii for Pb^{2+} and Cd^{2+} in solution are 1.20 Å and 0.97 Å respectively. Cd^{2+} with a smaller ionic radius will have more access to smaller pores than Pb^{2+} (Horsfall Jnr and Spiff, 2005). Although, for this case it may not be so since the Cd^{2+} is coming from a hydrated salt i.e. $Cd(NO_3)_2.4H_2O$. the water molecules may increase the bulkiness of the ion, hence reducing it's mobility and access to small pores.

4.3.2 Methylene blue adsorption from heavy metal environment

Figures 4.8(a), 4.8(b), 4.9(a), 4.9(b), 4.10(a) and 4.10(b) are bar graphs representing the percentage MB adsorbed from $Pb(NO_3)_2$, $Cd(NO_3)_2.4H_2O$ and [$Pb(NO_3)_2$ + $Cd(NO_3)_2.4H_2O$] mixture and their Cumulative % average graphs. Generally, no particular trend can be seen for all the graphs. The % values of MB adsorbed onto the different matrices from the different heavy metal environments fluctuates for all the graphs. The summary graphs also do not give one particular trend. These irregularities is strongly attributed to electronic

repulsions between the dye, the heavy metals and the acidic pH surface of the AC surfaces.

MB is a cationic dye with a positive charge, in a positively charged heavy metal environment. this will lead to repulsions since like charges are involved. The pH of CMAC and PMAC are 3.42 and 4.66 which is why CMAC had the least results; although PMAC's surface is acidic the modification process may have canceled it's surface pH effect by creating more active sites. Despite the irregular patterns, all the AC matrices still showed good adsorption with the adsorption range being 78% - 91%. Results from the summary graphs were further subjected to analysis.

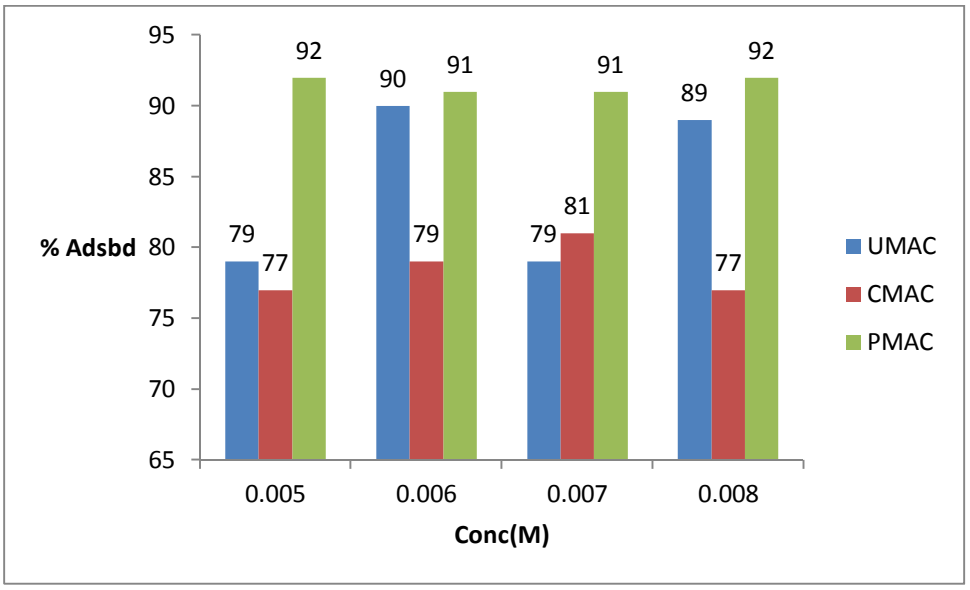


Figure 4.8(a): Percentage of MB adsorbed from aqueous $Pb(NO_3)_2$

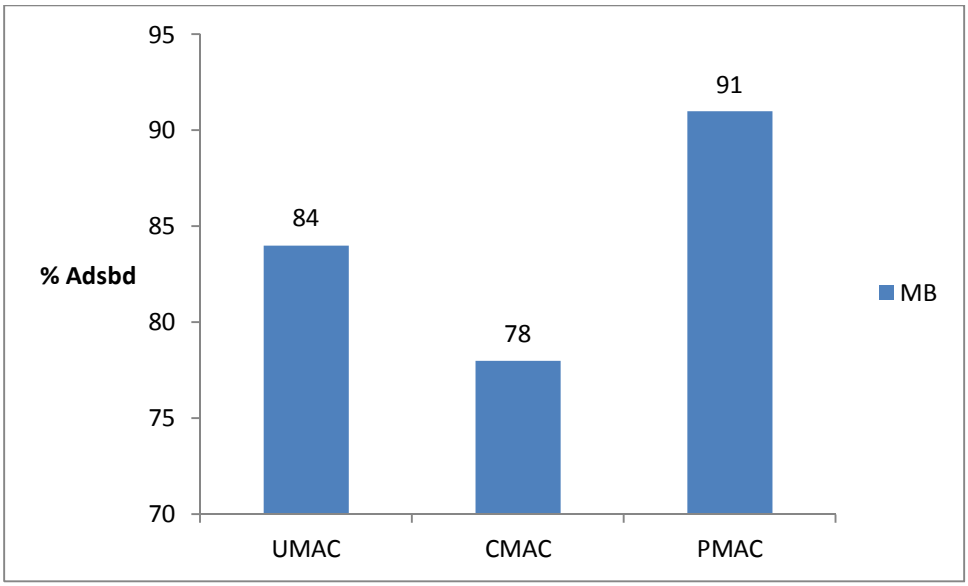


Figure 4.8(b): Cumulative percentage average of MB adsorbed from $Pb(NO_3)_2$

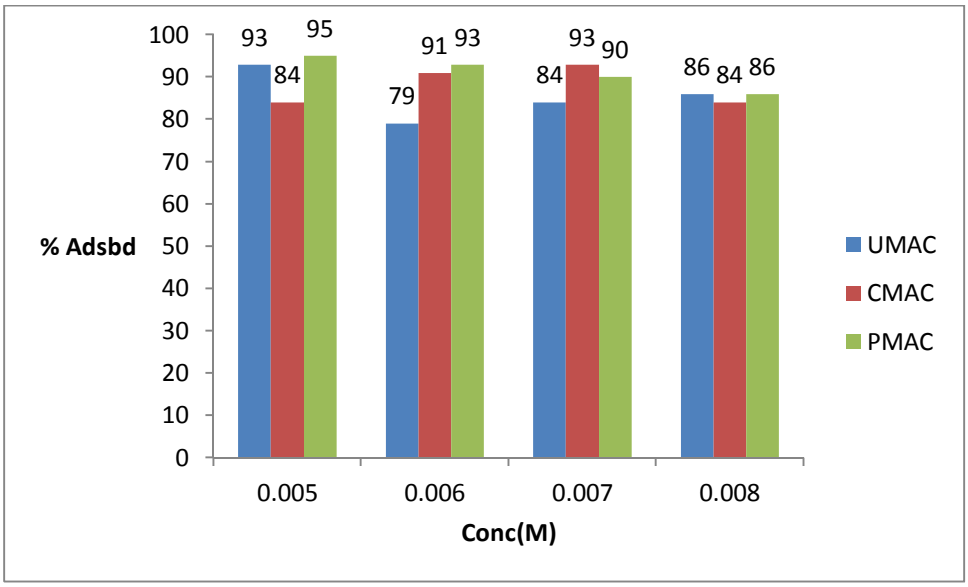


Figure 4.9(a): Percentage of MB adsorbed from aqueous $Cd(NO_3)_2.4H_2O$

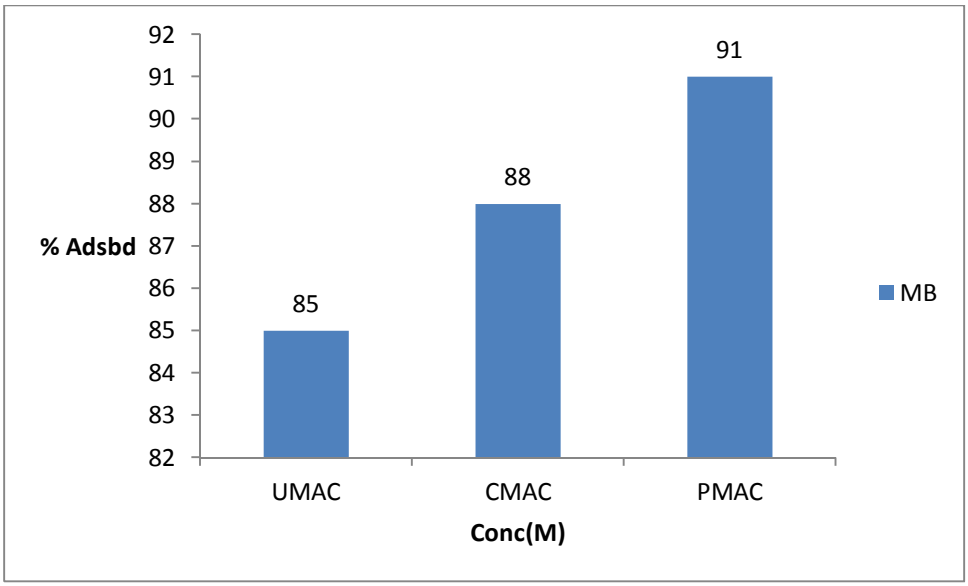


Figure 4.9(b): Cumulative Percentage average of MB adsorbed from aqueous $Cd(NO_3)_2.4H_2O$

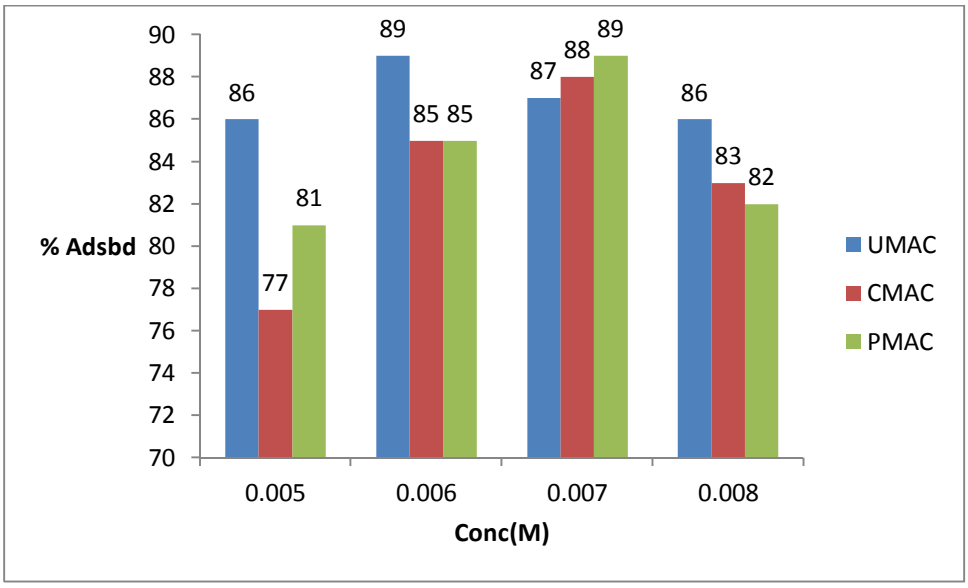


Figure 4.10(a): Percentage of MB adsorbed from aqueous $Pb(NO_3)_2$ and $Cd(NO_3)_2.4H_2O$ mixture

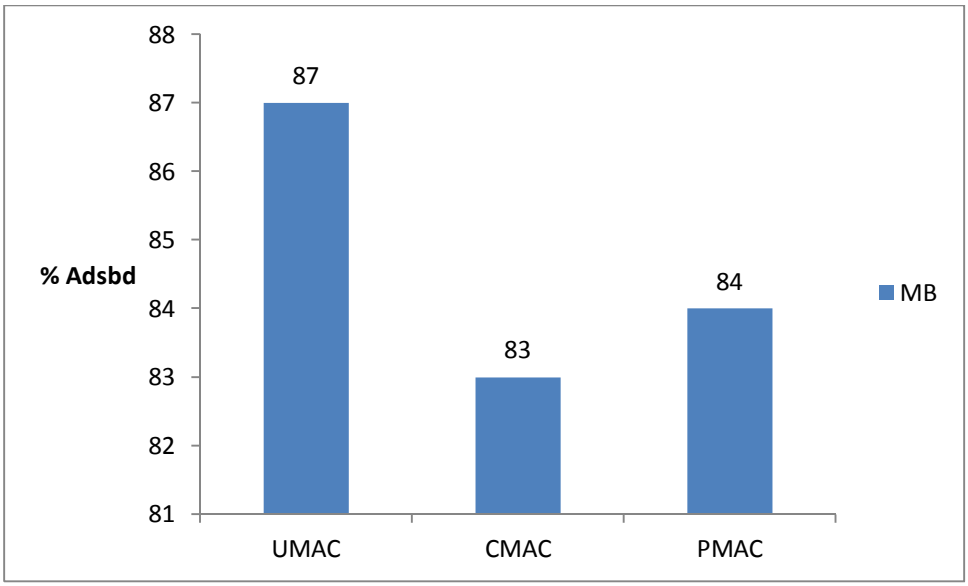


Figure 4.10(b): Cumulative Percentage average of MB adsorbed from aqueous $Pb(NO_3)_2$ and $Cd(NO_3)_2.4H_2O$ mixture

Table 4.4 Average percentage MB adsorption from summary graphs

	UMAC	CMAC	PMAC	Average
Pb nitrate	84	78	91	84
Cd nitrate	85	88	91	88
Pb/Cd nitrate	87	83	84	84
Average	85	83	87	

Table 4.4 shows the average percentage MB adsorbed onto the different AC matrices and the different heavy metal environments. This reveals the efficiency of the different AC matrices and also the heavy metal environment which affects MB adsorption the least. From the horizontal average row which shows efficiency of MB the order is

PMAC > UMAC > CMAC;

while for the average vertical column, it reveals the percentage MB adsorbed from the different heavy metal environment. the order is

Cd nitrate > Pb nitrate = Pb/Cd nitrate.

4.3.3 Methyl orange adsorption from heavy metal environment

Figures 4.11(a), 4.11(b), 4.12(a), 4.12(b), 4.13(a) and 4.13(b) are bar graphs representing the % MO adsorbed from $Pb(NO_3)_2$, $Cd(NO_3)_2.4H_2O$ and [$Pb(NO_3)_2$ + $Cd(NO_3)_2.4H_2O$] mixture and their Cumulative percentage average graphs.

Unlike the MB series graphs, the MO series is not as irregular. MO in acid solution carries a positive charge. From preliminary work conducted, the pH of aqueous MO in heavy metal environment is between 5-6. This suggests that it will carry a positive charge (see Figure 2.2(b)). The scenario recorded for MB would have been expected to be replayed. Yet it is not totally the case. The reason for this is strongly attributed to the same factor which favoured it in the rate

experiments. The range of the percentage MO (87-95%) adsorbed is higher than MB (78-91%).

This suggests that the pore-size network of the different AC samples is of comparable size with MO. Hence, it is the size factor and not the charge factor that is mainly responsible for MO's adsorption process results. Results for CMAC are generally lower compared to others. This can be attributed to it's low surface pH which tends to play down the benefit it has based on it's size.

Further analysis was also conducted on the cumulative % summary figures.

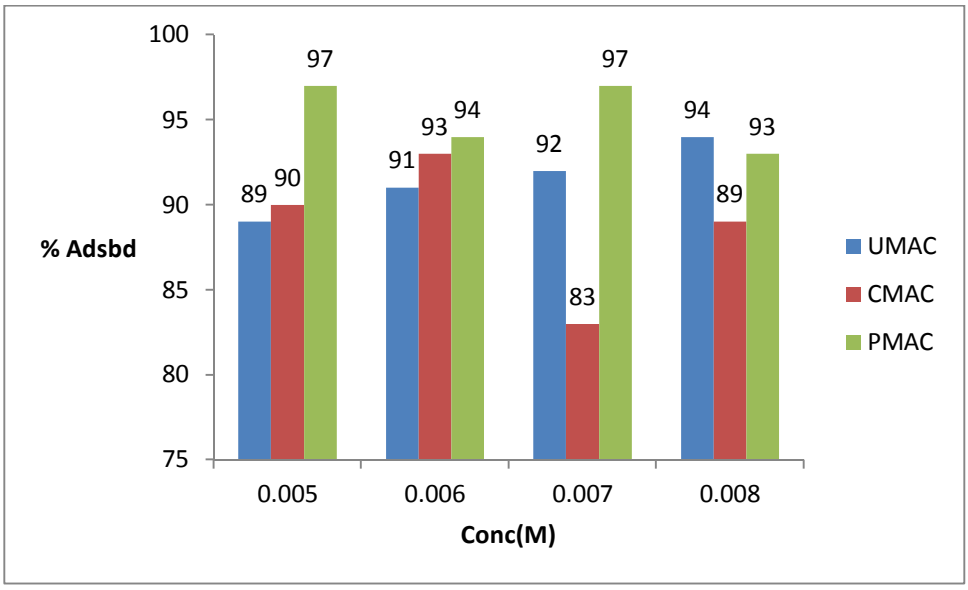


Figure 4.11(a): Percentage of MO adsorbed from aqueous $Pb(NO_3)_2$

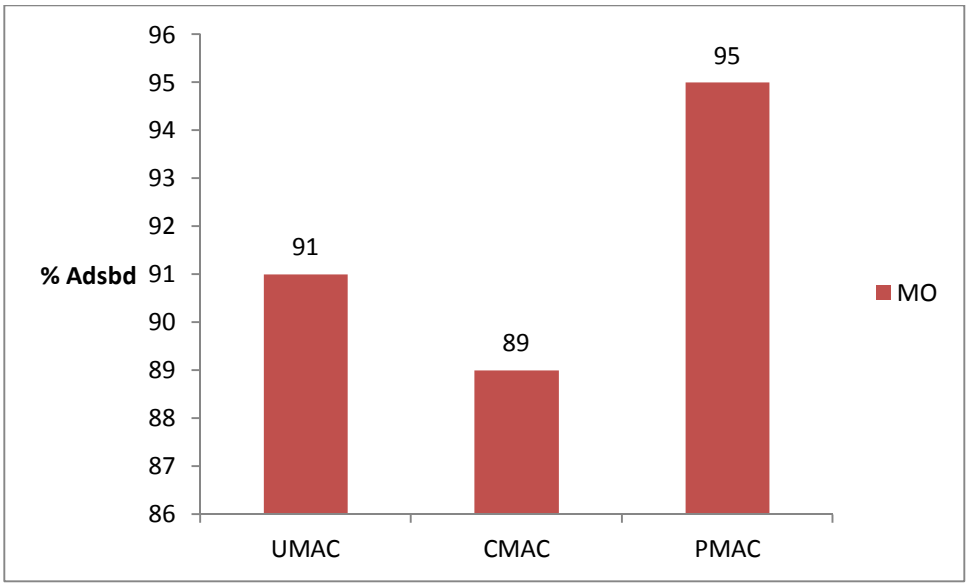


Figure 4.11(b): Cumulative percentage average of MO adsorbed from aqueous $Pb(NO_3)_2$

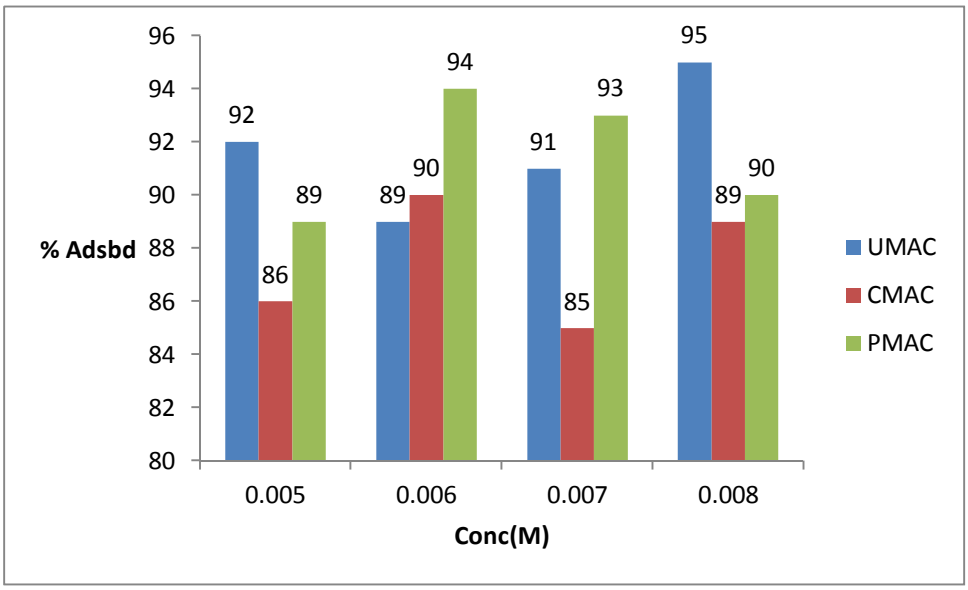


Figure 4.12(a): Percentage of MO adsorbed from $Cd(NO_3)_2.4H_2O$

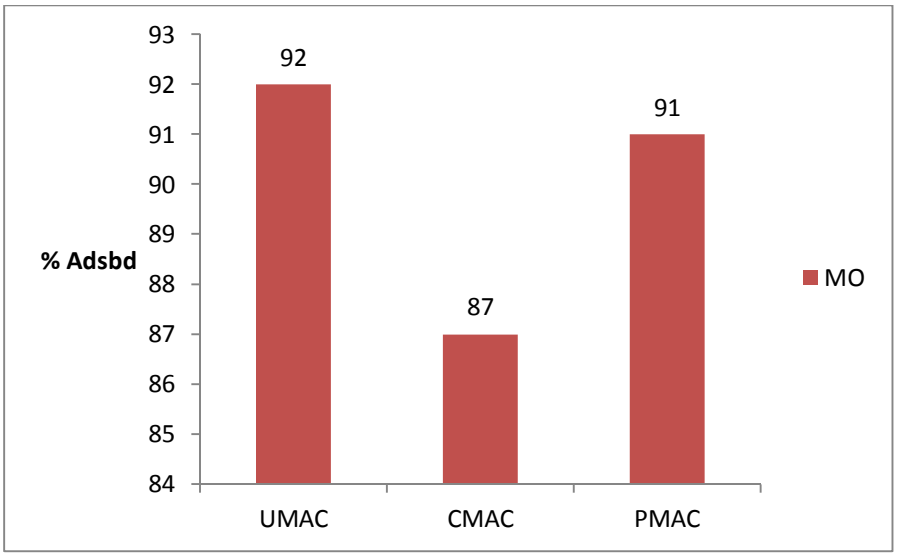


Figure 4.12(b): Cumulative percentage average of MO adsorbed from aqueous $Cd(NO_3)_2.4H_2O$

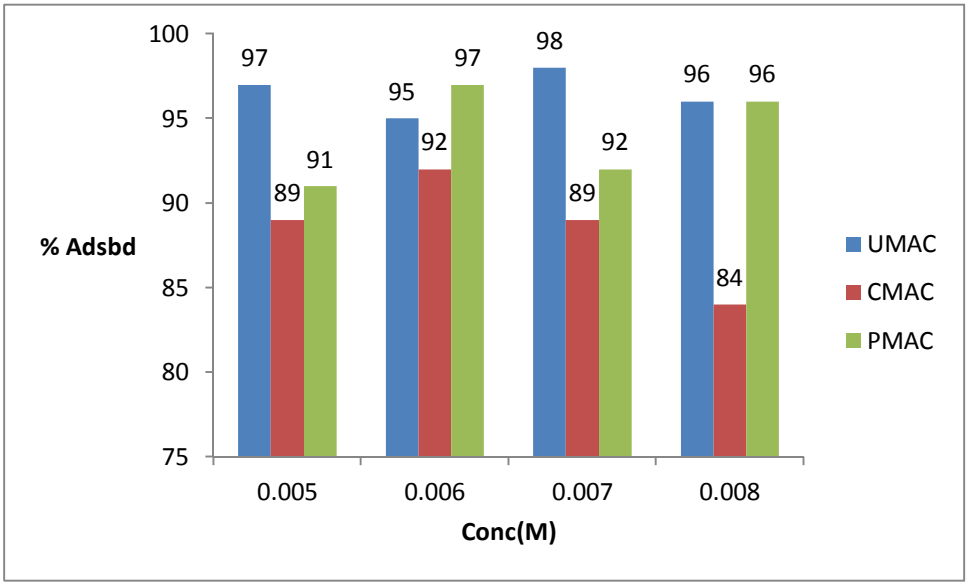


Figure 4.13(a): Percentage of MO adsorbed from aqueous $Pb(NO_3)_2$ and $Cd(NO_3)_2.4H_2O$ mixture

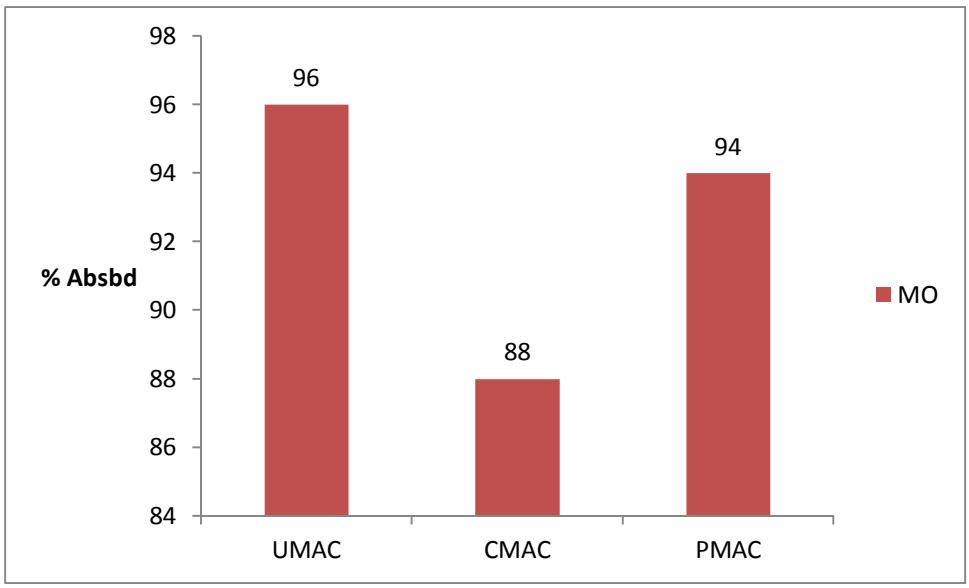


Figure 4.13(b): Cumulative percentage average of MO adsorbed from aqueous $Pb(NO_3)_2$ and $Cd(NO_3)_2.4H_2O$ mixture

Table 4.5 Average percentage MO adsorption from summary graphs.

	UMAC	CMAC	PMAC	Average
Pb nitrate	91	89	95	92
Cd nitrate	92	87	91	90
Pb/Cd nitrate	96	88	94	93
Average	93	88	93	

Like the similar table above, the horizontal average row gives the average for the different AC samples while the vertical average column is the averages for the heavy metal environment. The order for the AC samples is:

PMAC = UMAC > CMAC

While for the heavy metal environment the order will be:

Pb/Cd nitrate > Pb nitrate > Cd nitrate.

4.3.4 Indigo carmine adsorption from heavy metal environment

Figures 4.14(a), 4.14(b), 4.15(a), 4.15(b), 4.16(a) and 4.16(b) are bar graphs representing the % IG adsorbed from $Pb(NO_3)_2$, $Cd(NO_3)_2.4H_2O$ and [$Pb(NO_3)_2$ + $Cd(NO_3)_2.4H_2O$] mixture and their Cumulative percentage average graphs.

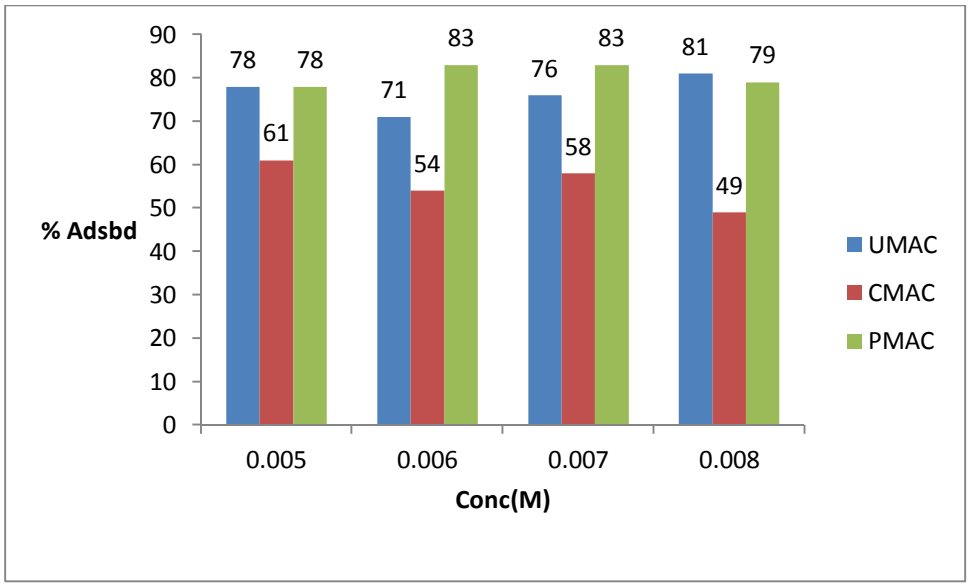


Figure 4.14(a): Percentage of IG adsorbed from aqueous $Pb(NO_3)_2$

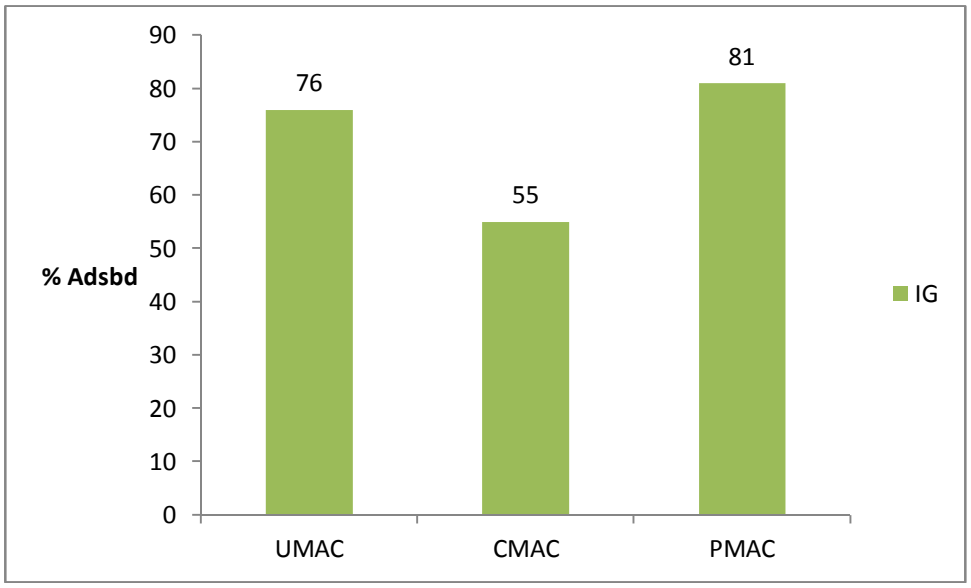


Figure 4.14(b): Cumulative percentage average of IG adsorbed from aqueous $Pb(NO_3)_2$

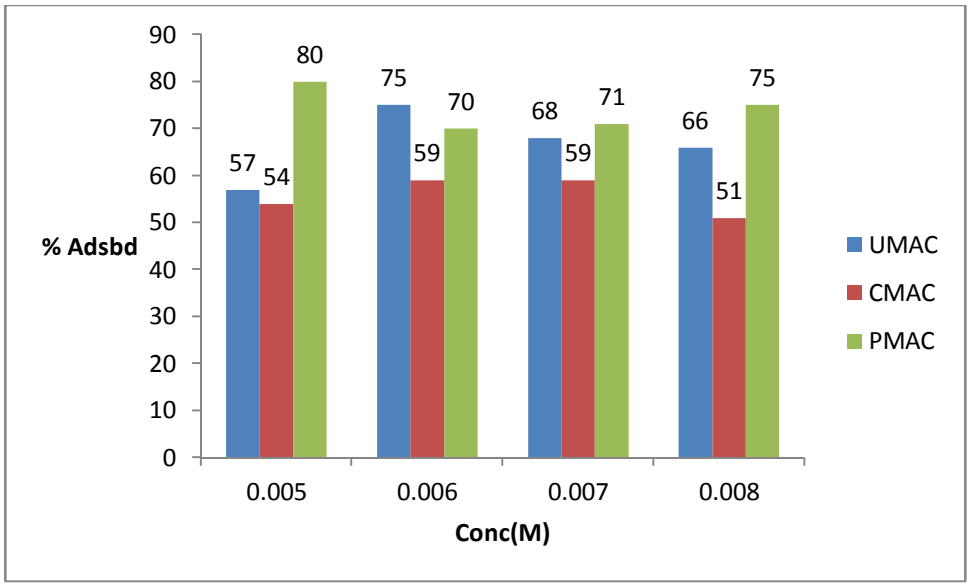


Figure 4.15(a): Percentage of IG adsorbed from aqueous $Cd(NO_3)_2.4H_2O$

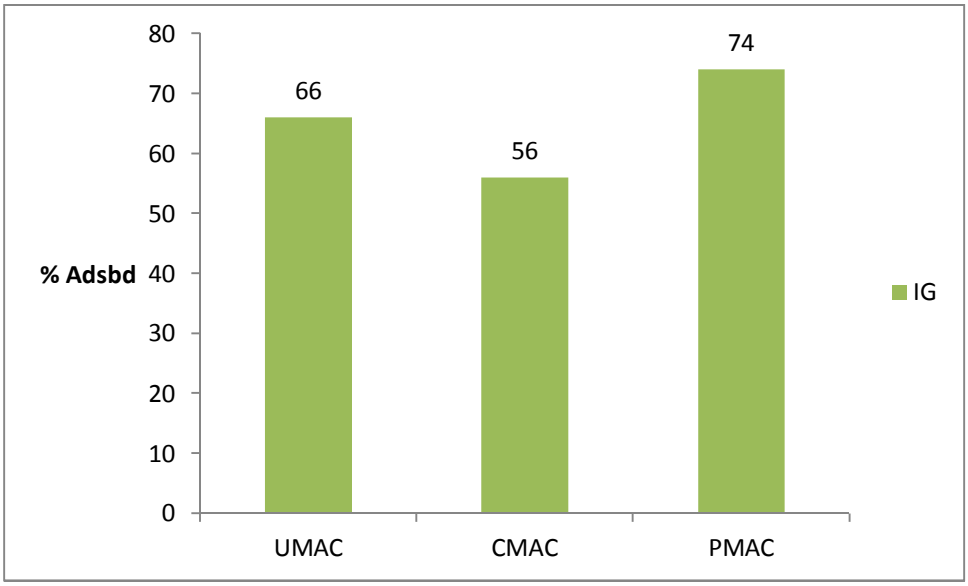


Figure 4.15(b): Cumulative percentage average of IG adsorbed from aqueous $Cd(NO_3)_2.4H_2O$ solution

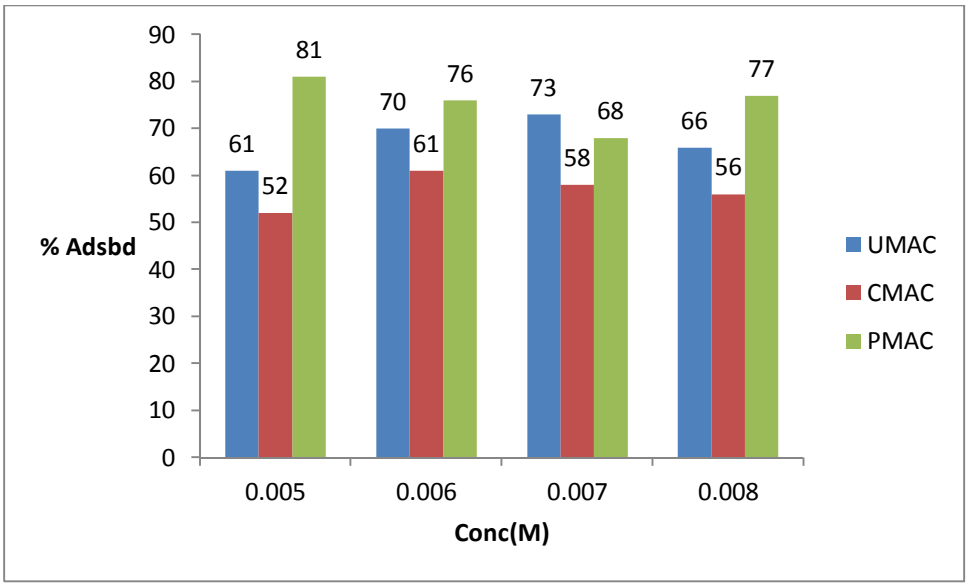


Figure 4.16(a): Percentage of IG adsorbed from aqueous $Pb(NO_3)_2$ and $Cd(NO_3)_2.4H_2O$ mixture

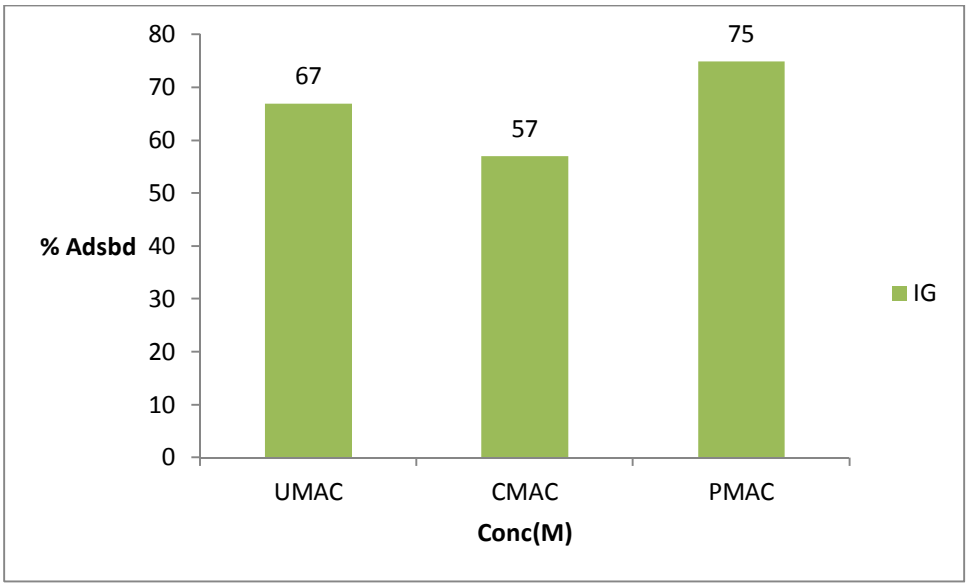


Figure 4.16(b): Cumulative percentage average of IG adsorbed from aqueous $Pb(NO_3)_2$ and $Cd(NO_3)_2.4H_2O$ mixture

The IG series compared to the other two series gives regular adsorption trends. From the summary graphs, the order for the % IG adsorbed from the different heavy metal environments can generally be given as below

PMAC > UMAC > CMAC

The range for the % IG (67 – 81%) adsorbed from the different heavy metal environments is lower than the MB (78 – 91%) and MO (87 – 95%) series. This is attributed to steric factors. i.e the large or bulky size is not favoured by the pore-sizes of the different AC samples. The relatively high amount of IG adsorbed onto the PMAC samples is as a result of well developed pore.sizes and good porous network which was developed on modification. It also suggests that new active sites where formed on modification.

The amount of IG adsorbed from the heavy metal environments was low compared to UMAC and PMAC. This was also the case for the other series. For CMAC, it's acidic surface and the bulky size of the IG molecules are perceived to be the reasons for the generally low IG adsorption onto the different AC samples. Also, the charge contributions of the heavy metal ions will also give rise to electronic repulsions.

Table 4.6: Average percentage IG adsorption from summary graphs.

	UMAC	CMAC	PMAC	Average
Pb nitrate	76	55	81	71
Cd nitrate	66	56	74	65
Cd/Pb nitrate	67	57	75	66
Average	70	56	75	

From the table above, the order for the amount IG adsorbed onto the different AC samples is: PMAC > UMAC > CMAC

While that for the heavy metal environment is

Pb nitrate > Cd/Pb nitrate > Cd nitrate.

4.3.5 Summary of results of adsorption of single dyes in heavy metal environment

The following summaries can be made from the adsorption results of the separate single dyes from heavy metal environment.

1. For the MB series the results did not follow any definite pattern. This was attributed mainly to electronic repulsions between MB(a cationic dye), and the

heavy metal ions. CMAC samples had the least result due to it's acidic surface.

2. For the MO series the good results is attributed mainly to it's small size; even though it is positively charged in solution. It also shows that the AC samples seem to have pore-size and porous network structure which favours MO adsorption.
3. The results for the IG series are the most regular but the least adsorbed when compared to the MB and MO series. This is strongly attributed to the IG molecular size which is the bulkiest of the dyes used (Karafnil *et al*., 1999; Newcomb, 1999).
4. The PMAC sample probably has the best pore size distribution and porous network structure compared to UMAC and CMAC.

4.4.0 Adsorption of Binary dye mixtures in heavy metal environment

The dye systems involved in this aspect of the work are

MBMO in $Pb(NO_3)_2$,

MBMO in $Cd(NO_3)_2.4H_2O$,

MBMO in [$Pb(NO_3)_2$ + $Cd(NO_3)_2.4H_2O$] mixture.

MOIG in $Pb(NO_3)_2$,

MOIG in $Cd(NO_3)_2.4H_2O$,

MOIG in [$Pb(NO_3)_2$ + $Cd(NO_3)_2.4H_2O$] mixture.

4.4.1 MBMO Adsorption in Heavy Metal Environment.

The results were represented using bar graphs which showed the percentage of each component adsorbed onto the different AC samples (i.e. UMAC, CMAC and PMAC), and 0.005, 0.006, 0.007 and 0.008M of the heavy metal salt solutions (i.e. $Pb(NO_3)_2$, $Cd(NO_3)_2.4H_2O$ and their mixture) provided the heavy metal environment.

4.4.1.1 MBMO adsorption from aqueous $Pb(NO_3)_2$ and $Cd(NO_3)_2.4H_2O$ mixture

Figures 4.17(a) – (c) represents bar graphs showing the percentages of the components of the MBMO mixture adsorbed from aqueous $Pb(NO_3)_2$ and $Cd(NO_3)_2.4H_2O$ mixture environment onto UMAC, CMAC and PMAC respectively; while Figure 4.17(d) is the summary graph.

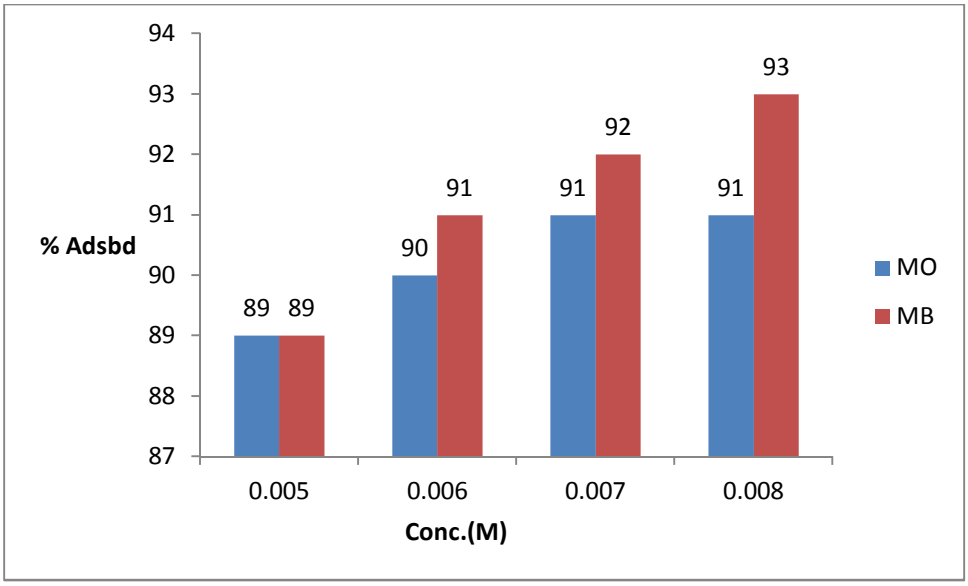


Figure 4.17(a): Percentage of components of MBMO adsorbed from aqueous $Pb(NO_3)_2$ and $Cd(NO_3)_2.4H_2O$ mixture onto UMAC

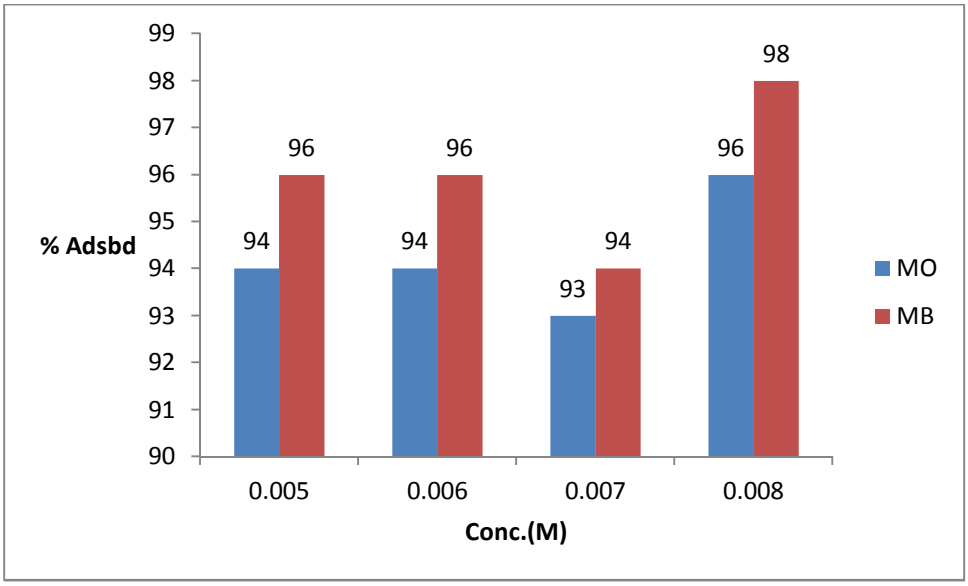


Figure 4.17(b): Percentage of components of MBMO adsorbed from aqueous $Pb(NO_3)_2$ and $Cd(NO_3)_2.4H_2O$ mixture onto CMAC

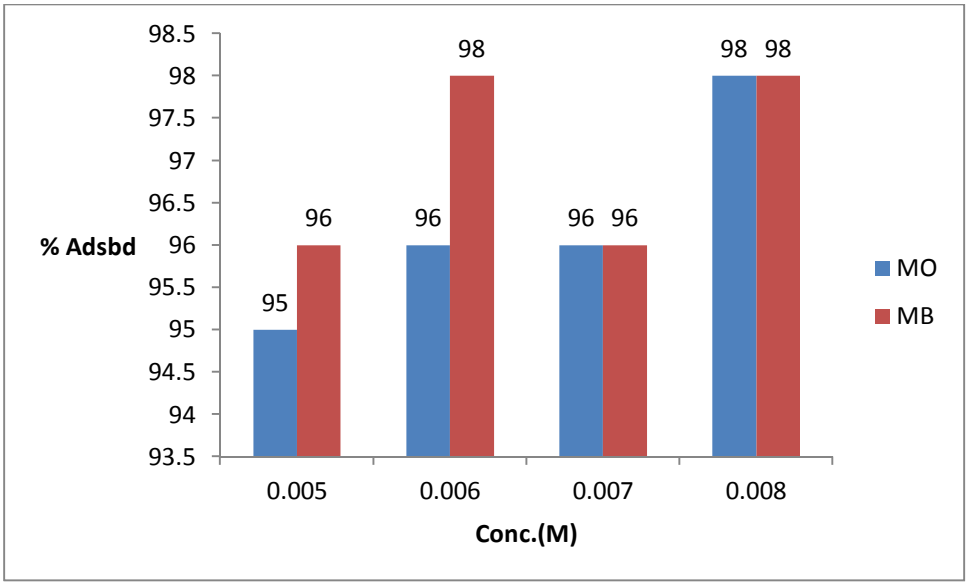


Figure 4.17(c): Percentage of components of MBMO adsorbed from aqueous $Pb(NO_3)_2$ and $Cd(NO_3)_2.4H_2O$ mixture onto PMAC

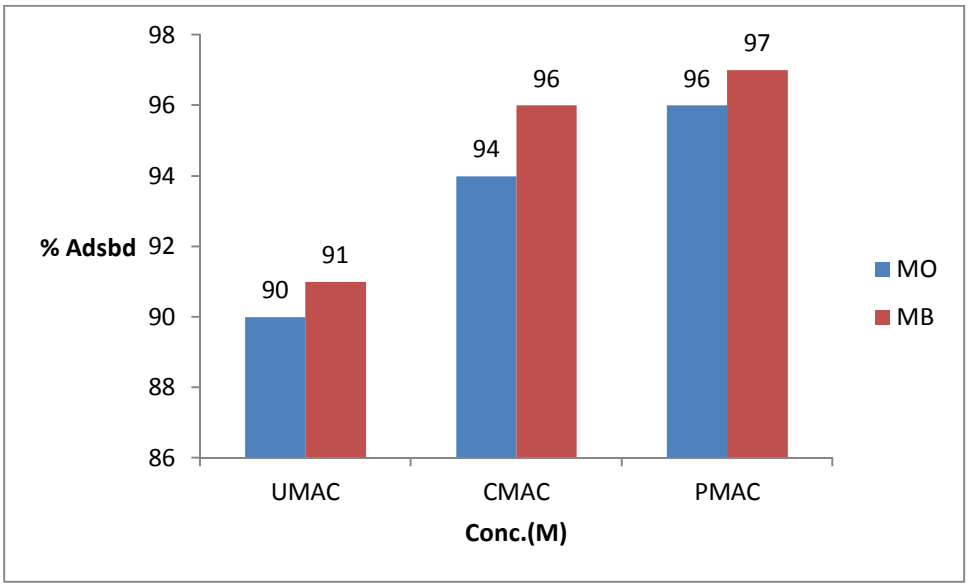


Figure 4.17(d): Cumulative percentage average of components of MBMO adsorbed from aqueous $Pb(NO_3)_2$ and $Cd(NO_3)_2.4H_2O$ mixture

The percentages of the components adsorbed is high for all the systems. The adsorption range considering all the systems is between 89 – 98%. For all the graphs, the results show that MB was preferentially adsorbed than MO except in Figure 4.17(c) where there were some ties in results. This seems to be contrary considering results from single dye systems where MO is adsorbed more compared to MB and IG. From their structures,(see Figures 2.1(a) and 2.2(b)) they are both positively charged on a N – atom; this means there will be electronic repulsions existing between them.

Because of the heavy metal environment (i.e. Pb^{2+} and Cd^{2+}) there will also be repulsions between the heavy metals and the dyes. The heavy metals will

also be repelling each other and also be acting as adsorbate ions competing for available active sites. Hence there is intra-dye repulsions between MB and MO; intra-heavy metal repulsion between Pb^{2+} and Cd^{2+} ; and inter-dye and heavy metal repulsions while all of the dyes and heavy metals are also acting as adsorbate species for the AC surfaces. This makes the competition in this system very stiff even though monitoring the adsorption of the heavy metals was not part of the scope of this work.

The observation for MB being preferentially adsorbed relative to MO can be explained using the "time" and "concentration" factor. From the trendline graphs in Figures 4.1(c) and 4.2(c), the linear equations for MB had the steepest slope compared to MO and IG, which suggests that MB adsorption is the most dependent on time; where the amount MB adsorbed increases steadily and even overtakes MO at the equilibrium time of 60 minutes. This can be seen by comparing results in Figures 4.3 and 4.4. In Figure 4.3, 20mg of UMAC was interacted with $10cm^3$ of 20ppm of the dyes separately, the amount adsorbed were 95% for MB and 94% for MO. In Figure 4.4, 10mg of UMAC was interacted with $10cm^3$ of the separate dyes. Results shows that the % MB adsorbed at 60 minutes interaction time was 77% while that for MO was 72% which gave a difference of 5%.compared to the 1% difference seen in Figure 4.3 results. This shows that at contact time of 60 minutes, the amount of MB adsorbed actually overtakes MO even though at initial periods, MO is adsorbed more. It also shows that the Set-Up of the adsorption process i.e. adsorbate concentrations, adsorbate dose, volume

of adsorbate solution are crucial in showing differences that may be happening in an adsorption process.

The sharpness and contrast of differences in results is revealed at the lower concentration used; where it is better to work at dilute concentrations for this particular system. For other systems it may not be the case. It can be seen from the results that what was applicable in the single dye system was extended in the binary system. From the summary graph on Figure 4.17(d), the order of the amounts of the components adsorbed onto the different AC samples was:

PMAC > CMAC > UMAC

This may be due to the surface pH of the different AC samples. Acidic pH doesn't favour heavy metals adsorption especially Pb^{2+} and Cd^{2+} (Corapcioglu and Huang, 1987; Huang and Ostovic, 1978). pH of MB (4.66) and MO (3.42) are acidic while UMAC (7.23) is neutral. More of the heavy metals are likely to be adsorbed onto UMAC as a result reducing the number of available active sites for the dyes which results in lower adsorption results compared to CMAC and PMAC.

4.4.1.2 MBMO Adsorption from $Pb(NO_3)_2$ solution

Figures 4.18(a) – (c) represents bar graphs showing the % of the components of the MBMO mixture adsorbed onto from Pb nitrate heavy metal environment onto UMAC, CMAC and PMAC respectively; while Figure 4.18(d) shows the cumulative percentage average of the components adsorbed onto the different AC samples.

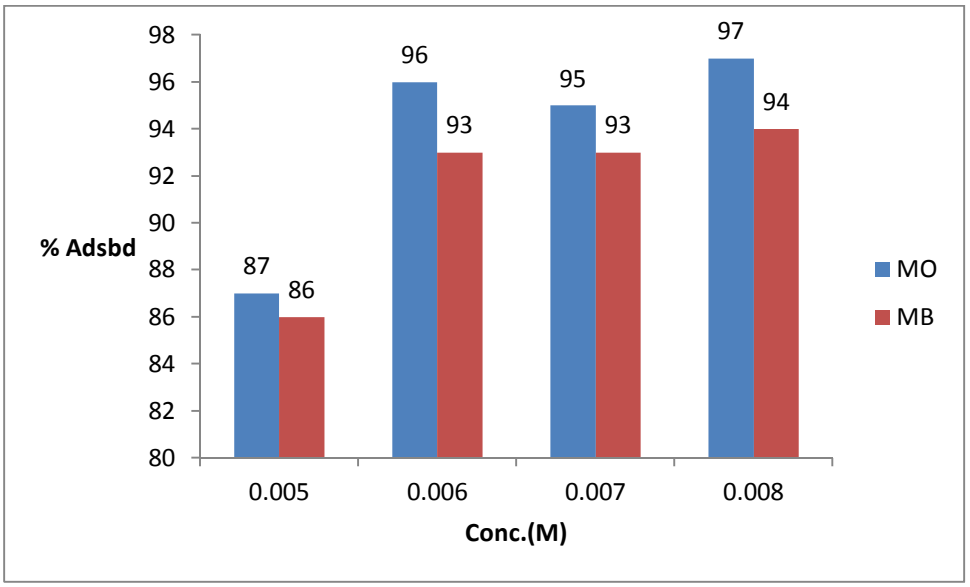


Figure 4.18(a): Percentage of components of MBMO adsorbed from aqueous $Pb(NO_3)_2$ onto UMAC

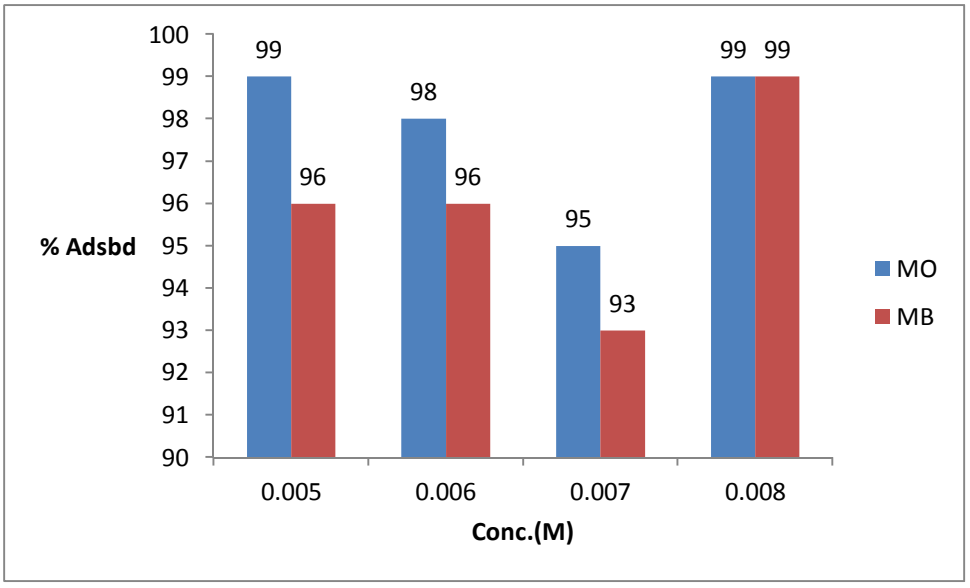


Figure 4.18(b): Percentage of components of MBMO adsorbed from aqueous $Pb(NO_3)_2$ onto CMAC

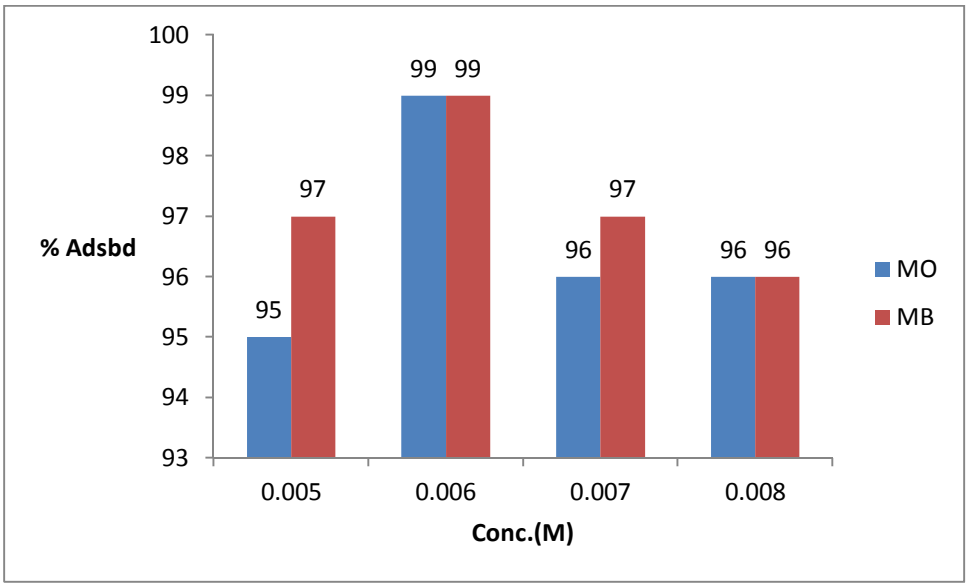


Figure 4.18(c): Percentage of components of MBMO adsorbed from aqueous $Pb(NO_3)_2$ onto PMAC

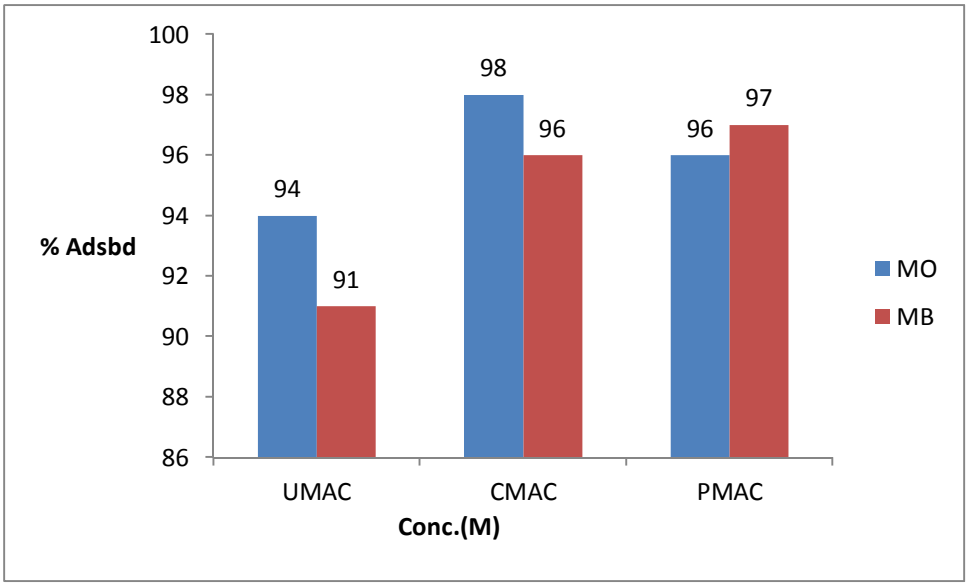


Figure 4.18(d): Cumulative percentage average of components of MBMO adsorbed from aqueous $Pb(NO_3)_2$

Generally, the results were very good with an adsorption range of between 91-98% and no general trend was observed as the percentage of the components adsorbed differed from one matrix to the other and as concentration of the $Pb(NO_3)_2$ was increased. For Figure 4.18(a), MO was preferentially adsorbed with the least amount at 0.005M and the highest at 0.008M. this may be that the presence of $Cd(NO_3)_2.4H_2O$ in the former system may be responsible.

For Figure 4.18(b), MO is preferentially adsorbed at all $Pb(NO_3)_2$ concentrations apart from 0.008M where there was a tie of 99% for each. In Figure 4.18(c), there were two ties at 0.006 and 0.008M with 99 and 96% adsorbed respectively and at two concentrations (0.005 and 0.007M), MO was preferentially adsorbed. From the summary graph, This suggests that the presence of $Pb(NO_3)_2$ specifically hinders or suppresses MB adsorption onto the different AC samples. The order of the percentage of the components adsorbed onto the three different surfaces is as below: CMAC > PMAC > UMAC

4.4.1.3 MBMO Adsorption from $Cd(NO_3)_2.4H_2O$ solution

Figures 4.19(a) – (c) represents bar graphs showing the percentage of the components of the MBMO mixture adsorbed from $Cd(NO_3)_2.4H_2O$ environment onto UMAC, CMAC and PMAC respectively; while Figure 4.19(d) shows the Cumulative percentage average of the components adsorbed onto the different AC samples.

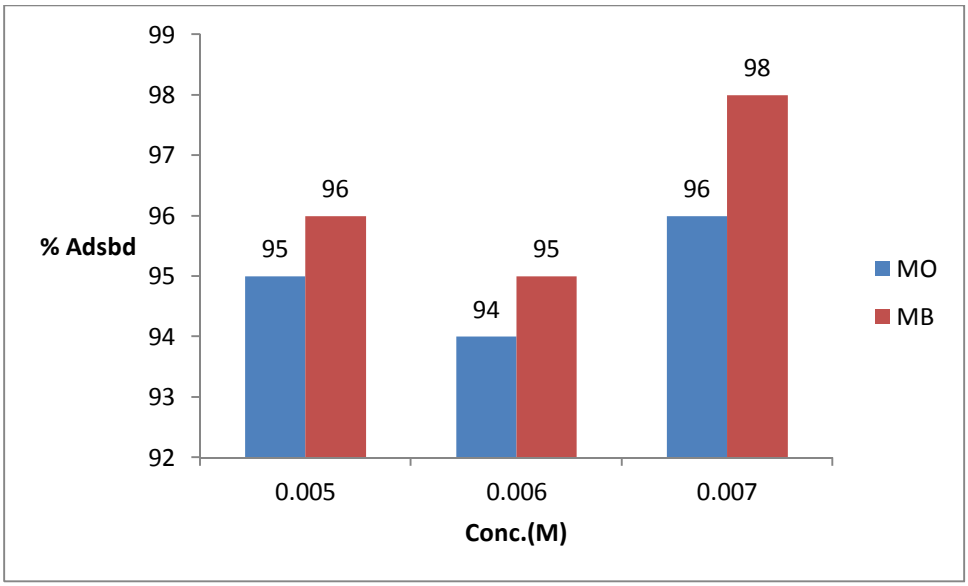


Figure 4.19(a): Percentage of components of MBMO adsorbed from aqueous $Cd(NO_3)_2.4H_2O$ onto UMAC

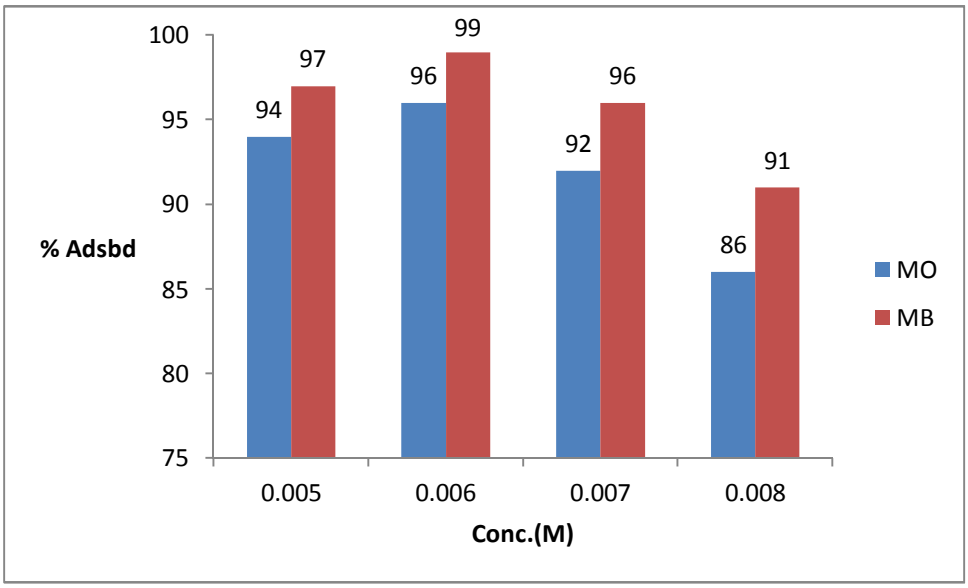


Figure 4.19(b): Percentage of components of MBMO adsorbed from aqueous $Cd(NO_3)_2.4H_2O$ onto CMAC

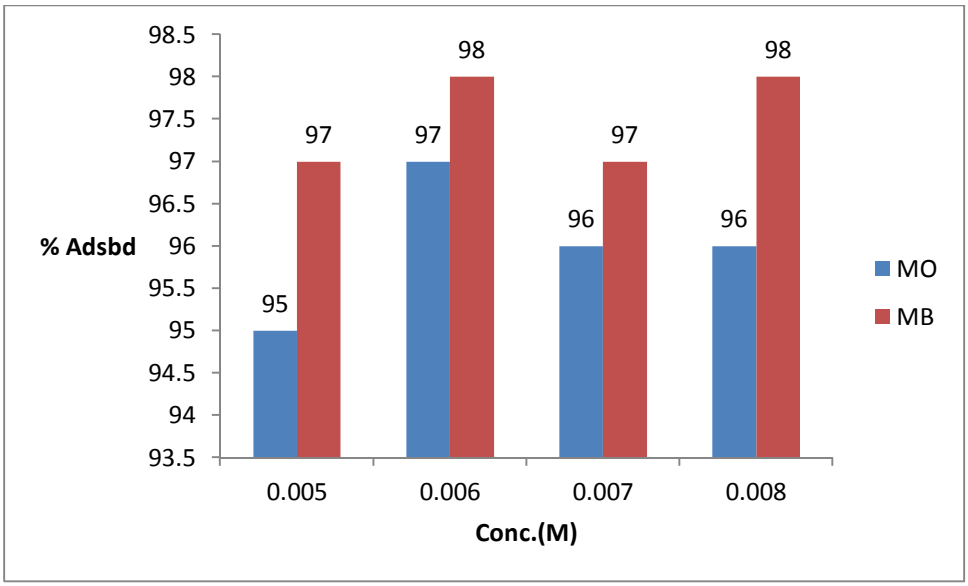


Figure 4.19(c): Percentage of components of MBMO adsorbed from aqueous $Cd(NO_3)_2.4H_2O$ onto PMAC

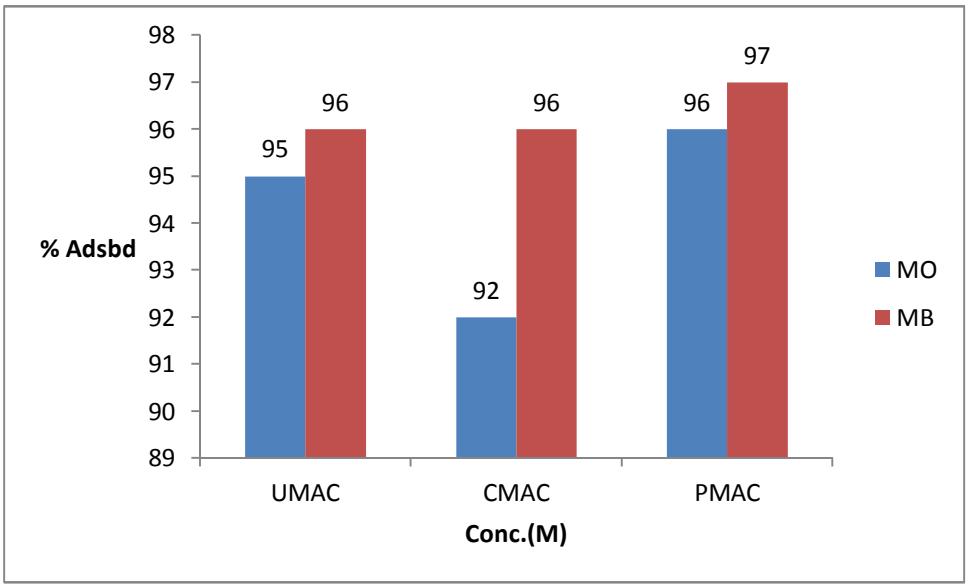


Figure 4.19(d): Cumulative percentage average of components of MBMO adsorbed from aqueous $Cd(NO_3)_2.4H_2O$

For this series the general trend is observed which is that MB is preferentially adsorbed compared to MO. This is the case in all the graphs. The result is seemingly opposite when compared to the former series where $Pb(NO_3)_2$ was involved, MO was preferentially adsorbed which is a reverse of this case. The amount of the components of the MBMO adsorbed was generally high irrespective of the $Cd(NO_3)_2.4H_2O$ concentration, or the AC sample, where the adsorption range was 92 – 98%.

On comparing these result with results of the former series which involed $Pb(NO_3)_2$, it is clear that $Pb(NO_3)_2$ hinders MB and aids MO adsorption, while in this current situation, it can be said that $Cd(NO_3)_2$.4H2O hinders MO adsorption and enhances MB adsorption There seems to be a correlation where it can be seen that $Cd(NO_3)_2$.4H2O hinders or screens MO more effectively than $Pb(NO_3)_2$ does against MB. This is why the adsorption trend for this current series is similar in all the graphs. This observation can also be linked to the sizes of the species involved.

MB has a larger size in bulk than MO due to the number of cyclic compounds or rings they possess. Article 4.2.1. of this work gives full details of this explanation. MB has three rings while MO has two. Pb^{2+} and Cd^{2+} on the other hand have ionic radii of 1.20Å and 0.97Å respectively. This means Pb^{2+} is larger in size than Cd^{2+}. Cd^{2+} hinders or screens MO from free adsorption while Pb^{2+} goes ahead to hinder MB. So the smaller cation hinders the smaller dye, while the bigger cation hinders the bigger dye. So in the MBMO dye mixture,

Pb^{2+} will assist MO to thrive in the adsorption process by screening MB, while Cd^{2+} on the other hand enhances MB adsorption by hindering MO adsorption.

It can be concluded that in the MBMO system the size of both the dyes and Cations will determine which will be preferentially adsorbed. The order of the percentage of the components adsorbed onto the different AC samples can be represented as:

` PMAC > UMAC > CMAC

Comparing this with the results in the Cd/Pb nitrate and Pb nitrate series, it can be seen that the rankings of the different AC samples differ. This suggests that the performance of the different AC samples is affected by the Heavy metal environment that they exist in . this may be tied to the relative affinities each AC sample may have for the adsorbate species and also the pH of the each surface may also be a factor. The table below summarizes the performances of each AC sample in the different heavy metal environment. Data from the summary Figures from the three different heavy metal environments is used.

Table 4.7: Table of percentage averages of components of MBMO adsorbed from different heavy metal environment onto different AC samples.

	UMAC		CMAC		PMAC		Average
	MO	MB	MO	MB	MO	MB	
Cd/Pbnitrate	90	91	94	96	96	97	94
Pb nitrate	94	91	98	96	96	97	95
Cd nitrate	95	96	92	96	96	97	95
Average	93	93	95	96	96	96	

From the table above it can be seen that for the different AC samples used, PMAC gave results that were consistent irrespective of the adsorbate species or the heavy metal environment involved. This proves that the modification process really had a positive influence on it's performance making it versatile. On the overall, the performance of the different AC samples is as below

PMAC > CMAC > UMAC

4.4.2 MOIG Adsorption in Heavy Metal Environment.

For the adsorption of components of MOIG in heavy metal environment, the results were represented using bar graphs which showed the percentage of each component adsorbed onto the different AC samples (i.e. UMAC, CMAC and

PMAC), and .0.005, 0.006, 0.007 and 0.008M of the heavy metal salt solutions (i.e. $Pb(NO_3)_2$, $Cd(NO_3)_2.4H_2O$ and their mixture).

4.4.1.4 MOIG Adsorption from aqueous $Pb(NO_3)_2$ and $Cd(NO_3)_2.4H_2O$ mixture

Figures 4.20(a) – (c) are bar graphs representing the percentage of components of MOIG adsorbed onto UMAC, CMAC and PMAC respectively from aqueous $Pb(NO_3)_2$ and $Cd(NO_3)_2.4H_2O$ mixture while Figure 4.20(d) is the cumulative percentage average of the components .

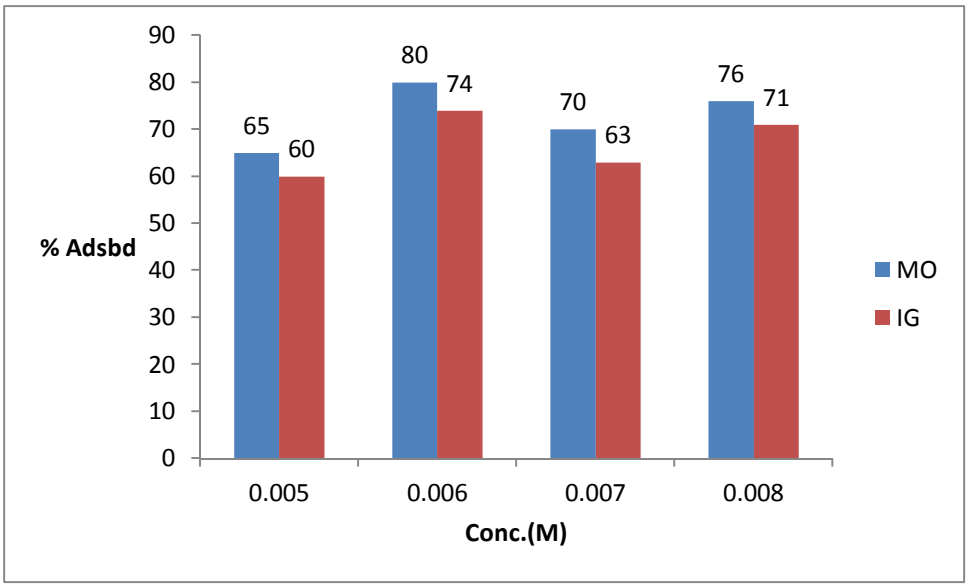


Figure 4.20(a): Percentage of components of MOIG adsorbed from aqueous $Pb(NO_3)_2$ and $Cd(NO_3)_2.4H_2O$ mixture onto UMAC

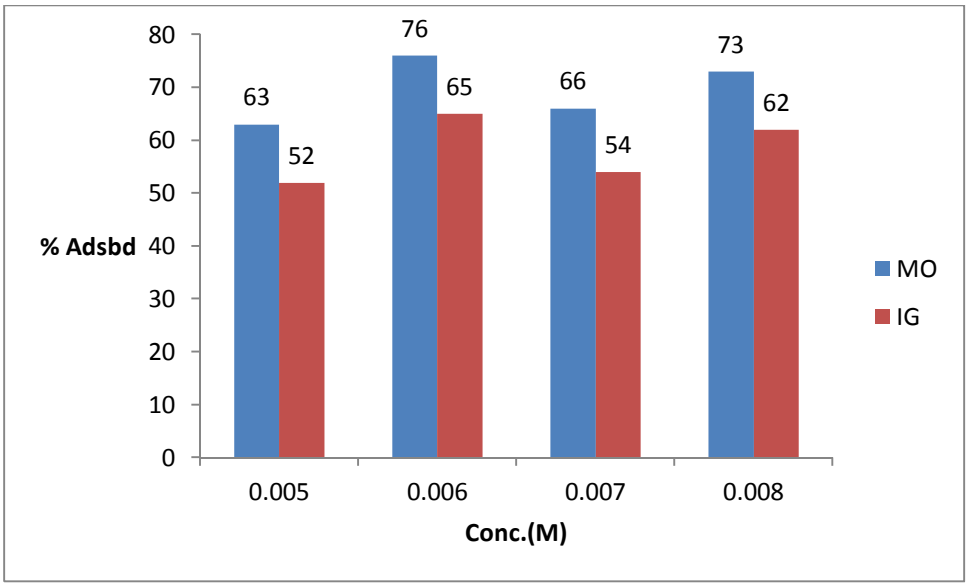


Figure 4.20(b): Percentage of components of MOIG adsorbed from aqueous $Pb(NO_3)_2$ and $Cd(NO_3)_2.4H_2O$ mixture onto CMAC

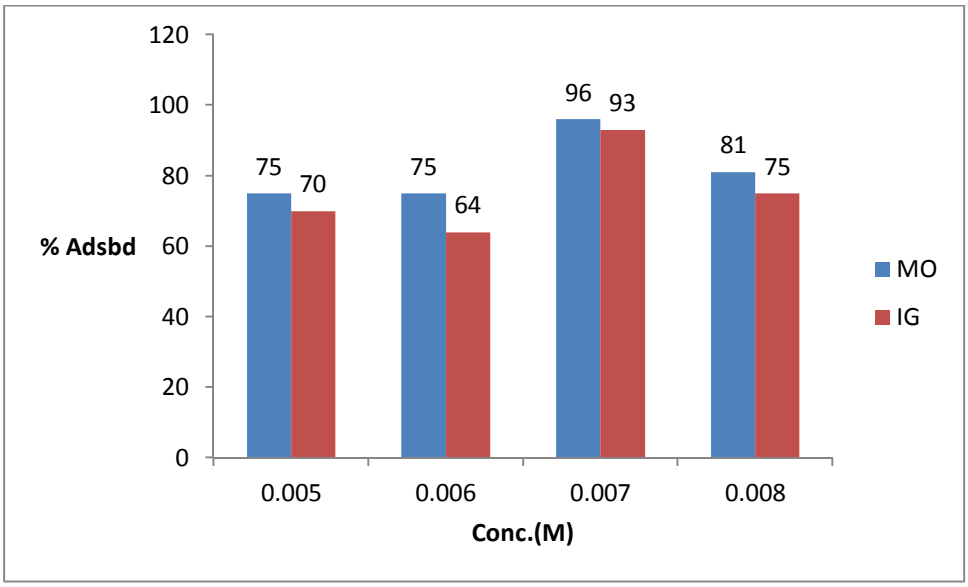


Fig 4.20(c): Percentage of components of MOIG adsorbed from aqueous $Pb(NO_3)_2$ and $Cd(NO_3)_2.4H_2O$ mixture onto PMAC

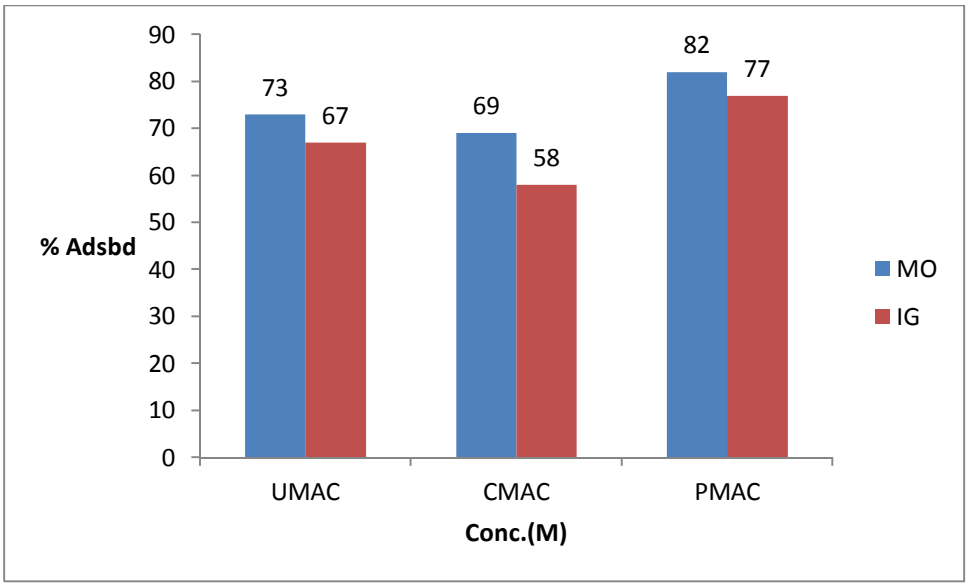


Figure 4.20(d): Cumulative percentage average of components of MOIG adsorbed from aqueous $Pb(NO_3)_2$ and $Cd(NO_3)_2.4H_2O$ mixture

For this series, a general adsorption trend was observed for all the graphs presented above which showed that MO was preferentially adsorbed relative to IG irrespective of the AC sample involved. The results were also generally lower when compared to the MBMO series

Figure 4.20(a) was the graph for adsorption of components of MOIG onto UMAC. The adsorption range was 60 – 80% which is low when compared to it's MBMO counterpart (i.e. Figure 4.17(a)) which had an adsorption range of 89 – 93%.

Figure 4.20(b) was the graph for adsorption of components of MOIG onto CMAC, the adsorption range was 52 – 76% which was lower than it's MBMO relative(Figure 4.17(b)) that had adsorption range of 93 – 98%, While Figure 4.20(c) was the graph for the PMAC matrix which had a range of 64 – 96% which

was the best of the series. It's MBMO relative (Figure 4.17(c)) had an adsorption range of 95 – 98%. These results can be tied to steric factors i.e the bulk differencein the size of the molecules involved. From Figure 4.20(d) which summarizes the results, the order of the % of the components adsorbed on the different AC samples is as : PMAC > UMAC > CMAC.

The good results of PMAC are due to it's improved qualities due to modification.

4.4.2.2 MOIG Adsorption from aqueous $Pb(NO_3)_2$ solution

Figures 4.21(a) – (c) are bar graphs representing the percentage of components of MOIG adsorbed onto UMAC, CMAC and PMAC respectively from aqueous $Pb(NO_3)_2$ solution, while Figure 4.21(d) is the cumulative percentage average of the components.

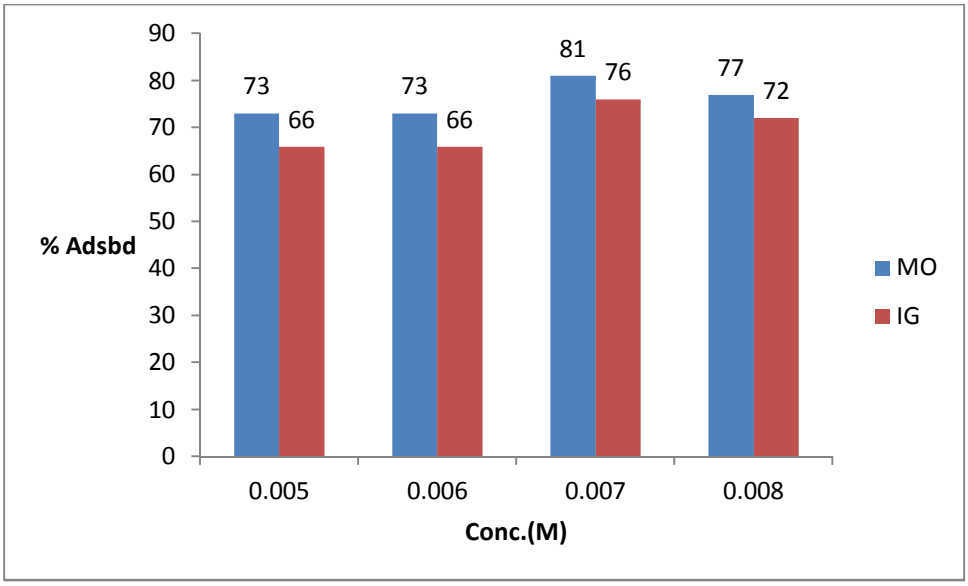


Figure 4.21(a): Percentage of components of MOIG adsorbed from aqueous $Pb(NO_3)_2$ onto UMAC

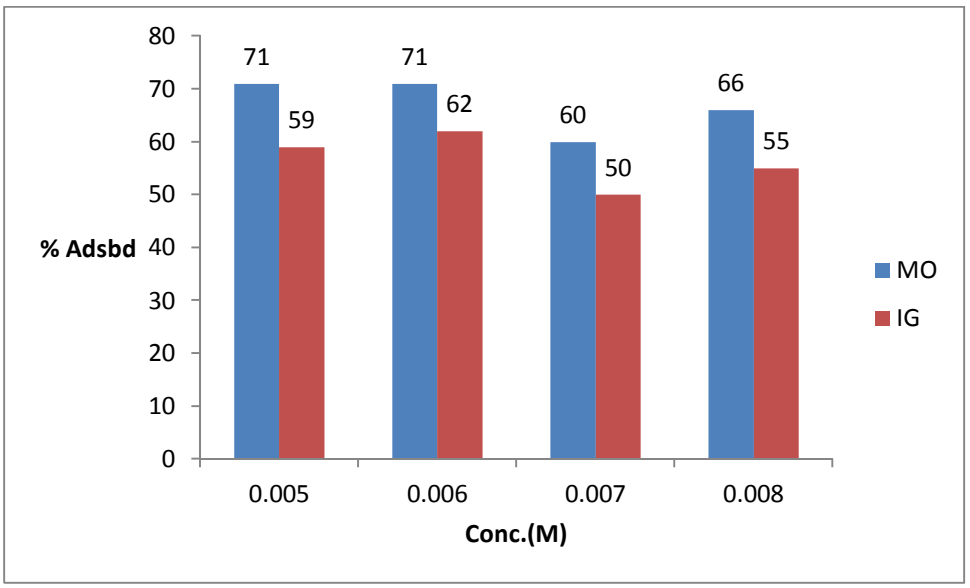


Figure 4.21(b): Percentage of components of MOIG adsorbed from aqueous $Pb(NO_3)_2$ onto CMAC

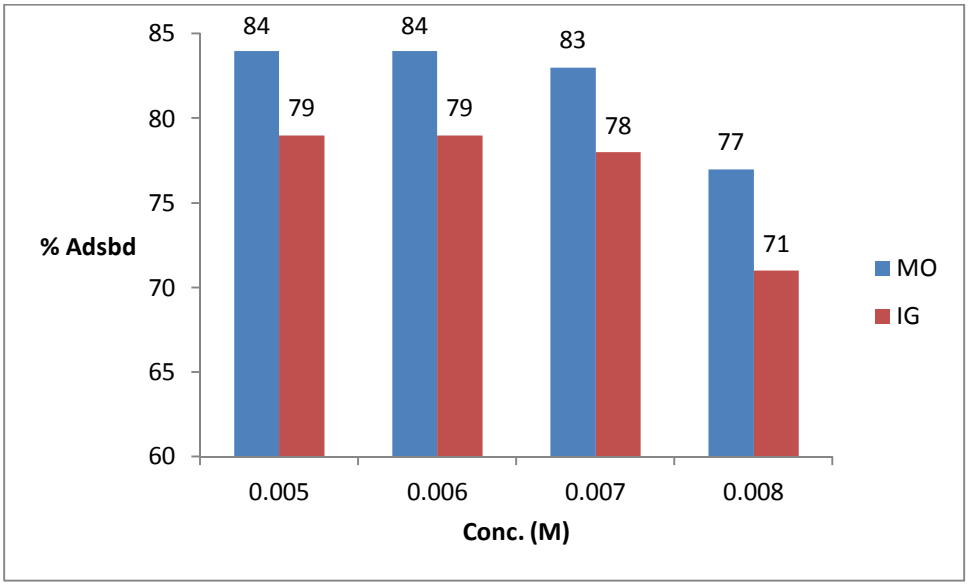


Figure 4.21(c): Percentage of components of MOIG adsorbed from aqueous $Pb(NO_3)_2$ onto PMAC

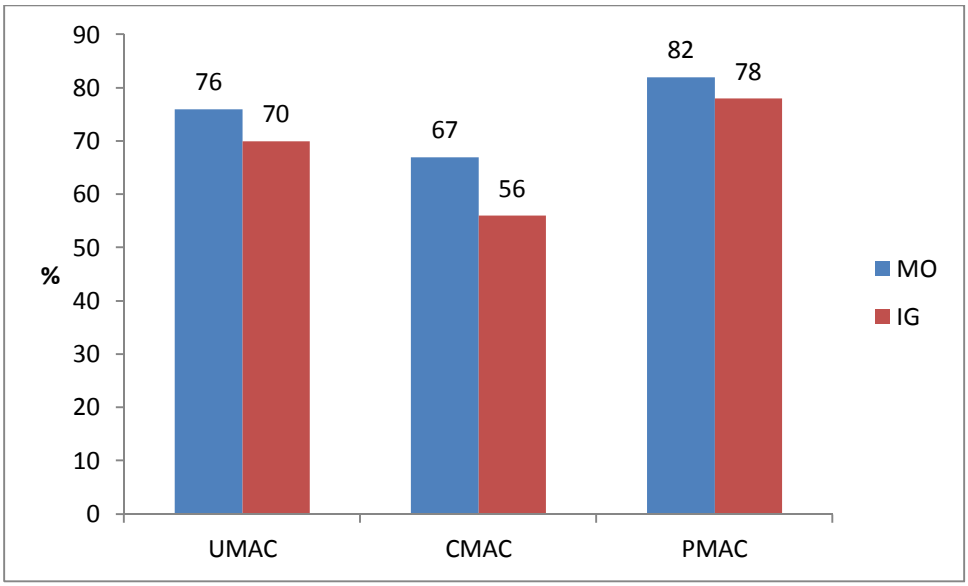


Figure 4.21(d): Cumulative percentage average of components of MOIG adsorbed from aqueous $Pb(NO_3)_2$

The general trend in this series showed that MO was preferentially adsorbed relative to IG. The trend is similar to that of the aqueous $Pb(NO_3)_2$ and $Cd(NO_3)_2.4H_2O$ mixture series. This can be generally attributed to the large difference in size between MO and IG, where the porous network of the various AC samples are favourable to the size of MO. On observing the structures of MO and IG, MO seems more linear while IG is broad and flat, which may be a hindering factor.

Figure 4.21(a) is the graph for components of MOIG in aqueous $Pb(NO_3)_2$ onto UMAC. The general adsorption range was 66 -81% but specifically the adsorption ranges were 73 – 81% for the MO component and 66 – 76% for the IG component. Figure 4.21(b) which is for the CMAC matrix gave a general adsorption range of 50 – 70% where the specific ranges were 60 – 71% and 50 – 62% for MO and IG respectively.

Figure 4.21(c) is for adsorption onto the PMAC sample where the general adsorption range was 71 – 84% and specific ranges of 77 – 84% and 71 – 79% for MO and IG respectively. The difference in the adsorption of the components is more pronounced in Figure 4.21(b) where CMAC was the adsorbent. This may be linked to the surface properties of CMAC. Which may repel IG more effectively than the UMAC and PMAC surfaces. The ranking for the different AC samples is of the order:

PMAC > UMAC > CMAC

4.4.2.3 MOIG Adsorption from $Cd(NO_3)_2.4H_2O$

Figures 4.22(a) – (c) are bar graphs representing the percentage of components of MOIG adsorbed onto UMAC, CMAC and PMAC from $Cd(NO_3)_2.4H_2O$ solution respectively, while Fig 4.22(d) is the cumulative percentage average of the components.

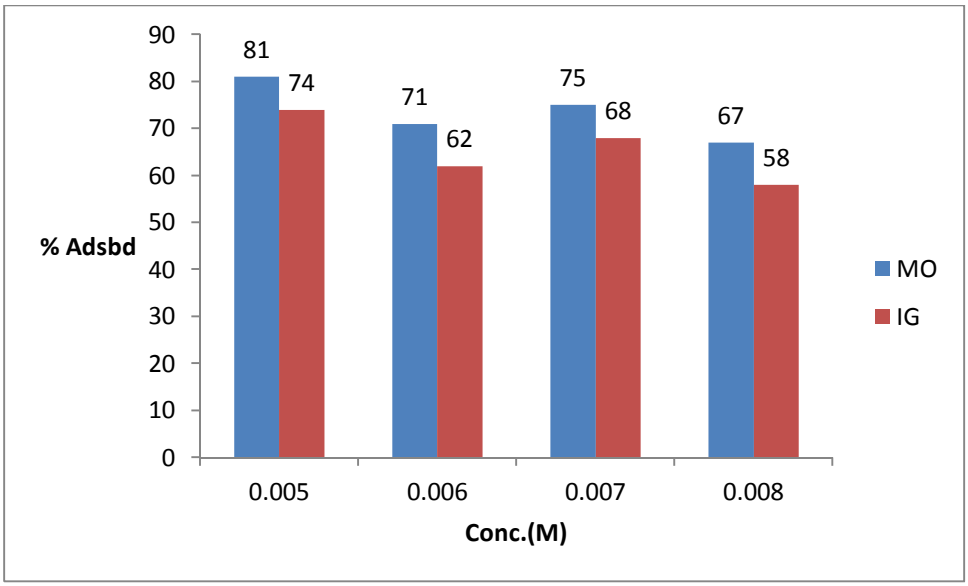


Figure 4.22(a): Percentage of components of MOIG adsorbed from aqueous $Cd(NO_3)_2.4H_2O$ onto UMAC

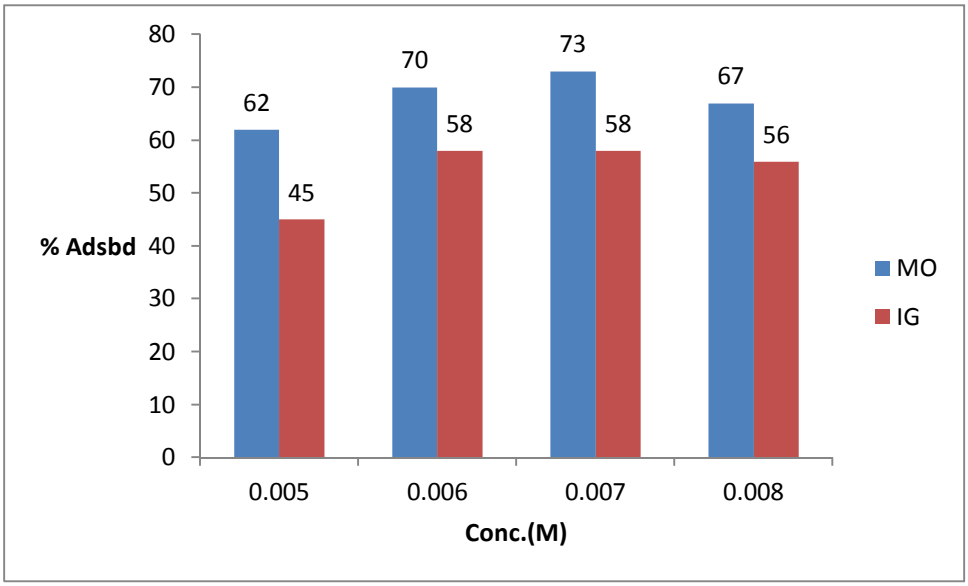


Figure 4.22(b): Percentage of components of MOIG adsorbed from aqueous $Cd(NO_3)_2.4H_2O$ onto CMAC

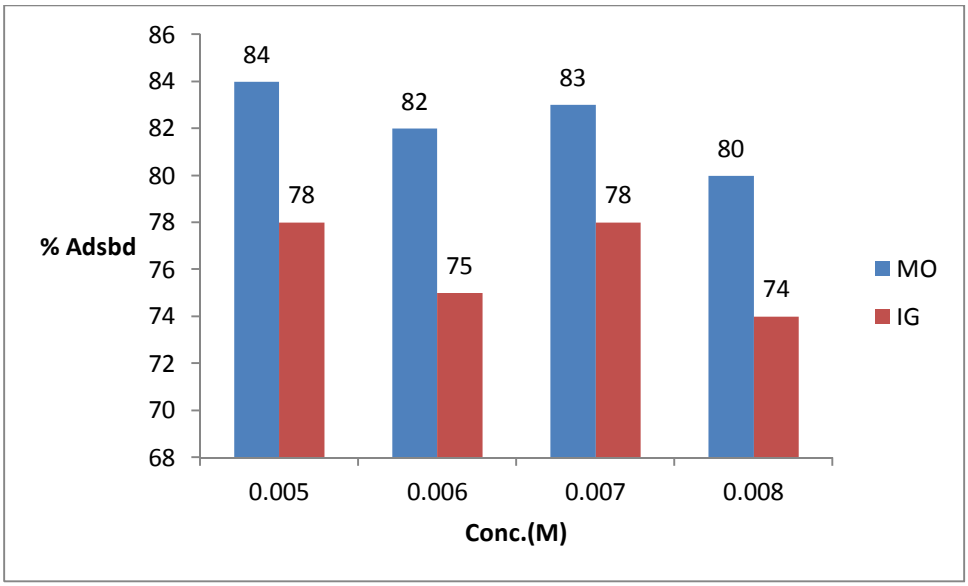


Figure 4.22(c): Percentage of components of MOIG adsorbed from aqueous $Cd(NO_3)_2.4H_2O$ onto PMAC

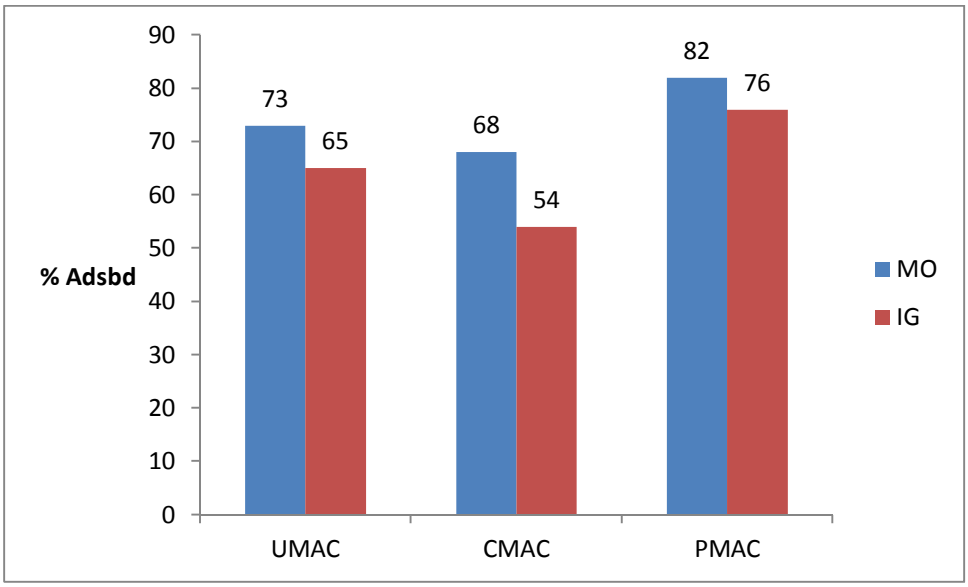


Figure 4.22(d): Cumulative percentage average of components of MOIG adsorbed from $Cd(NO_3)_2.4H_2O$ onto PMAC

The results in this series are similar to those in the aqueous $Pb(NO_3)_2$ and $Cd(NO_3)_2.4H_2O$ mixture and aqueous $Pb(NO_3)_2$ series. The reasons for the trend

are also similar which is mainly steric factors (i.e. differences in size of the dye molecules). The rankings of the different AC samples is also similar to those in the aqueous $Pb(NO_3)_2$ and $Cd(NO_3)_2.4H_2O$ mixture and aqueous $Pb(NO_3)_2$ series. above. i.e. PMAC > UMAC > CMAC

The summary results can be seen in Table 4.8.

Table 4.8: Table of % averages of components of MOIG adsorbed from different heavy metal environment onto different AC samples.

	UMAC		CMAC		PMAC		Average
	MO	IG	MO	IG	MO	IG	
Cd/Pbnitrate	73	67	69	58	82	77	71
Pb nitrate	76	70	67	56	82	78	71
Cd nitrate	73	65	68	54	82	76	70
Average	74	67	68	56	82	77	

The horizontal averages arising from the different columns shows that the amount of the dyes adsorbed is dependent on the adsorbate species and the adsorbent involved. From the vertical average it can be seen that on the average the heavy metal environment were similar.

4.4.3 Summary of results of adsorption of binary dyes in heavy metal environment

The following summaries can be made from the adsorption results of the separate binary dyes from heavy metal environment.

For the MBMO in aqueous $Pb(NO_3)_2$ and $Cd(NO_3)_2.4H_2O$ mixture:

1. series, adsorption was generally high irrespecvive of the AC sample. Adsorption range was 89 – 98%
2. MB was preferentially adsorbed relative to MO. This was attributed to time and concentration factors i.e. working at dilute concentration can enhance result details.
3. For MBMO in aqueous $Pb(NO_3)_2$, adsorption for the different components was generally high with adsorption range of 91 – 98%.
4. MO was preferentially adsorbed than MB, where Pb^{2+} can be said to hinder or suppress MB adsorption.
5. For MBMO in $Cd(NO_3)_2.4H_2O$, the adsorption range for the different components is averagely 92 – 97%.
6. MB is preferentially adsorbed than MO, where $Cd(NO_3)_2.4H_2O$ hinders or suppresses MO adsorption and assists MB adsorption.
7. For MOIG in the different heavy metal environments, adsorption was generally good but lower than results from the MBMO series. The adsorption range was 54 – 82%

8. MO was preferentially adsorbed in all cases irrespective of the heavy metal environment or AC sample. Steric factors is the main reason for results in this series.
9. PMAC generally performed better than UMAC and CMAC irrespective of the adsorbate system invoved.

4.5.0 Adsorption of Tertiary Dye Mixture in Heavy Metal Environment

Tertiary dye mixture in heavy metal solution was prepared by mixing equal amounts of MB, MO and IG in a 0.01M aqueous $Pb(NO_3)_2$ and $Cd(NO_3)_2.4H_2O$ mixture. 10 – 50ppm of the dye mixtures were prepared via serial dilution. Adsorption was done by interacting $10cm^3$ of the various dye mixture concentrations separately with 20mg of the different AC samples (i.e UMAC, CMAC and PMAC).

Figures 4.23(a) is the graph for adsorption of the tertiary dye mixture onto UMAC while Figure 4.23(b) is the cumulative percentage average of the components. Figures 4.24(a) and (b) are the bar graph and cumulative percentage average for CMAC while Figures 4.24(a) and (b) are graphs for PMAC.

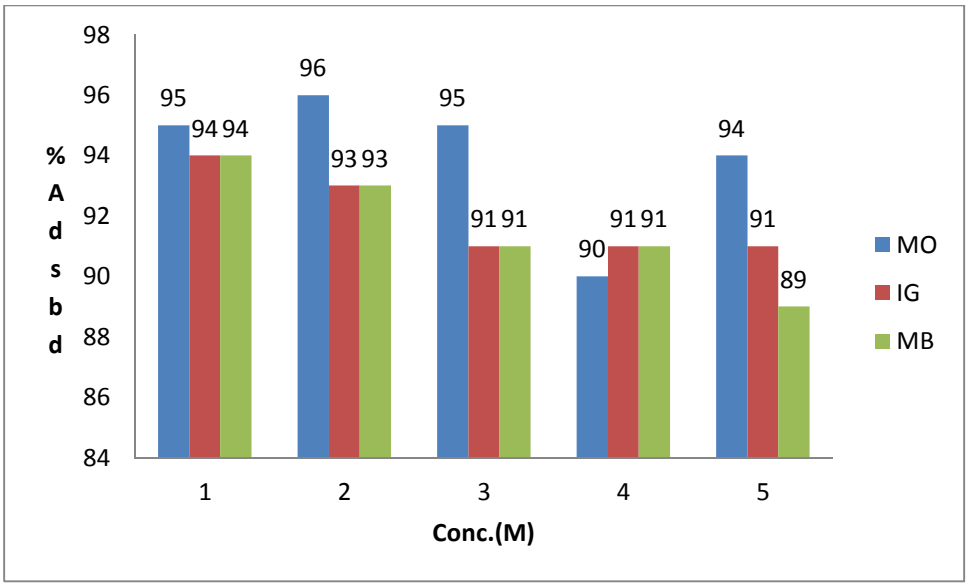


Figure 4.23(a): Percentage of components of MBMOIG adsorbed from aqueous $Pb(NO_3)_2$ and $Cd(NO_3)_2.4H_2O$ mixture onto UMAC

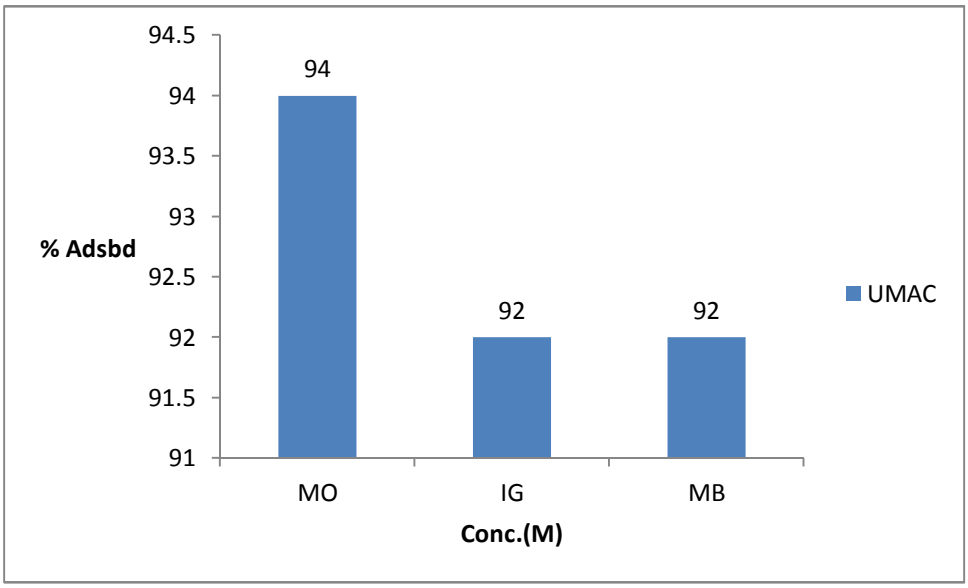


Figure 4.23(b): Cumulative percentage average of components of MOIGMB adsorbed from aqueous $Pb(NO_3)_2$ and $Cd(NO_3)_2.4H_2O$ mixture onto UMAC

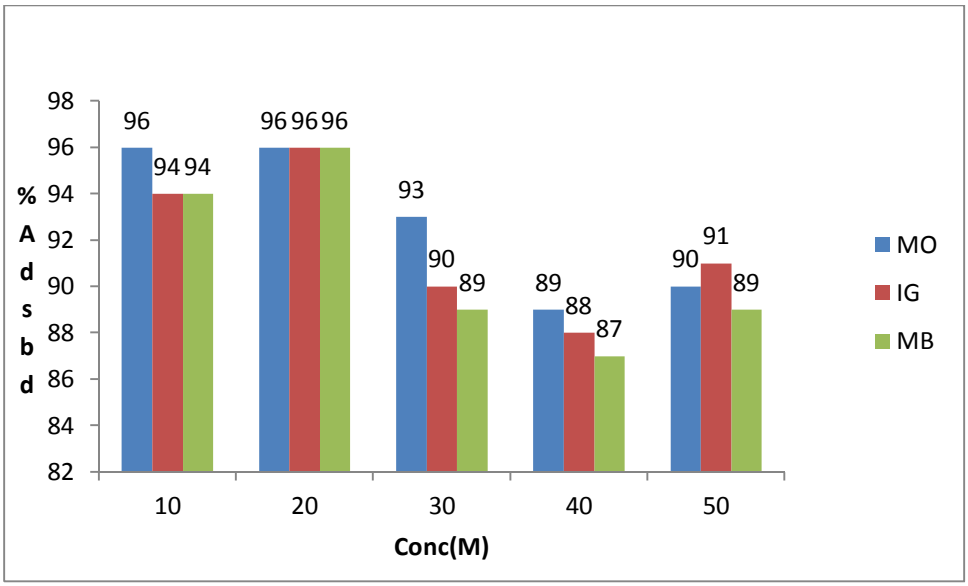


Figure 4.24(a): Percentage of components of MBMOIG adsorbed from aqueous $Pb(NO_3)_2$ and $Cd(NO_3)_2.4H_2O$ mixture onto CMAC



Figure 4.24(b): Cumulative percentage average of components of MOIGMB adsorbed from aqueous $Pb(NO_3)_2$ and $Cd(NO_3)_2.4H_2O$ mixture onto CMAC

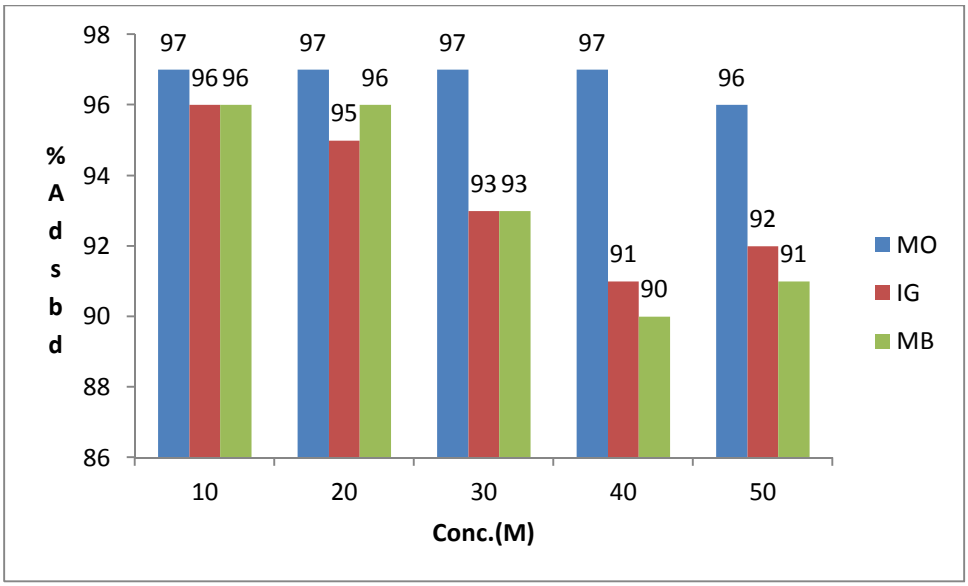


Figure 4.25(a): Percentage of components of MBMOIG adsorbed from aqueous $Pb(NO_3)_2$ and $Cd(NO_3)_2.4H_2O$ mixture onto PMAC

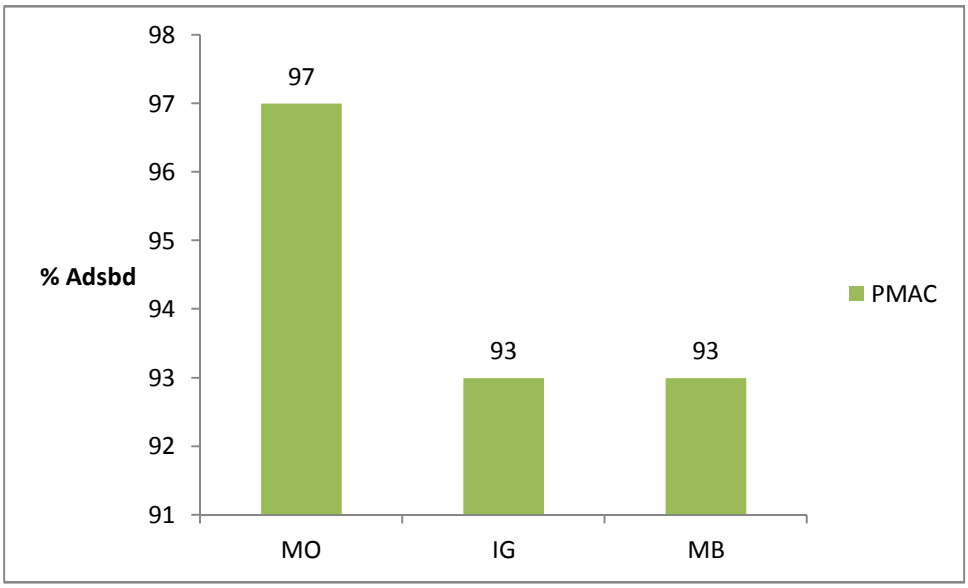


Fig 4.25(b): Cumulative percentage average of components of MBMOIG adsorbed from aqueous $Pb(NO_3)_2$ and $Cd(NO_3)_2.4H_2O$ mixture onto PMAC

Adsorption was generally favourable with readings above 90% adsorption apart from adsorption of the IG component onto CMAC which gave 73%. MO was preferentially adsorbed onto all the AC samples. This is still linked to it's favourable small size which allows it's easy diffusion to active sites of the AC samples. The PMAC samples gave the best results.

Table 4.9 is a summary table which gives the percentage averages of components of MBMOIG adsorbed from from aqueous $Pb(NO_3)_2$ and $Cd(NO_3)_2.4H_2O$ mixture onto different AC samples.

Table 4.9: Table of percentage average of components of MBMOIG adsorbed from from aqueous $Pb(NO_3)_2$ and $Cd(NO_3)_2.4H_2O$ mixture onto different AC samples.

	MO	IG	MB	Average
UMAC	94	92	92	93
CMAC	93	73	91	86
PMAC	97	93	93	94
Average	95	86	92	

From Table 4.9, it can be seen that that the values of the averages are very close to each other. i.e. both the horizontal and vertical averages, irrespective of the dye species in the columns or the AC samples in the rows. The results are higher than those in Table 4.8 which gives results for the binary dye systems. This is because in this arrangement, the amount of each component in solution is the

least compared to single and binary states. This affords less of each component interacting with available active sites which makes it easier for more of their adsorption.

If the average of the horizontal and vertical averages are taken the average of 91% is the result. Working with tertiary dye mixtures(if the individual dyes do not react in with each other in their mixed state) can be a good way of executing adsorption in aqueous media when small or marginal concentrations of dyes are needed. (i.e < 1ppm). However, when heavy metals are also involved, there should be caution especially because of some of the results that were observed in the MBMO in heavy metal series. On looking at the rankings of the AC sample performances and the dyes, the following orders can be seen

PMAC > UMAC > CMAC and

MO > MB > IG

From these, it can be seen that the performance order for the AC samples is the order that has been the major observation through out this work, which gives PMAC as better compare to UMAC and CMAC. This is still attributed to the modification process which seem to create more active sites while degassing was occurring.

It can also be seen that the rankings for the order of the dyes adsorbed is an order observed as a general trend apart from some instances where this was not so in some of the MBMO binary arrangement in different heavy metal environment. This order reveals that MO is preferentially adsorbed to MB and IG.

Here, it is seen that the order was tied to the size of the different dye molecules, where the smaller sized MO adsorbed better than the rest. This was the generous observartion trend.

This method of simultaneous adsorption of dyes can be a good analytical way of saving time for adsorption processes in the laboratory on the condition that no chemical interaction is occuring between the dyes.

4.6.0 Adsorption Isotherms

The data gotten from this research were also represented via four different types of adsorption isotherms. They are :

i. Adsorption Isotherm

ii. Freundlich Isotherm

iii. Langmuir Isotherm

iv. Temkin Isotherm

The Freundlich, Langmuir and Temkin Isotherms and their constants are featured in the appendix section of this work (Appendices XII and XIII). The Freundlich constants n and K_f [(mg^{-1}) $(mg^{-1})^{1/n}$] give an idea of the quasi-Gaussian energetic heterogeneity of the adsorbent's surface or adsorption intensity and adsorption capacity respectively (Bansal and Goyal, 2005; Hameed *et al.,* 2007). The Langmuir constants b (mg^{-1}) and Q reveals the energy of adsorption and adsorption capacity respectively (Hameed *et al.,* 2007) while the Temkin isotherm operates on the condition that the heat of adsorption decreases in a linear rather than in a logarithmic fasion (Deinz and Saygideger, 2010).

4.6.1 Adsorption Isotherms for Aqueous Single Dye Systems

Figure 4.26(a): Shows the adsorption profiles of aqueous MO onto the different AC samples. Where X/m is the amount of the dye adsorbed per unit weight of the adsorbent in mg/g. From the above, it can be seen that the MO adsorption onto UMAC and CMAC have a similar pattern where there is a steady rise in a linear fashion of the amount adsorbed then a gradual slanting off. This shows that at the 3rd point on the horizontal of the graph which corresponds to the 30ppm,is an optimum concentration range for adsorption studies using the samples involved. i.e. a 0 – 30ppm working range concentration is appropriate.

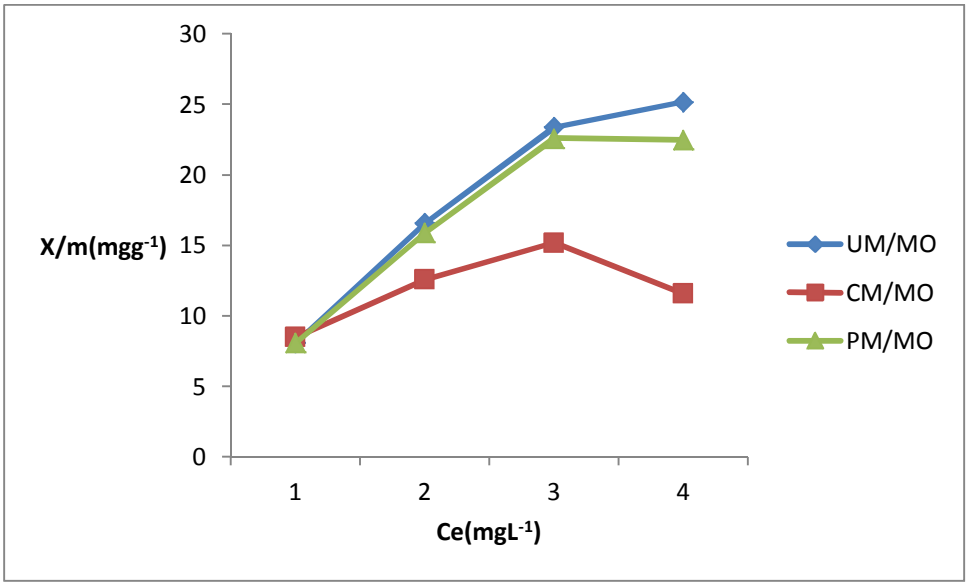


Figure 4.26(a): Adsorption isotherm of aqueous MO adsorbed onto UMAC,CMAC & PMAC

The similarities in the graph also shows that the two AC samples, i.e. UMAC and PMAC may have similar internal porous network which favours MO adsorption. These follows the Type I of the "General Types of Adsorption

Isotherms Classification," which depicts favourable adsorption. They also look like the L-2 types in the "System of Isotherm Classification." See Appendices XVII and XVIII.

From the graph, the MO adsorbed onto CMAC is not as that for the other matrices. It shows a gentle rise and then a fall. This is likened to the L-5 type adsorption isotherm. It shows that the adsorption onto this Matrix is not as good as that of the others. This may be linked to the process of modification which may have affected it's surface. For the CMAC matrix, it begins to slant at the 2^{nd} point of the X-axis which corresponds to 20ppm MO. This shows that for CMAC matrix, a working concentration range of 0 – 20ppm is recommended.

Figure 4.26(b) shows the adsorption pattern for MO in $Pb(NO_3)_2$ and $Cd(NO_3)_2.4H_2O$ mixture onto UMAC and PMAC. The graphs are curves. The curve of MO adsorption onto PMAC can be classified onto the L – 2 class, where there is a gentle rising curve, while that for UMAC can be classed as C – 2, where there is a gentle rising curve which peaks at a plateau. Comparing the results with that from aqueous only media, it can be seen that the PMAC has more space for adsorption even in $Pb(NO_3)_2$ and $Cd(NO_3)_2.4H_2O$ mixture.

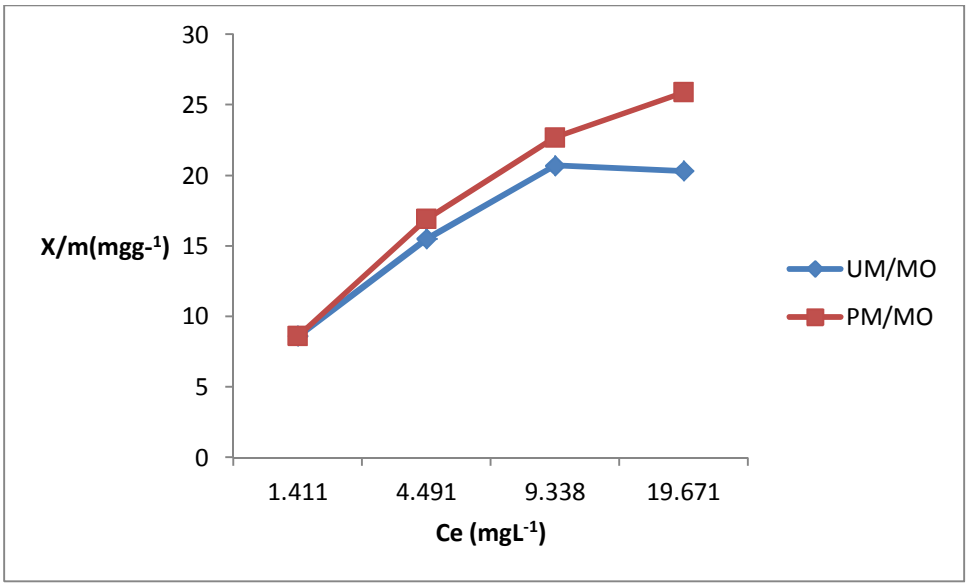


Figure 4.26(b): Adsorption isotherm of MO adsorbed from aqueous $Pb(NO_3)_2$ and $Cd(NO_3)_2.4H_2O$ mixture onto UMAC and PMAC

Fig 4.27(a) is the adsorption isotherm for aqueous MB adsorption onto UMAC, CMAC and PMAC samples. The adsorption trends of MB onto UMAC and PMAC are similar . There is a rise in linear fashion and then a fall. i.e. there is a steep and then a dip.

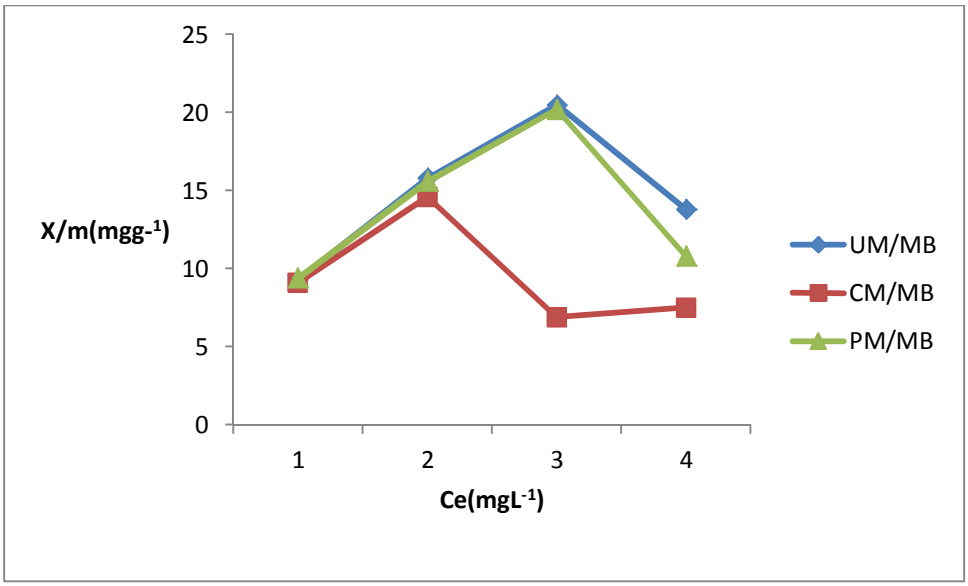


Figure 4.27(a): Adsorption Isotherm of aqueous MB adsorbed onto UMAC, CMAC, & PMAC

For the MB adsorption onto CMAC, there were three steps seen as the concentration of MB increase. There was a rise, an immediate drop at the next point and then a straight line to the last point. For the UMAC and PMAC samples, a good working concentration range will be 0 – 30ppm MB while for the CMAC sample it's 0 – 20ppm. These ranges are similar to results viewed in the MO series. This suggests that these dyes would be compatible for use for simultaneous adsorption studies. According to the adsorption isotherm classification system, the UMAC and CMAC can be classified into the L – mx class while the CMAC's isotherm can be classed into the H – mx class. Comparing these graphs with those from the MO series, it can be said that MO stays better or is better fitted onto AC sample surfaces than MB.

Figure 4.27(b) is the adsorption isotherm for MB from aqueous $Pb(NO_3)_2$ and $Cd(NO_3)_2.4H_2O$ mixture onto UMAC and PMAC. The graphs were distorted. This is attributed to the heavy metals (Cd^{2+} and Pb^{2+}) in solution and because of the high concentrations of MB involved. The repulsions were much which gave disorderly results. Although adsorption onto PMAC gave a normal adsorption curve up to the 3rd point where it dips.

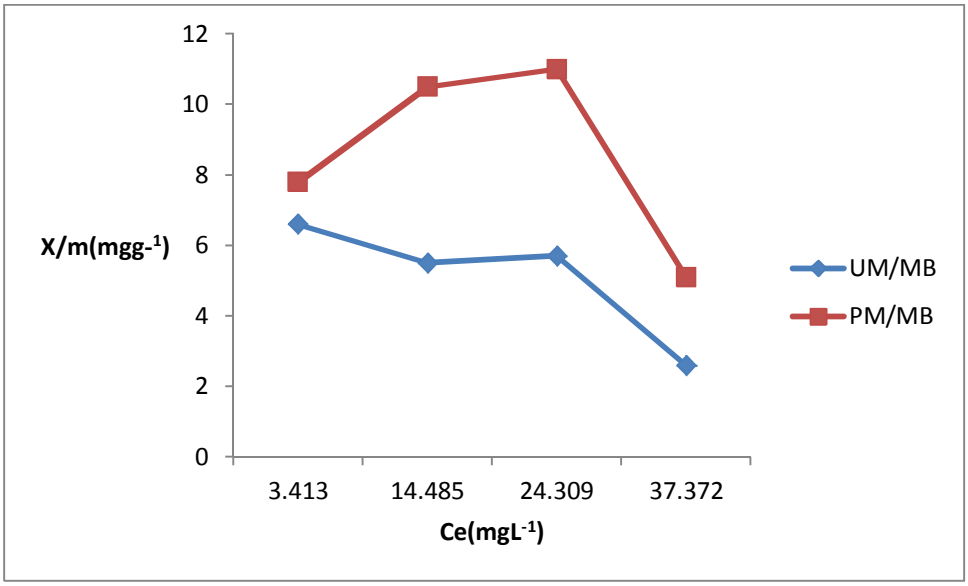


Figure 4.27(b): Adsorption isotherm of MB adsorbed from aqueous $Pb(NO_3)_2$ and $Cd(NO_3)_2.4H_2O$ mixture onto UMAC and PMAC

This shows that the adsorption process parameters and adsorbate's environment are crucial to adsorption results. Comparing the results with the MO series, it informs that MO is a more suitably adsorbed than MB. This is linked to their difference in size and shape.

Figure 4.28 shows the adsorption isotherm for aqueous IG onto UMAC, CMAC and PMAC.

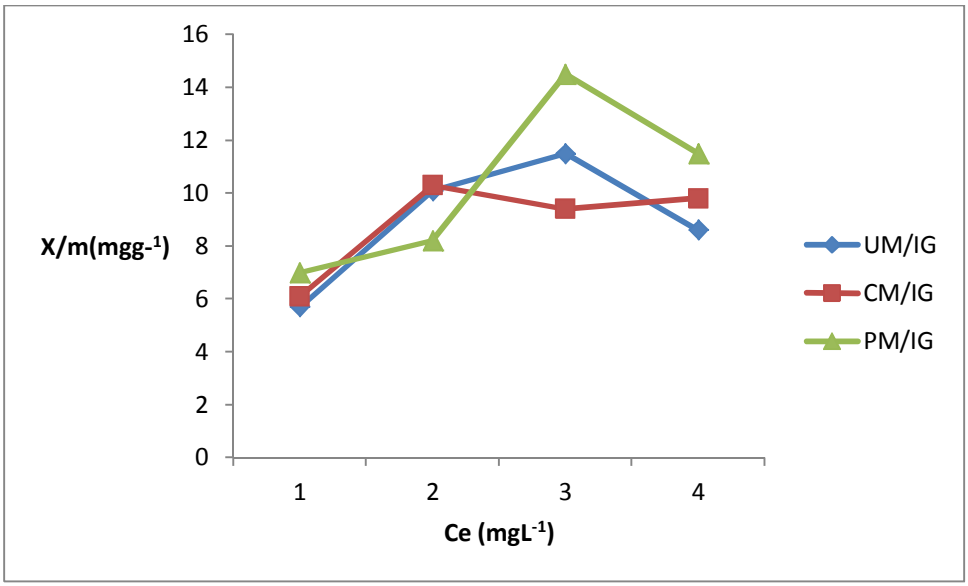


Figure 4.28(a): Adsorption isotherm of aqueous IG adsorbed onto UMAC, CMAC and PMAC

For the PMAC sample there were also three stages; a gentle rise followed by a steeper rise and then a relatively steep drop as the concentration of IG is increased. This shows that the adsorption profiles of a particular adsorbate molecule onto different AC samples can be different; especially as it's concentration increases. The working concentration range for the UMAC and CMAC samples can be set at 0 – 10ppm, while for PMAC it is 0 – 30ppm. It shows that IG has preferential affinity for PMAC. Even though the rise from 10 to 20ppm is small, the steep rise from 20 to 30ppm will make the amount adsorbed averagely higher than the amount adsorbed by the other matrices.

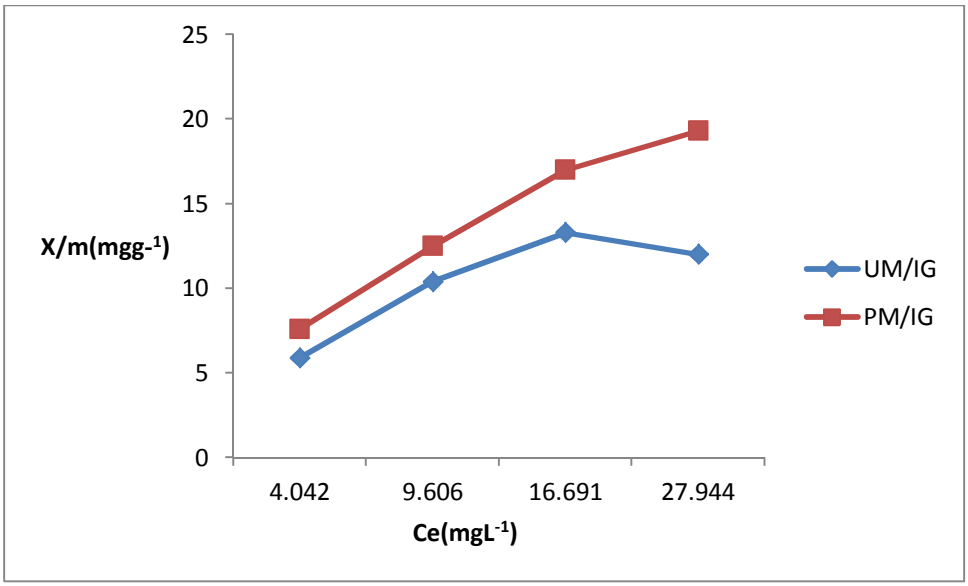


Figure 4.28(b): Adsorption isotherm of IG adsorbed from aqueous $Pb(NO_3)_2$ and $Cd(NO_3)_2.4H_2O$ mixture onto UMAC and PMAC

Figure 4.28(b) is the adsorption isotherm of IG from aqueous $Pb(NO_3)_2$ and $Cd(NO_3)_2.4H_2O$ mixture onto UMAC and PMAC . In terms of "orderliness" of the three different series, it can be seen that the most orderly or organized is the MO series followed by MB series and then IG series. Here again it is seen that the size of the dye molecules playing a role in the observed trend.

4.6.1.2 Summary of results of the adsorption isotherms of MO, MB, and IG onto the different AC samples.

1. For MO adsorption onto the different matrices, there was similarity in the adsorption trend of the UMAC and PMAC samples especially between the 0 - 30ppm concentration while in the case of CMAC, the adsorption was below the others. Which means a less amount of MO was adsorbed onto CMAC compared to UMAC and PMAC. The modification process may be responsible for this.

2. For MB adsorption onto the three different matrices, the UMAC and PMAC samples showed similarities in results with the MO series. The adsorption of MB onto CMAC was also lower as it was in the MO series. For IG adsorption onto the three different matrices, there was no particular similarity in the adsorption trends with the different matrices. The large size of the IG molecules may be responsible for this.

4.6.2 Adsorption Isotherm of Aqueous Binary Dye mixtures.

The adsorption isotherms for the binary dye mixtures both in aqueous and aqueous heavy metal environment is presented with the graphs that follows.

4.6.2.1 Adsorption of components of MBMO from aqueous and aqueo$Pb(NO_3)_2$ and $Cd(NO_3)_2.4H_2O$ mixture .

Figures 4.29(a) and 4.29(b) are adsorption isotherms for adsorption of components of MBMO from aqueous and aqueous heavy metal environment. Figure 4.29(a) shows that there was a similar adsorption trend for both components of the mixture up to the 30ppm where MB had a drop in the amount adsorbed suggesting desorption of the some of the MB molecules back into solution. This shows that MO is better attached to the UMAC surface. This can still be tied to the differences in the sizes of the molecules.

For results in Figure 4.29(b), it can be seen that there is a separation in the adsorption lines of both components. This shows that in the $Pb(NO_3)_2$ and $Cd(NO_3)_2.4H_2O$ mixture, MB adsorption is hindered more than MO. This also

implies that the AC surface is more inclined to MO or MO is more suited for the UMAC surface.

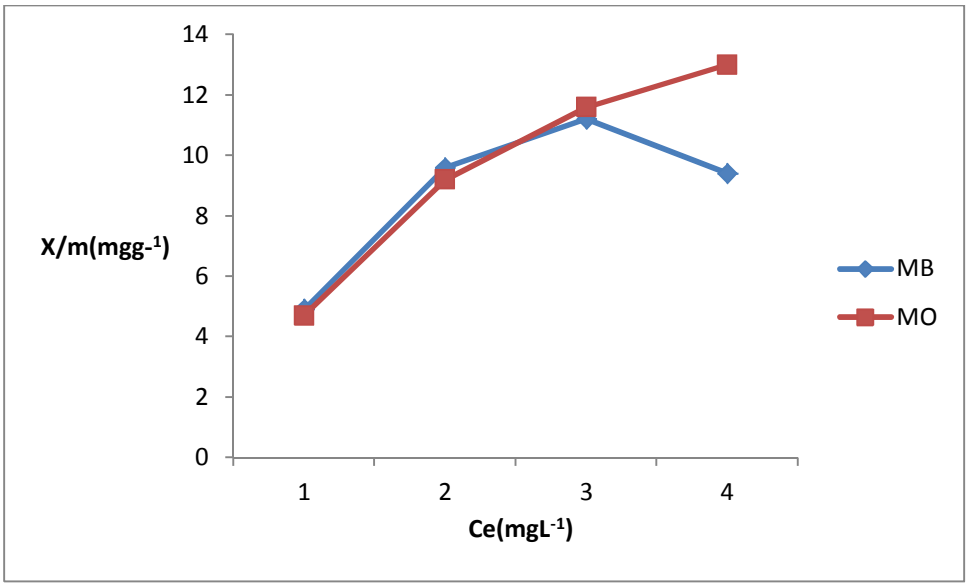


Figure 4.29(a): Adsorption isotherm of components of aqueous MBMO adsorbed onto UMAC

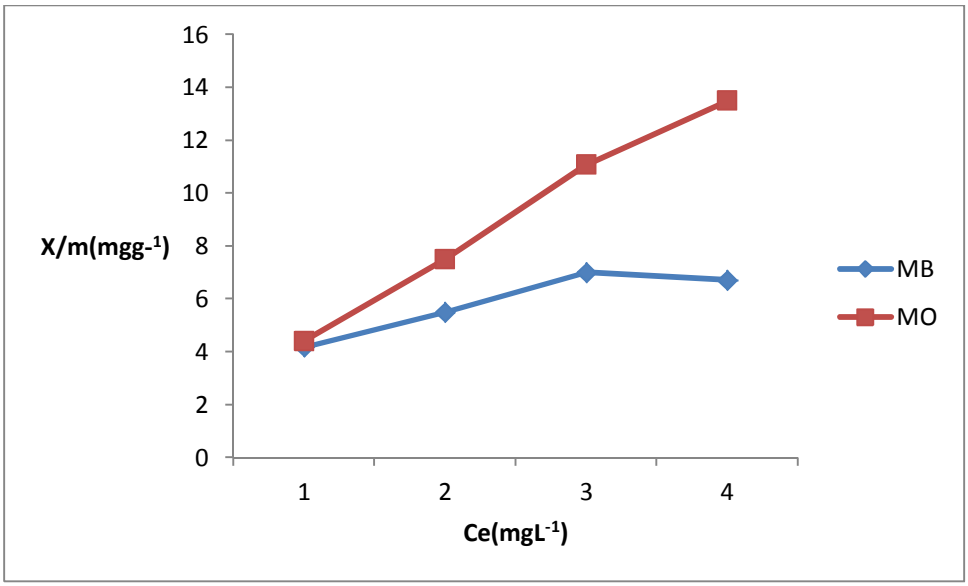


Figure 4.29(b): Adsorption isotherm of components of MBMO adsorbed from aqueous $Pb(NO_3)_2$ and $Cd(NO_3)_2.4H_2O$ mixture onto UMAC

Table 4.10 shows the average percentage of components of MBMO adsorbed from both aqueous and aqueous $Pb(NO_3)_2$ and $Cd(NO_3)_2.4H_2O$. It can be clearly observed that the average percentage of the components adsorbed is higher in the aqueous medium compared to the adsorption from aqueous $Pb(NO_3)_2$ and $Cd(NO_3)_2.4H_2O$ environment. This difference can be attributed to the adsorption of Cd^{2+} and Pb^{2+} which are also competing species for available active sites as adsorption progresses. The differences in these results can be used to estimate the amount of Cd^{2+} and Pb^{2+} adsorbed. This shows that the aqueous $Pb(NO_3)_2$ and $Cd(NO_3)_2.4H_2O$ environment opposes MB adsorption more than MO. This may be due to their size differences.

Table 4.10: Average percentage of components of MBMO adsorbed from both aqueous and aqueous $Pb(NO_3)_2$ and $Cd(NO_3)_2.4H_2O$ mixture

	UMAC		CMAC		PMAC	
	MO	MB	MO	MB	MO	MB
Aqueous	82	79	68	73	88	90
Cd/Pb nitrate	76	55	71	53	76	57

Figures 4.30(a) and (b) are adsorption isotherms for components of MBMO in aqueous and aqueous heavy metal environment.

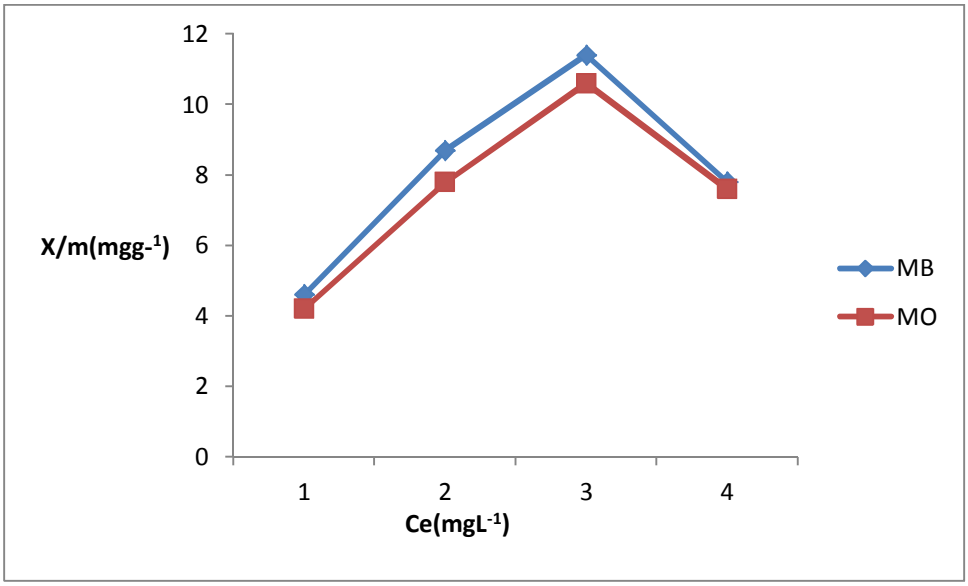


Figure 4.30(a): Adsorption isotherm of components of aqueous MBMO adsorbed onto CMAC

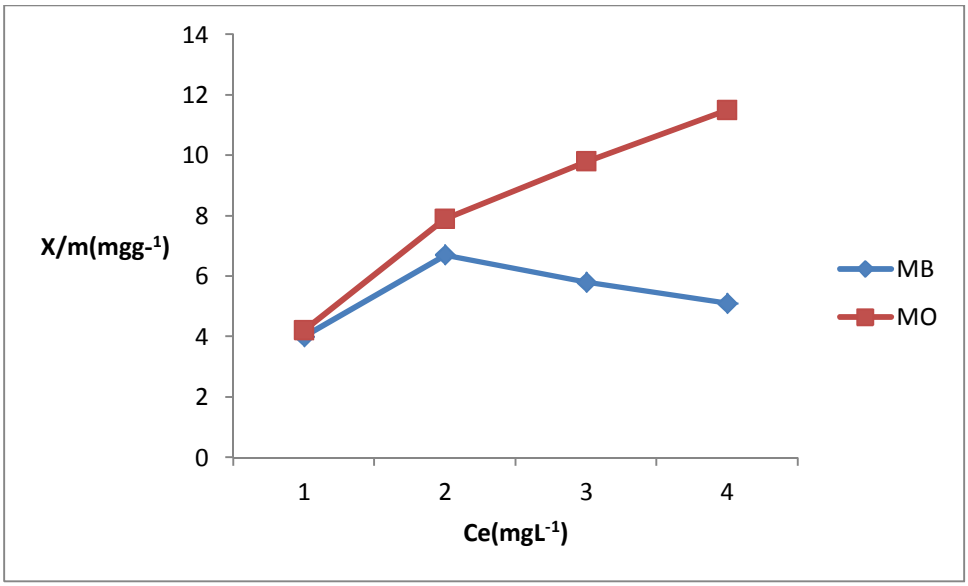


Figure 4.30(b): Adsorption isotherm of components of MBMO adsorbed from aqueous $Pb(NO_3)_2$ and $Cd(NO_3)_2.4H_2O$ mixture onto CMAC

In Figure 4.30(a), The adsorption curve for the two components is similar up to the 30ppm concentration. MB is slightly preferentially adsorbed compared to MO. This may be that the acidic surface of CMAC (pH = 3.66) affects or repels it more effectively than MB (due to it's small size). MB adsorption is also more time dependent; hence, the time factor also arises. The drop in the amount adsorbed at 40ppm suggests that as the concentration of the dyes increased, the degree of repulsion also increased which would not permit the dye species remain on the surface (i.e. desorption begins to occur). Since both dyes have a positive charge in solution.

In Figure 30(b), MO is preferentially adsorbed relative to MB. This is attributed to the presence of Cd^{2+} and Pb^{2+} which will also be simultaneously repelled by the acidic surface and because of the favourable size of MO. It is able

to have better access to the surface than the other species. Table 4.10 also confirms the above explanation where the average percentage of MO adsorbed is higher in aqueous $Pb(NO_3)_2$ and $Cd(NO_3)_2.4H_2O$ mixture, while the amount MB adsorbed is higher in aqueous medium.

Figures 4.31(a) and (b) are the adsorption isotherms for components of MBMO in aqueous and aqueous $Pb(NO_3)_2$ and $Cd(NO_3)_2.4H_2O$ mixture onto PMAC. In Figure 4.31(a) the isotherms for both components were the same at all concentrations. This is linked to the presence of active sites that may have been developed during the modification process for the matrix. Even though it's surface was acidic , the pH influence leading to repulsion of the components was over-ruled by the presence or availability of these sites and because of this the difference in their size did not play a major role in the results (i.e both the size and pH factors were reduced). It was the enhanced porous structure of the sample that was pronounce in this results.

In Figure 4.31(b), because of the presence of the other competing species for the available active sites, the size and pH factors came into play leading to the effective repulsion of MB which leads to a separation in the adsorption trend lines. This shows that MB adsorption is hindered more than MO in aqueous $Pb(NO_3)_2$ and $Cd(NO_3)_2.4H_2O$ mixture. Table 4.10 shows that the average percentage of both components adsorbed decrease in the aqueous $Pb(NO_3)_2$ and $Cd(NO_3)_2.4H_2O$ mixture

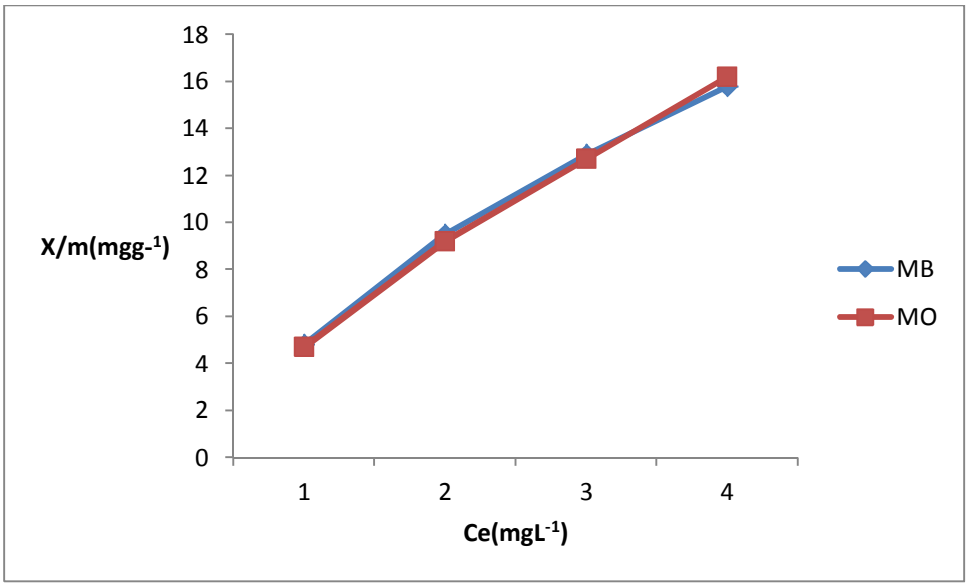


Figure 4.31(a): Adsorption isotherm of components of aqueous MBMO adsorbed onto PMAC

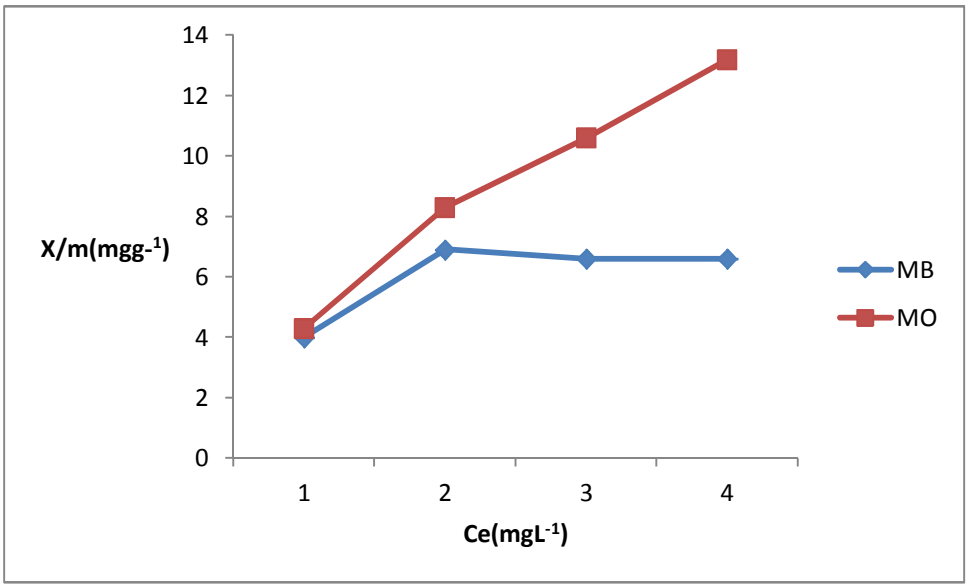


Figure 4.31(b): Adsorption isotherm of components of MBMO adsorbed from aqueous $Pb(NO_3)_2$ and $Cd(NO_3)_2.4H_2O$ mixture onto PMAC

4.6.2.2 Adsorption of components of MOIG from aqueous and aqueous $Pb(NO_3)_2$ and $Cd(NO_3)_2.4H_2O$ mixture

The graphs following are adsorption isotherms for the components of MOIG in both aqueous and aqueous $Pb(NO_3)_2$ and $Cd(NO_3)_2.4H_2O$ mixture.

Figures 4.32(a) and (b) are adsorption isotherms for components of MOIG onto UMAC in aqueous and aqueous $Pb(NO_3)_2$ and $Cd(NO_3)_2.4H_2O$ mixture. From Figures 4.32(a), it is observed that the adsorption isotherm for both MO and IG followed a similar pattern though the MO line was on the higher scale. Three distinct stages can be seen for the adsorption trends of both lines. First, there is a relatively steep rise, then a mild increase and then a steeper increase. This can be attributed to the rates of film-diffusion, intra- particle-diffusion and then diffusion to the active sites (Horsfall Jnr and Spiff, 2005). The difference being that the amount of MO adsorbed is more than IG. This can also be related to their size difference where MO is less bulky and more mobile than IG

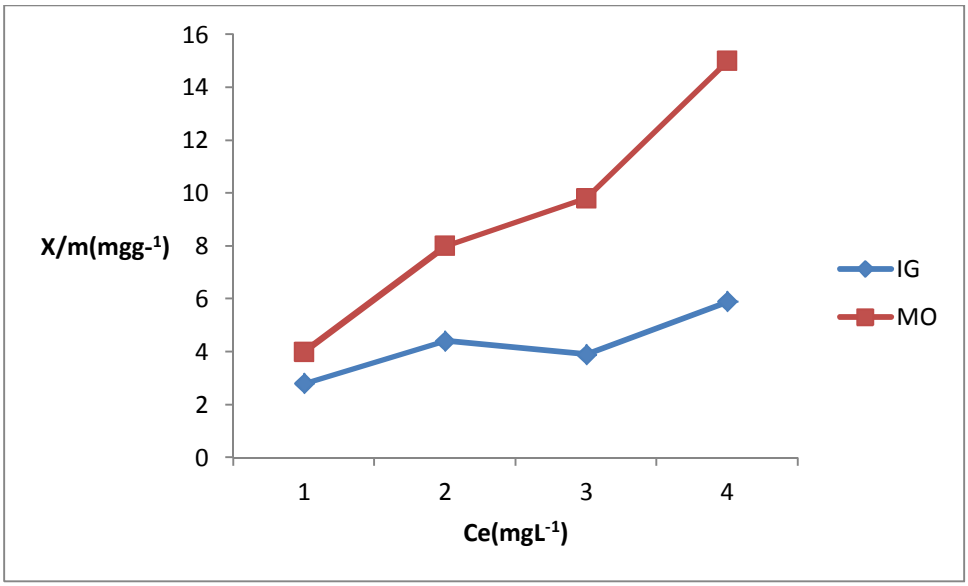


Figure 4.32(a): Adsorption isotherm of components of aqueous MOIG adsorbed onto UMAC

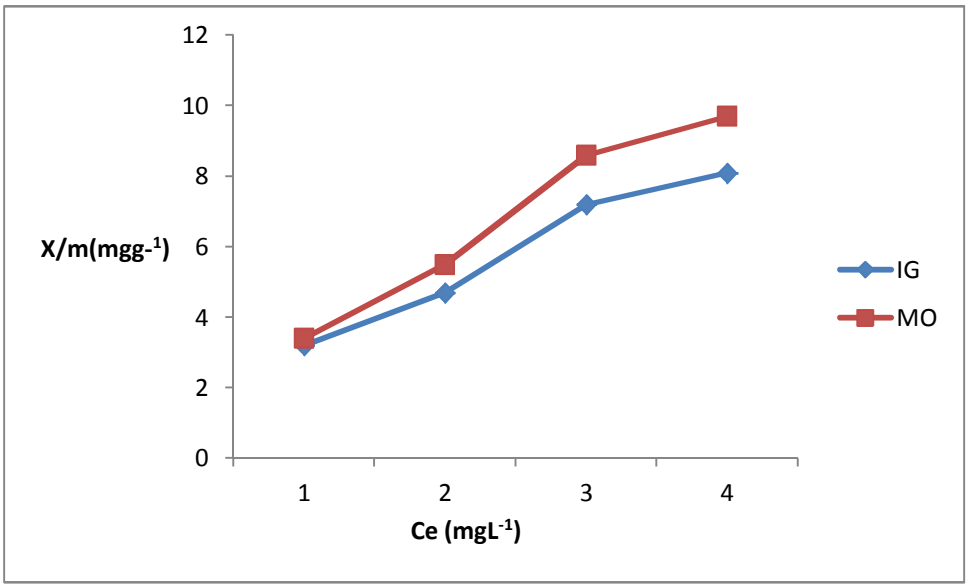


Figure 4.32(b): Adsorption isotherm of components of MOIG adsorbed from aqueous $Pb(NO_3)_2$ and $Cd(NO_3)_2.4H_2O$ mixture onto UMAC

Figure 4.32(b) is the adsorption trend for MOIG onto UMAC in a Cd/Pb nitrate environment. The trend is also similar to that in Figure 4.32(a) (i.e three stages) except that the graphs are steeper and the gap between the lines are narrower. This shows that the introduction of Cd^{2+} and Pb^{2+} into the aqueous medium lowers the difference in the amount between MO and IG. This is so because MO has a positive charge on it's skeleton which will lead to greater repulsion between the heavy metal ions in solution and itself. This will result in reducing the amount that would have been adsorbed if it was only in aqueous medium.

This interaction between MO and the Cd^{2+} and Pb^{2+}, will allow a greater amount of IG to be adsorbed ; though because of it's bulky size it doesn't overtake MO out rightly(i.e. due to steric hindrances). Hence, it can be said that while MO is slightly hindered in heavy metals environment, the presence of these same metal ions simultaneously enhance IG adsorption, indirectly. This can be clearly seen in the results in Table 4.11.

Table 4.11: Average percentage of components of MOIG adsorbed from both aqueous and Cd/Pb nitrate environment.

	UMAC		CMAC		PMAC	
	MO	IG	MO	IG	MO	IG
Aqueous	75	39	71	41	75	36
Cd/Pb nitrate	58	50	52	42	67	60

Figures 4.33(a) and (b) are adsorption isotherms for components of MOIG in aqueous, and aqueous $Pb(NO_3)_2$ and $Cd(NO_3)_2.4H_2O$ mixture onto CMAC. the observed trends in the two graphs are similar which shows a first steep rise followed by a mild increase. For Figure 4.33(a), the steep rise slants off at the 30ppm mark while for Figure 4.30(b), it slants at the 20ppm mark. This shows that there is more of both components adsorbed in the aqueous only medium than in the aqueous $Pb(NO_3)_2$ and $Cd(NO_3)_2.4H_2O$ mixture. This can be explained by the prence of Cd^{2+} and Pb^{2+} ions in solution in the latter which increases the competition for available sites. And with the positively charged CMAC surface, the repulsion for the charged species (in this case MO^+, Cd^{2+} and Pb^{2+}) is also increased which will turn out to favour IG adsorption. The results in Table 4.11 supports this.

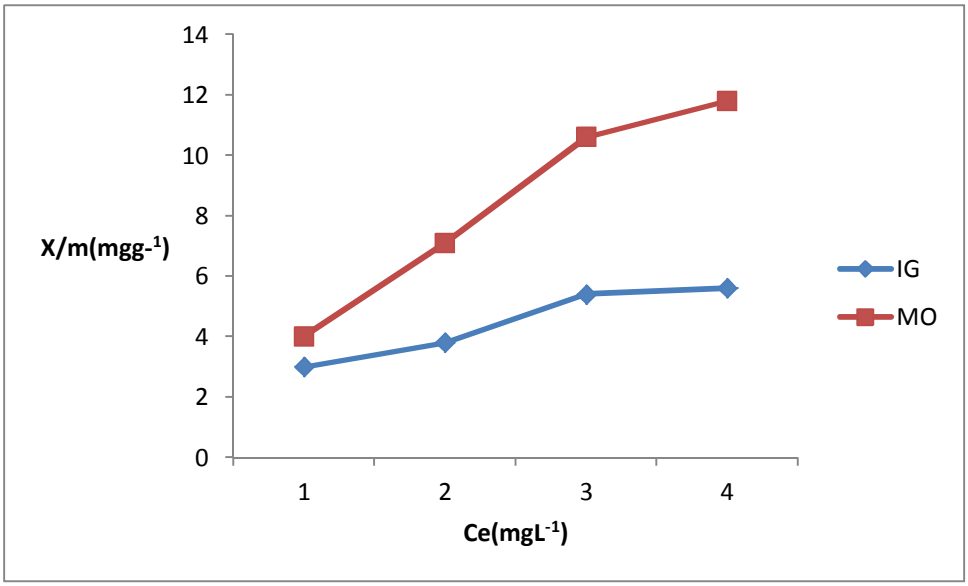


Figure 4.33(a): Adsorption isotherm of components of aqueous MOIG adsorbed onto CMAC

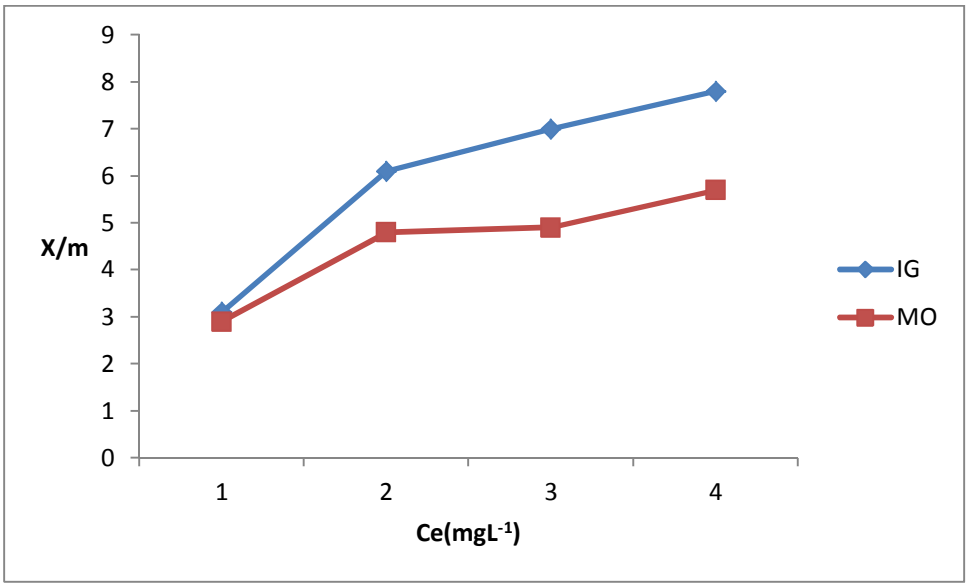


Figure 4.33(b): Adsorption isotherm of components of MOIG adsorbed from aqueous $Pb(NO_3)_2$ and $Cd(NO_3)_2.4H_2O$ mixture onto CMAC

Figures 4.34(a) and (b) are adsorption isotherms for components of MOIG in aqueous and aqueous $Pb(NO_3)_2$ and $Cd(NO_3)_2.4H_2O$ mixture onto PMAC. In Figure 4.34(a), the adsorption lines are straight lines for both components which depicts adsorption /absorbtion according to the "general type adsorption isotherms classification," while they can also be classified in the C – 1 class in the "system of isotherm classification." (Appendices vii and viii).

In Figure 4.34(b), the straight lines are slanted at the 20ppm mark. This is due to the presence of Cd^{2+} and Pb^{2+} ions which hinder the relative adsorption of both components. Though this still favours IG adsorption. From results in Table 4.11, IG has the best result in this scenario. This is because of the good porous

network structure of PMAC and also the electronic repulsions between MO and Cd^{2+} and Pb^{2+} which enhances it's adsorption.

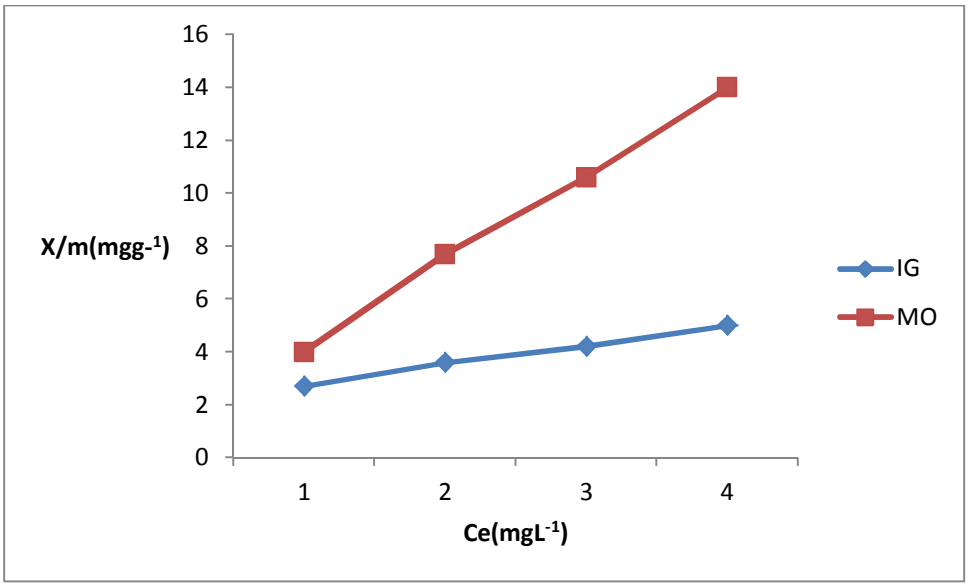


Figure 4.34(a): Adsorption isotherm of components of aqueous MOIG adsorbed onto PMAC

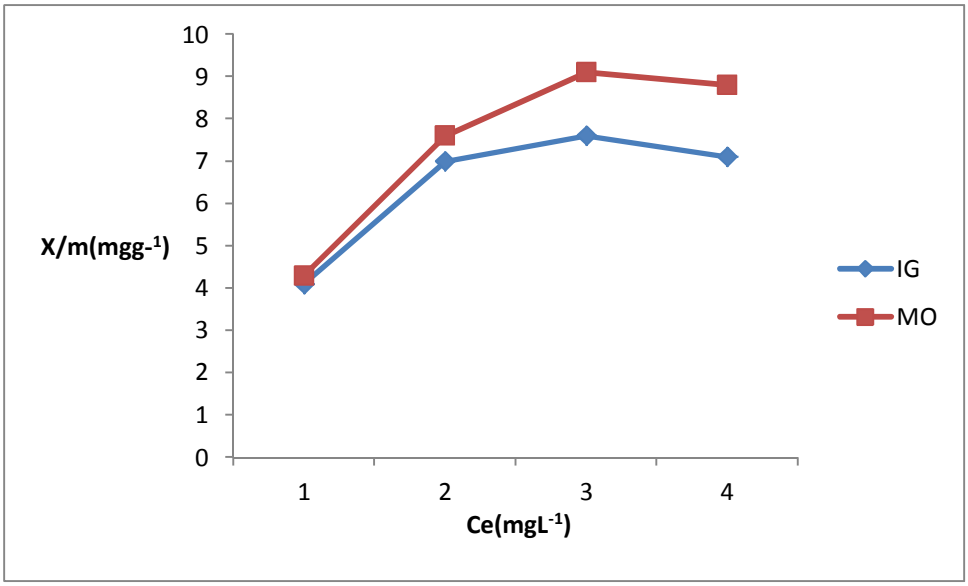


Figure 4.34(b): Adsorption isotherm of components of MOIG adsorbed from aqueous $Pb(NO_3)_2$ and $Cd(NO_3)_2.4H_2O$ mixture onto PMAC

4.7.0 Adsorption of components of MBMOIG from aqueous and aqueous $Pb(NO_3)_2$ and $Cd(NO_3)_2.4H_2O$ mixture

Adsorption of tertiary dye mixtures in both aqueous only and aqueous $Pb(NO_3)_2$ and $Cd(NO_3)_2.4H_2O$ mixture onto UMAC,CMAC and PMAC. The adsorption results can be seen in Figures 4.35(a), 4.35(b) and 4.35(c) respectively.

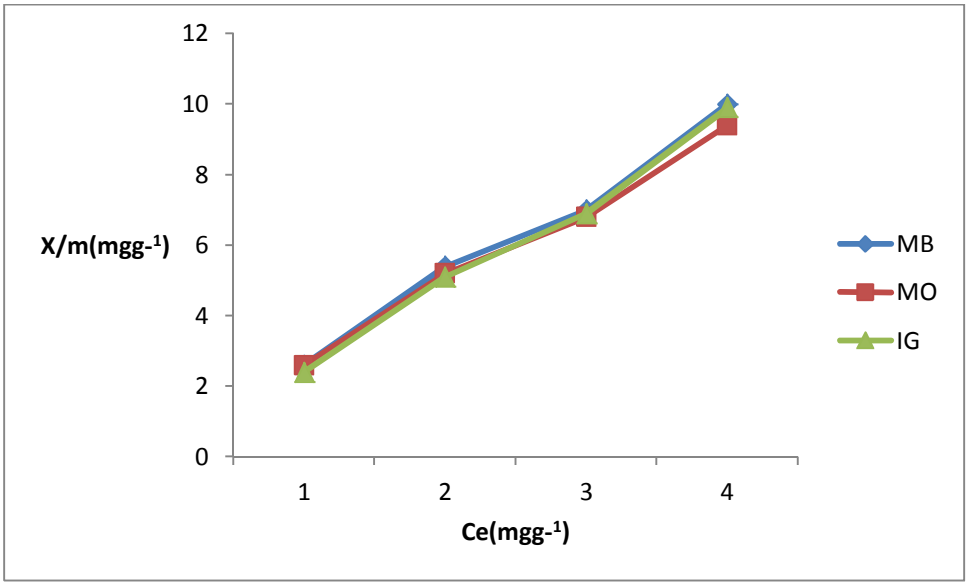


Figure 4.35(a): Adsorption isotherm of components of aqueous MBMOIG mixture onto UMAC

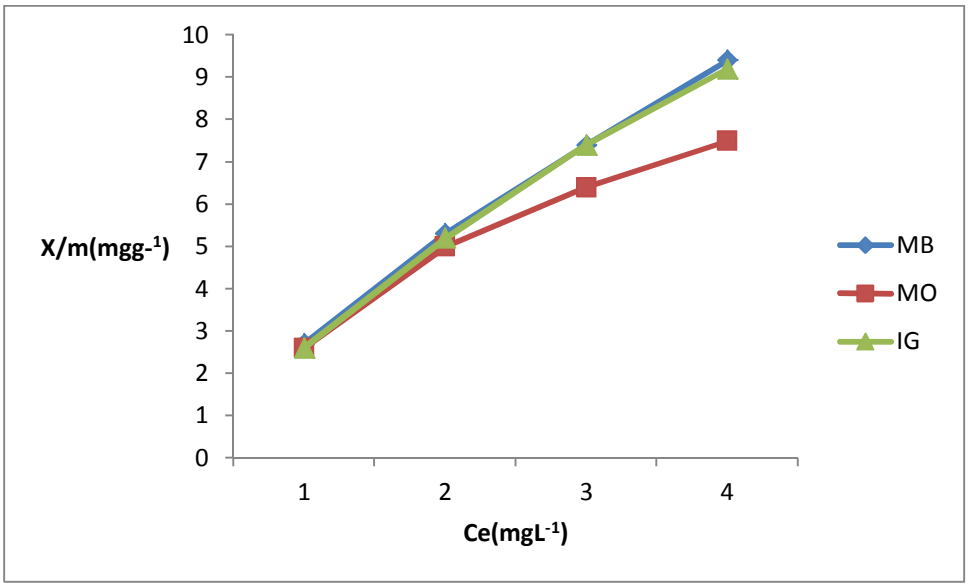


Figure 4.35(b): Adsorption isotherm of components of aqueous MBMOIG mixture onto CMAC

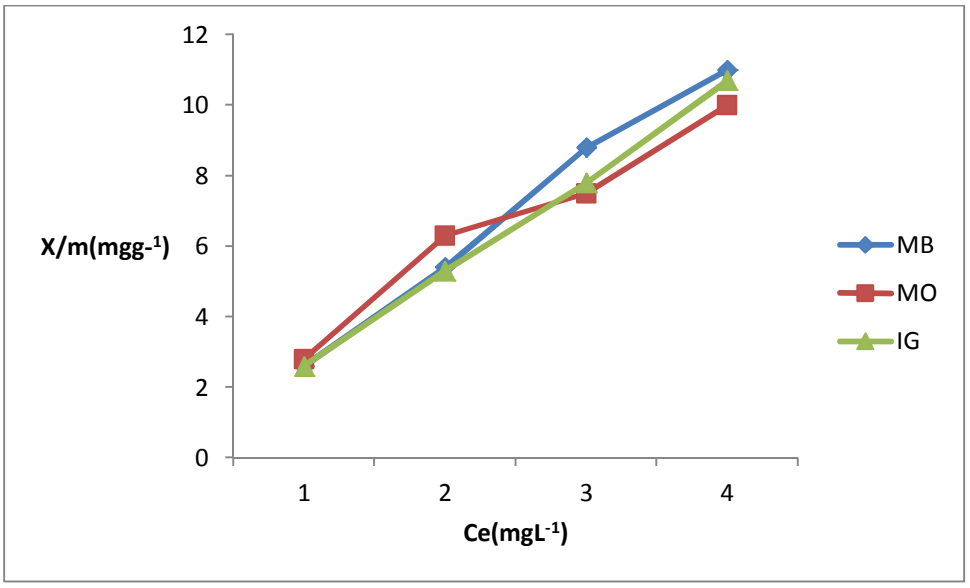


Figure 4.35(c): Adsorption isotherm of components of aqueous MBMOIG mixture onto PMAC

In Figure 4.35(a), it can be seen that the adsorption lines of the different components are similar with a steady increase for all. The lines tend to be linear which depicts adsorption/absorption in the general type of isotherm classification.(Weber Jnr, 1972). This is because in this set up, the amounts of the different components present in solution are the least compared to single and binary arrangements. So there is less of each component present for the available active sites which makes the competition less stiff.

Figure 4.35(b) is the adsorption isotherm for the components onto CMAC. Here, MB and IG give similar trend while MO slants at 20ppm mark. This can be attributed to the surface charge repulsion of CMAC for MO.where MB though is also positively charged, the degree of the repulsion for MO is more which leads to it's smaller amount being adsorbed compared to MB and IG especially as concentration is increased.

Figure 4.35(c) is the adsorption profile for the components onto PMAC. Here, each component follows a unique pattern to itself. This is the availability of enough active sites present for the components to exploit. Below is a table showing the percentage averages of the various components adsorbed onto the different matrices

Table 4.12 shows the average percentage of components of aqueous tertiary dye mixture (MBMOIG) adsorbed onto UMAC,CMAC and PMAC

Table 4.12: Average percentage components of aqueous tertiary dye mixture(MBMOIG) adsorbed onto UMAC,CMAC and PMAC

	MO	IG	MB	Average
UMAC	74	73	76	74
CMAC	69	74	76	73
PMAC	82	74	76	77
Average	75	74	76	

From Table 4.12, it can be seen that the component which is most affected by the changes in the different AC matrices is MO. It shows 74%, 69% and 82% adsorbed onto UMAC, CMAC and PMAC samples respectively. The IG and MB adsorbed is the same irrespective of the AC sample. On calculating the averages for each column, it can be seen that MB is preferentially adsorbed compared to MO and IG. The order of the amounts of each component onto the different matrices is MB > MO > IG while the order, when looking at the amounts adsorbed onto the different AC samples is shown to be PMAC > UMAC > CMAC.

Figures 4.36(a)–4.36(c) are adsorption isotherms for components of MBMOIG in Cd/Pb nitrate onto UMAC, CMAC and PMAC respectively. Here, the arrangement was different to what was obtained in the aqueous series arrangement. For these experiments 20mg of each sample was interacted with

$10cm^3$ of the separate concentrations; so there were more available active sites for the different components; hence, results were higher than those in the aqueous series. All the graphs were similar and linear.

For all the graphs, MO was preferentially adsorbed compared to the rest; though the differences are only slight. This set up shows the importance of how adsorbent dose and adsorbate concentrations can affect adsorption results. Table 4.13 shows the average percentage of the different components of MBMOIG adsorbed onto the different AC samples.

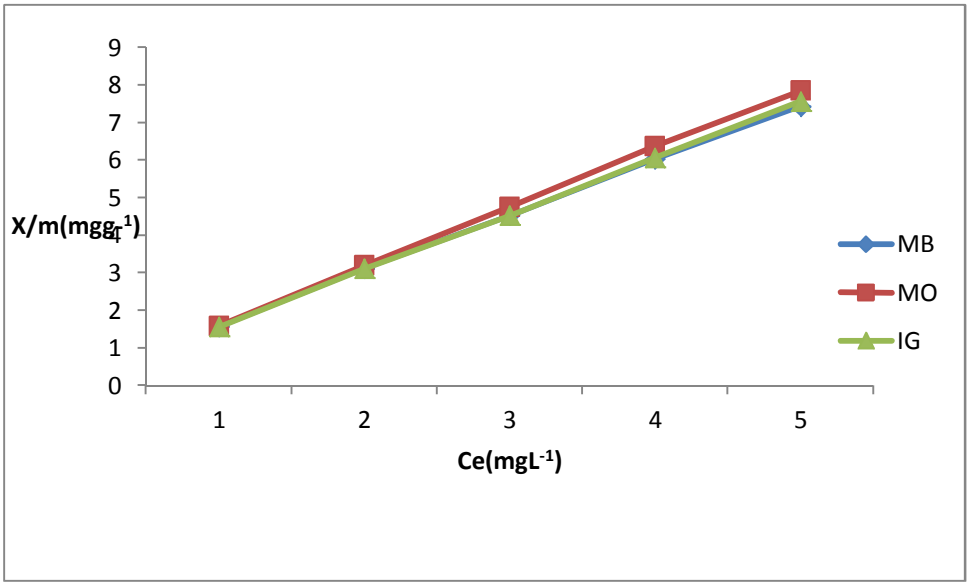


Figure 4.36(a): Adsorption isotherm of components of MBMOIG from aqueous $Pb(NO_3)_2$ and $Cd(NO_3)_2.4H_2O$ mixture onto UMAC

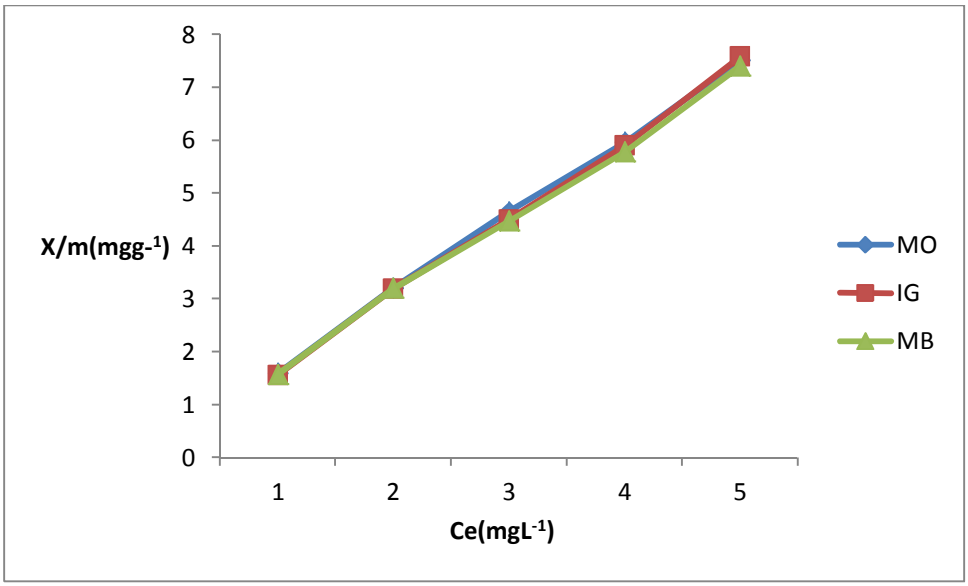


Figure 4.36(b): Adsorption isotherm of components of MBMOIG from aqueous $Pb(NO_3)_2$ and $Cd(NO_3)_2.4H_2O$ mixture onto CMAC

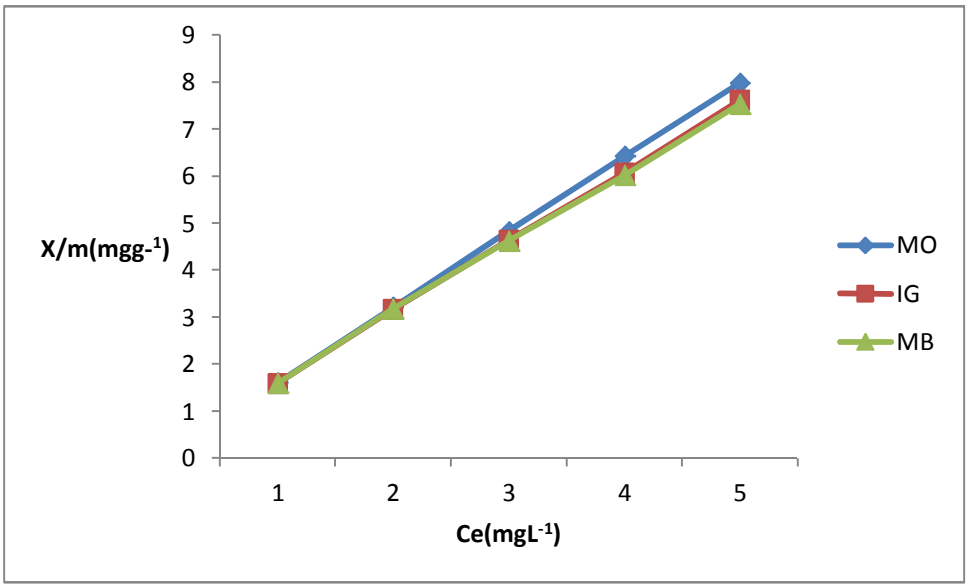


Figure 4.36(c): Adsorption isotherm of components of MBMOIG from aqueous $Pb(NO_3)_2$ and $Cd(NO_3)_2.4H_2O$ mixture onto PMAC

Table 4.13: Average percentage of components of MBMOIG aqueous $Pb(NO_3)_2$ and $Cd(NO_3)_2.4H_2O$ mixture adsorbed onto UMAC, CMAC and PMAC

	MO	IG	MB	Average
UMAC	94	92	92	93
CMAC	93	92	91	92
PMAC	97	93	93	94
Average	95	92	92	

From Table 4.13, the order of the average percentage of the different components adsorbed is MO > MB = IG, while the order with regards the performance of the different AC matrices is PMAC > UMAC > CMAC.

In summary, the adsorption of components slightly differs from what is observed in aqueous media (Table 4.12) in which the order of preferential adsorption of the different components is MB > MO > IG, while in both cases the performance of the different AC sample was PMAC > UMAC > CMAC.

4.8.0 Freundlich, Langmuir and Temkin constants

The Adsorption isotherm constants give important information about the adsorption processes. For the Freundlich isotherm, the *1/n* constant gives an idea of the adsorption intensity while K_f tells about the adsorbent's capacity. The R^2

values are the correlation coefficients which is a measure of how the experimental data fit into the different adsorption isotherms.

For the Langmuir isotherm, Q^o represents the monolayer adsorption capacity while *b* is indicative of the surface energy of the adsorption process. The Temkin constants are indicative of Chemisorption or Physisorption. The various graphs and table for the constants can be seen in the Appendices XII and XIII.

4.9.0 Adsorption of Real Textile Effluents onto AC samples

The textile effluent samples were randomly collected from CHELCO, textiles, Kaduna. They were coded TXT 1, TXT 2 and TXT 3.They were sieved through filter paper (Whattman no.1) and the filtrate were used after preparing 10, 20, 30 and 40% of the effluents using distilled water. The pH of the samples, the colour and their visible spectra were taken. The results are as follows:

Table 4.14: Colour and pH of textile effluent samples

	Colour	pH
TXT 1	Dirty green	6.49
TXT 2	Red	6.54
TXT 3	Emerald green	4.70

Figures 4.37, 4.38 and 4.39 are the visible spectra of the three different effluent samples. The all showed double peaks which were more pronounced at the 40% for TXT 1 and TXT 2. For TXT 3 sample, it was the 100% sample that gave the distinct peaks. This suggests that the effluent samples are binary dye mixtures. The wavelengths of absorption used for the different samples was in line with the peak values as given in Table 4.15.

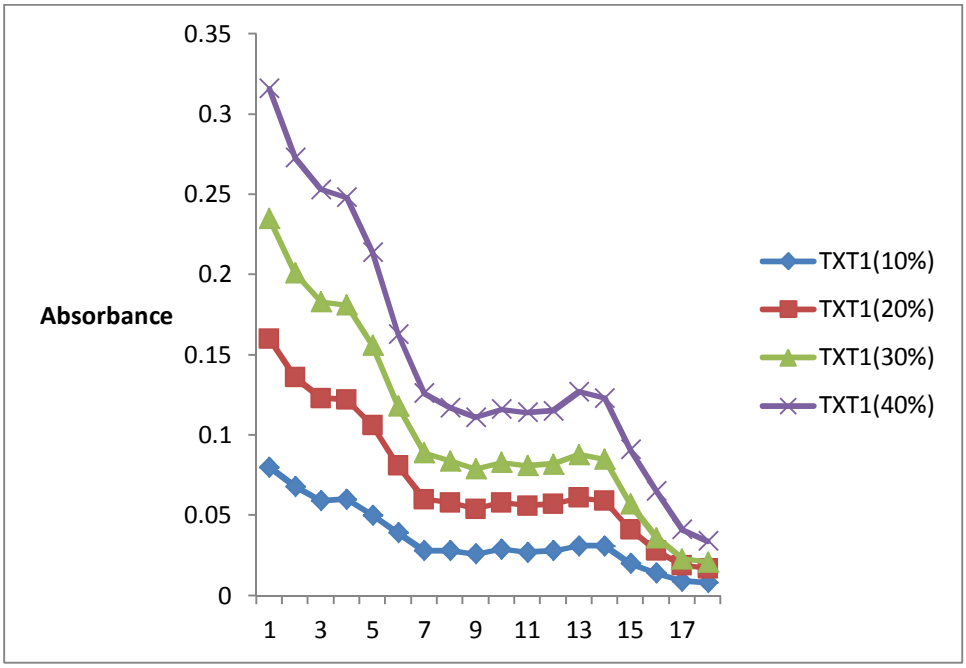


Figure 4.37: Visible spectra of TXT 1

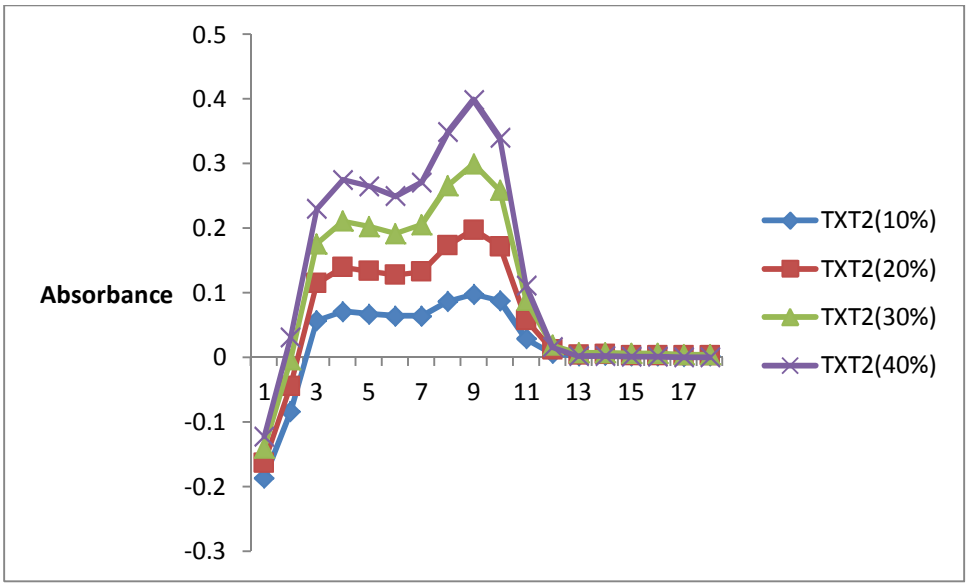


Figure 4.38: Visible spectra of TXT 2

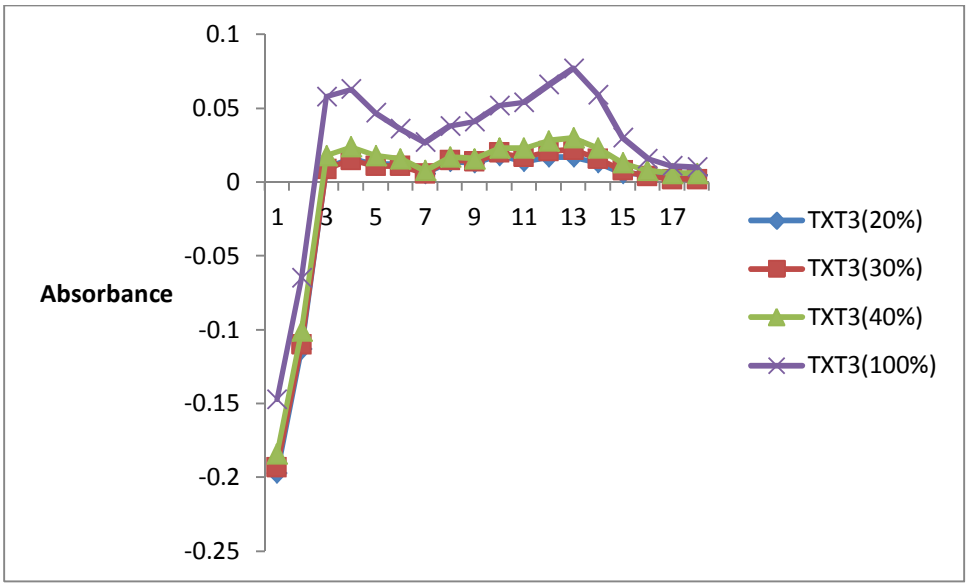


Fig4.39 : Visible Spectra of TXT3

Table 4.15: Wavelength of maximum (λ_{max}) absorption of effluents

Sample	Wavelengths (nm)	
TXT 1	380	620
TXT 2	440	540
TXT 3	440	620

Table 4.16 : Table of percentage of effluents adsorbed onto UMAC, CMAC and PMAC.

	TXT 1	
	380(nm)	620(nm)
UMAC	70	05
CMAC	02	04
PMAC	31	03
	TXT 2	
	440(nm)	540(nm)
UMAC	70	71
CMAC	72	71
PMAC	80	82
	TXT 3	
	440(nm)	620(nm)
UMAC	19	53
CMAC	36	68
PMAC	30	65

Figures 4.40, 4.41 and 4.42 are bar graphs representing the percentage of components of the various effluents adsorbed onto the various AC samples

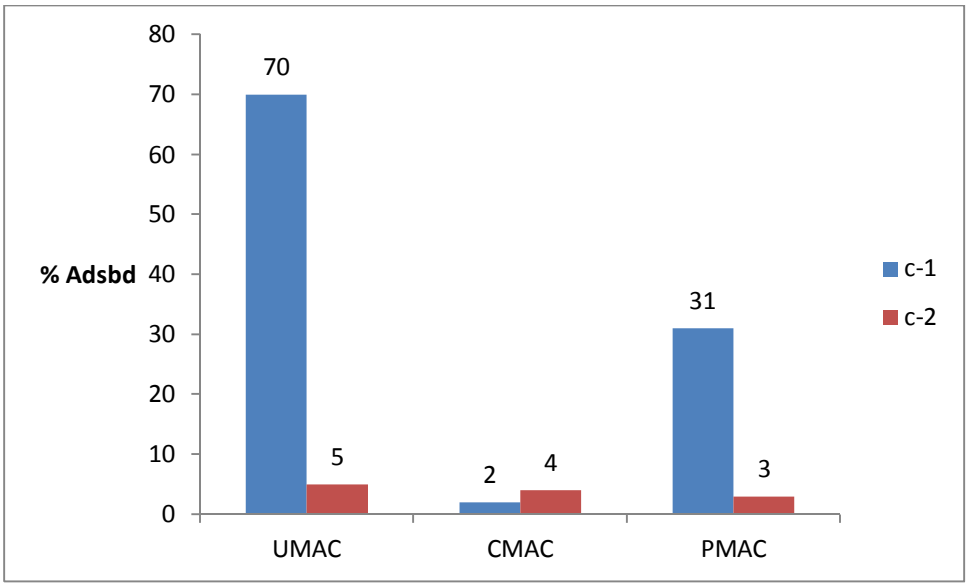


Figure 4.40: Percentage of components of TXT 1 adsorbed onto UMAC, CMAC and PMAC

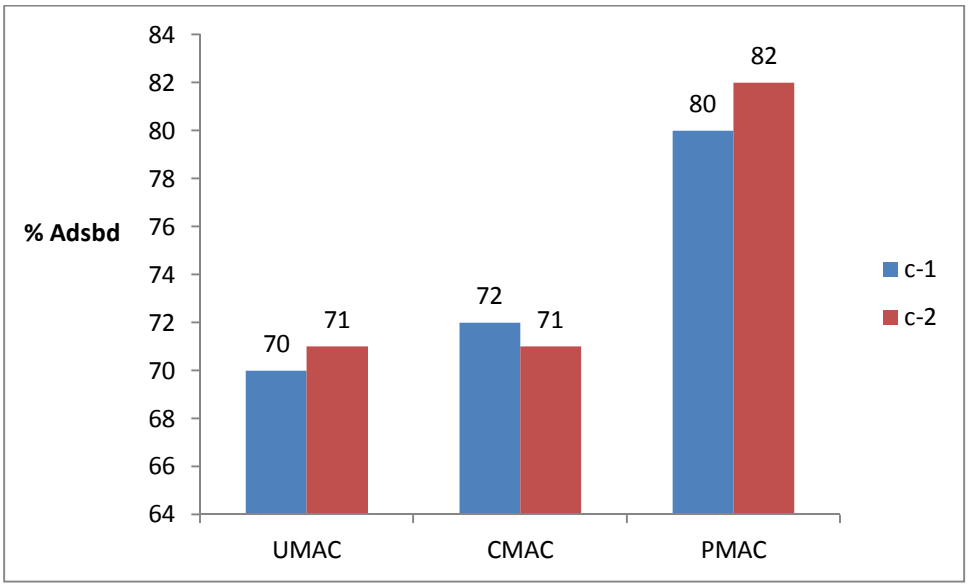


Figure 4.41: Percentage of components of TXT 2 adsorbed onto UMAC, CMAC and PMAC.

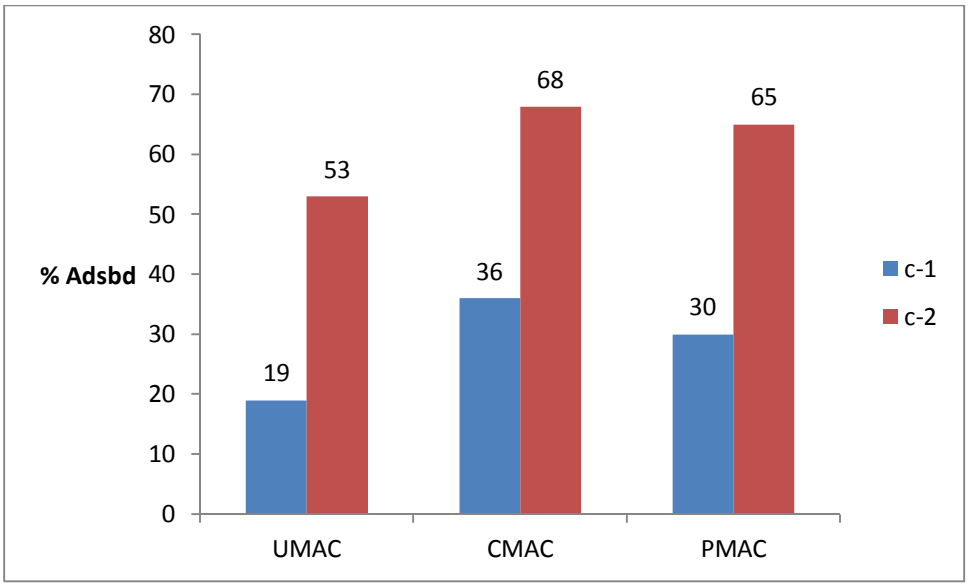


Figure 4.42: Percentage of components of TXT 3 adsorbed onto UMAC, CMAC and PMAC.

. In Figure 4.40, the adsorption range is between 2 – 70%. There was no precise pattern observed in the results. Adsorption onto CMAC was the least. PMAC did not perform appreciably following it's previous antecedents .

For Figure 4.41, the AC samples performed relatively better with the TXT 2 effluent sample with a general adsorption range of 70 – 82%. Here, PMAC gave better results compared to the others.

Figure 4.42 shows performances of the various AC samples where TXT 3 was the textile effluent sample. The general adsorption range was between 19 – 68% where the C-2 components were better adsorbed. Though the nature , quality and quantity of the species in the effluents were not investigated. It may be that the samples contain more than the two species that were observed from the visible

spectra. This is most likely the case where so many chemicals are involved in the production process of textiles which gives more components than we can see competing for the little available space on the adsorbent. This makes real effluent treatment difficult to handle.(Visa *et al.*, 2010)

CHAPTER FIVE

5.0. Summary, Conclusion and Recommendations.

5.1 Summary:

The work involved AC modification, preparation of simulated effluents and adsorption of the simulated and real effluents with the modified and unmodified AC samples.

The AC modification was done using simple techniques. For the chemical modification process, concentrated Nitric acid was used as the oxidizing agent, while for the physical modification, long term low temperature degassing was used where the temperature was 200^{o}C. The modification processes were meant to produce AC with opposing surface properties. The results showed that the chemical modification process achieved it's end by giving a product with pH of 3.42 from 7.23 which was the pH of the ummodified material.

The physically modified process did not achieve it's end; it rather produced an acidic surface with pH 4.66. Though it's performance was good. This modification method is a cleaner means of achieving the same end as that for the chemical modification process; since no reagent is used and only a relatively low temperature was employed.

Simulated effluents were prepared using various combinations of MB, MO, IG, $Pb(NO_3)_2$ and $Cd(NO_3)_2.4H_2O$; where a total of twenty two (22) systems were developed. Working range concentrations were established for the systems

at 0 -50 ppm for the dyes and their mixtures and 0.005 – 0.01M as concentrations for the heavy metal salts. The pH of the resultant systems fell within a 5.0 – 6.76 range which fell within range for the real textile effluent (pH 4.70 – 6.54). of which Three random samples were collected.

Adsorption studies was done using the batch mode of interaction, where experiments were done separately with the single dyes, binary dye mixtures and tertiary dye mixtures in both aqueous and aqueous heavy metal environment. The adsorption results show that results are unique to the effluent systems and AC sample involved. The factors responsible for these various results are:

1. The pH of the AC surface.
2. The pH of the simulated effluents / real effluents.
3. The size, shape and orientation of the adsorbate molecules.
4. The contact or residence agitation periods.
5. Adsorbate – adsorbate attraction or repulsions
6. Adsorbate – adsorbent attraction or repulsions
7. The porous network structure of the AC samples.

Initial rate experiments were conducted for the individual dyes from which it was observed that the percentage adsorbed as time increased for the different dyes was MO > MB > IG.

In single dye experiments, the general order of ranking for the amount of dye adsorbed on the different AC samples is PMAC > UMAC > CMAC.

In the binary dye system experiment, there were variations in observation which can be seen in the table below

Table 5.1 : preferentially adsorbed component and ranking of AC sample in binary dye system

System	Preferentially adsorbed	Ranking of AC sample
MBMO(Cd/Pb)	MB	PMAC>CMAC>UMAC
MBMO(Pb)	MO	CMAC>PMAC>UMAC
MBMO(Cd)	MB	PMAC>CMAC>UMAC
MOIG(Cd/Pb)	MO	PMAC>UMAC>CMAC
MOIG(Pb)	MO	PMAC>UMAC>CMAC
MOIG(Cd)	MO	PMAC>UMAC>CMAC

For the tertiary dye mixture the summary results can be seen in Table 5.2

Table 5.2: Order of component adsorbed and ranking of AC sample in tertiary dye mixtures.

System	Order for dye adsorbed	Ranking for AC sample
MBMOIG(aq)	MB>MO>IG	PMAC>CMAC>UMAC
MBMOIG(Cd/PB)	MO>MB=IG	PMAC>CMAC>UMAC

For adsorption of real effluents the amount of the components adsorbed onto the different matrices follows : TXT 2 > TXT 3 > TXT 1 while the ranking for the matrices is PMAC = UMAC > CMAC.

5.2 Conclusion.

This research work has shown that:

1. Long term low temperature degassing is a good means of improving existing AC samples which can be employed for adsorption of dyes and real textile effluents
2. The size, shape and orientation of adsorbate molecules plays a major role in adsorption studies; though other factors are also involved
3. MB depends more on time as a factor for it's maximum adsorption.
4. The adsorption of the individual dyes (i.e. MB, MO and IG) is mainly chemisorptions as seen from the rate experiment.
5. The sorption process for the dyes involved is particle - diffusion controlled.
6. The environment in which dyes exist in plays a significant role in which dye will be preferentially adsorbed when in binary or tertiary dye mixtures.
7. Heavy metals in solution can enhance or hinder the uptake of components of dye mixtures .
8. The AC samples can be used for treatment of real textile effluents.

5.3 Recommendations

The following is recommended for further studies:

1. Carry out long term low temperature degassing both in an inert environment and air-circulating situations.
2. Carry out detailed kinetic and thermodynamic studies for the dyes in this work and their mixtures both in aqueous only and heavy metal environment.
3. Look at effect of pH on the adsorption profiles of these dyes and their mixtures in both aqueous only and aqueous heavy metal environment.
4. Carry out adsorption studies for lead and cadmium ions when present in dye environment.
5. Carry out adsorption studies at lower concentrations of the dyes and lower doses of the AC samples.
6. Carry out adsorption of these dyes when other heavy metals are involved e.g. chromium, iron, mercury… etc
7. Blending of the AC samples with other suitable adsorbents to make them more versatile
8. Look more into the chemical species of the textile effluents involved.

References

Abdulrasaq, O.O.and Basiru,O.G.(2010). Removal of copper(II), iron(III) and lead(II) ions from mono-component Simulated Waste effluent by Adsorption on Coconut Husk. *African Journal of Enviromental Science and Technology*. 4(6): 382-387.

Abechi, E.S., (2006). Adsorption characteristics of titanium(IV) and zinc(II) oxide coated activated carbon from walnut shell and sawdust. An M.Sc. thesis, Dept. of Chemistry, ABU- Zaria.

Abechi,E.S., (2011). Kinetics and Thermodynamic studies of the adsorption of methylene blue onto activated carbon prepared from palm kernel shell. A Ph.D dissertation, Dept. of Chemistry, ABU- Zaria.

Abram, J.C. (1973). The characteristics of activated carbon. Papers and proceedings of a *Water Research Association Conference*, University of Reading, 3rd – 5th April, 1973. The Water Research Association, England.

Aggarwal, D. (1998). Ph.D dissertation , Panjab University. In: Bansal, R.C. and Goyal, M. (Ed)(2005) *Activated Carbon*, CRC press . pp 44.

Aksu, Z. and Donmez, G. (2003). *Chemosphere*, 50: 1075-1083. In: Kathiresan, S., Vinoth, M., Lim, H.Y., Xavier, R., Marimuthu, K., Sreeramanan S. and Mas Rosemal, H.M.H. (2010). Removal of Methyl Orange from solutions using yam leaf Fibers. *Int. J. of ChemTech Res*, 2(4): 1892-1900.

Argaman, Y. and Weddle,C.L. (1973). *Alchem Symposium Series*. In: Bansal, R.C. and Goyal, M. (Ed)(2005) *Activated Carbon*, CRC press . pp 299

Atkins, P.W.(1999). *Physical Chemistry*. 6th edition , Oxford University Press. Pp 857-864.

Bansal, R.C. and Goyal, M. (Ed) (2005) *Activated Carbon*, CRC press.

Bari, M.B., (2010). Methyl orange adsorption unto phosphoric acid activated carbon from *Delonix regia* pods , A B.Sc project, Dept. of Chemistry, ABU- Zaria.

Cenens, J. and Schoonheydt, R.A. (1988). Visible Spectroscopy of methylene blue on Hectorite, Laponite B and Barasym in aqueous suspension. *Clay and Clay minerals*. 36(3): 214-224.

Cheng, J., Subramanian, K., Chakrabati, C., Guo, R., Ma, X., Lu, Y. and Pickering, W.F., (1993) *Jour. Environ. Scie. Health.A*., 28:51. In: Bansal, R.C. and Goyal, M. (Ed)(2005) *Activated Carbon*, CRC press . pp 351.

Cheremisinoff, P. and Ellerbusch, F.(1978). *Carbon Adsorption Handbook* , Ann Arbor Science Publishers Inc. pp 72, 689-690.

Cheremisinoff,P.N. and Habib,Y.H.(1972). *Water Sewer Works*. In: Bansal, R.C. and Goyal, M. (Ed) (2005) *Activated Carbon*, CRC press . pp 299.

Chiou, M.S. and Chuang, G.S. (2006) *Chemosphere* 62, 731 -740. In: Deinz, F. and Saygideger, S.D. (2010) Equilibrium, kinetic and thermodynamic studies of Acid Orange 52 dye biosorption by *Paulownia tomentosa* Steud. Leaf powder as a low-cost natural adsorbent. *Bioresource Technology*, 101, 5137-5143.

Corapcioglu, M.D. and Huang, C.P.(1987). *Water Res.*, 21:1031. In: Bansal, R.C. and Goyal, M. (Ed) (2005) *Activated Carbon,* CRC press . pp 351.

Daintith, J. (2000). *A Dictionary of Chemistry*, 4th edition. Oxford University Press.

Deinz, F. and Saygideger, D. (2010) Equilibrium, kinetic and thermodynamic studies of Acid Orange 52 dye biosorption by *Paulownia tomentosa* Steud. Leaf powder as a low-cost natural adsorbent. *Bioresource Technology* 101, 5137-5143.

Dika, J.,(2009). Adsorption studies of activated carbon from coconut shell, sawdust and combined precursor matrices. A B.Sc project, Dept. of Chemistry, ABU- Zaria

Dobrowolski,R., Jaroniec,M., and Kosmulski, M.,(1986). *Carbon*, 24:15 in Bansal, R.C. and Goyal, M. (Ed) (2005) *Activated Carbon*, CRC press . pp 301.

Garg, V.K, Gupta, R., Yadav, A. and Kumar, K. (2003) Dye removal from aqueous solution by adsorption on treated sawdust. *Bioresource Technology*, 89:121-124.

Gaur,V. and Shankar, P.A.,(2008). Surface Modificatioin of Activated Carbon for the removal of water impurities. *Water Conditioning and purification*.

Gimba, C.E. (2001). Preparation and adsorption of activated carbon from coconut shell. Ph.D dissertation, Dept. of Chemistry, ABU- Zaria.

Gimba,C.E., Ocholi, O., Egwaikhide, P.A., Muyiwa, T., and Akporhonor, E.E.,(2009). New material for activated carbon . I. Methylene blue adsorption on activated carbon prepared from *Khaya senegalensis* fruits. *Jour. Of agricultureand natural resources*, 36(1):107-114.

Goyal, M. and Bansal, R.C.(1997). Symposium on Porous Carbons. In: Bansal, R.C. and Goyal, M. (Ed) (2005) *Activated Carbon*, CRC press . pp 44.

Goyal, M.,Bansal, R.C. and Rattan, V.K. (1999) *Indian jour. Chem. tech.* 6:305 In: Bansal, R.C. and Goyal, M. (Ed) (2005) *Activated Carbon*, CRC press . pp 44.

Goyal, M.,Bansal, R.C. , and Aggarwal, D., (1989) *Carbon*, 37. In: Bansal, R.C. and Goyal, M. (Ed) (2005) *Activated Carbon,* CRC press . pp 44.

Goyal, M.,Bansal, R.C., Rattan, V.K., and Aggarwal, D. (2001). Colloids and surfaces. *A Physico-chemical and Engg aspects,*190: 229. In: Bansal, R.C. and Goyal, M. (Ed) (2005) *Activated Carbon,* CRC press . pp 44.

Graham, D.(1955). *Jour. Phys.Chem*. 59: 896. In: Bansal, R.C. and Goyal, M. (Ed) (2005) *Activated Carbon*, CRC press . pp 154.

Griffiths, J. (1986). Introduction: The Evolution of Present-Day Dye Technology in: Waring, D.R. and Hallas, G.(Ed) *The Chemistry and Application of Dyes*. Plenum Press, New York and London. pp 1

Gupta, V.K., Jain, R., Varshney, S. and Saini, V.K. (2007). *J. Colloid Interface Sci.* In: Kathiresan, S., Vinoth, M., Lim, H.Y., Xavier, R., Marimuthu, K., Sreeramanan S. and Mas Rosemal, H.M.H. (2010). Removal of Methyl Orange from solutions using yam leaf Fibers. *Int. J. of ChemTech Res*. 2(4): 1892-1900.

Guzel, F., (1996). Sep. Sci. Technol., 31:283 In: Bansal, R.C. and Goyal, M. (Ed) (2005) *Activated Carbon*, CRC press . pp 421.

Hameed, B.H., Din, A.T.M., and Ahmad,A.L.,(2007). Adsorption of methylene blue onto Bamboo-based activated carbon: kinetic and equilibrium studies. *J. Hazard Matter*. 141(2007) 819-825.

Hameed, B.H., Mahmoud, D.K. and Ahmad, A.L., (2008). *J. Hazard Matter*. In: In: Sreeramanan, S.,Vinoth, M., Xavier, R., Marimuthu, K., Mas Rosemal, H.M.H. and Kathiresan, S. (2010) Removal of methyl orange from solutions using yam leaf fibres. *Int. J. of ChemTech Research.* 2(4): 1892 – 1900.

Hartman, J.R. (1974). *Colloid Chemistry*, Houghton Mifflin Company, Cambridge. pp 47-51.

Hestekin, J.A., Bhattacharrya, D., Sikdarand, S.K. and Kim, B.M. (1998). Membranes for treatment of hazardous wastewater, In: R.A. Meyers (ed), *Encyclopedia of Environmental Analysis and Pre-mediation*, John Wiley and Sons Inc.

Ho, S.Y., Wase, D.A.J. and Forster, C.F. Water Res. (1995) 29:1327. In: Horsfall Jnr, M. and Spiff, A.I.(2005). Kinetics of the sorption of Pb^{2+} and Cd^{2+} from aqueous solutions by *C. bicolor* biomass. *Bull. Chem. Soc. Ethiop.*19(1): 88-102.

Horsfall Jnr, M. and Spiff, A.I.(2005). Kinetics of the sorption of Pb^{2+} and Cd^{2+} from aqueous solutions by *C. bicolor* biomass. *Bull. Chem. Soc. Ethiop.*19(1): 88-102.

Huheey, J.E. (1972). *Inorganic Principles of structure and Reactivity*. Harper and Row Publishers New York, Evanston, San Francisco . pp201.

Huang, C.P. and Ostovic , F.(1978). *Jour. Enviroment Engg*. In: Bansal, R.C. and Goyal, M. (Ed)(2005) *Activated Carbon*, CRC press . pp 301.

Ishizaki,C., Marti,I. and Ruiz, M. (1983). In: *Advances in Chemistry*; No 202 I.H. Suffet and M.J. Mc Guire (Ed) Amer. Chem. Soc. Washington D.C. pp 95. In: Bansal, R.C. and Goyal, M. (Ed)(2005) *Activated Carbon*, CRC press. pp 375.

Kadrivelu, K., Kavipriya, M., Karthika, C., Radhika, M., Vennilamani, N. and Pattabhi, S. (2003). Utilization of various agricultural wastes for activated carbon preparation and application for the removal of dyes and metal ions from aqueous solutions. *Bioresource Technology*, 87: 129-132.

Kannan, N., and Meenakshisundaram, M. (2002). Adsorption of Congo red on Activated Carbons: A comparative Study. *Water, Air and Soil Pollution*, 138: 289-305.

Karanfil, T., Kitis, M., Kilduf, J.E. and Wigton, A. (1999). *Environ.Sci. Technol.* 33: 3225. In: Bansal, R.C. and Goyal, M. (Ed)(2005) *Activated Carbon*, CRC press. pp 384.

Kipling, J.J (1965). *In Adsorption from Solution from Electrolytes*. Academic Press. Newyork. In: Bansal, R.C. and Goyal, M. (Ed)(2005) *Activated Carbon,* CRC press . pp 44.

Kipling, J.J. and Gasser, C.G (1960). In: Proc. 4th conf. on carbon, Univ. of Buffalo, Pergamon Press . New York. In: Bansal, R.C. and Goyal, M. (Ed) (2005) *Activated Carbon*, CRC press . pp 45.

Kipling, J.J. and Tester, D.A.(1952), *J. Chem. Soc.*, London , pp 4123 in Bansal, R.C. and Goyal, M. (Ed)(2005) *Activated Carbon*, CRC press . pp 45.

Langmuir, I.,(1918). *Jour.Amer. Chem. Soc* . 40(1): 1361 in Bansal, R.C. and Goyal, M. (Ed) (2005) *Activated Carbon*, CRC press . pp 78.

Leechart, P., Nakbanpote, W. and Thiravetyan, P. (2009). *J. Environ. Manage*. In: Vinoth, M., Xavier, R., Marimuthu, K., Sreeramanan, S., Mas Rosemal, H.M.H. and Kathiresan, S. (2010). Removal of methyl orange from solutions using yam leaf fibres. *Int. J. of ChemTech Research,* 2(4): 1892 – 1900.

Linstedt,K.D., Houck,C.P. and O'Conner, J.T. (1971). *Jour.Water Poll. Control.Fed.* In: Bansal, R.C. and Goyal, M. (Ed) (2005) *Activated Carbon*, CRC press . pp 299.

Meevasana K. and Pavasant P. (2008). Quantitative measurement techniques for binary dye mixtures : a case study in an adsorption system. *ScienceAsia*, 34: 390-394.

Netzer, A. and Hughes, D.E.(1984). Water Res., 18:927. In: Bansal, R.C. and Goyal, M. (Ed) (2005). *Activated Carbon*, CRC press . pp 351.

Newcomb, G.(1999). Water Sci. Technol, 40:191. In: Bansal, R.C. and Goyal, M. (Ed)(2005) *Activated Carbon*, CRC press. pp 385.

Ocholi, O. (2001). Studies on cyanide binding in micro-columns with activated carbon matrix from groundnut and coconut shells. A B.Sc. project, Dept. of Chemistry, ABU- Zaria.

Ocholi, O.(2006). Studies on the preparation and adsorption of activated carbon matrices from *Delonix regia* pods and *Khaya senegalensis* fruits. An M.Sc. thesis, Dept. of Chemistry, ABU- Zaria.

Okpe, J.O., (2010). Methylene blue adsorption unto phosphoric acid activated carbon from *Delonix regia* pods , A B.Sc. project, Dept. of Chemistry, ABU- Zaria.

Ong, S., Lee, W., Keng, P., Lee, S. and Hung, Y.(2010). Optimization of basic and reactive dye uptakes in binary dye solution using statistical

experimental methodology. *International Journal of the Physical Sciences*. 5(14): 2171-2178.

Özacar M. and Şengil İ.A. (2005). Adsorption of metal complex dyes from aqueous solutions by pine sawdust. *Bioresource Technology*, 96: 791-795.

Puri , B.R. (1981). In: *Activated Carbon Adsorption*, Suffet,I.H. and McGuire, M.J.(Ed) Ann Arbor Science Publishers. pp 353. In: Bansal, R.C. and Goyal, M. (Ed) (2005) *Activated Carbon,* CRC press . pp 44.

Qin, F., Wen, B., Shan, X., Xie, Y., Liu, T., Zhang, S. and Khan, S.U. (2006). Mechanisms of competitive adsorption of Pb, Cu and Cd on peat. *Environmental Pollution*, 144: 669-680.

Quinlivan,P.A.,(2001). Effects of activated carbon surface chemistry and pore structure on the adsorption of methyl tertiary- butyl ether and trichloroethene from natural water. An M.Sc thesis, Dept. of Civil Engineering/Water Resources and Enviromental Engineering,North Carolina State University.

Ribeiro, M.H.L., Lourenco, P.A.S., Monteiro, J.P. and Ferroira-Dias, S. (2001). Kinetics of selective adsorption of impurities from a crude vegetable in hexane to activated earths and carbon. *Euro Food Res. Tech*, 213: 132-138.

Saffaj, N., Loukili, H., Younssi, S.A., Albizine A., Bouhria, M., Persin, M., and Larbot, A. (2004). Filtration of solution containing heavy metals and dyes by means of ultrafiltration membranes deposited on support made of Moroccan clay. *Desalination*,168: 301-306.

Sarin, V., Sarvinder, S. and Pant, K.K. (2006). Thermodynamic and Breakthrough column studies for the selective sorption of chromium from industrial effluent on activated . *Bioresource Technology*, 97: 1986-1993.

SIGMA (1991). Biochemicals, Organic Compounds for Research and Diagonistic Reagents. SIGMA Chemical Company.

Siyaka, Z.M. (2000). Comparative studies on the adsorption of azodyes using activated carbon arachis hypogeal and cocos nucifera shells. A B.Sc thesis, Dept. of Chemistry, ABU- Zaria.

Skanthakumar, S., Wilson, R.E., Sigmon, G., Burns, P.C. and Soderholm, L. (2007) Structures of Dimeric Hydrolysis products of Thorium. *Inorg. Chem*., 46(7): 2368.

Taylor, R.M., and Kuennen, R.,(1994). *Environ. Prog.*, 13:65. In: Bansal, R.C. and Goyal, M. (Ed)(2005) *Activated Carbon*, CRC press . pp 351.

Thomas, J.W., and Crittenden, B. (1998). *Adsorption technology and design*, Butterworth Heinmann. pp1-51.

Vasu, E.A.,(2008). Surface Modification for Activated Carbon for enhancement of Nickel(II) Adsorption.*E-Journal of Chemistry,* 5(4): 814-819.

Vinod, V.P. and Anirudhan, T.S. (2001). *J. Chem. Technol. Biotechnol.* In Horsfall Jnr, M. and Spiff, A.I.(2005). Kinetics of the sorption of Pb^{2+} and Cd^{2+} from aqueous solutions by *C. bicolor* biomass. *Bull. Chem. Soc. Ethiop.*19(1): 88-102.

Visa, M., Bogatu, C. and Duta, A. (2010). Simultaneous adsorption of dyes and heavy metals from multicomponent solutions using fly ash. *Applied surface Science* . article in press. DOI: 10.1016/j.apsusc.2009.12.145

Weber, W.J.Jnr. (1972) *Physicochemical processes for water quality control*. Wiley-Interscience, London. pp 199-245.

Yasin Y., Hussein, M.Z. and Ahmad, F. (2007). Adsorption of methylene blue onto treated activated carbon. *The Malaysian Journal of Analytical Sciences,* 11(11): 400-406.

Yileng,M.T.(2008). Adsorption of Pesticides unto Activated carbon from *Canarium Schweinforthii*. An M.Sc thesis, Dept. of Chemistry, ABU-Zaria.

Appendices

Appendix I(a): Table of pH measurements of dye and heavy metal solutions

	Conc(ppm)	pH1	pH2	pH3	Average
MB	10	6.76	6.65	6.43	6.61
	20	6.58	6.55	6.27	6.47
	30	6.58	6.48	6.23	6.43
	40	6.67	6.52	6.27	6.49
	50	6.69	6.69	6.35	6.58
MO	10	6.41	6.50	6.51	6.47
	20	6.49	6.44	6.38	6.44
	30	6.50	6.57	6.48	6.52
	40	6.39	6.57	6.40	6.48
	50	6.55	6.56	6.45	6.52
MBMO	10	6.30	6.34	6.41	6.35
	20	6.30	6.28	6.32	6.30
	30	6.26	6.28	6.22	6.29
	40	6.33	6.32	6.33	6.33
	50	6.32	6.36	6.30	6.33
	Conc(M)				
Lead nitrate	0.01	5.29	5.33	5.31	5.31
	0.02	5.15	5.18	5.14	5.16

	0.03	5.12	5.16	5.17	5.15
	0.04	5.00	5.05	5.07	5.04
	0.05	5.09	5.12	5.12	5.11
Cadmium nitrate.X	0.01	6.13	6.27	6.16	6.19
	0.02	6.14	6.21	6.02	6.12
	0.03	6.07	6.18	5.99	6.08
	0.04	6.07	6.07	5.89	6.01
	0.05	6.00	6.04	5.85	5.96
Lead/Cadmium nitrate	0.01	5.32	5.37	5.38	5.36
	0.02	5.41	5.42	5.36	5.40
	0.03	5.31	5.32	5.29	5.31
	0.04	5.27	5.27	5.27	5.27
	0.05	5.23	5.23	5.20	5.22
Dye/Heavy metal mixture	10/0.01	5.59	5.63	5.65	5.62
	20/0.02	5.49	5.50	5.57	5.52
	30/0.03	5.35	5.49	5.39	5.41
	40/0.04	5.39	5.40	5.41	5.40
	50/0.05	5.35	5.36	5.37	5.36

Appendix I(b): pH of Textile Effluent Samples.

Sample	pH
TXT 1	6.49
TXT 2	6.54
TXT 3	4.70

Summary of pH readings, midpoints and ranges for dye and heavy metal solutions and mixtures

	Range	Mid point	Difference
MB	6.52-6.76	6.64	0.24
MO	6.39-6.57	6.48	0.18
MBMO	6.26-6.36	6.31	0.10
Lead nitrate	5.00-5.33	5.16	0.33
Cadmium nitrate	6.00-6.27	6.13	0.27
Lead/Cadmium nitrate	5.23-5.42	5.32	0.19
Dye/heavy metal mixture	5.35-5.63	5.49	0.28

Appendix II

Table of Absorbances of dyes in aqueous $Pb(NO_3)_2$ and $Cd(NO_3)_2.4H_2O$

	Conc.(M)	Abs 1	Abs 2	Abs 3
MB in $Pb(NO_3)_2$	0.000	2.373	2.380	2.380
	0.005	2.348	2.391	2.392
	0.006	2.395	2.398	2.400
	0.007	2.381	2.387	2.387
	0.008	2.385	2.398	2.390
	0.009	2.381	2.386	2.384
	0.010	2.317	2.315	2.314
	0.020	2.339	2.336	2.334
	0.030	2.332	2.330	2.328
	0.040	2.363	2.361	2.358
	0.050	2.382	2.375	2.373
MB in $Cd(NO_3)_2.4H_2O$	0.000	2.373	2.380	2.380
	0.005	2.387	2.387	2.387
	0.006	2.385	2.385	2.385
	0.007	2.387	2.387	2.387
	0.008	2.395	2.395	2.395
	0.009	2.393	2.393	2.393
	0.010	2.285	2.283	2.283
	0.020	2.303	2.302	2.301
	0.030	2.303	2.299	2.297

	0.040	2.300	2.299	2.298
	0.050	2.302	2.301	2.300
MO in $Pb(NO_3)_2$	0.000	2.625	2.623	2.624
	0.005	2.618	2.615	2.617
	0.006	2.621	2.614	2.617
	0.007	2.627	2.629	2.626
	0.008	2.626	2.627	2.626
	0.009	2.623	2.624	2.619
	0.010	2.498	2.494	2.501
	0.020	2.460	2.454	2.456
	0.030	2.488	2.489	2.494
	0.040	2.469	2.468	2.468
	0.050	2.485	2.488	2.492
MO in $Cd(NO_3)_2.4H_2O$	0.000	2.627	2.622	2.626
	0.005	2.628	2.628	2.625
	0.006	2.606	2.603	2.608
	0.007	2.612	2.612	2.610
	0.008	2.598	2.597	2.592
	0.009	2.574	2.573	2.569
	0.010	2.439	2.435	2.424
	0.020	2.379	2.378	2.381
	0.030	2.187	2.191	2.193

	0.040	1.888	1.886	1.923
	0.050	1.697	1.710	1.718
IG in $Pb(NO_3)_2$	0.000	0.828	0.829	0.828
	0.010	0.250	0.248	0.246
	0.020	0.304	0.291	0.272
	0.030	0.310	0.313	0.311
	0.040	0.359	0.370	0.361
	0.050	0.352	0.339	0.342
IG in $Cd(NO_3)_2.4H_2O$	0.000	0.828	0.829	0.829
	0.010	0.787	0.789	0.789
	0.020	0.756	0.757	0.756
	0.030	0.722	0.722	0.723
	0.040	0.722	0.720	0.718
	0.050	0.727	0.727	0.726

Appendix III(a)

Table of Absorbances of dyes in aqueous $Pb(NO_3)_2$ and $Cd(NO_3)_2.4H_2O$

	Conc.(M)	Abs 1	Abs 2	Abs 3
MB in $Pb(NO_3)_2$	0.000	2.373	2.380	2.380
	0.005	2.348	2.391	2.392
	0.006	2.395	2.398	2.400
	0.007	2.381	2.387	2.387
	0.008	2.385	2.398	2.390
	0.009	2.381	2.386	2.384
	0.010	2.317	2.315	2.314
	0.020	2.339	2.336	2.334
	0.030	2.332	2.330	2.328
	0.040	2.363	2.361	2.358
	0.050	2.382	2.375	2.373
MB in $Cd(NO_3)_2.4H_2O$	0.000	2.373	2.380	2.380
	0.005	2.387	2.387	2.387
	0.006	2.385	2.385	2.385
	0.007	2.387	2.387	2.387
	0.008	2.395	2.395	2.395
	0.009	2.393	2.393	2.393
	0.010	2.285	2.283	2.283
	0.020	2.303	2.302	2.301
	0.030	2.303	2.299	2.297
	0.040	2.300	2.299	2.298
	0.050	2.302	2.301	2.300
MO in $Pb(NO_3)_2$	0.000	2.625	2.623	2.624
	0.005	2.618	2.615	2.617
	0.006	2.621	2.614	2.617
	0.007	2.627	2.629	2.626
	0.008	2.626	2.627	2.626
	0.009	2.623	2.624	2.619
	0.010	2.498	2.494	2.501
	0.020	2.460	2.454	2.456
	0.030	2.488	2.489	2.494
	0.040	2.469	2.468	2.468
	0.050	2.485	2.488	2.492
MO in $Cd(NO_3)_2.4H_2O$	0.000	2.627	2.622	2.626
	0.005	2.628	2.628	2.625
	0.006	2.606	2.603	2.608
	0.007	2.612	2.612	2.610

	0.008	2.598	2.597	2.592
	0.009	2.574	2.573	2.569
	0.010	2.439	2.435	2.424
	0.020	2.379	2.378	2.381
	0.030	2.187	2.191	2.193
	0.040	1.888	1.886	1.923
	0.050	1.697	1.710	1.718
IG in $Pb(NO_3)_2$	0.000	0.828	0.829	0.828
	0.010	0.250	0.248	0.246
	0.020	0.304	0.291	0.272
	0.030	0.310	0.313	0.311
	0.040	0.359	0.370	0.361
	0.050	0.352	0.339	0.342
IG in $Cd(NO_3)_2.4H_2O$	0.000	0.828	0.829	0.829
	0.010	0.787	0.789	0.789
	0.020	0.756	0.757	0.756
	0.030	0.722	0.722	0.723
	0.040	0.722	0.720	0.718
	0.050	0.727	0.727	0.726

Appendix III(b)

Table of Absorbances of MBMO in aqueous $Pb(NO_3)_2$ and $Cd(NO_3)_2.4H_2O$

MO/MB in $Pb(NO_3)_2$	Conc(M)	MO Abs 1	Abs 2	Abs 3	MB Abs 1	Abs 2	Abs 3
	0.000	1.004	1.004	1.003	0.812	0.811	0.813
	0.005	0.972	0.985	0.993	1.035	1.037	1.038
	0.006	1.009	1.009	1.012	1.055	1.054	1.052
	0.007	1.002	1.000	1.000	1.018	1.020	1.023
	0.008	1.000	1.002	1.004	0.993	0.993	0.985
	0.009	0.985	0.985	0.985	0.983	0.986	0.987
	0.010	0.844	0.929	0.938	1.603	1.586	1.623
	0.020	1.046	1.039	1.020	1.620	1.626	1.622
	0.030	1.071	1.104	1.111	1.673	1.676	1.647
	0.040	1.068	1.106	1.083	1.703	1.692	1.726
	0.050	1.091	1.103	1.081	1.724	1.761	1.722

MO/MB in $Cd(NO_3)_2.4H_2O$	0.000	1.000	1.000	1.000	0.811	0.812	0.820
	0.005	0.996	1.034	1.163	0.924	0.926	0.928
	0.006	1.040	1.073	1.055	0.919	0.927	0.923
	0.007	1.055	1.014	1.122	0.936	0.934	0.936
	0.008	1.020	1.005	1.003	0.910	0.913	0.912
	0.009	1.028	1.031	1.027	0.930	0.928	0.930
	0.010	1.010	0.989	0.981	1.485	1.505	1.504
	0.020	0.936	0.891	0.890	1.272	1.287	1.285
	0.030	1.030	0.986	1.003	1.487	1.486	1.513
	0.040	1.075	1.045	1.031	1.624	1.590	1.603
	0.050	1.075	1.028	1.023	1.587	1.621	1.707

Appendix IV: **Table of Effect of Time on amount of MB, MO and IG adsorbed onto UMAC**

	Time(min)	Abs 1	Abs 2	Average	%Absbd
10ppmMB/10mg UMAC	0	1.463	1.463	1.463	0
	15	1.149	1.197	1.173	20
	30	0.928	0.826	0.877	40
	45	0.644	0.451	0.547	63
	60	0.270	0.409	0.340	77
10ppmMO/10mg UMAC	0	0.744	0.744	0.744	0
	15	0.530	0.462	0.496	33
	30	0.392	0.336	0.364	51
	45	0.197	0.233	0.215	71
	60	0.190	0.226	0.208	72
10ppmIG/10mg UMAC	0	0.104	0.104	0.104	0
	15	0.072	0.074	0.073	30
	30	0.069	0.059	0.064	38
	45	0.052	0.052	0.052	50
	60	0.037	0.039	0.038	62
20ppmMB/20mg UMAC	0	1.46	1.46	1.46	0
	5	1.13	1.12	1.12	23
	10	0.93	0.94	0.93	34
	15	0.67	0.68	0.67	54
	20	0.55	0.59	0.57	61
	30	0.39	0.35	0.37	75
	45	0.10	0.10	0.10	93
	60	0.07	0.08	0.07	95

20ppmMO/20mg UMAC	0	0.84	0.84	0.84	0
	5	0.58	0.58	0.58	31
	10	0.45	0.46	0.45	46
	15	0.32	0.31	0.31	62
	20	0.27	0.26	0.26	68
	30	0.14	0.13	0.13	84
	45	0.06	0.05	0.05	93
	60	0.06	0.04	0.04	94
20ppmIG/20mg UMAC	0	0.20	0.20	0.20	0
	5	0.16	0.15	0.15	22
	10	0.13	0.13	0.13	35
	15	0.11	0.11	0.11	45
	20	0.10	0.12	0.11	45
	30	0.08	0.08	0.08	60
	45	0.08	0.06	0.07	65
	60	0.08	0.05	0.06	67

Appendix IV(a): **One Way Anova for rate experiment**

One Way Analysis of Variance Sunday, July 29, 2012, 6:34:56 PM

Data source: Data 1 in Notebook1

Normality Test: Passed (P = 0.388)

Equal Variance Test: Passed (P = 0.500)

Group Name	N	Missing	Mean	Std Dev	SEM
Col 1	7	0	62.143	27.655	10.453
Col 2	7	0	68.286	23.963	9.057
Col 3	7	0	48.429	16.612	6.279

Source of Variation	DF	SS	MS	F	P
Between Groups	2	1446.952	723.476	1.344	0.286
Residual	18	9690.000	538.333		
Total	20	11136.952			

The differences in the mean values among the treatment groups are not great enough to exclude the possibility that the difference is due to random sampling variability; there is not a statistically significant difference (P = 0.286).

Power of performed test with alpha = 0.050: 0.094

The power of the performed test (0.094) is below the desired power of 0.800.
Less than desired power indicates you are less likely to detect a difference when one actually exists. Negative results should be interpreted cautiously.

Appendix IV(b): **One-Sample t-test for rate experiment**.

One-Sample t-test Sunday, July 29, 2012, 6:41:59 PM

Data source: Data 1 in Notebook1

Normality Test: Passed (P = 0.567)

Group Name	N	Missing	Mean	Std Dev	SEM
Col 5	3	0	59.333	10.263	5.925

Hypothesized population mean 0.000

t = 10.013 with 2 degrees of freedom. (P = 0.010)

95 percent confidence interval for the population mean: 33.838 to 84.829

There is a statistically significant difference between the mean of the sampled population and the hypothesized population mean (P = 0.010).

Power of performed test with alpha = 0.050: 0.993

Appendix V

Performance(%) of UMAC,CMAC and PMAC after interaction with components of MBMOIG in aqueous $Pb(NO_3)_2$ and $Cd(NO_3)_2.4H_2O$ mixture.

	Conc.(ppm)	MO(%)	IG(%)	MB(%)
UMAC	10	95	94	94
	20	96	93	94
	30	95	91	91
	40	90	91	91
	50	94	91	89
CMAC	10	96	94	94
	20	96	96	96
	30	93	90	89
	40	89	88	87

	50	90	91	89
PMAC	10	97	96	96
	20	97	95	96
	30	97	93	93
	40	97	91	90
	50	96	92	91

Appendix VI(a)

Data for MBMO adsorption from aqueous $Pb(NO_3)_2$ and $Cd(NO_3)_2.4H_2O$ mixture

UMCA/MO	Co (mg/L)	Ce (mg/L)	Co-Ce	X(mg)	X/m	logX/m	logCe	lnCe	1/Ce	1/qe
	5	0.577	4.423	0.044	4.4	0.643	-0.239	-0.550	1.733	0.227
	10	2.534	7.466	0.075	7.50	0.875	0.404	0.930	0.395	0.133
	15	3.916	11.084	0.111	11.08	1.044	0.593	1.365	0.255	0.090
	20	6.521	13.479	0.135	13.50	1.130	0.814	1.875	0.153	0.074
UMCA/MB	5	0.820	4.180	0.042	4.18	0.621	-0.086	-0.198	1.219	0.239
	10	4.514	5.486	0.055	5.5	0.740	0.654	1.507	0.221	0.182
	15	8.008	6.992	0.070	7.0	0.845	0.903	2.080	0.125	0.143
	20	13.260	6.74	0.067	6.70	0.832	1.122	2.585	0.075	0.149
CMAC/MO	5	0.794	4.206	0.042	4.2	0.623	-0.100	-0.231	1.259	0.238
	10	2.051	7.949	0.079	7.9	0.898	0.312	0.718	0.487	0.126
	15	5.247	9.753	0.098	9.8	0.991	0.720	1.658	0.190	0.102
	20	8.494	11.506	0.115	11.5	1.061	0.929	2.139	0.118	0.087
CMAC/MB	5	1.048	3.952	0.040	4.0	0.602	0.020	0.047	0.954	0.25
	10	3.313	6.687	0.067	6.7	0.826	0.520	1.198	0.302	0.149
	15	9.193	5.807	0.058	5.8	0.763	0.963	2.218	0.109	0.172
	20	14.919	5.081	0.051	5.1	0.707	1.173	2.702	0.067	0.196
PMAC/MO	5	0.742	4.258	0.043	4.3	0.633	-0.129	-0.298	1.348	0.232
	10	1.704	8.296	0.083	8.3	0.919	0.231	0.533	0.587	0.120
	15	4.377	10..623	0.106	10.6	1.025	0.641	1.477	0.228	0.094
	20	6.837	13.163	0.132	13.2	1.119	0.835	1.922	0.146	0.076
PMAC/MB	5	1.042	3.958	0.040	4.0	0.602	0.018	0.041	0.960	0.25
	10	3.032	6.968	0.069	6.9	0.839	0.482	1.109	0.330	0.145
	15	8.396	6.604	0.066	6.6	0.819	0.924	2.128	0.119	0.15
	20	13.410	6.59	0.066	6.6	0.819	0.924	2.128	0.074	0.15

Appendix VI(b): **Data for adsorption of aqueous MOMB**

	Co (mg/L)	Ce (mg/L)	Co-Ce	X (mg)	X/m	logX/m	logCe	lnCe	1/Ce	1/qe
UMCA/MO	5	0.325	4.675	0.047	4.7	0.672	-0.488	-1.124	3.077	0.213
	10	0.776	9.224	0.092	9.2	0.964	-0.110	-0.254	1.289	0.109
	15	3.363	11.637	0.116	11.6	1.064	0.527	1.213	0.297	0.086
	20	7.012	12.988	0.130	13.0	1.114	0.846	1.948	0.143	0.077
UMCA/MB	5	0.095	4.905	0.049	4.9	0.690	-1.022	-2.354	10.526	0.204
	10	0.434	9.566	0.096	9.6	0.982	-0.362	-0.362	2.304	0.104
	15	3.781	11.219	0.112	11.2	1.049	1.330	1.330	0.264	0.089
	20	10.595	9.405	0.941	9.4	0.97	2.360	2.360	0.094	0.106
CMAC/MO	5	0.784	4.216	0.042	4.2	0.623	-0.243	-0.243	1.275	0.238
	10	2.207	7.793	0.078	7.8	0.892	0.792	0.792	0.453	0.128
	15	4.403	10.597	0.106	10.6	1.025	1.483	1.483	0.227	0.094
	20	12.387	7.613	0.076	7.6	0.881	2.517	2.517	0.081	0.131
CMAC/MB	5	0.448	4.552	0.046	4.6	0.663	-0.349	-0.803	2.232	0.217
	10	1.259	8.741	0.087	8.7	0.939	0.100	0.230	0.794	0.115
	15	3.571	11.429	0.114	11.4	1.057	0.553	1.273	0.280	0.088
	20	12.24	7.76	0.078	7.8	0.892	1.088	2.505	0.082	0.128
PMAC/MO	5	0.296	4.704	0.047	4.7	0.672	-0.529	-1.218	3.378	0.213
	10	0.761	9.239	0.092	9.2	0.964	-0.119	-0.273	1.314	0.109
	15	2.257	12.743	0.127	12.7	1.104	0.353	0.814	0.443	0.079
	20	3.765	16.235	0.162	16.2	1.209	0.576	1.326	0.266	0.062
PMAC/MB	5	0.163	4.837	0.048	4.8	0.681	-0.788	-1.814	6.135	0.208
	10	0.509	9.491	0.095	9.5	0.978	-0.293	-0.675	1.965	0.105
	15	2.088	12.912	0.129	12.9	1.110	0.320	0.736	0.479	0.077
	20	4.156	15.844	0.158	15.8	1.199	0.619	1.424	0.241	0.063

Appendix VII(a): **Data for MOIG adsorption from aqueous $Pb(NO_3)_2$ and $Cd(NO_3)_2.4H_2O$ mixture**

	Co(ppm)	Ce(mg/L)	Co-Ce	X(mg)	X/m	logX/m	LogCe	lnCe	1/Ce	1/qe
UMCA/MO	5	1.568	3.431	0.034	3.4	0.531	0.195	0.450	0.638	0.294
	10	4.466	5.534	0.055	5.5	0.740	0.650	1.497	0.224	0.182
	15	6.382	8.618	0.086	8.6	0.934	0.805	1.854	0.157	0.116
	20	10.272	9.728	0.097	9.7	0.987	1.012	2.330	0.097	0.103
UMCA/IG	5	1.759	3.241	0.032	3.2	0.505	0.245	0.565	0.568	0.312
	10	5.315	4.685	0.047	4.7	0.672	0.725	1.671	0.188	0.213
	15	7.777	7.223	0.072	7.2	0.857	0.891	2.052	0.128	0.139
	20	11.907	8.093	0.081	8.1	0.908	1.076	2.477	0.084	0.123
CMAC/MO	5	1.853	3.147	0.031	3.1	0.491	0.268	0.617	0.540	0.322
	10	3.887	6.113	0.061	6.1	0.785	0.590	1.358	0.257	0.164
	15	8.043	6.957	0.070	7.0	0.845	0.905	2.085	0.124	0.143

	20	12.143	7.857	0.078	7.8	0.892	1.084	2.497	0.082	0.128
CMAC/IG	5	2.068	2.932	0.029	2.9	0.462	0.315	0.727	0.483	0.345
	10	5.164	4.836	0.048	4.8	0.681	0.713	1.642	0.194	0.208
	15	10.097	4.903	0.049	4.9	0.690	1.004	2.313	0.099	0.204
	20	14.332	5.668	0.057	5.7	0.756	1.156	2.663	0.070	0.175
PMAC/MO	5	0.737	4.263	0.043	4.3	0.633	-0.132	-0.305	1.357	0.232
	10	2.355	7.645	0.076	7.6	0.881	0.372	0.856	0.425	0.131
	15	5.885	9.115	0.091	9.1	0.959	0.770	1.772	0.170	0.110
	20	11.174	8.826	0.088	8.8	0.944	1.048	2.413	0.089	0.089
PMAC/IG	5	0.889	4.111	0.041	4.1	0.613	-0.889	-0.118	1.125	0.244
	10	2.972	7.028	0.070	7.0	0.845	0.473	1.089	0.336	0.143
	15	7.355	7.645	0.076	7.6	0.959	0.866	1.996	0.136	0.132
	20	12.943	7.057	0.071	7.1	0.851	1.112	2.561	0.077	0.141

Appendix VII(b): **Data for adsorption of aqueous MOIG mixture**

	Co(ppm)	Ce(mg/L)	Co-Ce	X(mg)	X/m	logX/m	logCe	lnCe	1/Ce	1/qe
UMCA/MO	5	0.954	4.046	0.040	4.0	0.602	-0.020	-0.047	1.048	0.25
	10	2.010	7.99	0.080	8.0	0.903	0.303	0.698	0.497	0.125
	15	5.172	9.828	0.098	9.8	0.991	0.714	1.643	0.193	0.102
	20	5.295	14.705	0.15	15.0	1.176	0.724	1.667	0.189	0.067
UMCA/IG	5	2.156	2.844	0.028	2.8	0.447	0.334	0.768	0.464	0.357
	10	5.598	4.402	0.044	4.4	0.643	0.748	1.722	0.179	0.227
	15	11.059	3.941	0.039	3.9	0.591	1.044	2.403	0.090	0.256
	20	14.093	5.907	0.059	5.9	0.771	1.149	2.646	0.071	0.169
CMAC/MO	5	0.966	4.033	0.040	4.0	0.602	-0.015	-0.034	1.035	0.250
	10	2.875	7.125	0.071	7.1	0.851	0.459	1.056	0.348	0.141
	15	4.416	10.583	0.106	10.6	1.025	0.645	1.485	0.226	0.094
	20	8.202	11.798	0.118	11.8	1.072	0.914	2.104	0.122	0.085
CMAC/IG	5	2.014	2.986	0.030	3.0	0.477	0.304	0.700	0.497	0.333
	10	6.172	3.828	0.038	3.8	0.580	0.790	1.820	0.162	0.263
	15	9.458	5.542	0.054	5.4	0.732	0.978	2.247	0.106	0.185
	20	14.404	5.596	0.056	5.6	0.748	1.158	2.668	0.069	0.179
PMAC/MO	5	0.966	4.034	0.040	4.0	0.602	-0.015	-0.034	1.035	0.25
	10	2.303	7.697	0.077	7.7	0.886	0.362	0.834	0.434	0.130
	15	4.430	10.570	0.106	10.6	1.025	0.646	1.489	0.226	0.094
	20	5.985	14.015	0.140	14.0	1.146	0.777	1.789	0.167	0.071

PMAC/IG	5	2.251	2.749	0.027	2.7	0.431	0.352	0.811	0.444	0.370
	10	6.435	3.565	0.036	3.6	0.556	0.808	1.862	0.155	0.278
	15	10.830	4.170	0.042	4.2	0.623	1.035	2.382	0.092	0.238
	20	15.000	5.000	0.050	5.0	0.699	1.176	2.708	0.067	0.200

Appendix VIII(a): **Data for single aqueous MO,MB & IG solutions**

	Co(ppm)	Ce	Co-Ce	X	X/m	logX/m	logCe	lnCe	1/Ce	1/qe
UMAC/MO	10	1.909	8.091	0.081	8.1	0.908	0.281	0.647	0.524	0.123
	20	3.364	16.636	0.166	16.6	1.220	0.527	1.213	0.297	0.060
	30	6.631	23.369	0.234	23.4	1.369	0.821	1.892	0.151	0.043
	40	14.757	25.243	0.252	25.2	1.401	1.169	2.692	0.068	0.040
CMAC/MO	10	1.519	8.481	0.085	8.5	0.929	0.182	0.418	0.658	0.118
	20	7.402	12.598	0.126	12.6	1.100	0.869	2.002	0.135	0.079
	30	14.832	15.168	0.152	15.2	1.182	1.171	2.697	0.067	0.066
	40	28.394	11.606	0.116	11.6	1.064	1.453	3.347	0.035	0.086
PMAC/MO	10	1.882	8.118	0.081	8.1	0.908	0.275	0.632	0.531	0.123
	20	4.080	15.92	0.159	15.9	1.201	0.611	1.406	0.245	0.063
	30	7.439	22.561	0.226	22.6	1.354	0.871	2.007	0.134	0.044
	40	14.516	25.484	0.255	22.5	1.352	1.162	2.675	0.069	0.044
UMAC/MB	10	0.670	9.33	0.093	9.3	0.968	-0.174	-0.400	1.492	0.107
	20	4.159	15.841	0.158	15.8	1.199	0.619	1.425	0.240	0.063
	30	9.453	20.547	0.205	20.5	1.312	0.975	2.247	0.106	0.049
	40	26.227	13.773	0.138	13.8	1.140	1.419	3.267	0.038	0.072
CMAC/MB	10	0.950	9.05	0.091	9.1	0.959	-0.022	-0.051	1.053	0.110
	20	5.350	14.650	0.146	14.6	1.164	0.728	1.677	0.187	0.068
	30	23.093	6.907	0.069	6.9	0.839	1.363	3.140	0.043	0.145
	40	32.492	7.508	0.075	7.5	0.875	1.512	3.482	0.031	0.133
PMAC/MB	10	0.608	9.392	0.094	9.4	0.973	-0.216	-0.497	1.645	0.106
	20	4.408	15.592	0.156	15.6	1.193	0.644	1.483	0.227	0.064
	30	9.820	20.180	0.202	20.2	1.305	0.992	2.284	0.102	0.049
	40	29.195	10.805	0.108	10.8	1.033	1.465	3.374	0.034	0.092
UMAC/IG	10	4.289	5.711	0.057	5.7	0.756	0.632	1.456	0.233	0.175
	20	9.894	10.106	0.101	10.1	1.004	0.995	2.292	0.101	0.100
	30	18.444	11.556	0.115	11.5	1.061	1.266	2.915	0.054	0.087
	40	31.401	8.599	0.086	8.6	0.934	1.497	3.447	0.032	0.116

CMAC/IG	10	3.858	6.142	0.061	6.1	0.785	0.586	1.350	0.259	0.164
	20	9.735	10.265	0.103	10.3	1.013	0.988	2.276	0.103	0.097
	30	20.636	9.364	0.094	9.4	0.968	1.315	3.027	0.048	0.106
	40	30.223	9.777	0.098	9.8	0.991	1.480	3.409	0.033	0.102
PMAC/IG	10	2.995	7.005	0.070	7.0	0.845	0.476	1.097	0.334	0.143
	20	11.751	8.249	0.082	8.2	0.914	1.070	2.464	0.085	0.122
	30	15.512	14.488	0.145	14.5	1.161	1.191	2.742	0.064	0.069
	40	28.535	11.465	0.115	11.5	1.061	1.455	3.352	0.035	0.087

Appendix VIII(b): **Data for Single MO,MB & IG in aqueous $Pb(NO_3)_2$ and $Cd(NO_3)_2.4H_2O$ mixture**

	Co(ppm)	Ce	Co-Ce	X	X/m	logX/m	logCe	lnCe	1/Ce	1/qe
UMAC/MO	10	1.411	8.588	0.086	8.6	0.934	0.149	0.344	0.709	0.116
	20	4.491	15.509	0.155	15.5	1.190	0.652	1.502	0.223	0.064
	30	9.338	20.662	0.207	20.7	1.316	0.970	2.234	0.107	0.048
	40	19.671	20.329	0.203	20.3	1.307	1.294	2.980	0.051	0.049
CMAC/MO	10	-	-	-	-	-	-	-	-	-
	20	-	-	-	-	-	-	--	-	---
	30	-	-	-	-	-	-	-	-	-
	40	-	-	-	-	-	-	-	-	-
PMAC/MO	10	1.387	8.612	0.086	8.6	0.934	0.142	0.327	0.720	0.116
	20	3.077	16.923	0.169	16.9	1.228	0.488	1.124	0.324	0.059
	30	7.324	22.676	0.227	22.7	1.356	0.865	1.992	0.136	0.044
	40	14.055	25.944	0.259	25.9	1.413	1.148	2.643	0.071	0.039
UMAC/MB	10	3.413	6.587	0.066	6.6	0.819	0.533	1.227	0.293	0.151
	20	14.485	5.515	0.055	5.5	0.740	1.161	2.673	0.069	0.182
	30	24.309	5.691	0.057	5.7	0.755	1.386	3.191	0.041	0.175
	40	37.372	2.628	0.026	2.6	0.415	1.572	3.621	0.027	0.385
CMAC/MB	10	-	-	-	-	-	-	-	-	-
	20	-	-	-	-	-	-	-	-	-
	30	-	-	-	-	-	-	-	-	-
	40	-	-	-	-	-	-	-	-	-
PMAC/MB	10	2.226	7.774	0.078	7.8	0.892	0.347	0.800	0.449	0.128
	20	9.465	10.534	0.105	10.5	1.021	0.976	2.248	0.106	0.095

	30	18.943	11.057	0.110	11.0	1.041	1.277	2.941	0.090	0.091
	40	34.843	5.156	0.051	5.1	0.707	0.712	3.551	0.029	0.196
UMAC/IG	10	4.042	5.958	0.059	5.9	0.771	0.606	1.397	0.247	0.169
	20	9.606	10.394	0.104	10.4	1.017	0.982	2.262	0.104	0.096
	30	16.691	13.309	0.133	13.3	1.124	1.222	2.815	0.060	0.075
	40	27.944	12.056	0.120	12.0	1.079	1.079	3.330	0.036	0.083
CMAC/IG	10	-	-	-	-	-	-	-	-	-
	20	-	-	-	-	-	-	-	-	-
	30	-	-	-	-	-	-	-	-	-
	40	-	--	-	-	-	-	-	-	-
PMAC/IG	10	2.375	7.625	0.076	7.6	0.881	0.376	0.865	0.421	0.131
	20	7.488	12.512	0.125	12.5	1.097	0.874	2.014	0.133	0.080
	30	12.982	17.018	0.170	17.0	1.230	1.113	2.564	0.077	0.059
	40	20.676	19.324	0.193	19.3	1.285	1.315	3.029	0.048	0.052

Appendix IX: **Data for adsorption of components of aqueous MBMOIG mixture onto different AC matrices**

	Co	Ce	Co-Ce	X	X/m	logX/m	log Ce	lnCe	1/Ce	1/qe
UMAC/MO	3.333	0.729	2.604	0.026	2.6	0.415	-0.137	-0.316	1.372	0.385
	6.667	1.411	5.256	0.052	5.2	0.716	0.149	0.344	0.709	0.192
	10.000	3.212	6.788	0.068	6.8	0.832	0.508	1.167	0.311	0.147
	13.333	3.923	9.410	0.094	9.4	0.973	0.594	1.367	0.255	0.106
UMAC/IG	3.333	0.901	2.432	0.024	2.4	0.380	-0.045	-0.104	1.110	0.417
	6.667	1.543	5.124	0.051	5.1	0.707	0.188	0.434	0.649	0.196
	10.000	3.093	6.907	0.069	6.9	0.839	0.490	1.129	0.323	0.145
	13.333	3.471	9.862	0.099	9.9	0.996	0.540	1.245	0.288	0.101
UMAC/MB	3.333	0.748	2.585	0.026	2.6	0.415	-0.126	-0.290	1.337	0.385
	6.667	1.280	5.387	0.054	5.4	0.732	0.107	0.247	0.781	0.185
	10.000	2.972	7.028	0.070	7.0	0.845	0.473	1.089	0.336	0.143
	13.333	3.343	9.990	0.100	10.0	1.000	0.524	1.207	0.299	0.100
CMAC/MO	3.333	0.679	2.654	0.026	2.6	0.415	-0.168	-0.387	1.473	0.385
	6.667	1.636	5.029	0.050	5.0	0.699	0.214	0.493	0.610	0.200
	10.000	3.628	6.372	0.064	6.4	0.806	0.560	1.289	0.276	0.156
	13.333	5.871	7.462	0.075	7.5	0.875	0.769	1.770	0.170	0.133
CMAC/IG	3.333	0.721	2.612	0.026	2.6	0.415	-0.142	-0.327	1.387	0.385
	6.667	1.451	5.216	0.052	5.2	0.716	0.162	0.372	0.689	0.192

	10.000	2.553	7.447	0.074	7.4	0.869	0.407	0.937	0.392	0.135
	13.333	4.095	9.238	0.092	9.2	0.964	0.612	1.410	0.244	0.109
CMAC/MB	3.333	0.636	2.697	0.027	2.7	0.431	-0.196	-0.453	1.572	0.370
	6.667	1.358	5.309	0.053	5.3	0.724	0.133	0.306	0.736	0.189
	10.000	2.596	7.404	0.074	7.4	0.869	0.414	0.954	0.385	0.135
	13.333	3.898	9.435	0.094	9.4	0.973	0.591	1.361	0.256	0.106
PMAC/MO	3.333	0.541	2.792	0.028	2.8	0.447	-0.267	-0.614	1.848	0.357
	6.667	0.315	6.352	0.063	6.3	0.799	-0.502	-1.155	3.175	0.159
	10.000	2.471	7.529	0.075	7.5	0.875	0.393	0.905	0.405	0.133
	13.333	3.347	9.986	0.100	10.0	1.000	0.525	1.208	0.299	0.100
PMAC/IG	3.333	0.751	2.582	0.026	2.6	0.415	-0.124	-0.286	1.331	0.385
	6.667	1.373	5.294	0.053	5.3	0.724	0.138	0.317	0.728	0.189
	10.000	2.177	7.823	0.078	7.8	0.892	0.338	0.778	0.459	0.128
	13.333	2.663	10.67	0.107	10.7	1.029	0.425	0.979	0.375	0.093
PMAC/MB	3.333	0.706	2.627	0.026	2.6	0.415	-0.151	-0.348	1.416	0.385
	6.667	1.243	5.424	0.054	5.4	0.732	0.094	0.217	0.804	0.185
	10.000	1.202	8.798	0.088	8.8	0.944	0.080	0.184	0.832	0.114
	13.333	2.378	10.955	0.110	11.0	1.041	0.376	0.866	0.420	0.091

Appendix X: Data for adsorption of components of MBMOIG from aqueous $Pb(NO_3)_2$ and $Cd(NO_3)_2.4H_2O$ mixture onto different AC matrices.

Data for MO adsorption from MBMOIG in $0.01PbNO_3$+$Cd(NO_3)_2.4H_20$ mixture onto UMAC

Co(mg/L)	Ce(mg/L)	Co-Ce	X(mg)	X/m	logX/m	logCe	lnCe	1/Ce	1/qe
3.333	0.159	3.174	0.032	1.587	0.200	-0.799	-1.839	6.289	0.630
6.667	0.277	6.389	0.064	3.195	0.504	-0.558	-1.284	3.610	0.313
10.000	0.489	9.511	0.095	4.756	0.677	-0.311	-0.715	2.045	0.210
13.333	0.594	12.739	0.127	6.370	0.804	-0.226	-0.521	1.684	0.157
16.667	0.967	15.700	0.157	7.850	0.895	-0.014	-0.033	1.634	0.127

Data for IG adsorption from MOIGMB in $0.01PbNO_3$+$Cd(NO_3)_2.4H_20$ mixture onto UMAC

Co(mg/L)	Ce(mg/L)	Co-Ce	X(mg)	X/m	logX/m	logCe	lnCe	1/Ce	1/qe
3.333	0.207	3.127	0.031	1.564	0.194	-0.684	-1.575	4.831	0.639
6.667	0.445	6.221	0.062	3.111	0.493	-0.352	-0.810	2.247	0.321
10.000	0.952	9.048	0.090	4.524	0.655	-0.021	-0.049	1.050	0.221
13.333	1.192	12.141	0.121	6.071	0.783	0.076	0.176	0.839	0.165
16.667	1.538	15.129	0.151	7.565	0.879	0.187	0.430	0.650	0.132

Data for MB adsorption from MOIGMB in 0.01$PbNO_3$+$Cd(NO_3)_2.4H_20$ mixture onto UMAC

Co(mg/L)	Ce(mg/L)	Co-Ce	X(mg)	X/m	logX/m	logCe	lnCe	1/Ce	1/qe
3.33	0.21	3.12	0.03	1.56	0.19	-0.68	-1.57	4.83	0.64
6.67	0.44	6.22	0.06	3.11	0.49	-0.35	-0.81	2.25	0.32
10.0	0.95	9.05	0.09	4.52	0.65	-0.02	-0.05	1.05	0.22
13.3	1.19	12.1	0.12	6.07	0.78	0.08	0.18	0.84	0.16
16.7	1.54	15.1	0.15	7.56	0.88	0.19	0.43	0.65	0.13

Data for MO adsorption from MOIGMB in 0.01$PbNO_3$+$Cd(NO_3)_2.4H_20$ mixture onto CMAC

Co(mg/L)	Ce(mg/L)	Co-Ce	X(mg)	X/m	logX/m	logCe	lnCe	1/Ce	1/qe
3.333	0.148	3.185	0.032	1.593	0.202	-0.830	-1.911	6.756	0.628
6.667	0.251	6.416	0.064	3.208	0.506	-0.600	-1.382	3.984	0.312
10.000	0.701	9.299	0.093	4.650	0.667	-0.154	-0.355	1.427	0.215
13.333	1.414	11.919	0.119	5.959	0.775	0.150	0.346	0.707	0.168
16.667	1.629	15.037	0.150	7.518	0.876	0.212	0.488	0.614	0.133

Data for IG adsorption from MOIGMB in 0.01$PbNO_3$+$Cd(NO_3)_2.4H_20$ mixture onto CMAC

Co(mg/L)	Ce(mg/L)	Co-Ce	X(mg)	X/m	logX/m	logCe	lnCe	1/Ce	1/qe
3.333	0.207	3.127	0.031	1.563	0.194	-0.684	-1.575	4.831	0.639
6.667	0.273	6.394	0.064	3.197	0.505	-0.564	-1.298	2.247	0.321
10.000	0.996	9.004	0.090	4.502	0.653	-0.002	-0.004	1.050	0.221
13.333	1.537	11.796	0.118	5.898	0.771	0.187	0.430	0.839	0.165
16.667	1.507	15.16	0.152	7.58	0.880	0.178	0.410	0.650	0.132

Data for MB adsorption from MOIGMB in 0.01$PbNO_3$+$Cd(NO_3)_2.4H_20$ mixture onto CMAC

Co(mg/L)	Ce(mg/L)	Co-Ce	X(mg)	X/m	logX/m	logCe	lnCe	1/Ce	1/qe
3.333	0.190	3.144	0.031	1.572	0.196	-0.721	-1.661	5.263	0.636
6.667	0.261	6.406	0.064	3.203	0.506	-0.583	-1.343	3.831	0.312
10.000	1.055	8.945	0.089	4.472	0.651	0.023	0.054	0.948	0.224
13.333	1.775	11.558	0.115	5.779	0.762	0.249	0.574	0.563	0.173
16.667	1.855	14.811	0.148	7.405	0.869	0.268	0.618	0.539	0.135

Data for MO adsorption from MOIGMB in 0.01$PbNO_3$+$Cd(NO_3)_2.4H_20$ mixture onto PMAC

Co(mg/L)	Ce(mg/L)	Co-Ce	X(mg)	X/m	logX/m	logCe	lnCe	1/Ce	1/qe

3.333	0.102	3.231	0.032	1.615	0.208	-0.991	-2.283	9.8	0.619
6.667	0.224	6.442	0.064	3.221	0.508	-0.650	-1.496	4.460	0.310
10.000	0.331	9.669	0.097	4.834	0.684	-0.480	-1.106	3.021	0.207
13.333	0.467	12.867	0.129	6.433	0.808	-0.331	-0.761	2.141	0.155
16.667	0.677	15.990	0.160	7.995	0.903	-0.169	-0.390	1.477	0.125

Data for IG adsorption from MOIGMB in 0.01$PbNO_3$+$Cd(NO_3)_2.4H_20$ mixture onto PMAC

Co(mg/L)	Ce(mg/L)	Co-Ce	X(mg)	X/m	logX/m	logCe	lnCe	1/Ce	1/qe
3.333	0.146	3.187	0.032	1.593	0.202	-0.836	-1.924	6.849	0.628
6.667	0.316	6.351	0.063	3.175	0.502	-0.500	-1.152	3.164	0.315
10.000	0.717	9.283	0.093	4.641	0.667	-0.144	-0.333	1.395	0.215
13.333	1.192	12.141	0.121	6.070	0.783	0.076	0.176	0.839	0.165
16.667	1.412	15.254	0.152	7.627	0.882	0.150	0.345	0.708	0.131

Data for MB adsorption from MOIGMB in 0.01$PbNO_3$+$Cd(NO_3)_2.4H_20$ mixture onto PMAC

Co(mg/L)	Ce(mg/L)	Co-Ce	X(mg)	X/m	logX/m	logCe	lnCe	1/Ce	1/qe
3.333	0.130	3.203	0.032	1.601	0.204	-0.886	-2.040	7.692	0.625
6.667	0.291	6.376	0.064	3.188	0.503	-0.536	-1.234	3.436	0.314
10.000	0.742	9.258	0.092	4.629	0.665	-0.130	-0.298	1.348	0.216
13.333	1.289	12.044	0.120	6.022	0.780	0.110	0.254	0.776	0.166
16.667	1.576	15.091	0.151	7.545	0.878	0.197	0.455	0.634	0.132

Appendix XI: **Absorbances of textile eflluents(TXT 1, TXT 2 & TXT 3)**

		TXTE 1		
Wavelength(nm)	10%	20%	30%	40%
380	0.080	0.160	0.235	0.316
400	0.068	0.136	0.201	0.273
420	0.059	0.123	0.183	0.253
440	0.060	0.122	0.181	0.248
460	0.050	0.106	0.156	0.214
480	0.039	0.081	0.118	0.163
500	0.028	0.060	0.089	0.126
520	0.028	0.058	0.084	0.117
540	0.026	0.054	0.079	0.111
560	0.029	0.058	0.083	0.116
580	0.027	0.056	0.081	0.114
600	0.028	0.057	0.082	0.115
620	0.031	0.061	0.088	0.127

640	0.031	0.059	0.085	0.123
660	0.020	0.041	0.057	0.091
680	0.014	0.028	0.036	0.065
700	0.009	0.019	0.023	0.041
710	0.008	0.017	0.021	0.034

		TXTE 2		
Wavelength(nm)	10%	20%	30%	40%
380	-0.187	-0.163	-0.140	-0.122
400	-0.084	-0.044	-0.004	0.031
420	0.057	0.115	0.176	0.230
440	0.071	0.140	0.211	0.275
460	0.067	0.134	0.203	0.265
480	0.064	0.128	0.192	0.250
500	0.064	0.133	0.206	0.271
520	0.087	0.174	0.266	0.349
540	0.098	0.198	0.300	0.399
560	0.088	0.172	0.259	0.340
580	0.029	0.058	0.089	0.111
600	0.006	0.012	0.019	0.016
620	0.002	0.004	0.007	0.002
640	0.003	0.005	0.007	0.002
660	0.002	0.003	0.006	0.001
680	0.002	0.003	0.006	0.001
700	0.001	0.003	0.004	0.000
710	0.002	0.003	0.004	0.000

		TXTE 3		
Wavelength(nm)	20%	30%	40%	100%
380	-0.197	-0.193	-0.184	-0.147
400	-0.113	-0.110	-0.101	-0.065
420	0.010	0.009	0.018	0.058
440	0.016	0.015	0.024	0.063
460	0.012	0.011	0.018	0.047
480	0.012	0.011	0.016	0.036
500	0.006	0.006	0.008	0.027
520	0.014	0.015	0.017	0.038
540	0.013	0.014	0.016	0.041
560	0.018	0.020	0.023	0.052
580	0.014	0.017	0.023	0.054
600	0.017	0.021	0.028	0.066
620	0.017	0.022	0.030	0.077
640	0.013	0.016	0.023	0.059
660	0.006	0.008	0.013	0.030
680	0.005	0.004	0.008	0.016
700	0.004	0.002	0.006	0.011

710	0.005	0.002	0.006	0.010

Appendix XII: **Freundlich, Langmuir and Temkin isotherms constants**.

	Freundlich			Langmuir			Temkin		
	R2	n	Kf	R2	Qo	b	R2	A	B
IG/Cd/Pb/PMAC	0.993	2.26	5.20	0.982	22.22	0.22	0.982	1.56	5.49
IG/Cd/Pb/UMAC	0.985	1.69	2.63	0.958	18.18	0.12	0.810	1.67	3.51
MB/Cd/Pb/UMAC	0.282	2.16	1.87	0.608	0.12	6.61			
MB/Cd/Pb/PMAC									
MO/Cd/Pb/PMAC	0.912	2.15	8.41	0.982	38.46	0.22	0.975	2.65	7.42
MO/Cd/Pb/UMAC	0.887	2.91	8.37	0.992	25	0.38	0.906	5.17	4.78
IG(aq)/PMAC	0.578	3.82	5.23	0.641	12.5	0.41	0.485	5.74	2.47
IG(aq)/CMAC	0.613	4.83	5.15	0.852	11.63	0.31	0.591	20.30	1.610
IG(aq)/UMAC	0.431	4.29	4.80	0.750	12.50	0.21	0.369	12.97	1.76
MB(aq)/PMAC	0.133	12.99	11.72	0.471	15.15	2.87	.11	2 .24E5	1.0
MB(aq)/CMAC	0.217	-10.42	11.12	0.048	8.40	-7.93	0.158	2.16E5	-0.867
MB(aq)/UMAC	0.439	7.09	11.32				0.352	828	1.78
MO(aq)/PMAC	0.858	1.94	6.73	0.973	41.67	0.13	0.891	1.89	7.46
MO(aq)/CMAC	0.544	7.04	8.65	0.827	14.08	1.04	0.479	311	1.52
MO(aq)/UMAC	0.814	1.89	7.13	0.992	25	0.38	0.91	5.17	4.776
Binary dye mixtures									
MOIG/PMAC (MO)	0.991	1.51	4.17	0.992	15.15	0.41	0.962	2.09	5.165
(IG)	0.984	3.11	2.71	0.932	9.52	0.82	0.962	9.65	1.179
MOIG/CMAC MO	0.961	1.88	4.17	0.997	20	0.14	0.951	2.81	3.83
IG	0.905	3.18	2.99	0.961	6.53	0.44	0.882	9.38	1.31
MOIG/UMAC MO	0.873	1.60	4.46	0.955	23.25	0.22	0.792	2.41	
	0.593	3.47	3.08	0.743	5.85	1.02	0.542	15.05	
MOIG/Cd/Pb/PMAC MO	0.844	3.69	5.18	0.993	11.76	0.79	0.872	22.2	1.74
IG	0.661	4.33	4.99	0.951	8.40	1.35	0.726	85.05	1.15
MOIG/Cd/Pb/CMAC/ MO	0.875	2.13	2.62	0.96	12.19	0.19	0.931	2.38	2.39
IG	0.845	3.06	2.59	0.937	6.99	0.40	0.874	5.90	1.34
MOIG/Cd/Pb/UMACMO	0.956	1.71	2.56	0.953	13.16	0.22	0.919	1.54	3.46
IG	0.943	3.27	2.47	0.925	9.80	0.30	0.906	1.87	2.69
MBMO(aq)/PMAC MB	0.952	2.24	9.12	0.994	19.61	1.13	0.989	11.39	4.14
MO	0.963	2.16	8.99	0.994	19.61	1.08	0.985	10.26	4.30

MBMO(aq)CMAC MB	0.384	11.36	6.12	0.805	11.23	0.95	0.299	150	1.32
MO	0.471	10.10	5.52	0.858	10.87	0.85	0.384	70.99	1.40
MBMO(aq)UMAC MB	0.549	5.13	7.65	0.869	12.19	2.28	0.541	293	1.43
MO	0.85	3.31	7.85	0.869	15.15	1.47	0.927	29.18	2.52
MBMO/CdPb/PMACMB	0.846	5.05	4.91	0.846	1.18	9.95	0.561	147	1.02
MO	0.985	2.10	5.44	0.985	17.54	0.45	0.978	4.52	3.77
MBMO/CdPb/CMACMB	0.181	11.36	4.82	0.527	6.25	2.67	0.13	4.1E5	0.39
MBMO/CdPb/UMACMB	0.918	4.59	4.71	0.914	7.04	2.53	0.879	64.03	1.15
MO	0.971	2.14	5.48	0.943	13.70	0.81	0.915	4.88	3.66
Tertiary Dye Mixture									
MBMOIG/HM/PM-MB	0.995	1.20	11.04	0.999	24.4	0.69	0.971	14.37	3.15
MO	0.994	1.15	11.91	0.998	31.25	0.53	0.966	13.74	3.41
IG	0.995	1.19	11.19	0.999	25.64	0.65	0.969	14.16	3.20
MBMOIG/HM/CM-MB				0.944	10.42	1.31	0.936	15.40	2.10
MO				0.951	10.87	1.26	0.948	15.11	2.13
IG	0.969	0.31	3E8	0.956	10.99	1.21	0.936	14.76	2.14
MBMOIG/HM/UM-MB				0.986	-66.7	-0.1	0.978	9.62	3.27
MO				0.987	-40	-0.2	0.978	9.32	3.51
IG				0.985	-55.5	-0.2	0.976	9.43	3.34
MBMOIG(aq)/PMACMB	0.603	2.42	5.83	0.232	7.94	2.68	0.746	11.13	2.78
MO	0.427	3.22	5.86	0.138	7.09	4.55	0.540	29.56	1.91
IG	0.582	2.47	5.61	0.226	7.52	2.95	0.702	12.53	2.52
MBMOIG(aq)/CM MB	0.979	1.76	3.58	0.997	13.70	0.36	0.993	3.51	3.027
	0.950	2.08	3.41	0.993	10.47	0.50	0.991	5.07	2.22
	0.977	1.73	3.48	0.997	13.89	0.34	0.997	3.44	3.01
MBMOIG(aq)/UM MB	0.932	1.41	3.55	0.966	22.73	0.18	0.908	2.74	3.79
	0.939	1.47	3.50	0.970	19.61	0.22	0.923	2.88	3.53
	0.942	1.33	3.31	0.970	27.03	0.14	0.915	2.52	3.88

Appendix XIII: Freundlich, Langmuir and Temkin isotherms

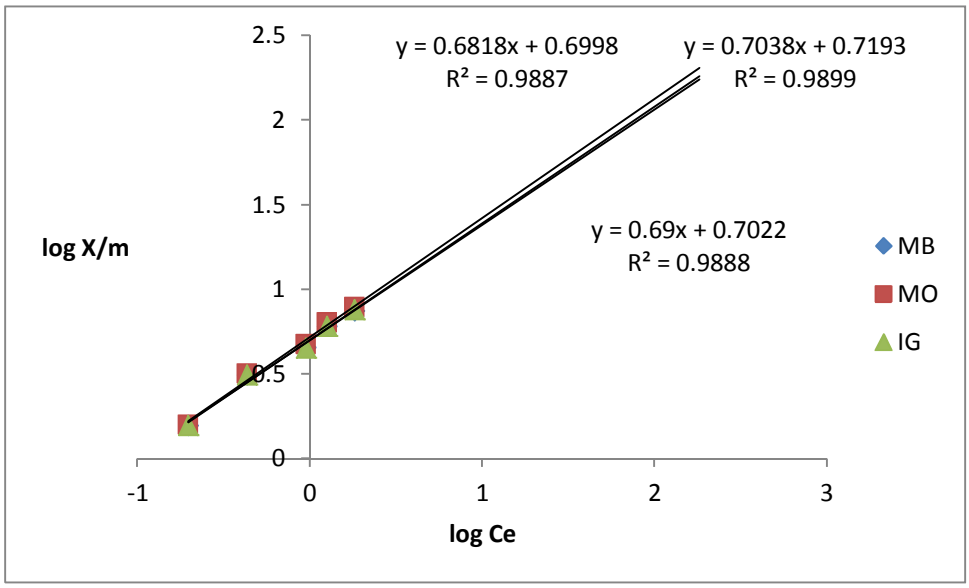


Figure 1: Freundlich isotherm for components of MBMOIG from aqueous $Pb(NO_3)_2$ and $Cd(NO_3)_2.4H_2O$ mixture onto UMAC

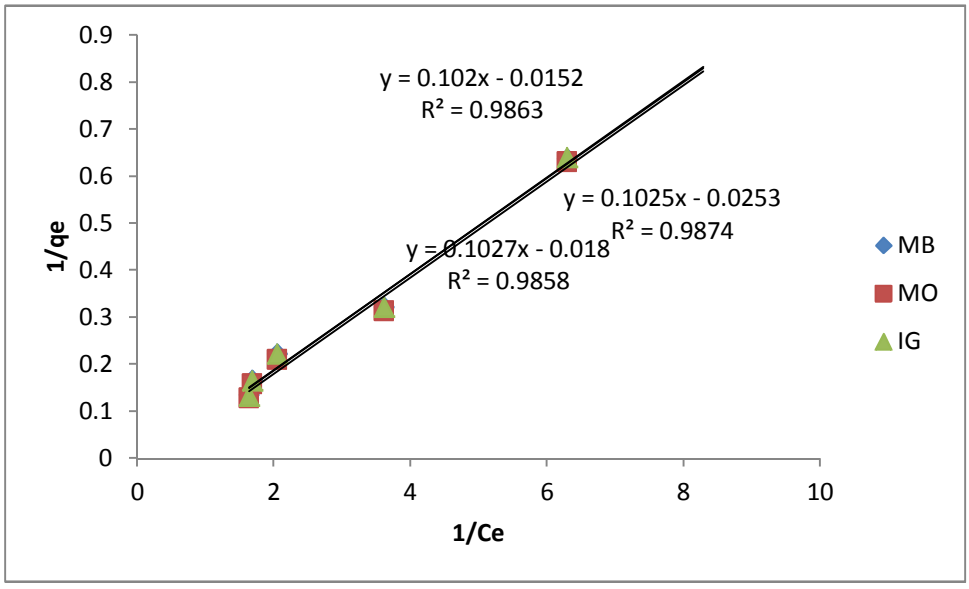


Figure 2 : Langmuir isotherm of components of MBMOIG from aqueous $Pb(NO_3)_2$ and $Cd(NO_3)_2.4H_2O$ mixture mixture onto UMAC

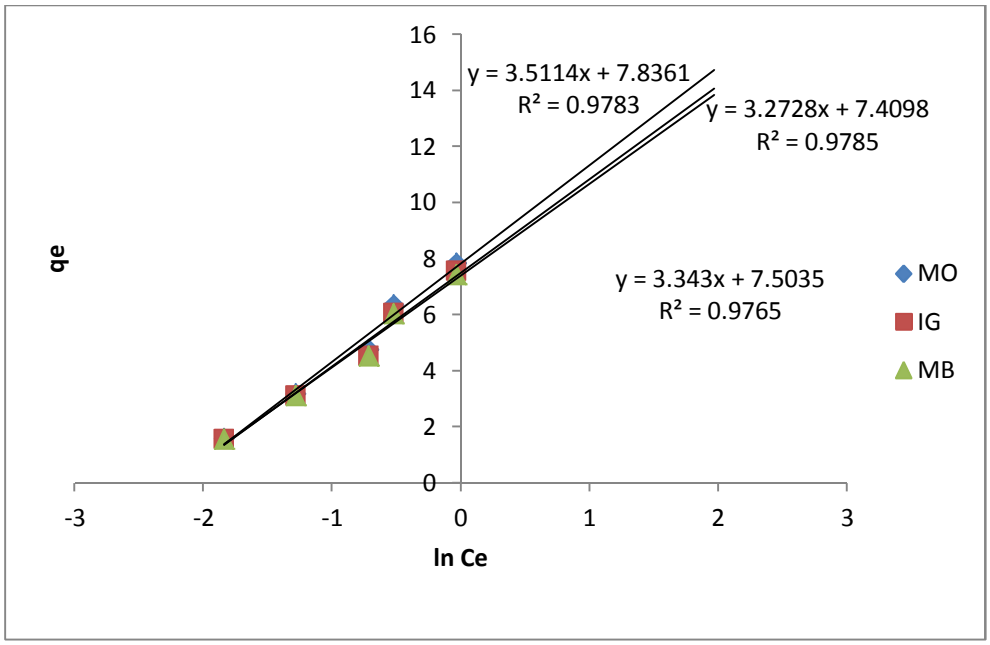


Figure 3: Temkin isotherm of components of MBMOIG from aqueous $Pb(NO_3)_2$ and $Cd(NO_3)_2.4H_2O$ mixture onto UMAC

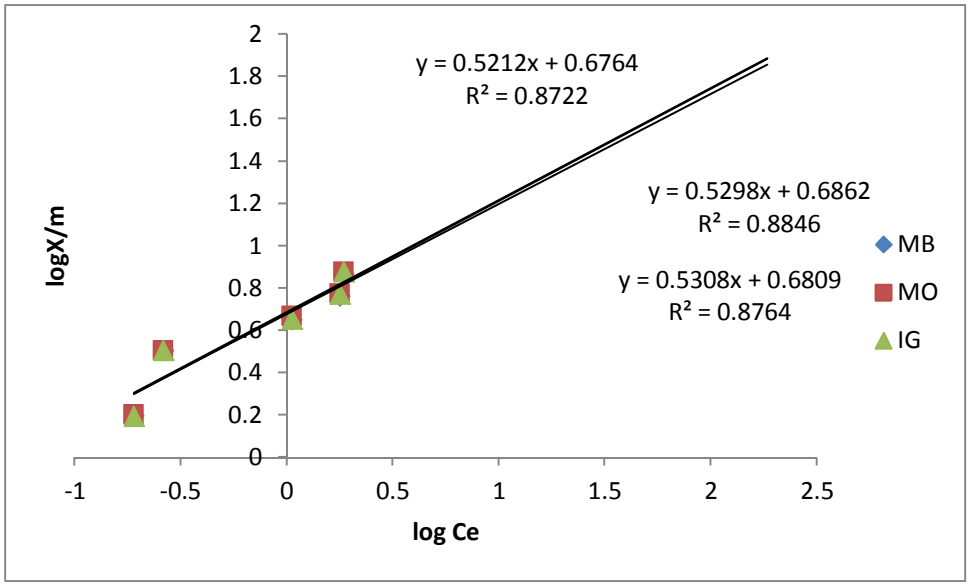


Figure 4: Freundlich isotherm of components of MBMOIG from aqueous $Pb(NO_3)_2$ and $Cd(NO_3)_2.4H_2O$ mixture onto CMAC

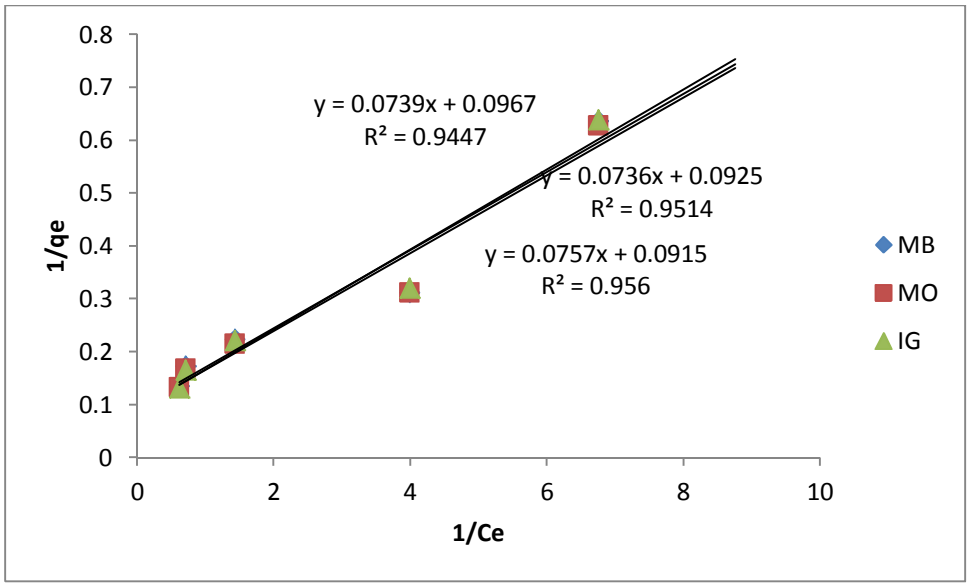


Figure 5: Langmuir isotherm of components of MBMOIG from aqueous $Pb(NO_3)_2$ and $Cd(NO_3)_2.4H_2O$ mixture onto CMAC

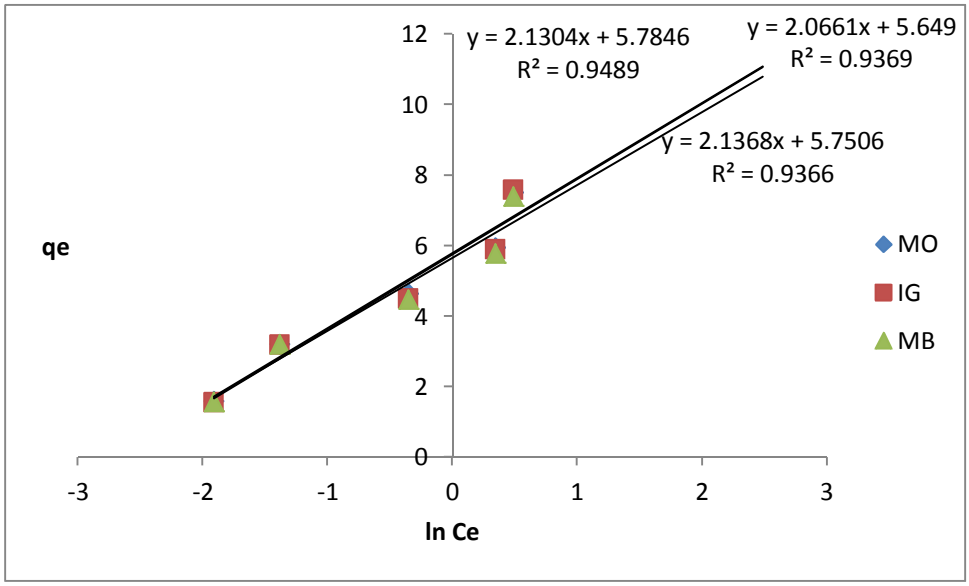


Figure 6: Temkin isotherm for components of MBMOIG from aqueous $Pb(NO_3)_2$ and $Cd(NO_3)_2.4H_2O$ mixture onto CMAC

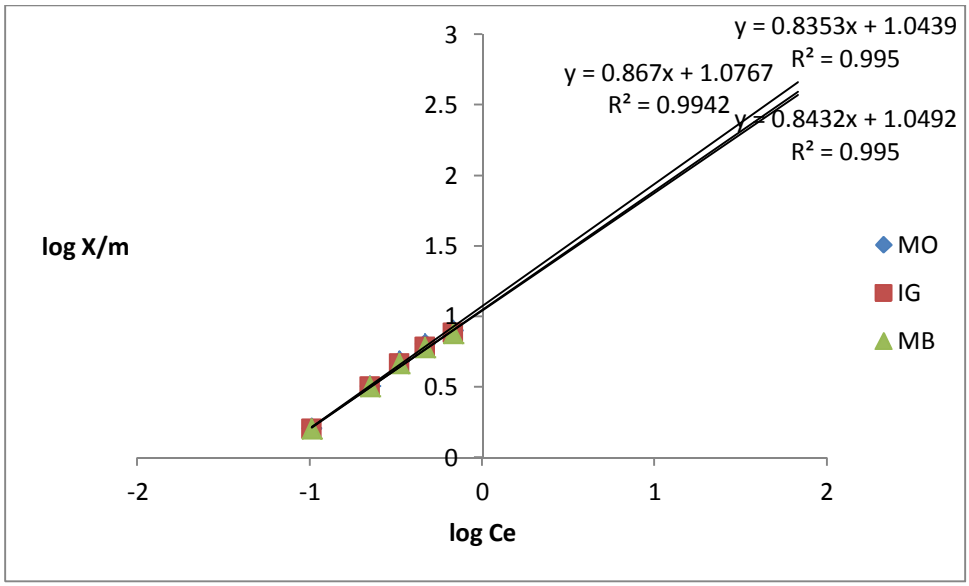


Figure 7: Freundlich isotherm of components of MBMOIG from aqueous $Pb(NO_3)_2$ and $Cd(NO_3)_2.4H_2O$ mixture onto PMAC

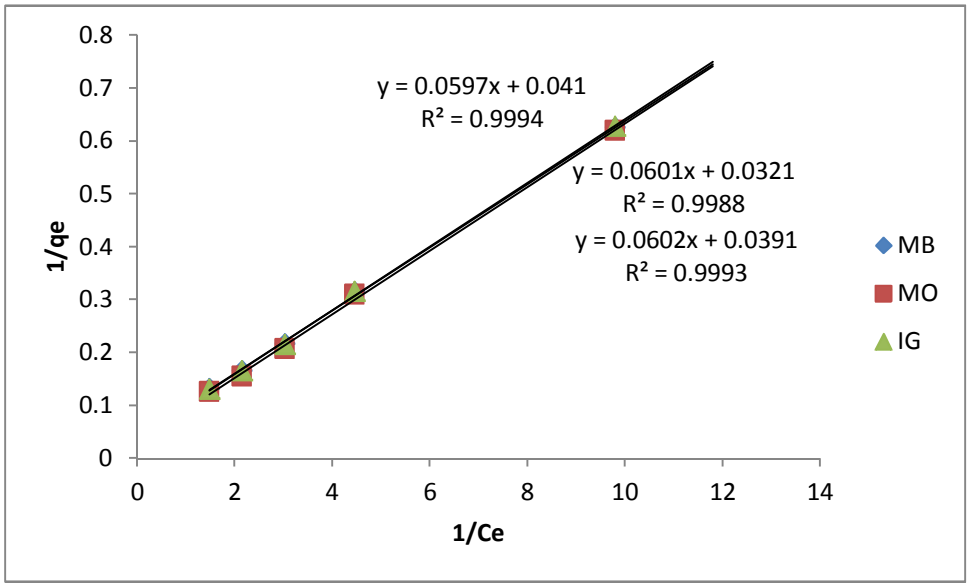


Figure 8: Langmuir isotherm of cmponents of MBMOIG from aqueous $Pb(NO_3)_2$ and $Cd(NO_3)_2.4H_2O$ mixture onto PMAC

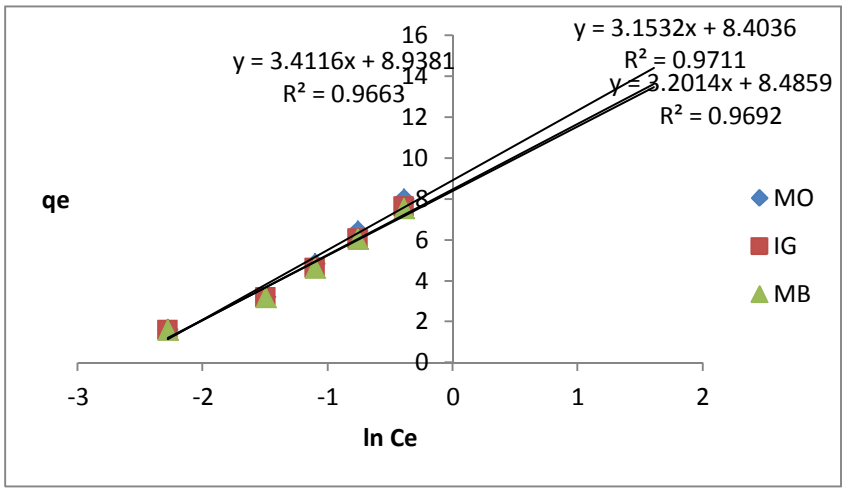


Figure 9: Temkin isotherm of components of MBMOIG from aqueous $Pb(NO_3)_2$ and $Cd(NO_3)_2.4H_2O$ mixture onto PMAC

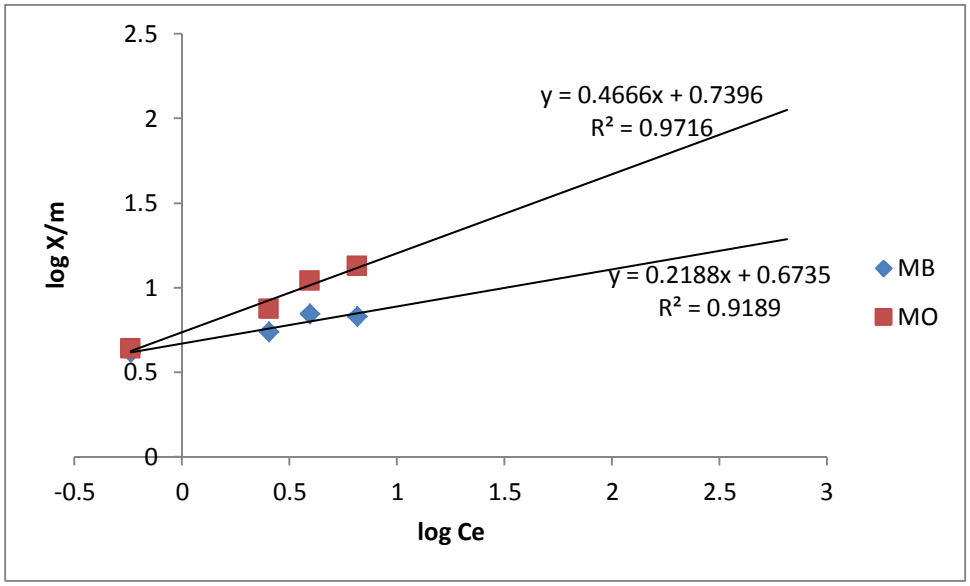


Figure 10: Freundlich isotherm of components of MBMO from aqueous $Pb(NO_3)_2$ and $Cd(NO_3)_2.4H_2O$ mixture onto UMAC

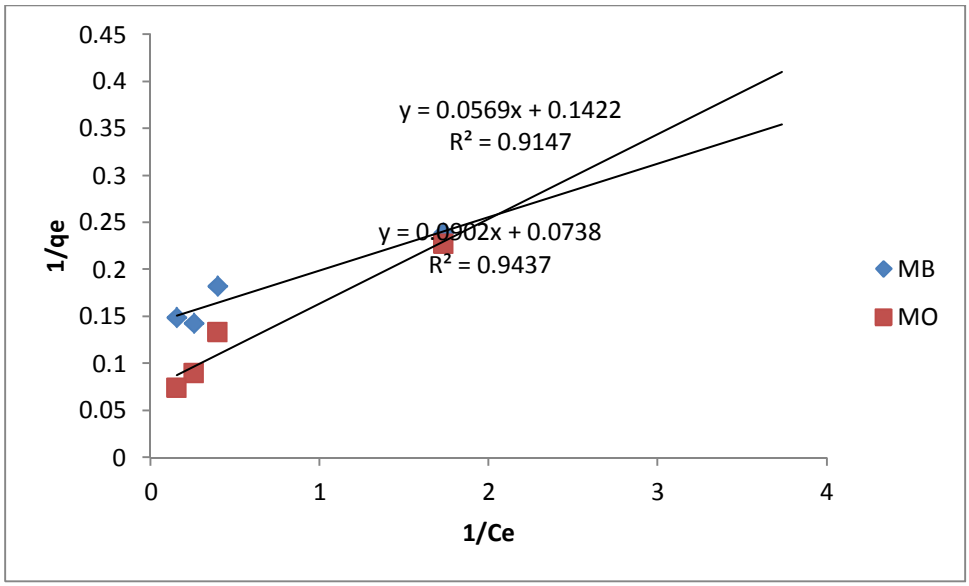


Figure 11: Langmuir isotherm of components of MBMO from aqueous $Pb(NO_3)_2$ and $Cd(NO_3)_2.4H_2O$ mixture onto UMAC

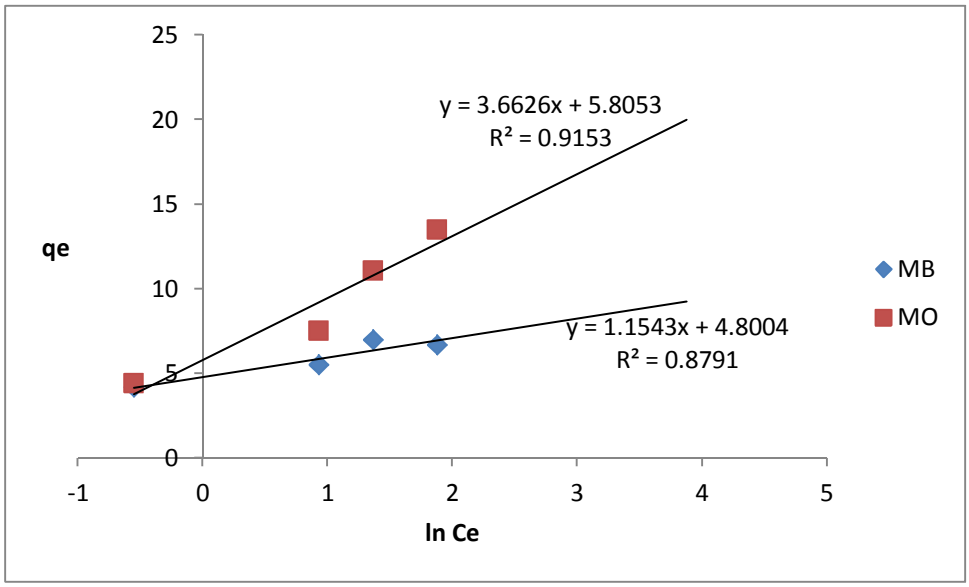


Figure 12: Temkin isotherm of components of MOMB from aqueous $Pb(NO_3)_2$ and $Cd(NO_3)_2.4H_2O$ mixture onto UMAC

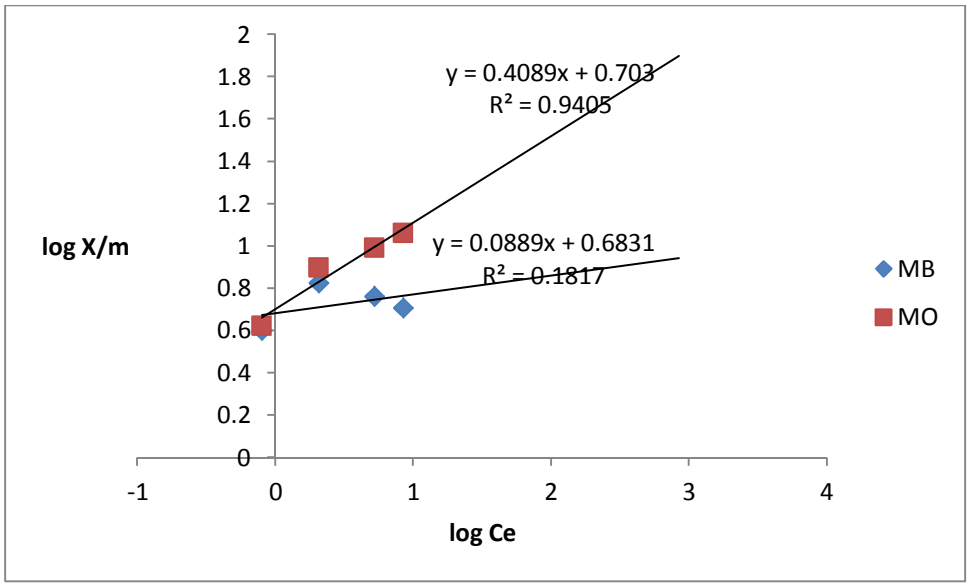


Figure 13: Freundlich isotherm for components of MBMO from aqueous $Pb(NO_3)_2$ and $Cd(NO_3)_2.4H_2O$ mixture onto CMAC

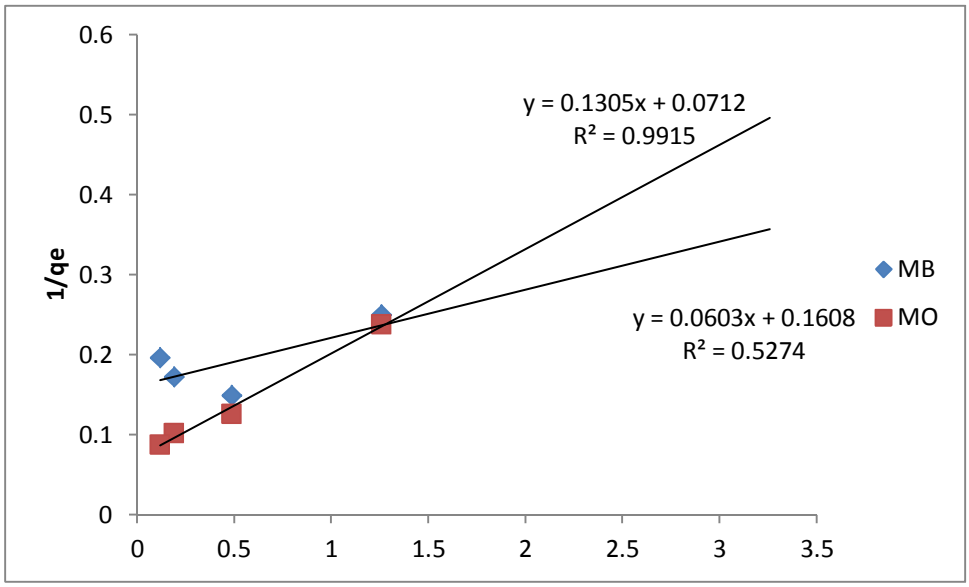


Figure 14: Langmuir isotherm of components of MBMO from aqueous $Pb(NO_3)_2$ and $Cd(NO_3)_2.4H_2O$ mixture onto CMAC

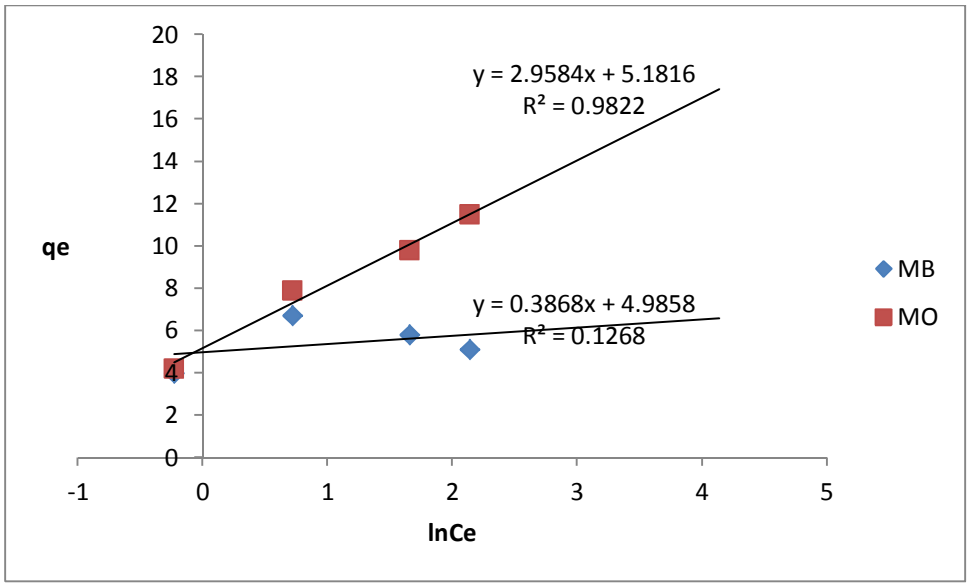


Figure 15: Temkin isotherm of components of MBMO from aqueous $Pb(NO_3)_2$ and $Cd(NO_3)_2.4H_2O$ mixture onto CMAC

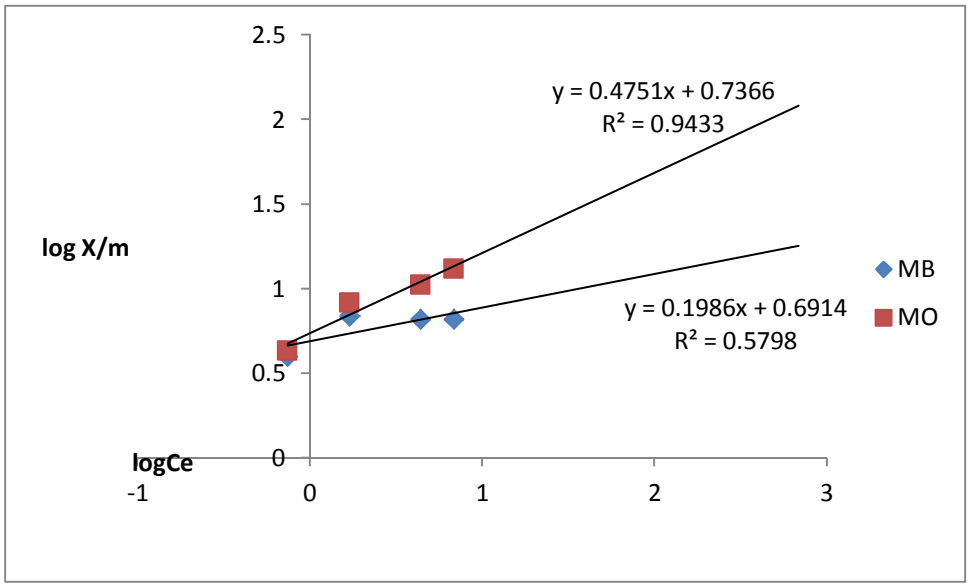


Figure 16: Freundlich isotherm of components of MBMO from aqueous $Pb(NO_3)_2$ and $Cd(NO_3)_2.4H_2O$ mixture onto PMAC

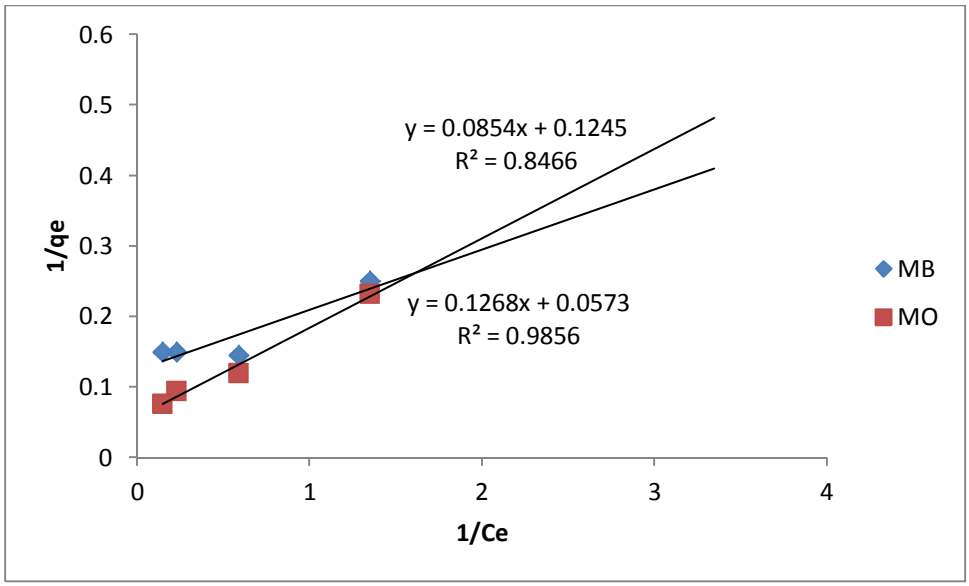


Figure 17: Langmuir isotherm of components of MBMO from aqueous $Pb(NO_3)_2$ and $Cd(NO_3)_2.4H_2O$ mixture onto PMAC

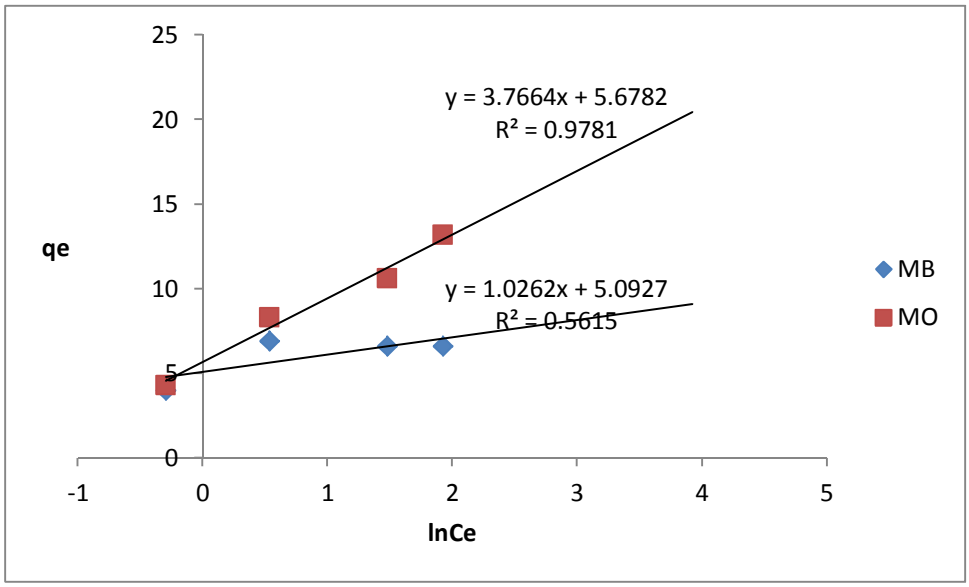


Figure 18: Temkin isotherm of components of MBMO from aqueous $Pb(NO_3)_2$ and $Cd(NO_3)_2.4H_2O$ mixture onto PMAC

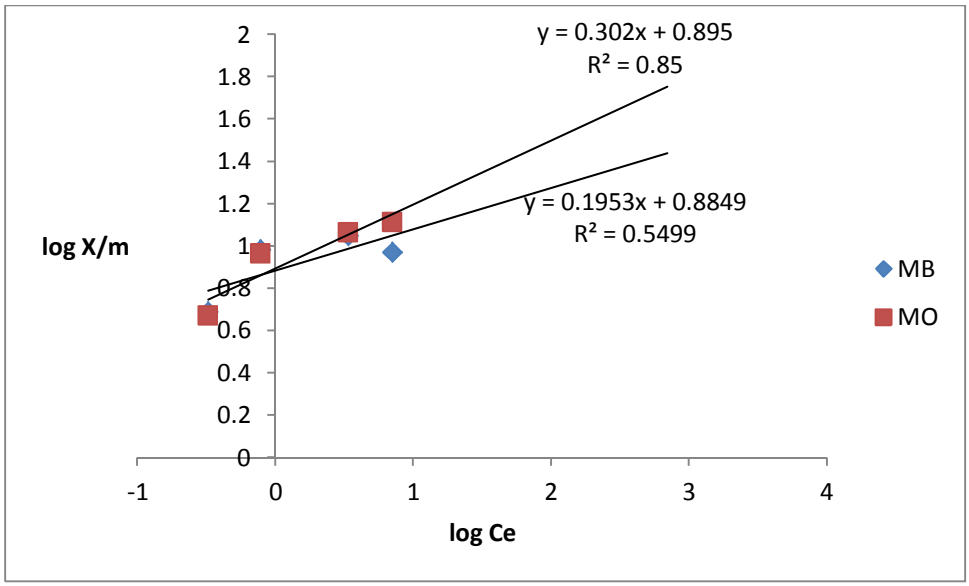


Figure 19: Freundlich isotherm of components of aqueous MBMO onto UMAC

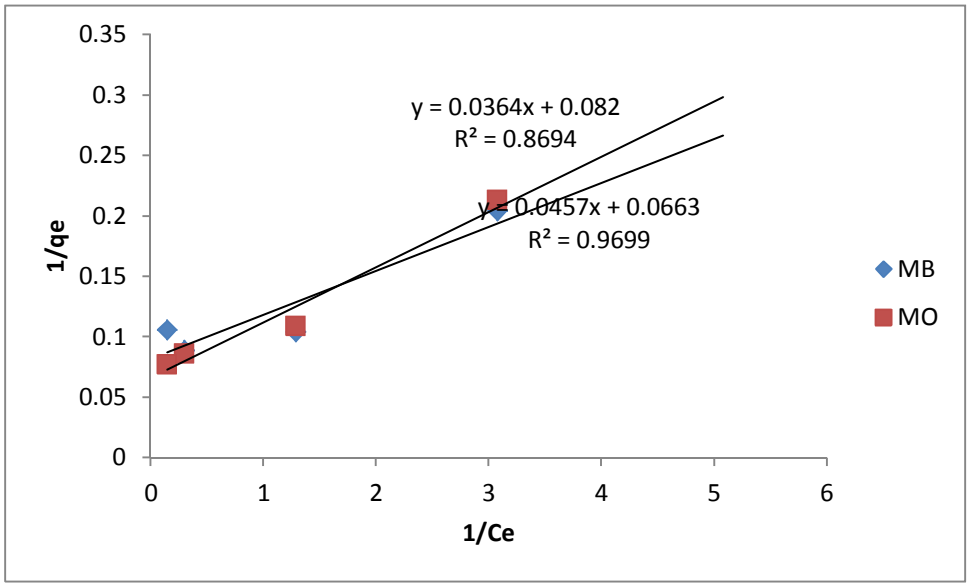


Figure 20 :Langmuir isotherm of components of aqueous MBMO onto UMAC

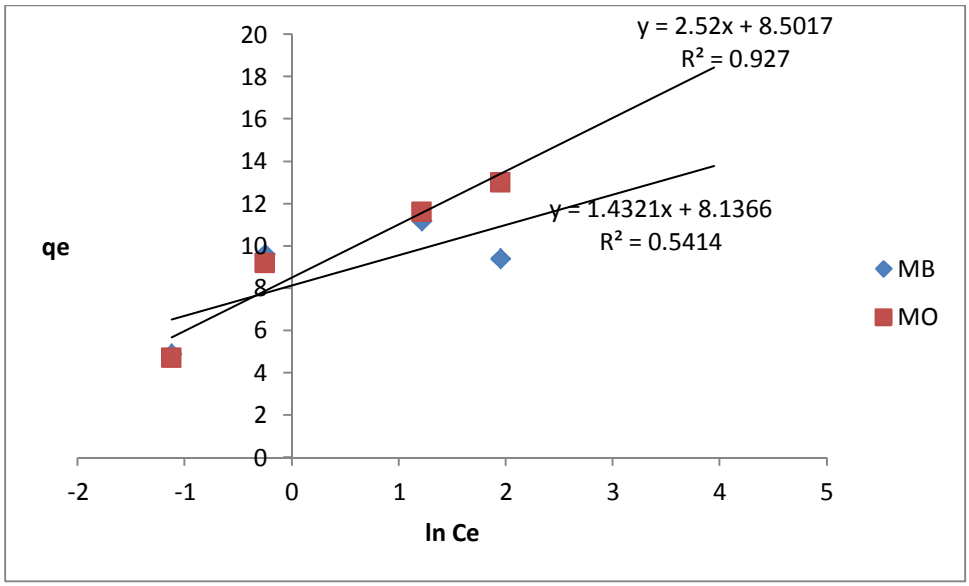


Figure 21: Temkin isotherm of components of aqueous MBMO mixture onto UMAC

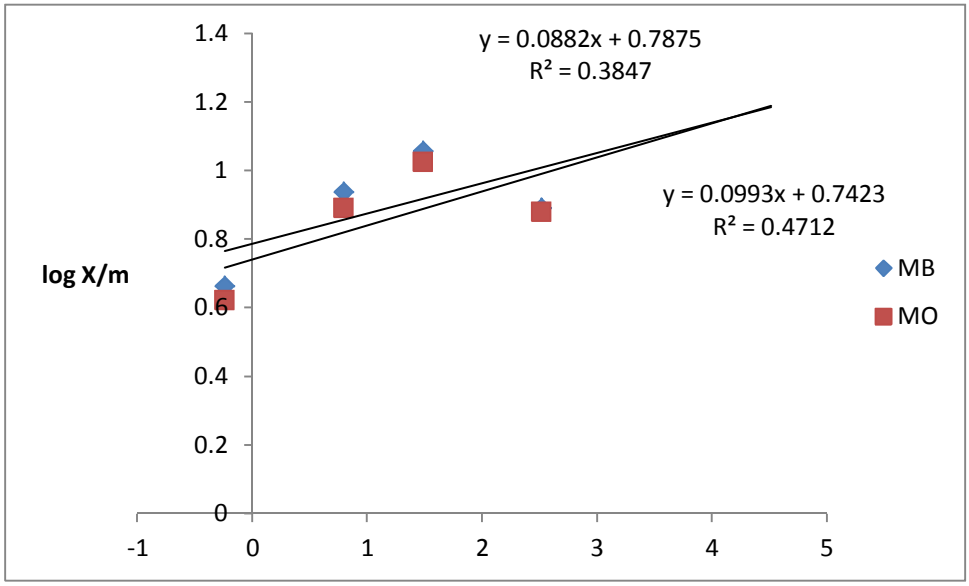


Figure 22: Freundlich isotherm of components of aqueous MBMO mixture onto CMAC

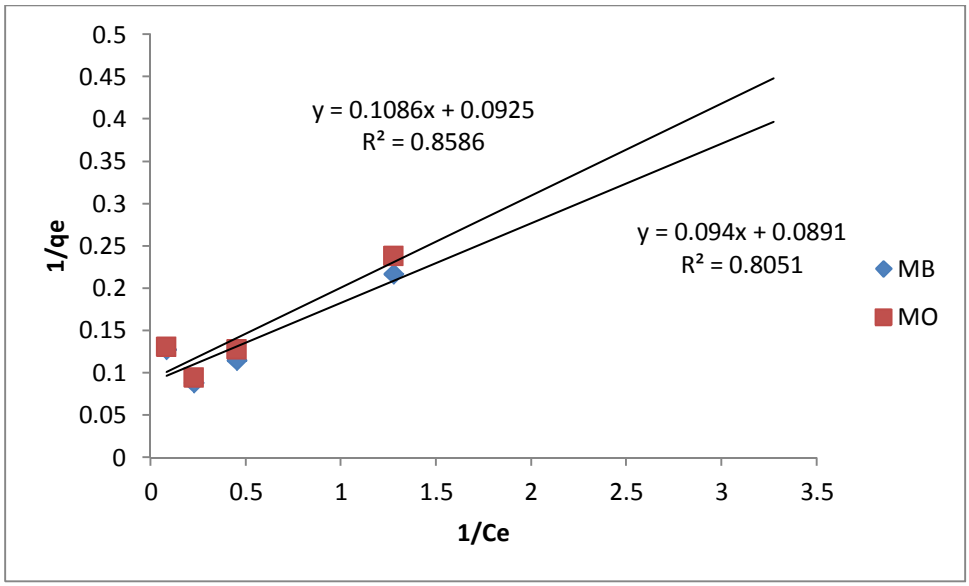


Figure 23: Langmuir isotherm of components of aqueous MBMO onto CMAC

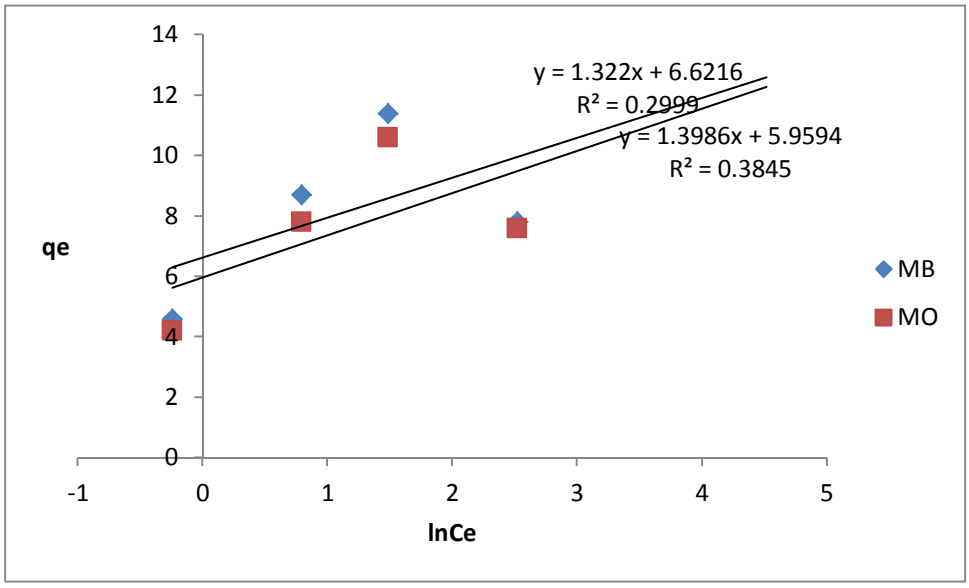


Figure 24: Temkin isotherm of components of aqueous MBMO mixture onto CMAC

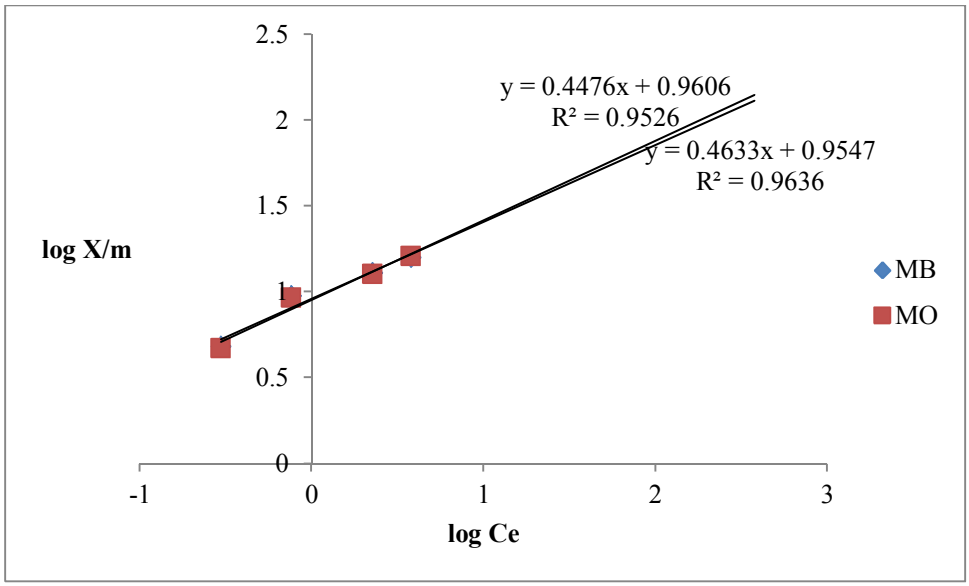


Figure 25: Freundlich isotherm of components of aqueous MBMO mixture onto PMAC

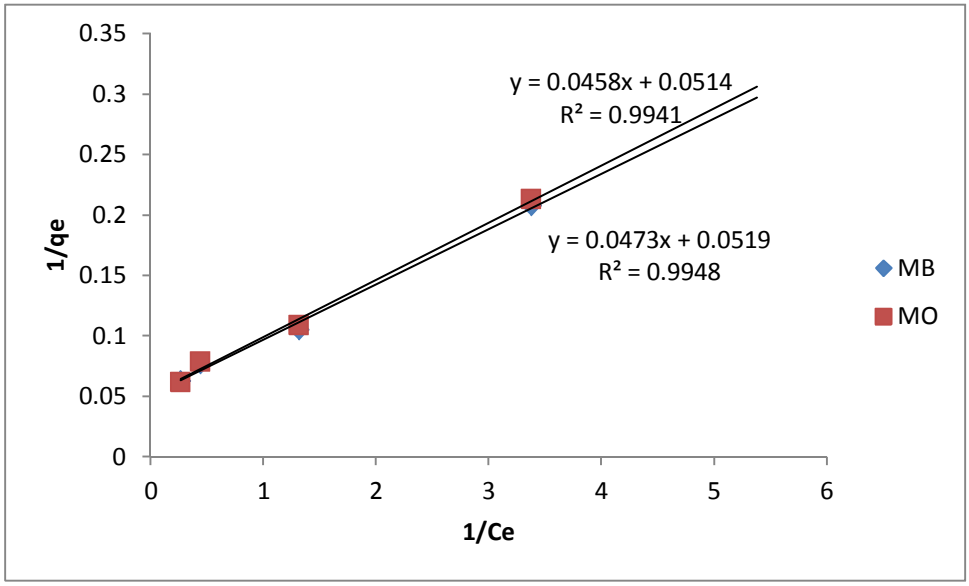


Figure 26: Langmuir isotherm of components of aqueous MBMO onto PMAC

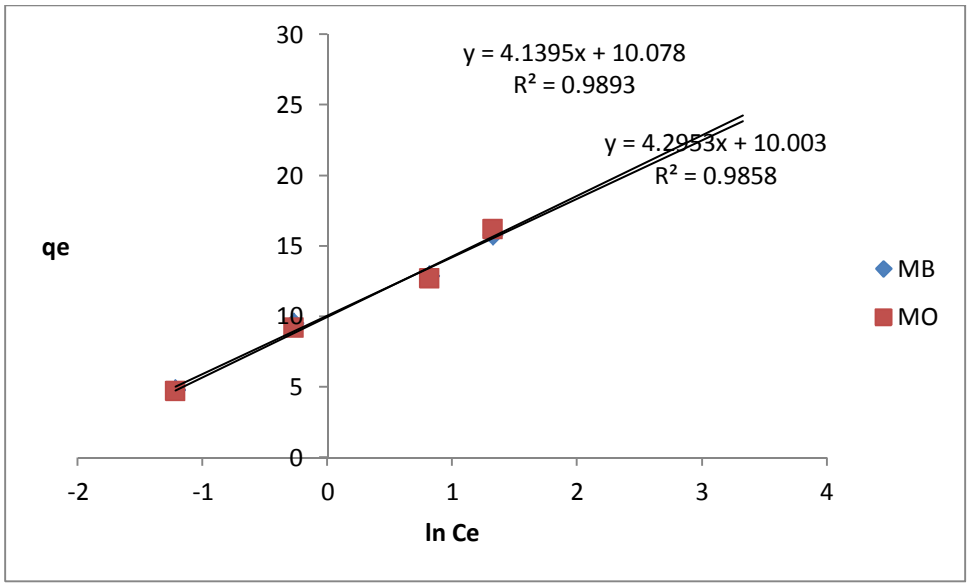


Figure 27: Temkin isotherm of components of aqueous MBMO mixture onto PMAC

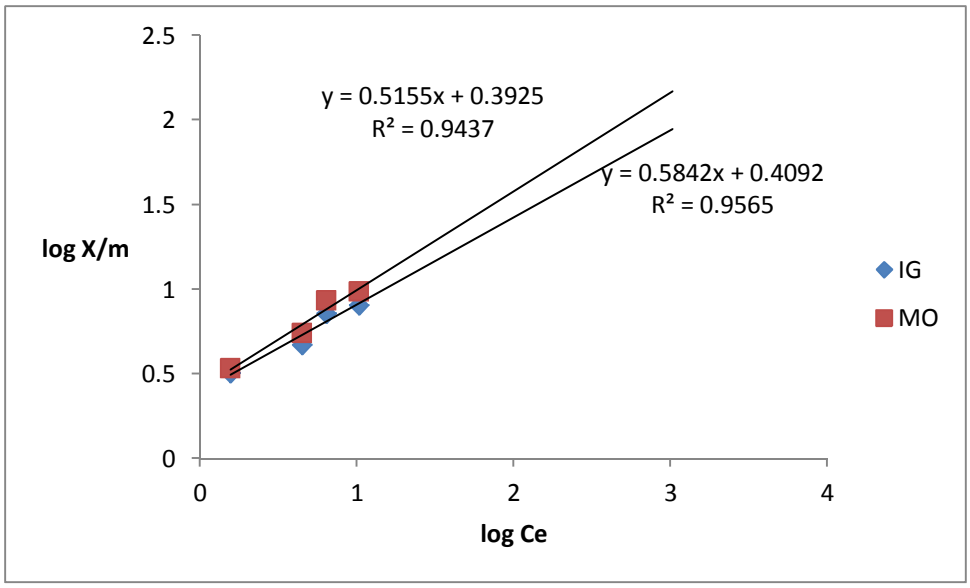


Figure 28: Freundlich isotherm of MOIG in Cd/Pb nitrate mixture onto UMAC

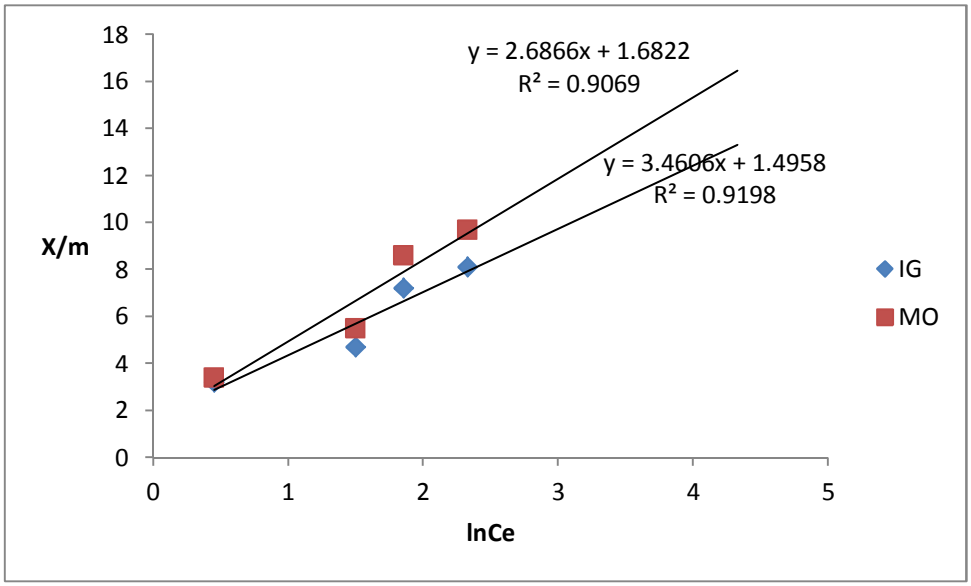


Figure 29: Temkin isotherm of components of MOIG from aqueous $Pb(NO_3)_2$ and $Cd(NO_3)_2.4H_2O$ mixture onto UMAC

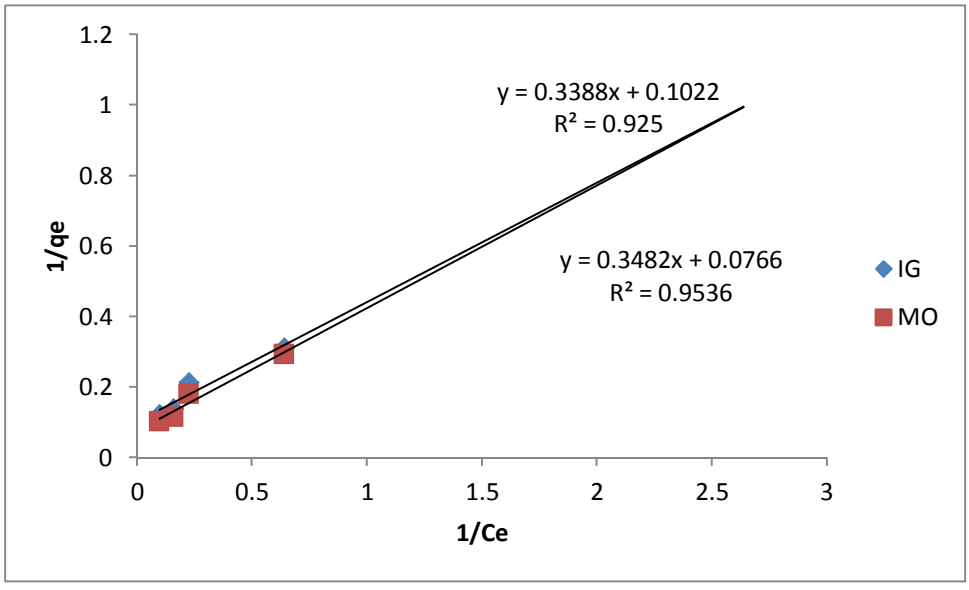


Figure 30: Langmuir isotherm of components of MOIG from aqueous $Pb(NO_3)_2$ and $Cd(NO_3)_2.4H_2O$ mixture onto UMAC

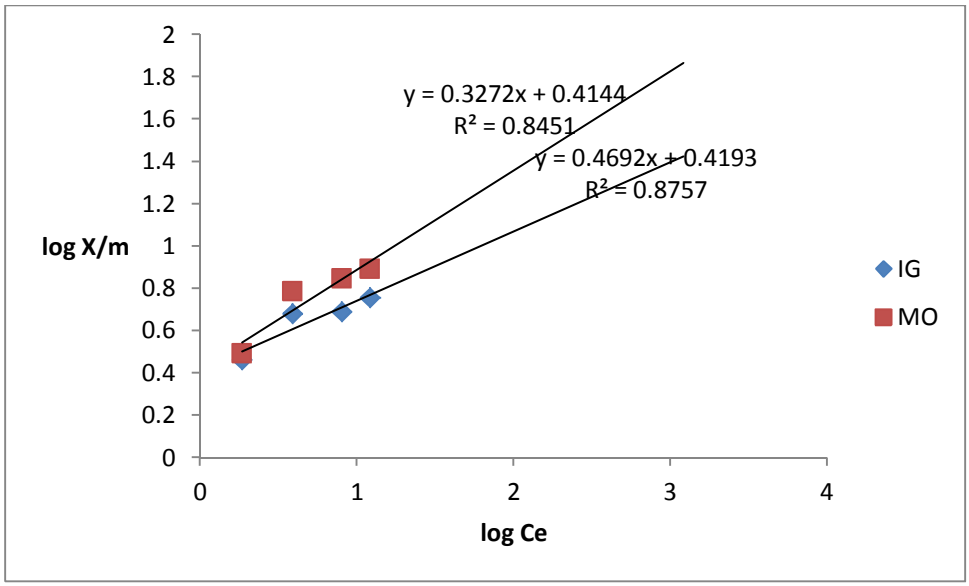


Figure 31: Freundlich isotherm of components of MOIG from aqueous $Pb(NO_3)_2$ and $Cd(NO_3)_2.4H_2O$ mixture onto CMAC

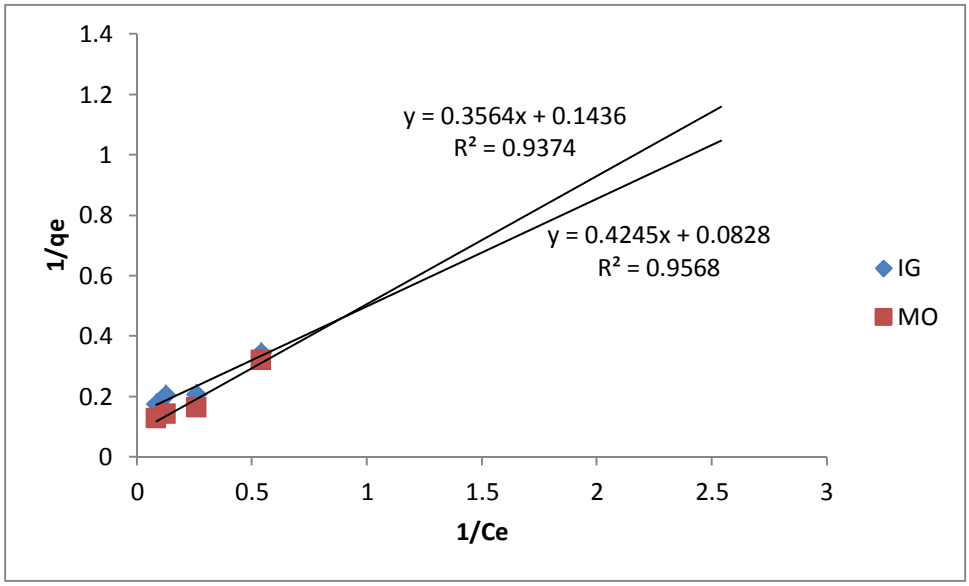


Figure 32: Langmuir isotherm of components of MOIG from aqueous $Pb(NO_3)_2$ and $Cd(NO_3)_2.4H_2O$ mixture onto CMAC

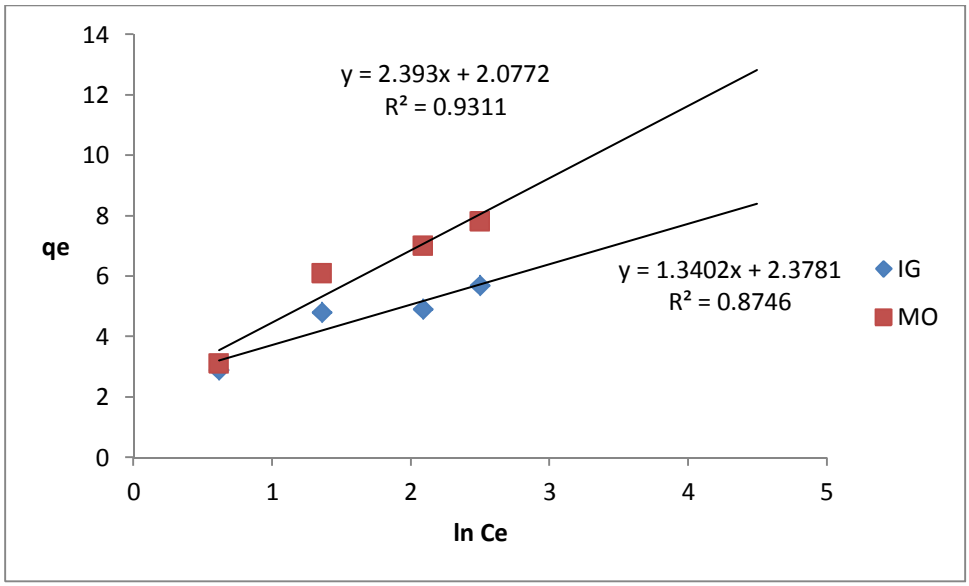


Figure 33: Temkin isotherm of components of MOIG from aqueous $Pb(NO_3)_2$ and $Cd(NO_3)_2.4H_2O$ mixture onto CMAC

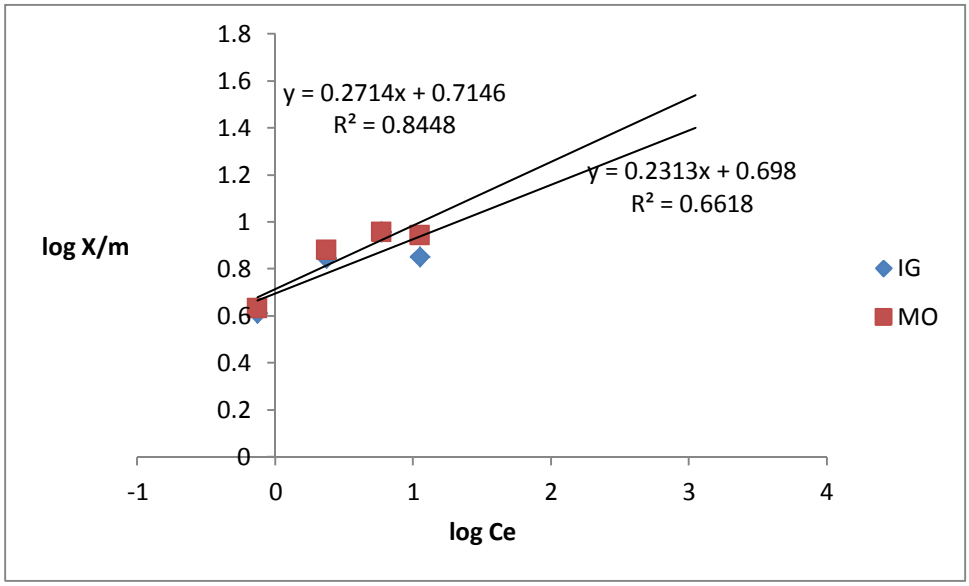


Figure 34: Freundlich isotherm of components of MOIG from aqueous $Pb(NO_3)_2$ and $Cd(NO_3)_2.4H_2O$ mixture onto PMAC

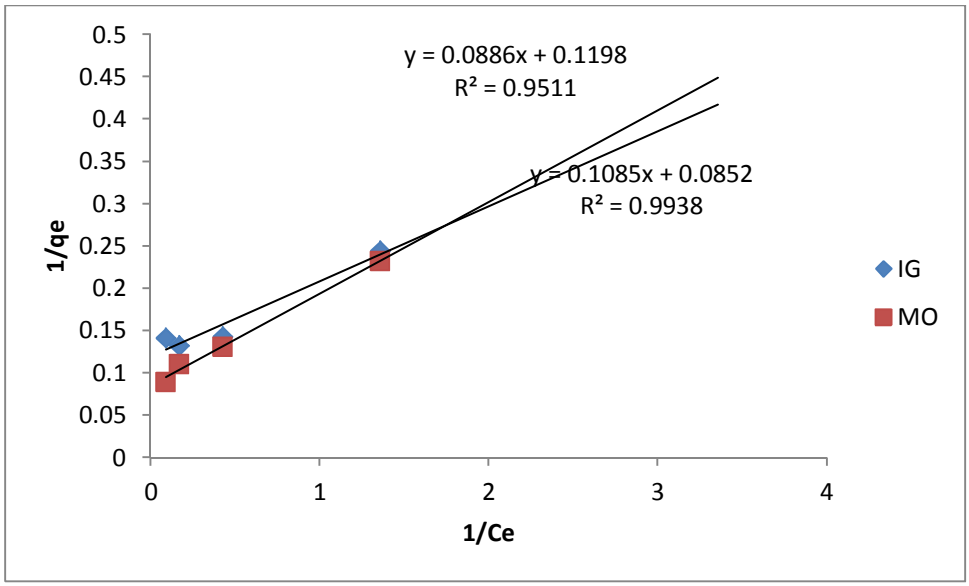


Figure 35: Langmuir isotherm of components of MOIG from aqueous $Pb(NO_3)_2$ and $Cd(NO_3)_2.4H_2O$ mixture onto PMAC

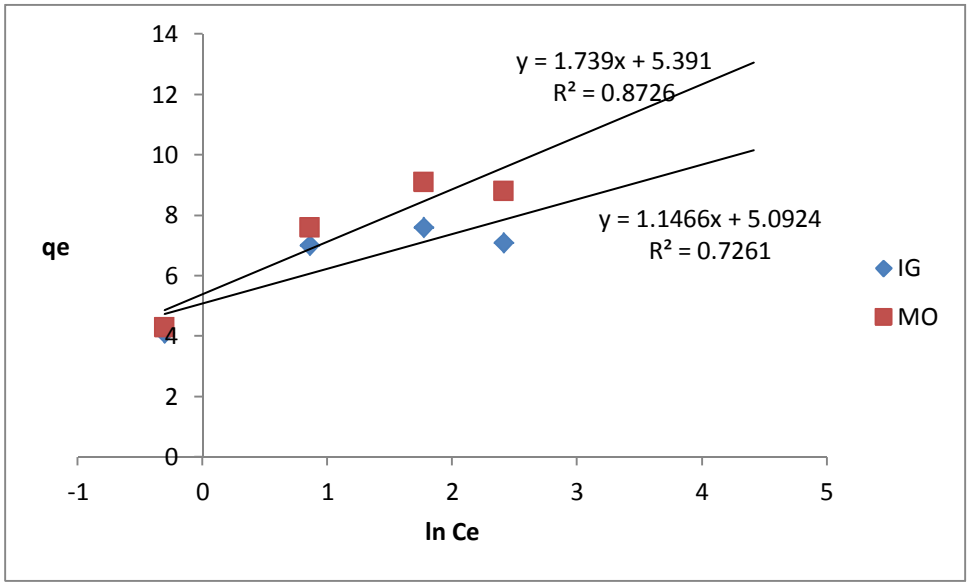


Figure 36: Temkin isotherm of components of MOIG from aqueous $Pb(NO_3)_2$ and $Cd(NO_3)_2.4H_2O$ mixture onto PMAC

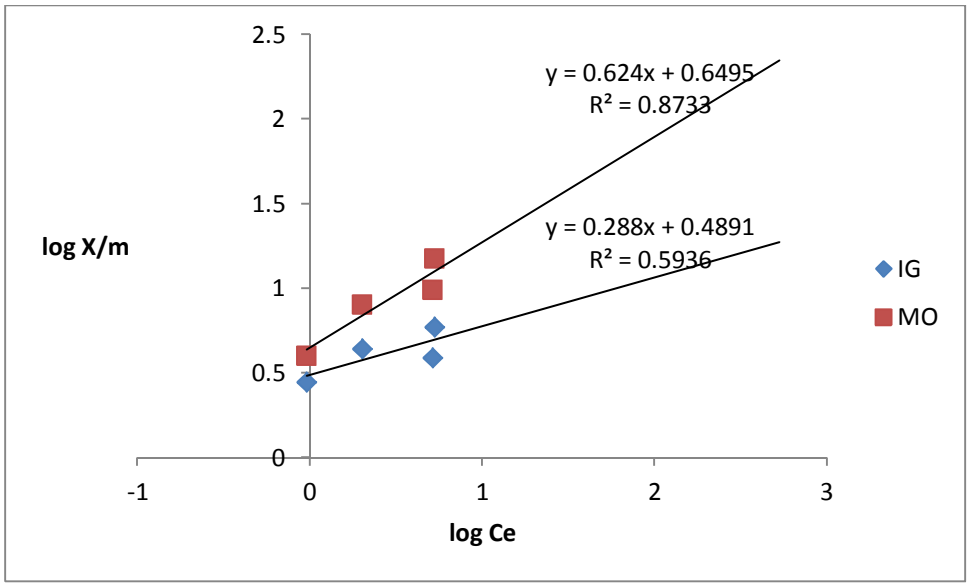


Figure 37 : Freundlich isotherm of components of aqueous MOIG mixture onto UMAC

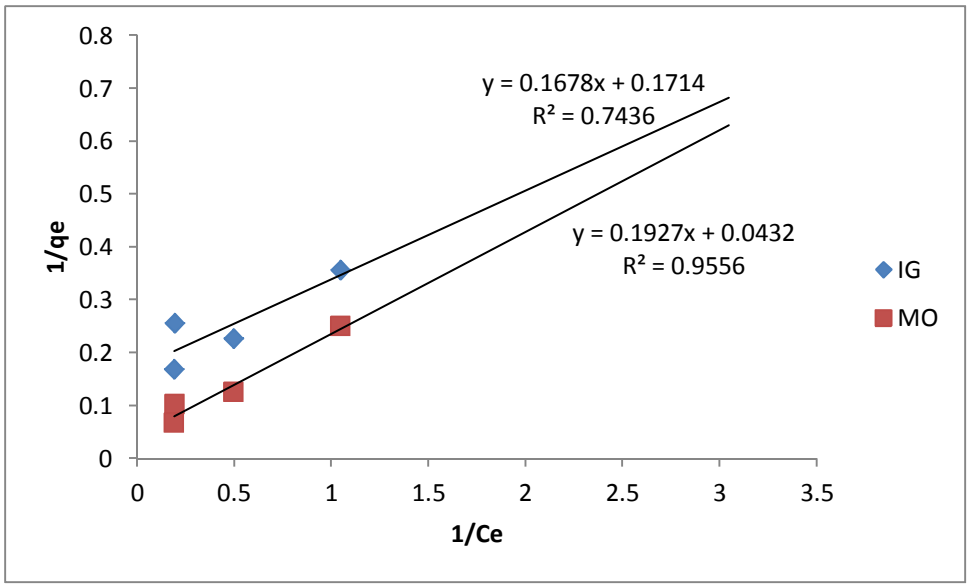


Figure 38: Langmuir sotherm of components of aqueous MOIG mixture onto UMAC

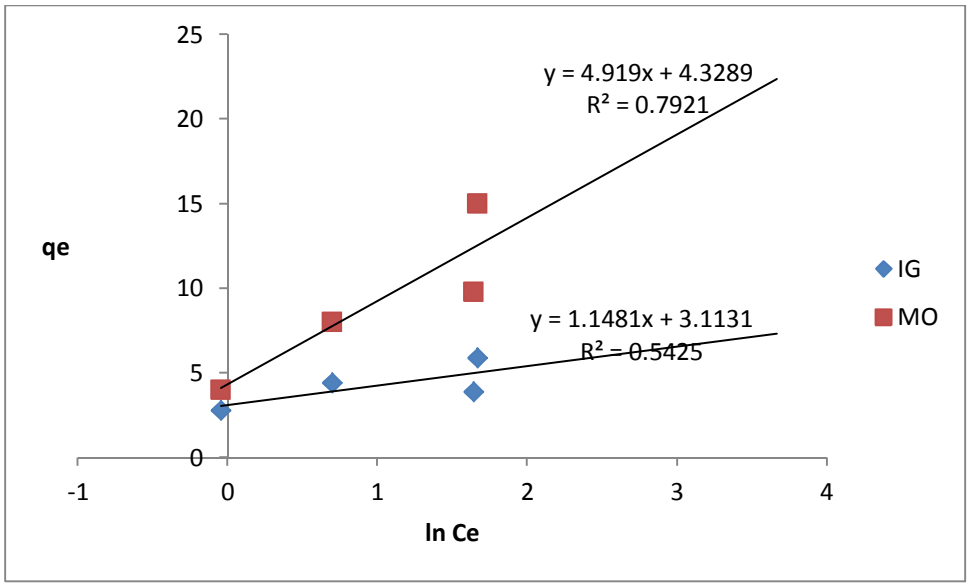


Figure 39 : Temkin isotherm of components of aqueous MOIG mixture onto UMAC

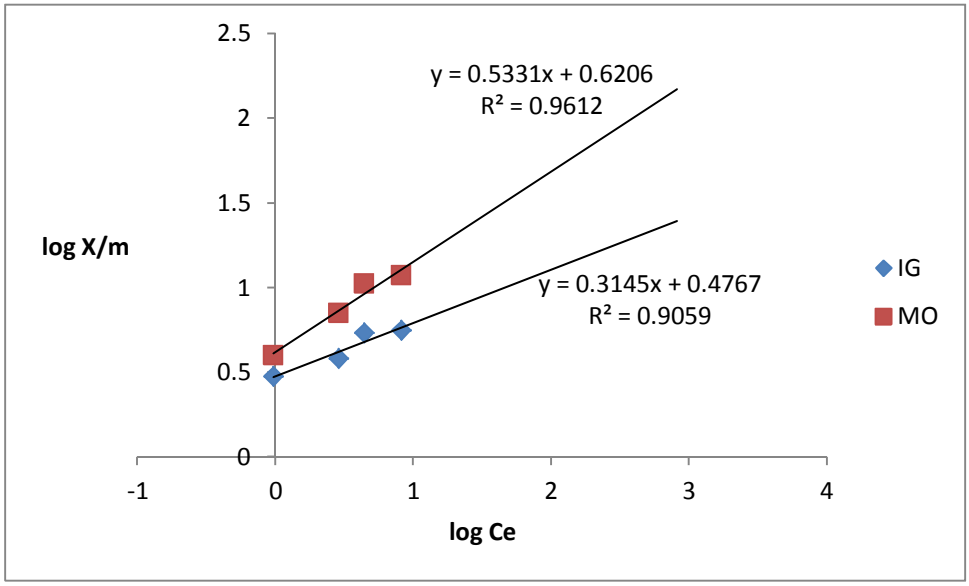


Figure 40: Freundlich isotherm of components of aqueous MOIG mixture onto CMAC

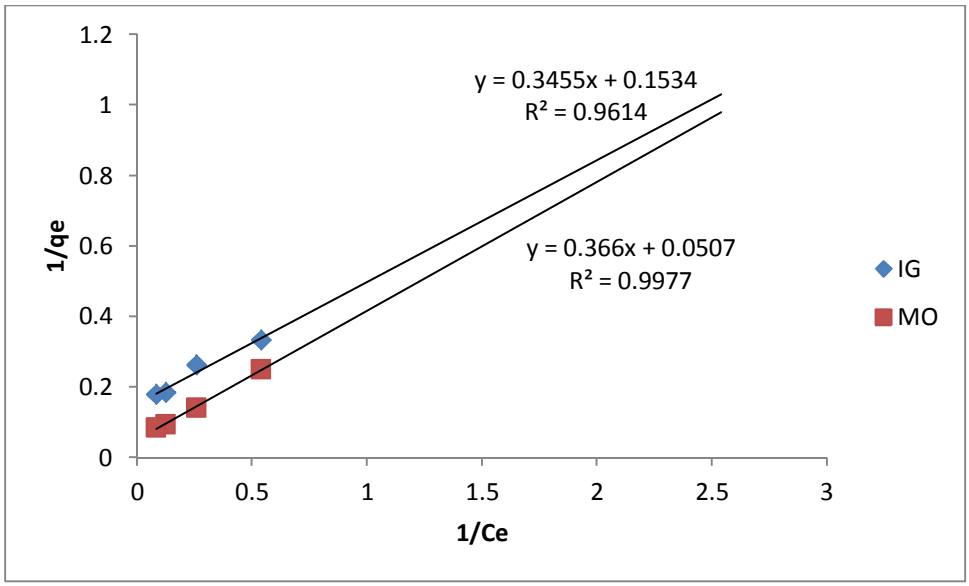


Figure 41: Langmuir isotherm of components of aqueous MOIG mixture onto CMAC

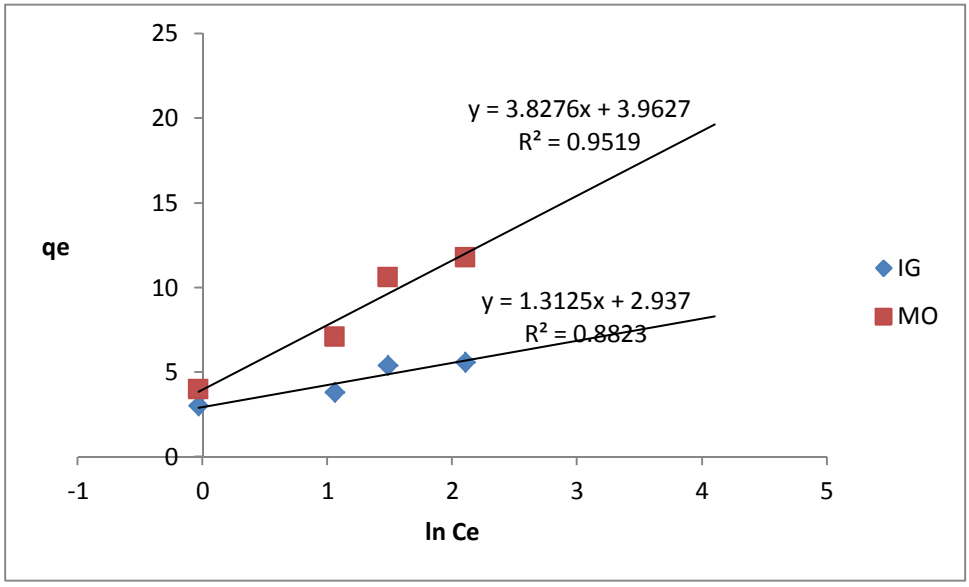


Figure 42: Temkin isotherm of components of aqueous MOIG mixture onto CMAC

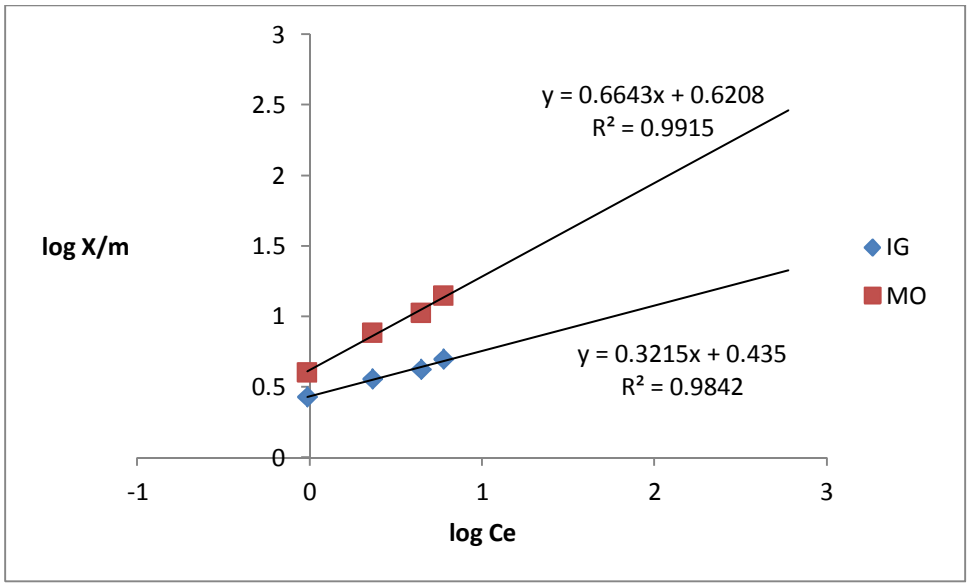


Figure 43: Freundlich isotherm of components of aqueous MOIG mixture onto PMAC

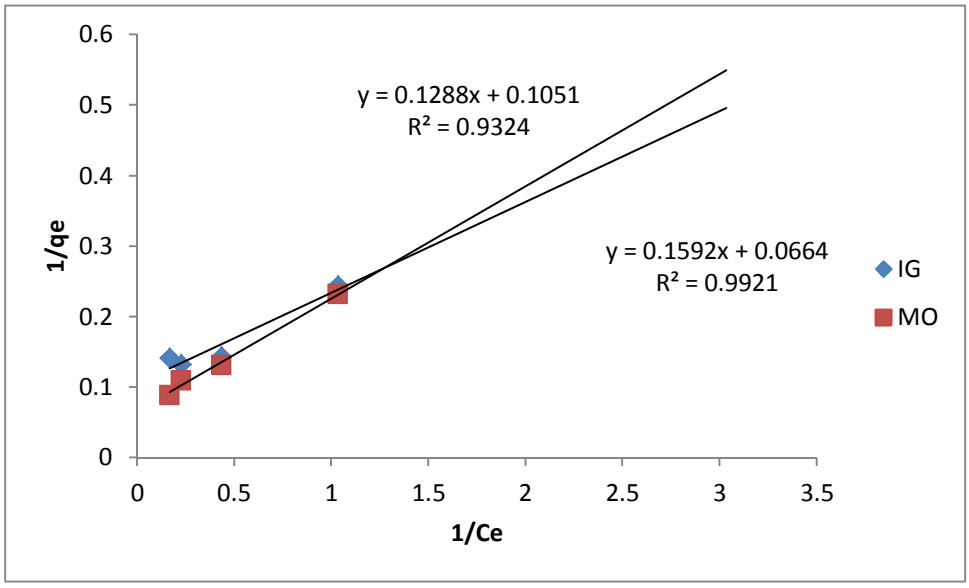


Figure 44: Langmuir isotherm of components of aqueous MOIG mixture onto PMAC

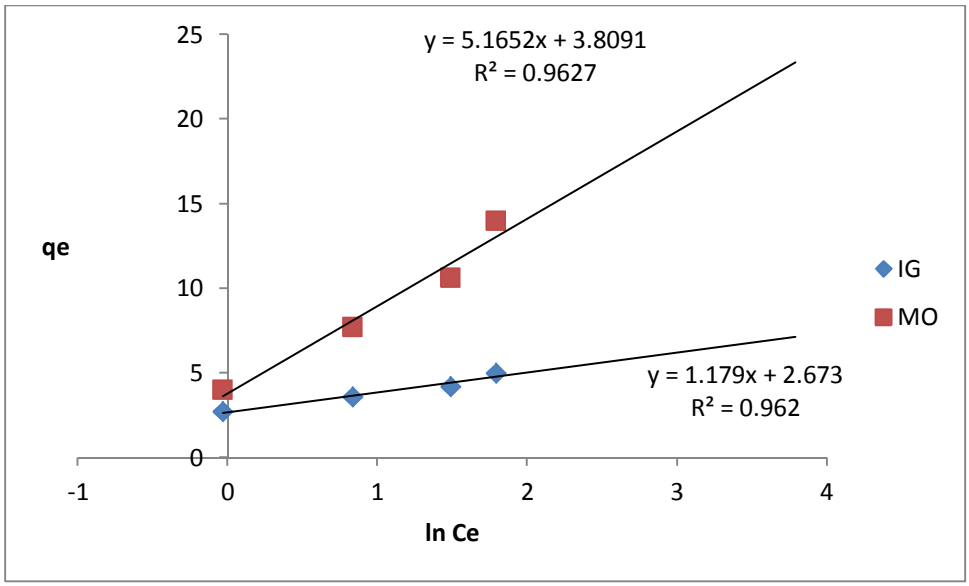


Figure 45 : Temkin isotherm of components of aqueous MOIG mixture onto PMAC

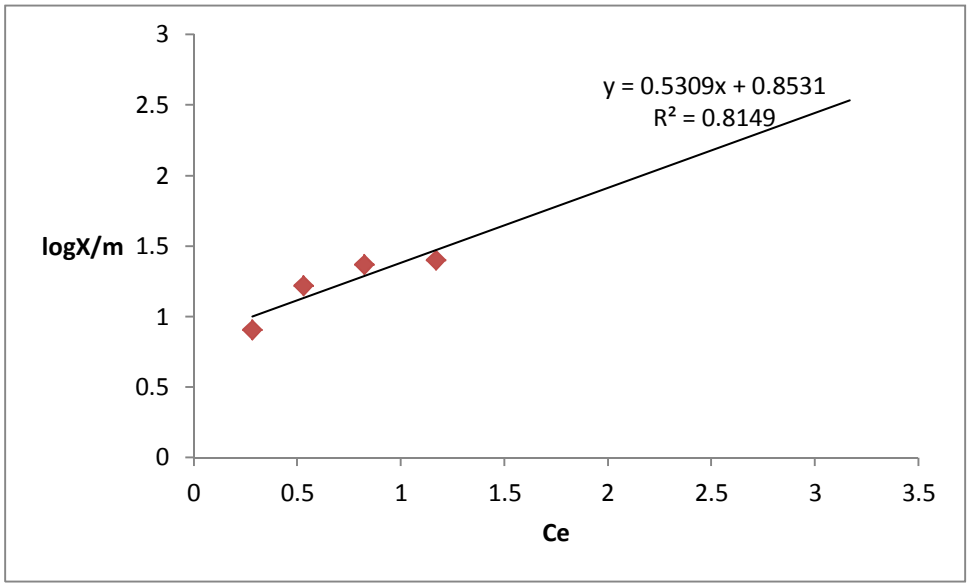


Fig 46: Freundlich isotherm of aqueous MO adsorbed onto UMAC

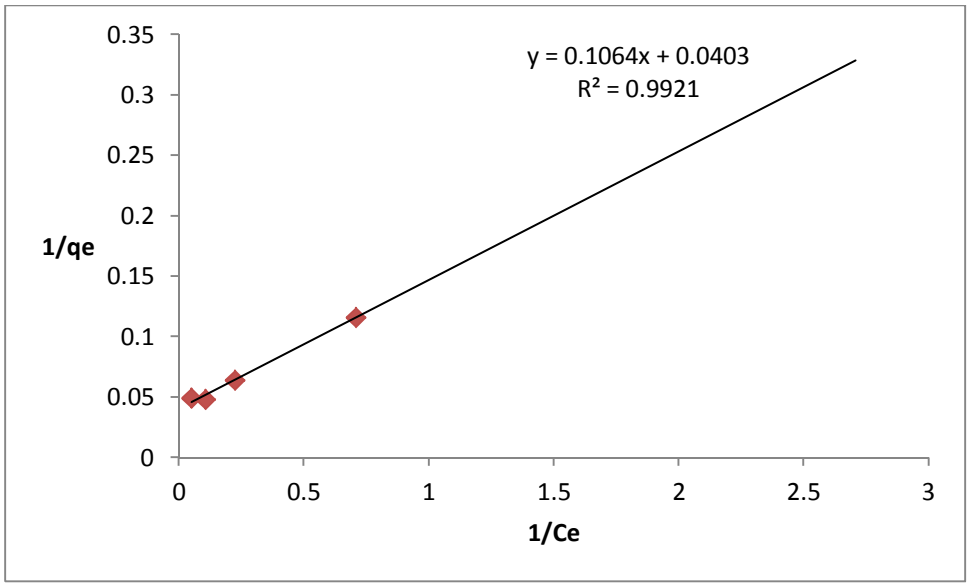


Figure 47: Langmuir isotherm of aqueous MO adsorbed onto UMAC

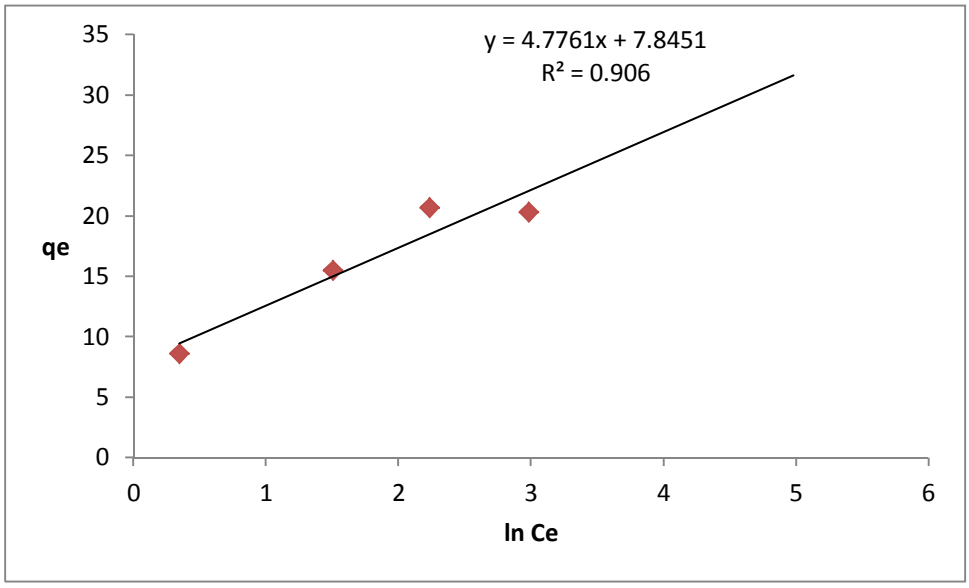


Figure 48: Temkin isotherm of aqueous MO adsorbed onto UMAC

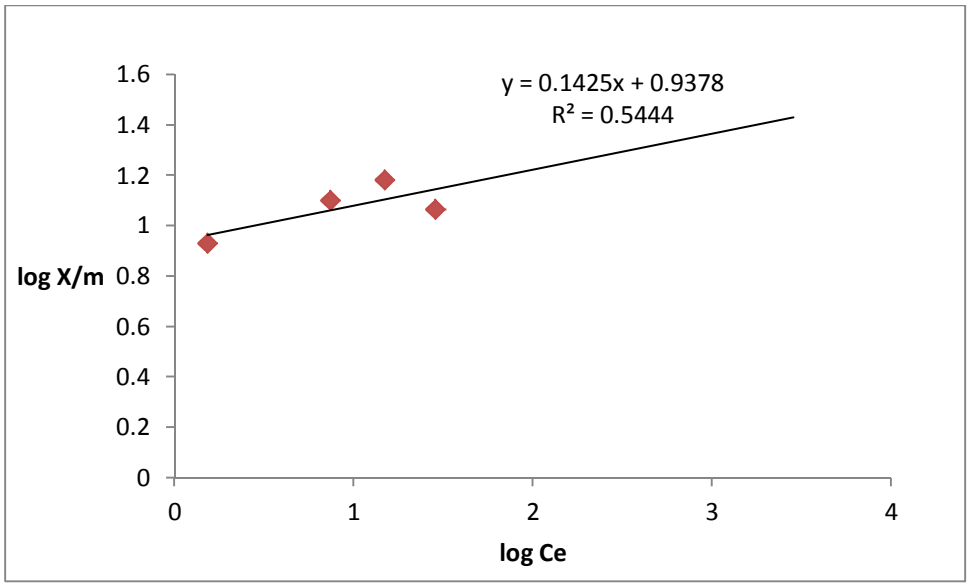


Figure 49: Freundlich isotherm For Aqueous MO onto CMAC

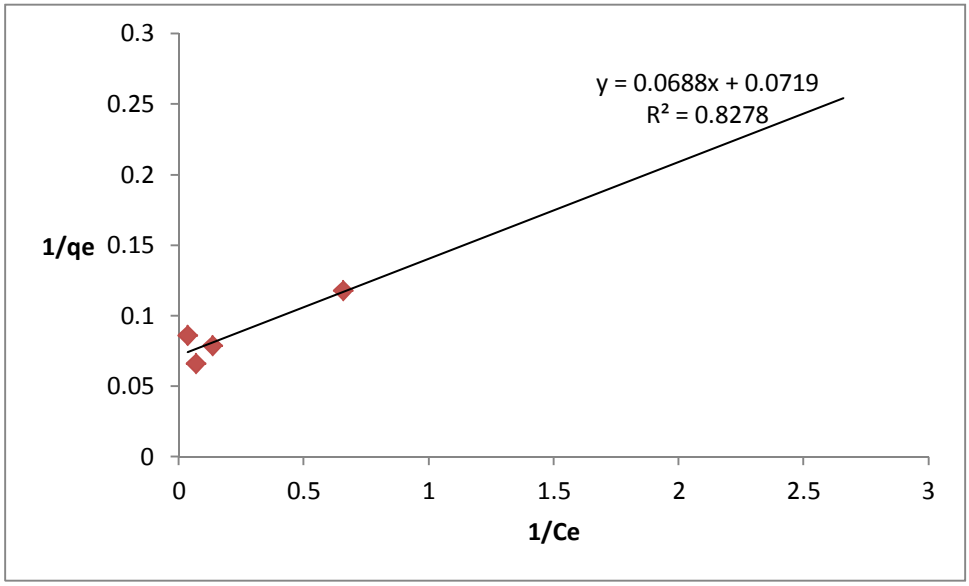


Figure 50: Langmuir isotherm of aqueous MO adsorbedonto CMAC

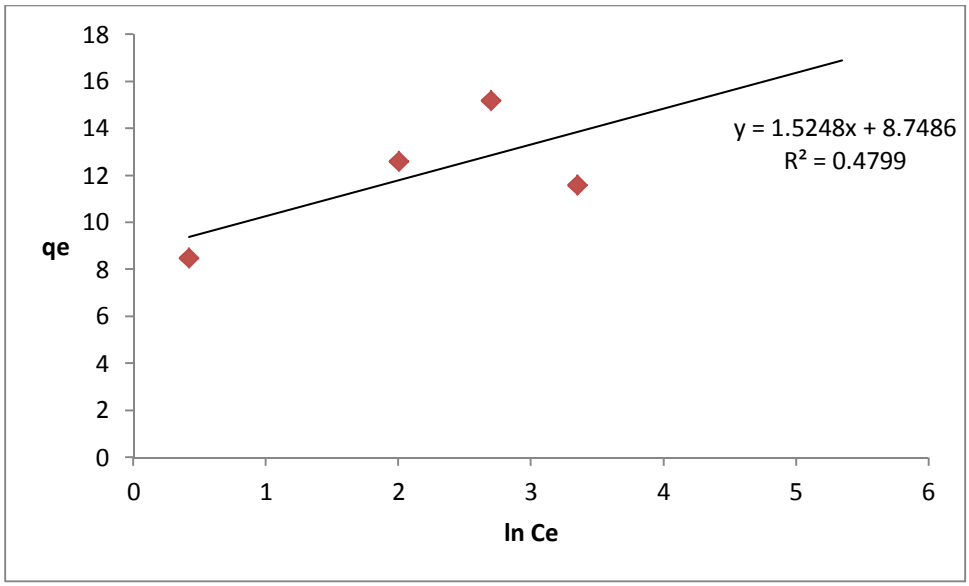


Figure 51: Temkin isotherm of aqueous MO adsorbed onto CMAC

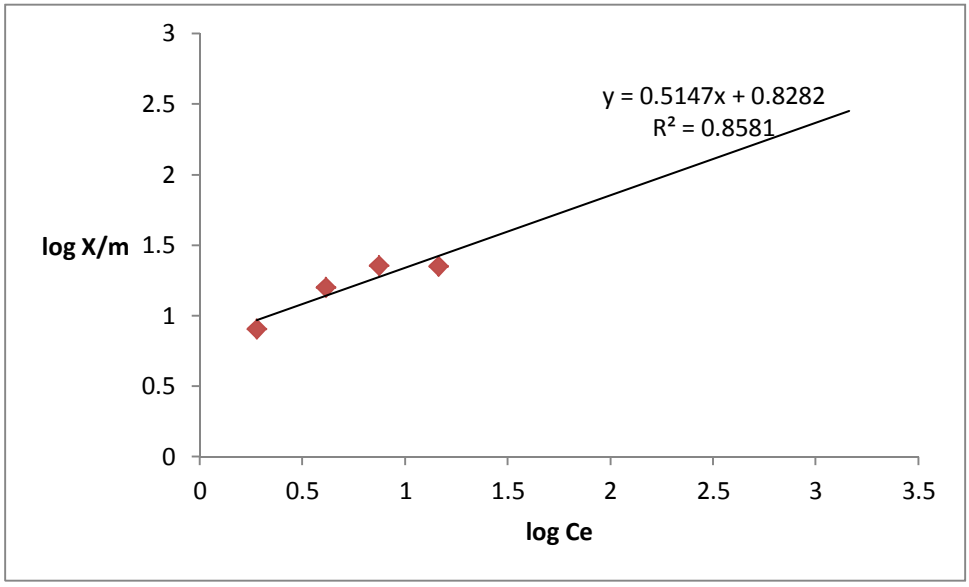


Figure 52: Freundlich isotherm of aqueous MO adsorbed onto PMAC

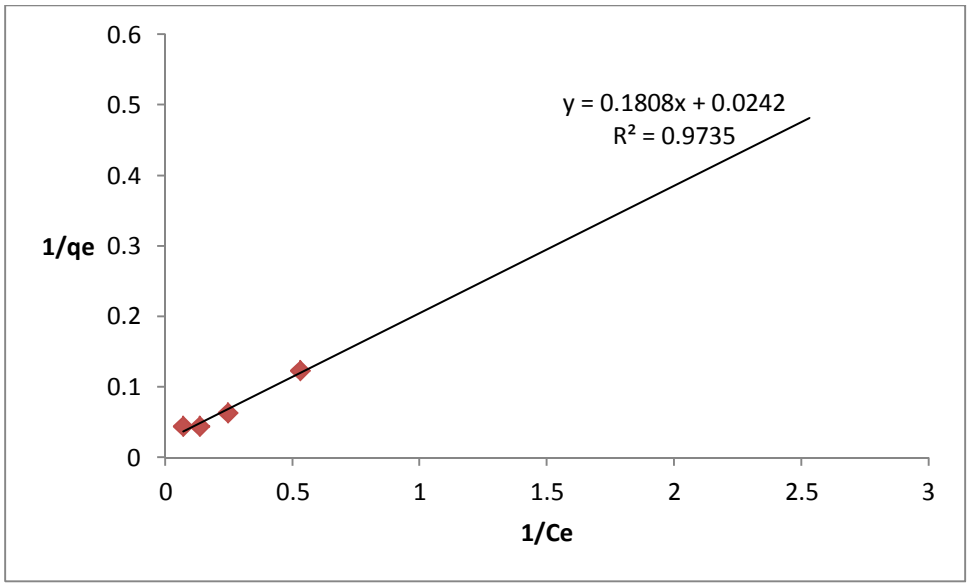


Figure 53: Langmuir isotherm of aqueous MO adsorbed onto PMAC

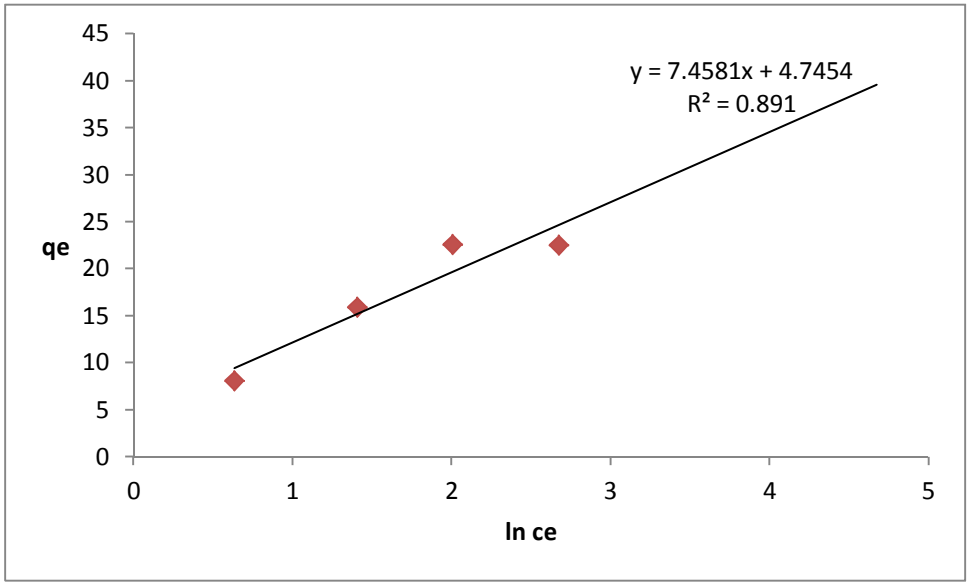


Figure 54: Temkin isotherm of aqueous MO adsorbed onto PMAC

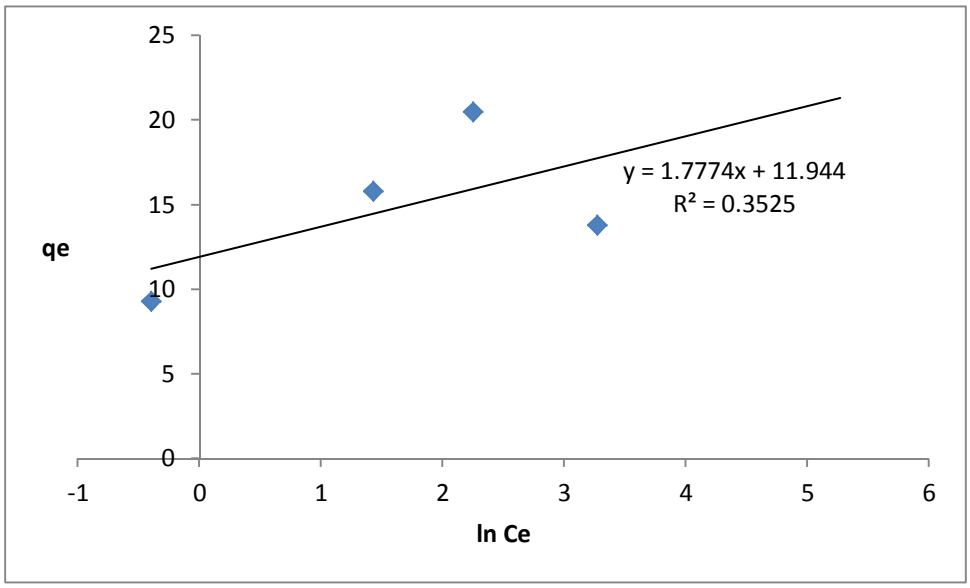


Figure 55: Temkin isotherm of aqueous MB adsorbed onto UMAC

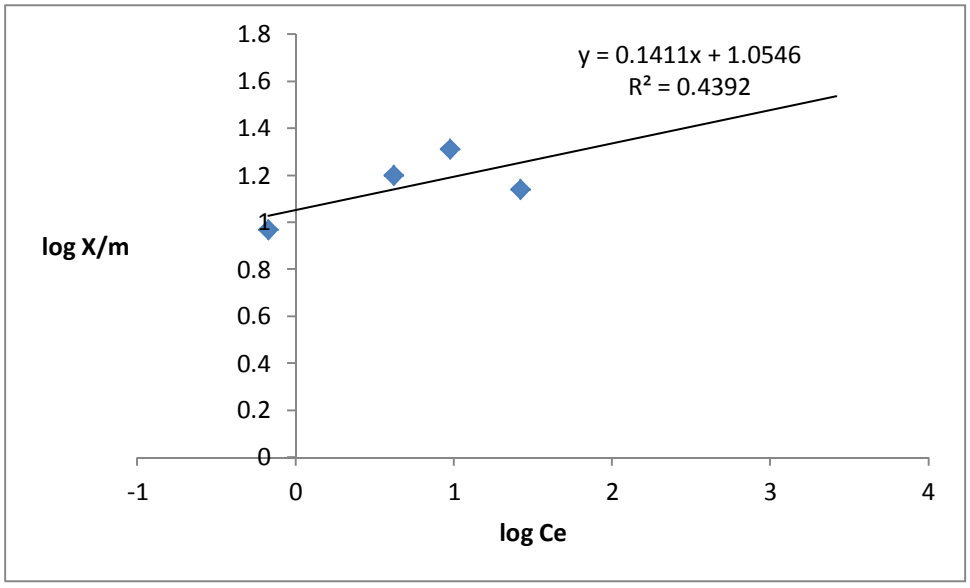


Figure 56: Freundlich isotherm of aqueous MB adsorbed onto UMAC

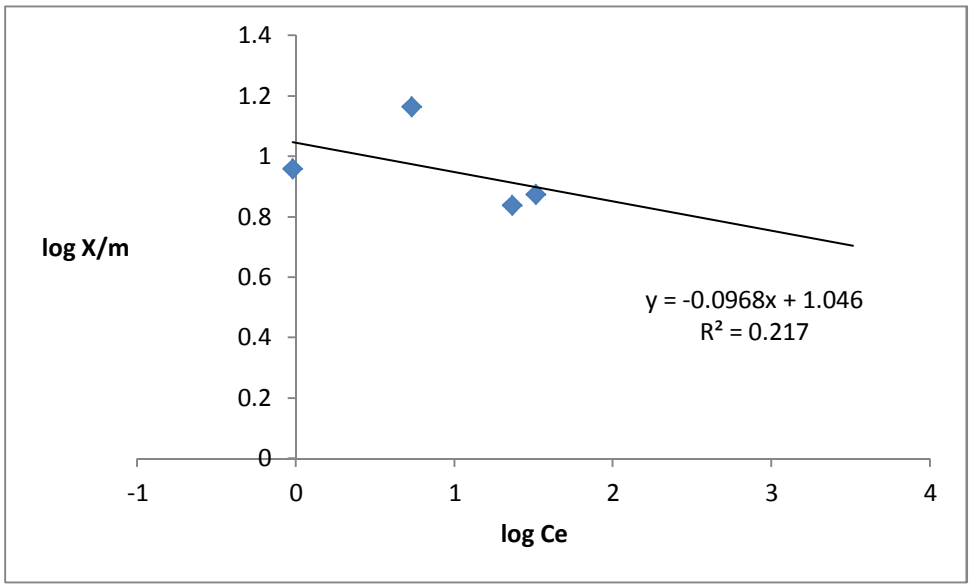


Figure 57: Freundlich isotherm for aqueous MB adsorbed onto CMAC

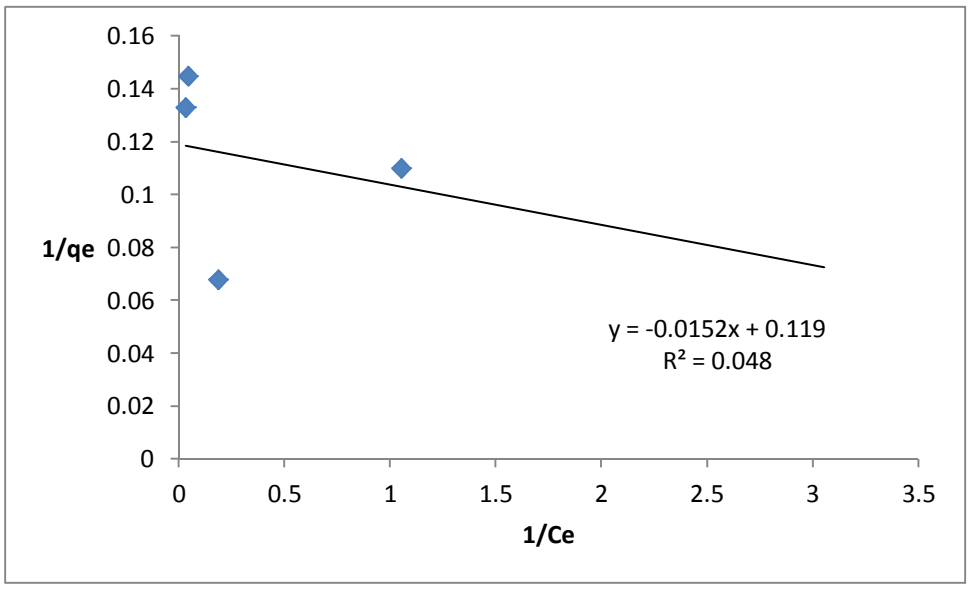


Figure 58: Langmuir isotherm of aqueous MB adsorbed onto CMAC

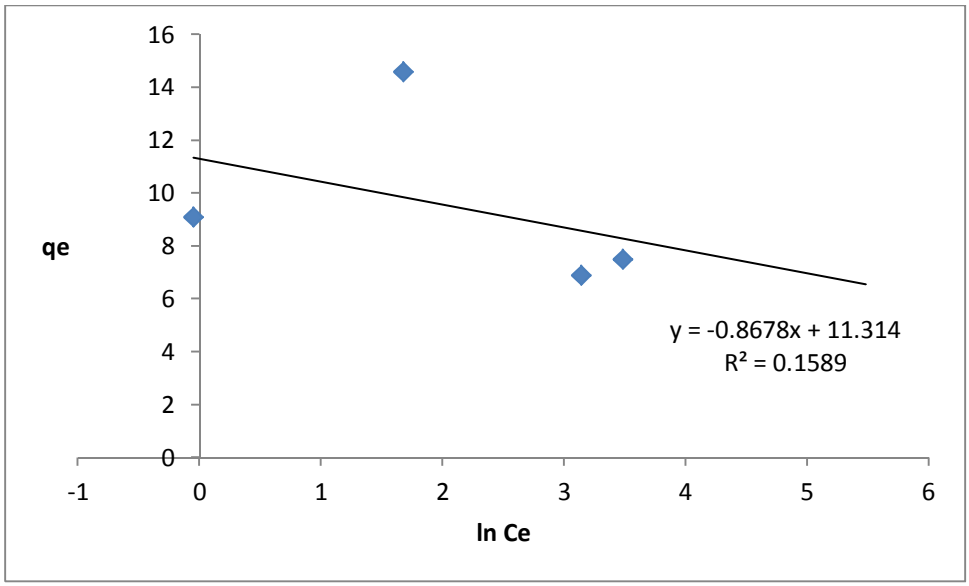


Figure 59: Temkin isotherm of aqueous MB adsorbed onto CMAC

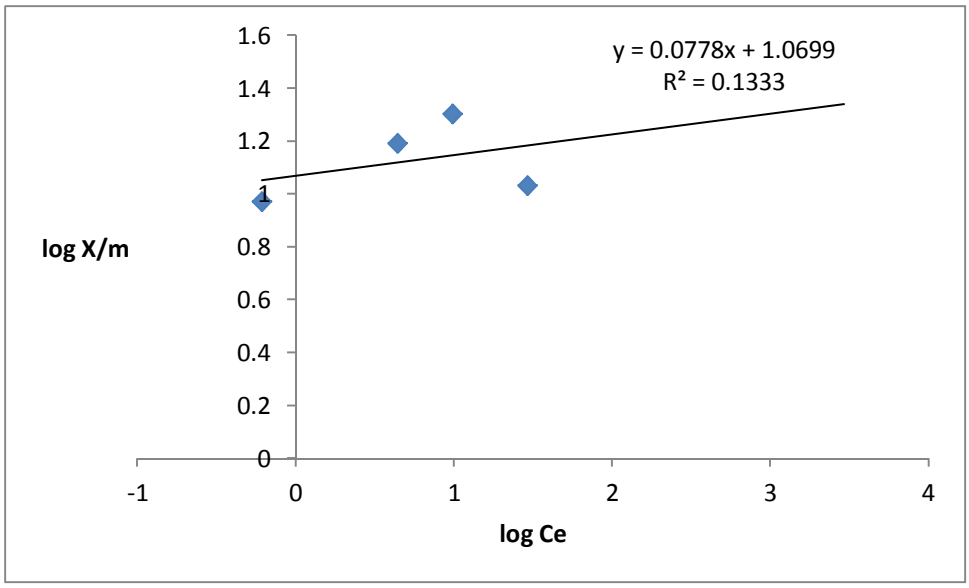


Figure 60: Freundlich isotherm of aqueous MB adsorbed onto PMAC

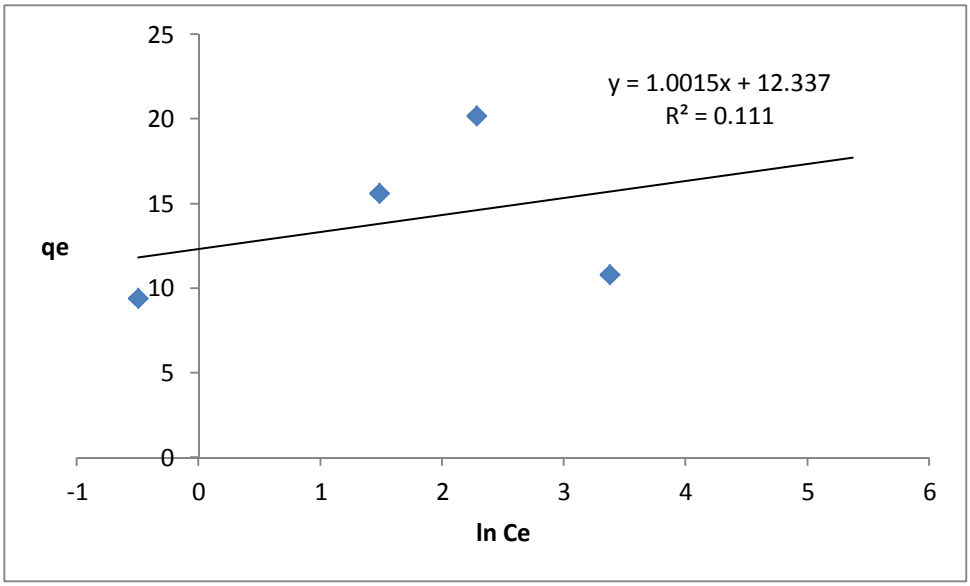


Figure 61: Temkin isotherm of aqueous MB adsorbed onto PMAC

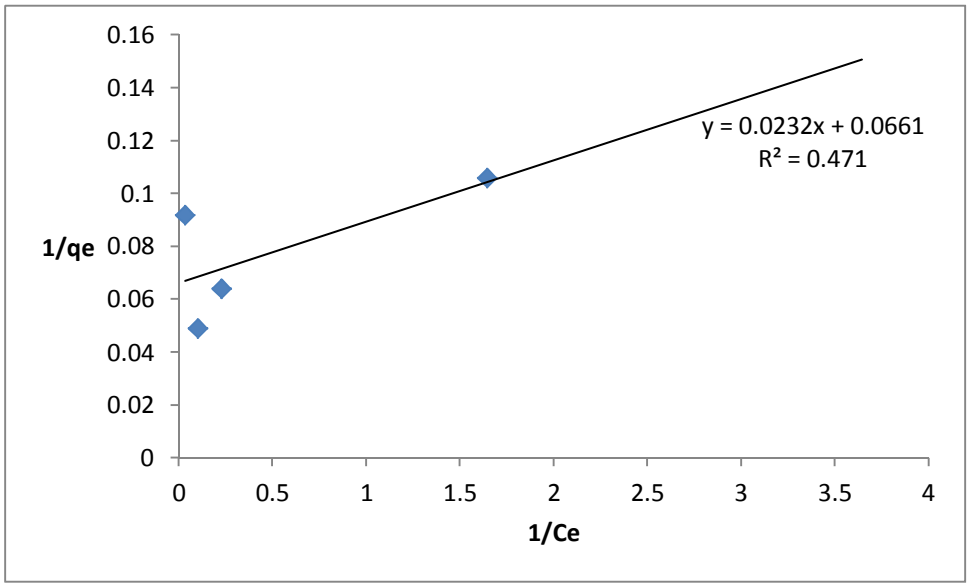


Figure 62: Langmuir isotherm of aqueous MB adsorbed onto PMAC

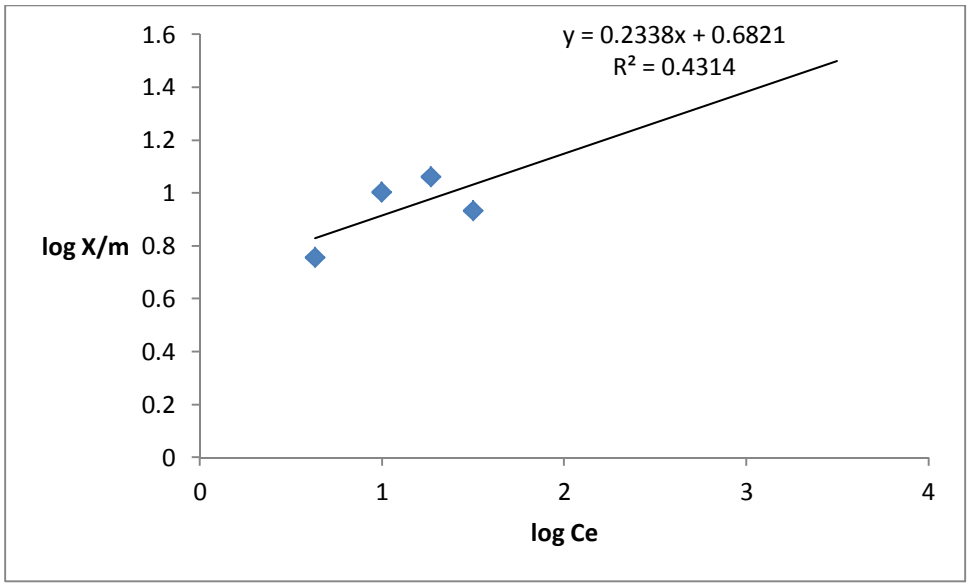


Figure 63: Freundlich isotherm of aqueous IG adsorbed onto UMAC

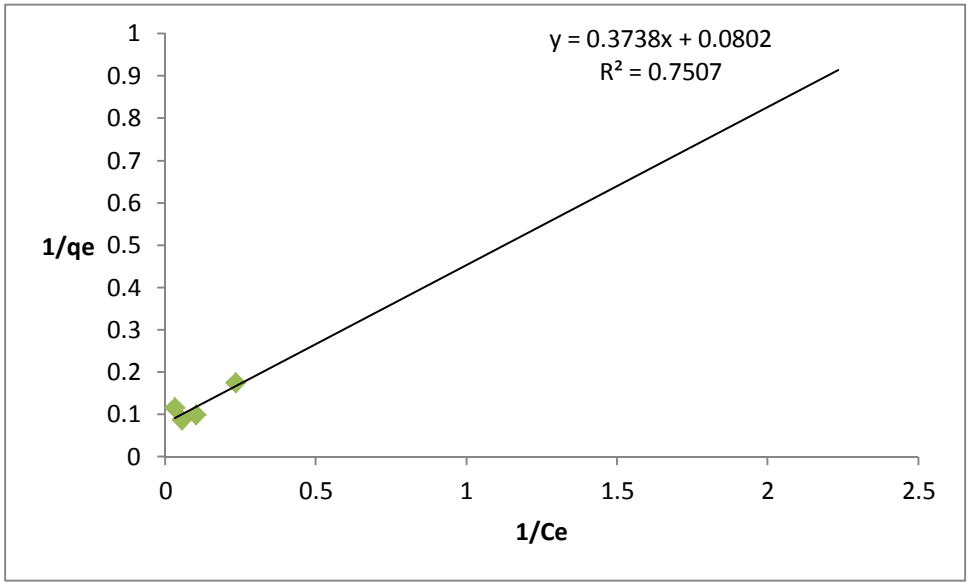


Figure 64: Langmuir isotherm of aqueous IG adsorbed onto UMAC

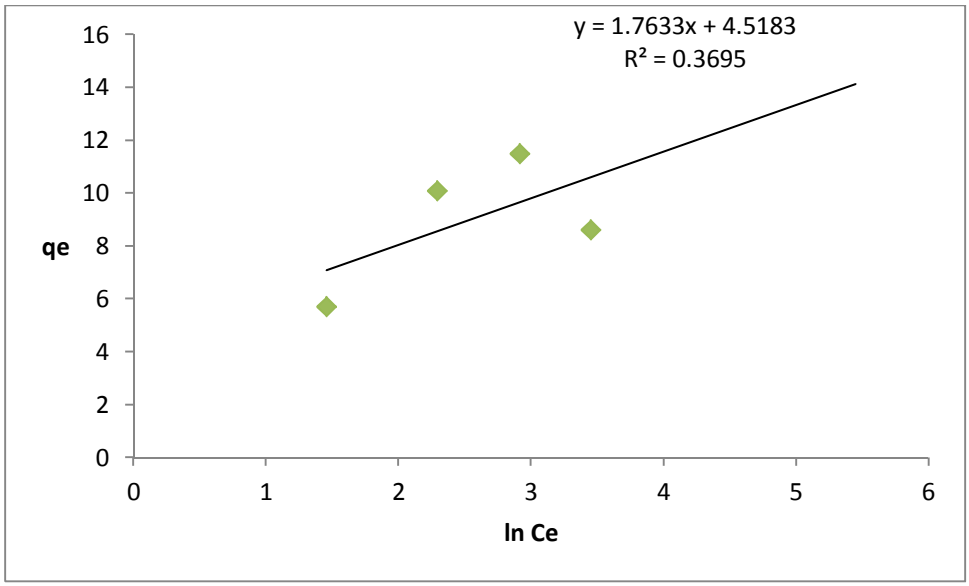


Figure 65: Temkin isotherm of aqueous IG adsorbed onto UMAC

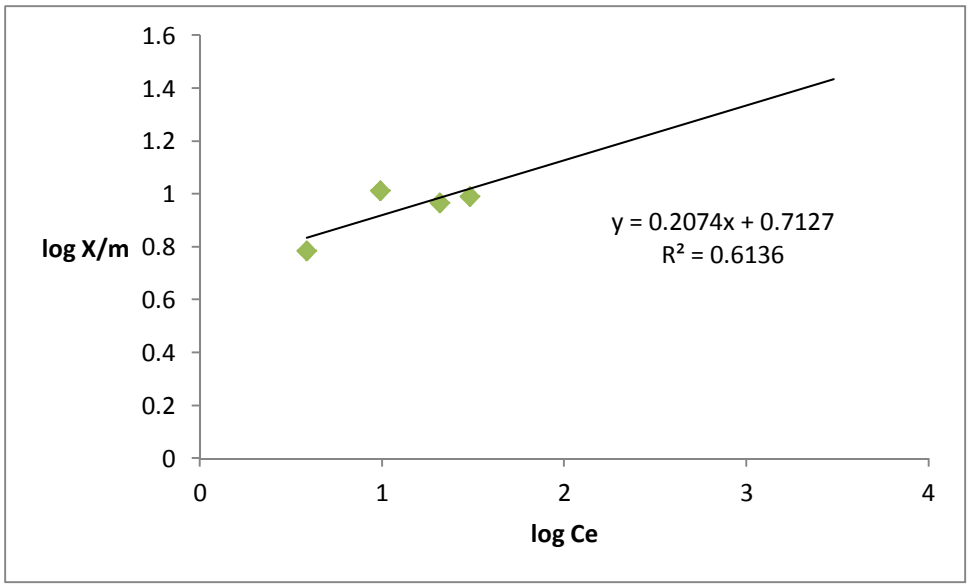


Figure 66: Freundlich isotherm of aqueous IG adsorbed onto CMAC

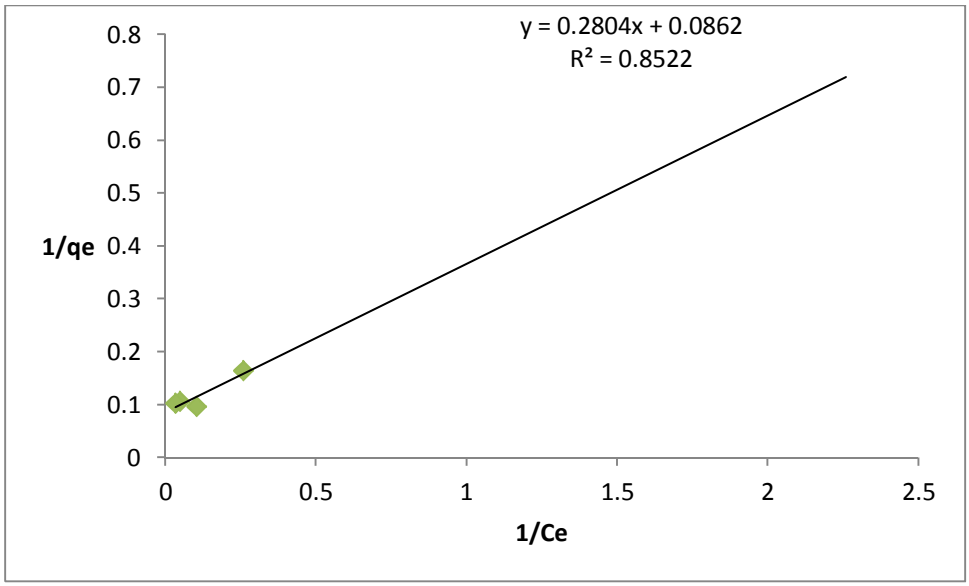


Figure 67 : Langmuir isotherm of aqueous IG onto CMAC

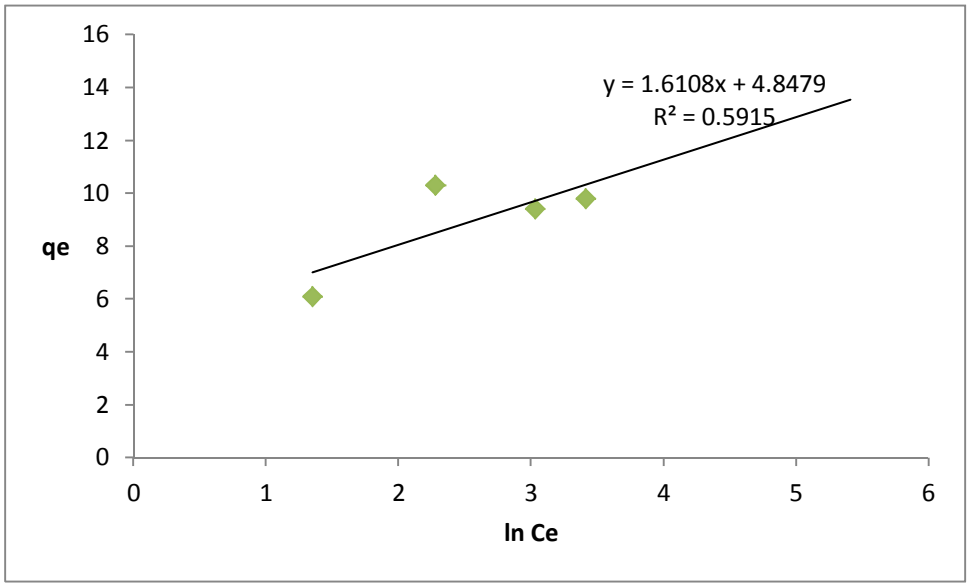


Figure 68: Temkin isotherm of aqueous IG adsorbed onto CMAC

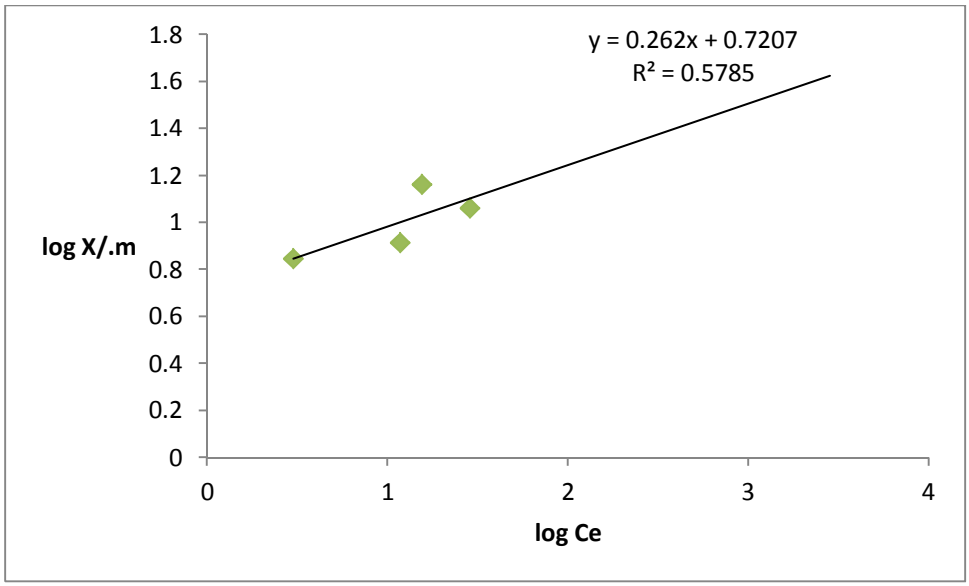


Figure 69 : Freundlich isotherm of aqueous IG adsorbed onto PMAC

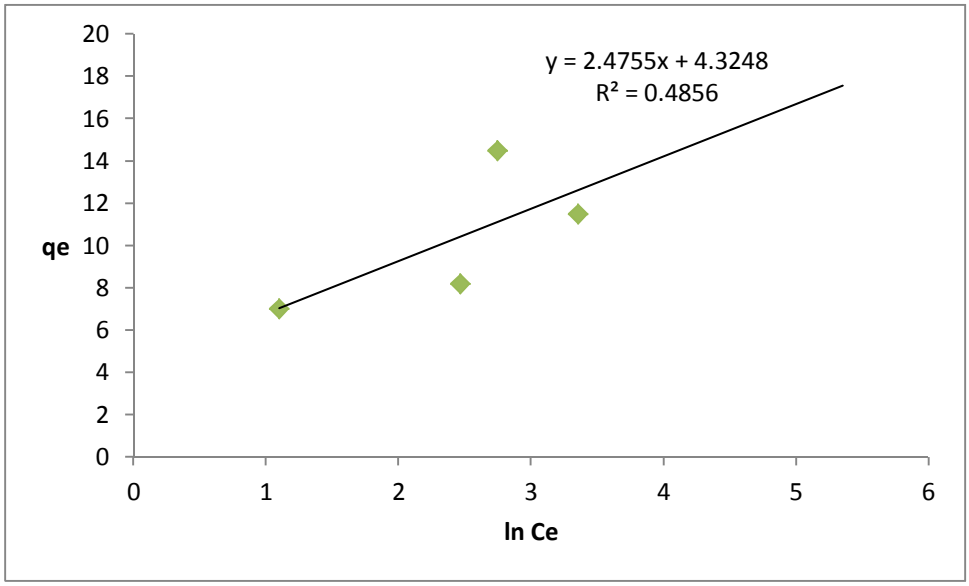


Figure 70: Temkin isotherm of aqueous IG adsorbed onto PMAC

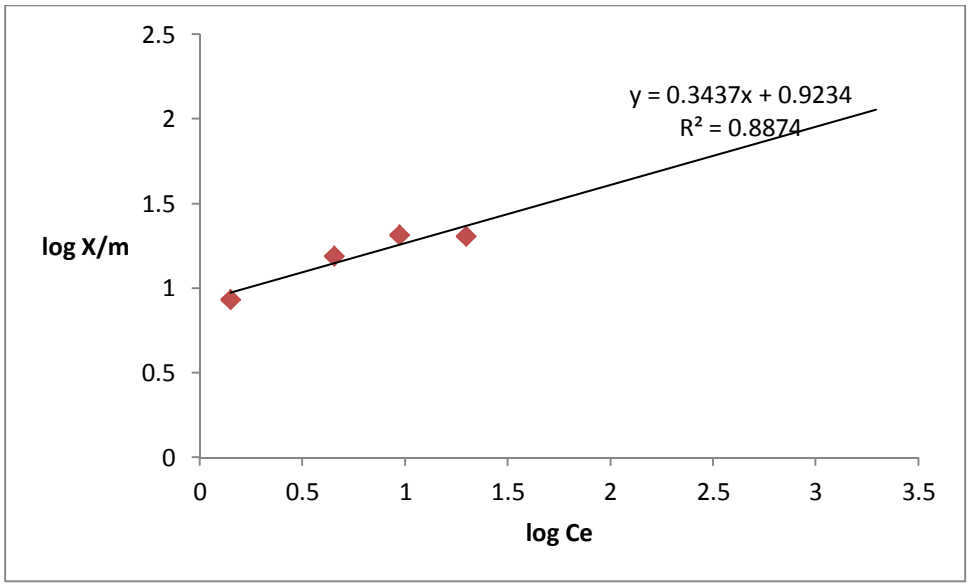


Figure 71: Freundlich isotherm of MO adsorbed from aqueous $Pb(NO_3)_2$ and $Cd(NO_3)_2.4H_2O$ mixture onto UMAC

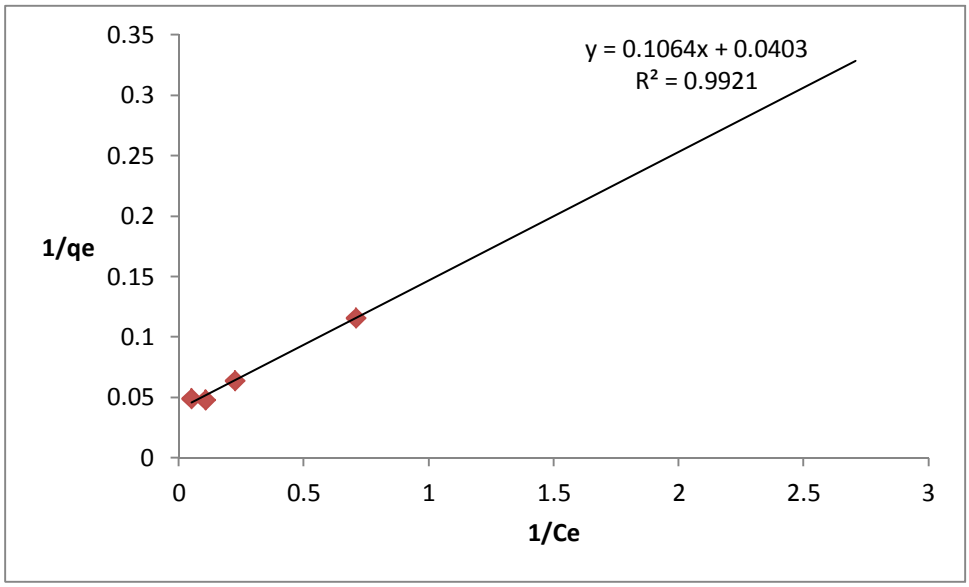


Figure 72: Langmuir isotherm of MO adsorbed from aqueous $Pb(NO_3)_2$ and $Cd(NO_3)_2.4H_2O$ mixture onto UMAC

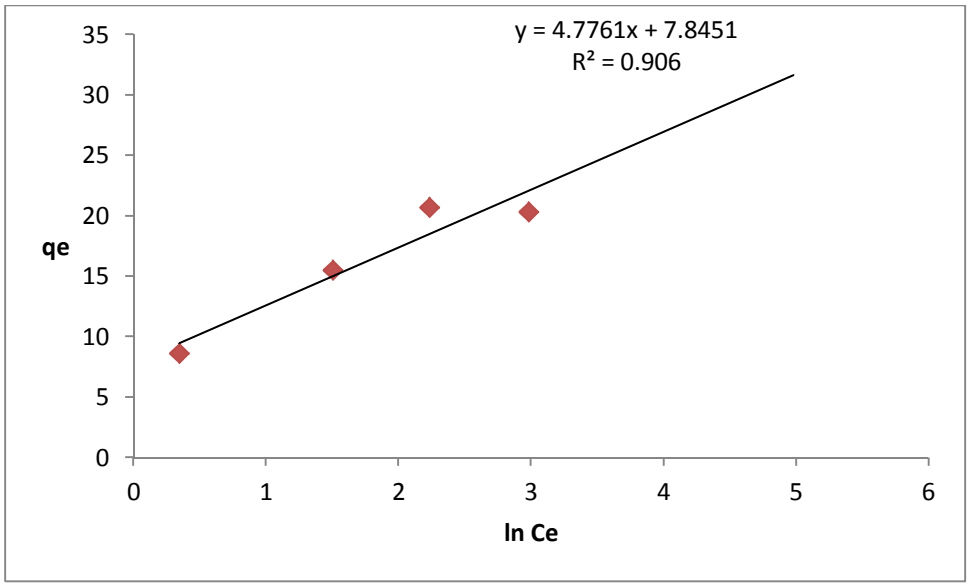


Figure 73: Temkin isotherm of MO from aqueous $Pb(NO_3)_2$ and $Cd(NO_3)_2.4H_2O$ mixture onto UMAC

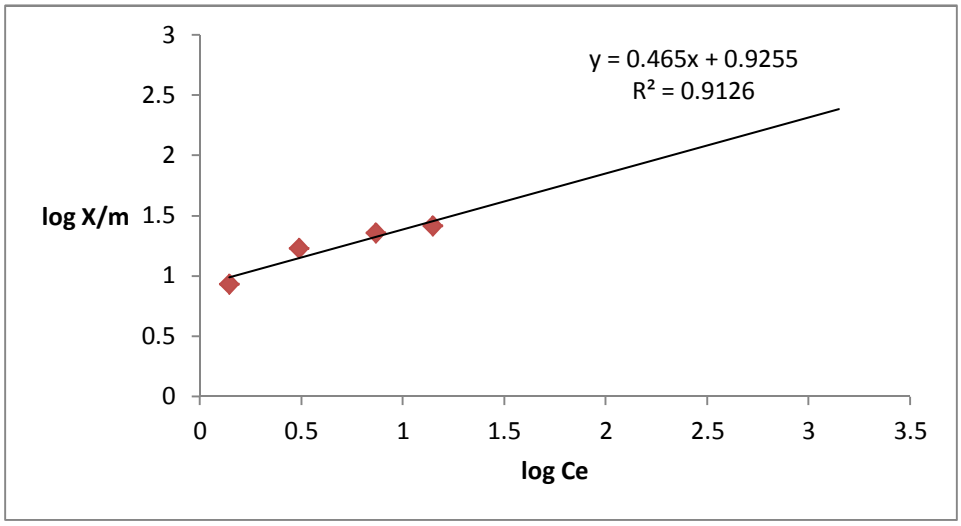


Figure 74: Freundlich isotherm of MO from aqueous $Pb(NO_3)_2$ and $Cd(NO_3)_2.4H_2O$ mixture onto PMAC

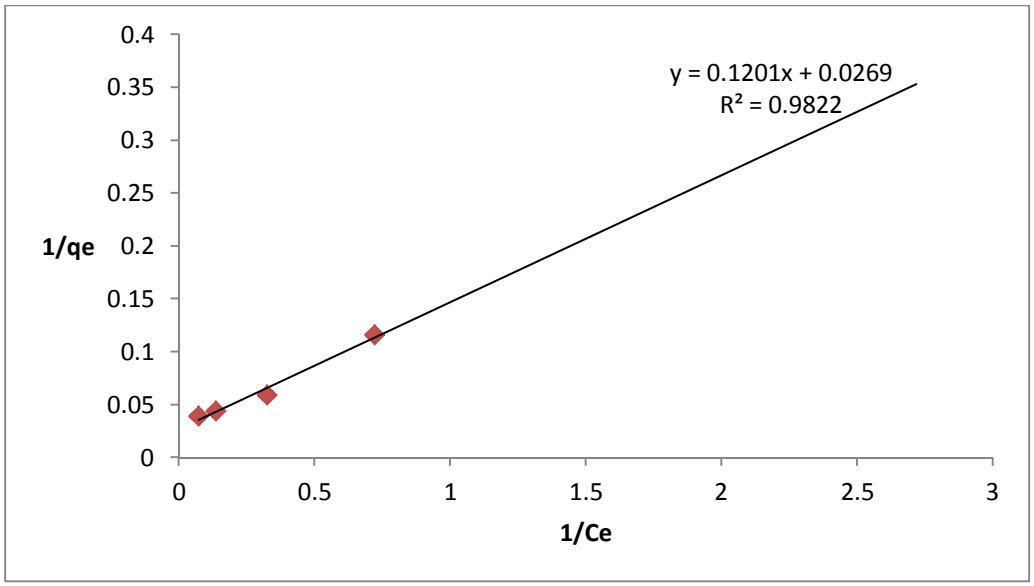


Figure 75: Langmuir isotherm of MO from aqueous $Pb(NO_3)_2$ and $Cd(NO_3)_2.4H_2O$ mixture onto PMAC

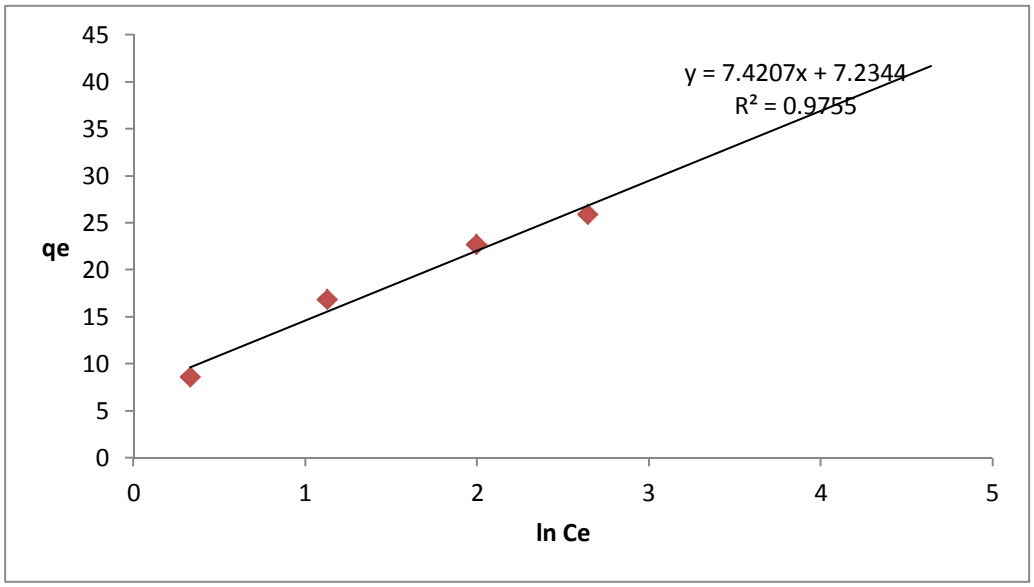


Figure 76: Temkin isotherm of MO from aqueous $Pb(NO_3)_2$ and $Cd(NO_3)_2.4H_2O$ mixture onto PMAC

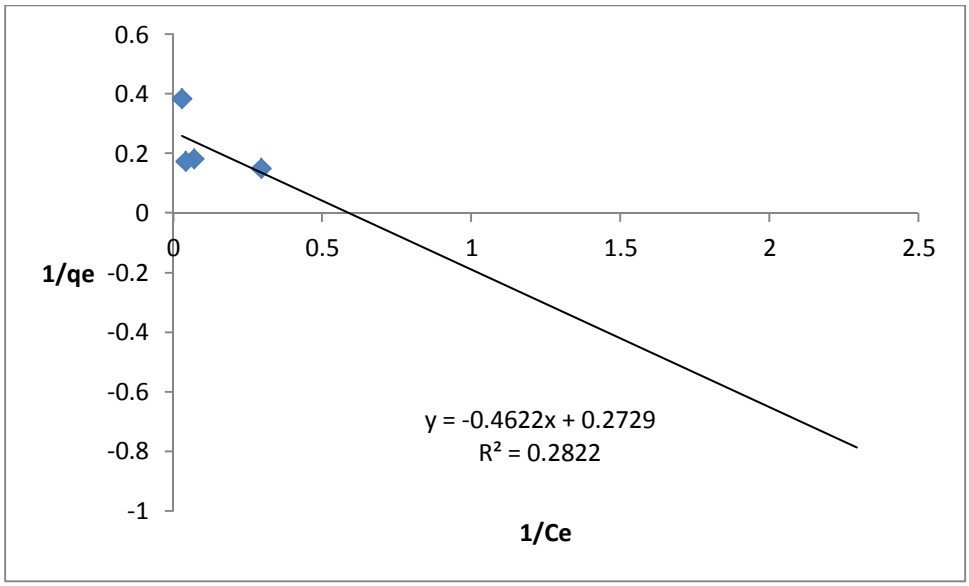


Figure 77: Langmuir isotherm of MB from aqueous $Pb(NO_3)_2$ and $Cd(NO_3)_2.4H_2O$ mixture onto UMAC

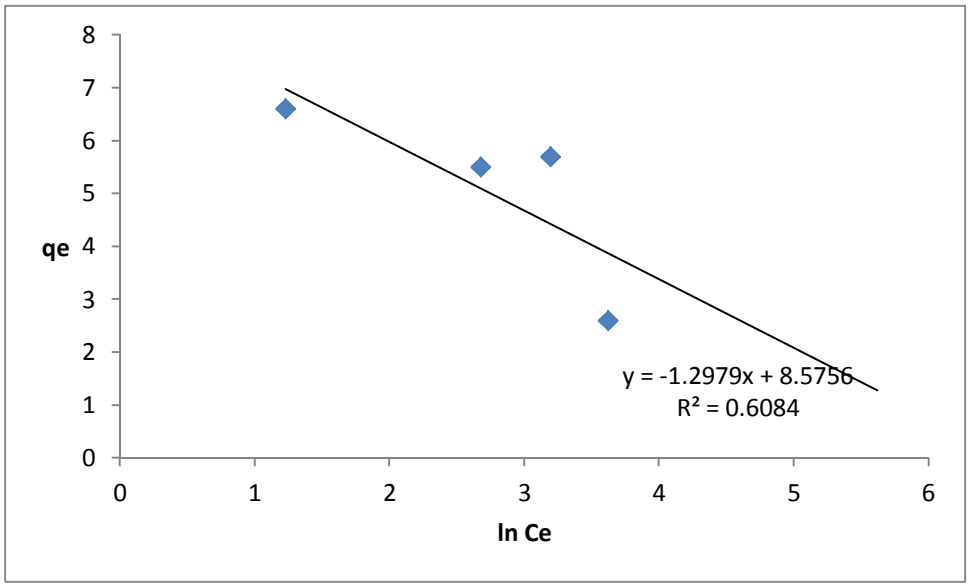


Figure 78: Temkin isotherm MB from aqueous $Pb(NO_3)_2$ and $Cd(NO_3)_2.4H_2O$ mixture onto UMAC

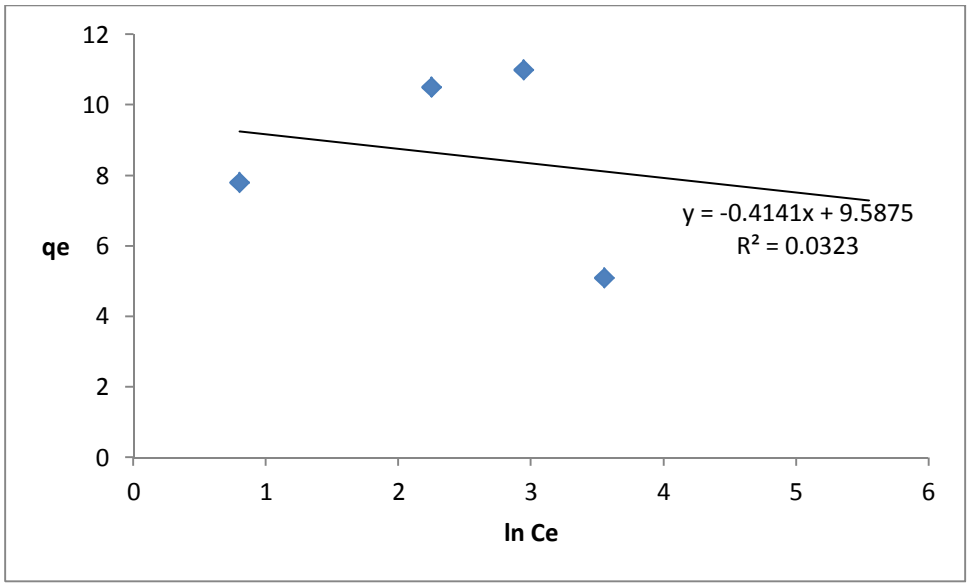


Figure 79: Temkin isotherm MB from aqueous $Pb(NO_3)_2$ and $Cd(NO_3)_2.4H_2O$ mixture onto PMAC

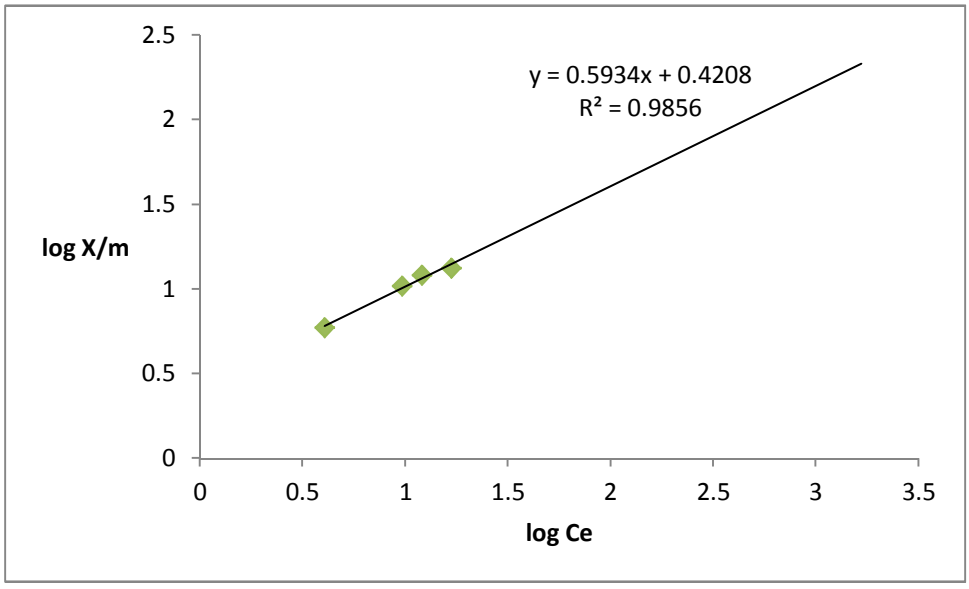


Figure 80: Freundlich isotherm IG from aqueous $Pb(NO_3)_2$ and $Cd(NO_3)_2.4H_2O$ mixture onto UMAC

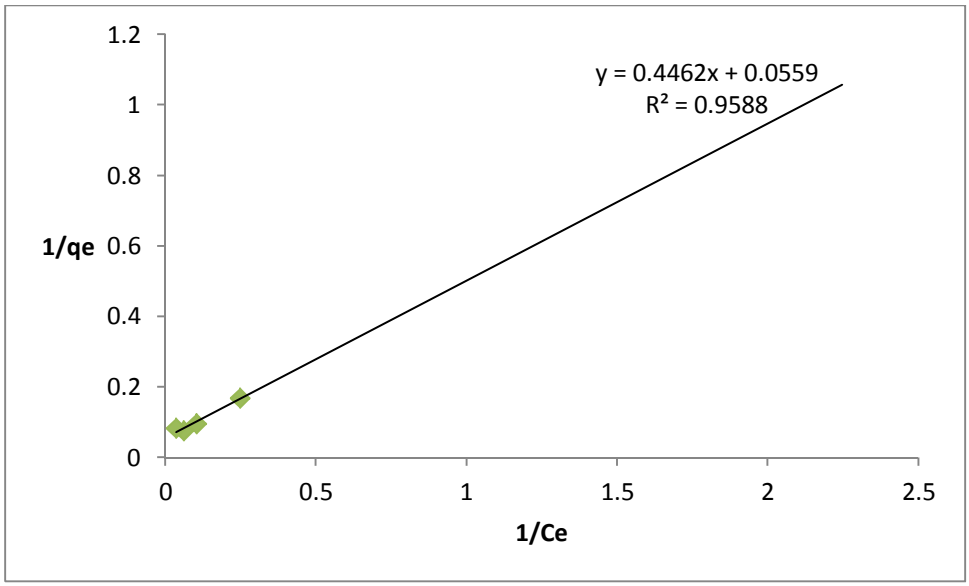


Figure 81: Langmuir isotherm IG from aqueous $Pb(NO_3)_2$ and $Cd(NO_3)_2.4H_2O$ mixture onto UMAC

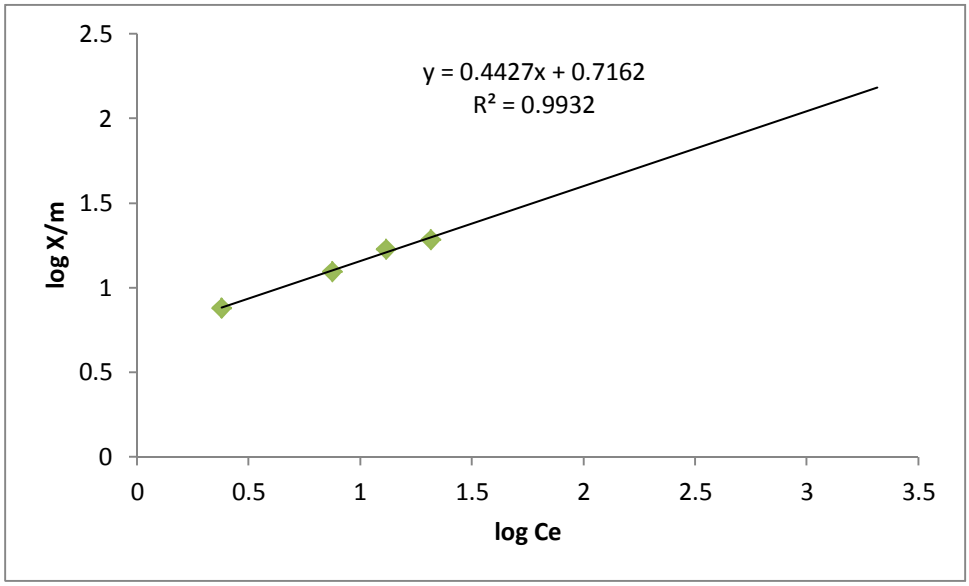


Figure 82 : Freundlich isotherm IG from aqueous $Pb(NO_3)_2$ and $Cd(NO_3)_2.4H_2O$ mixture onto PMAC

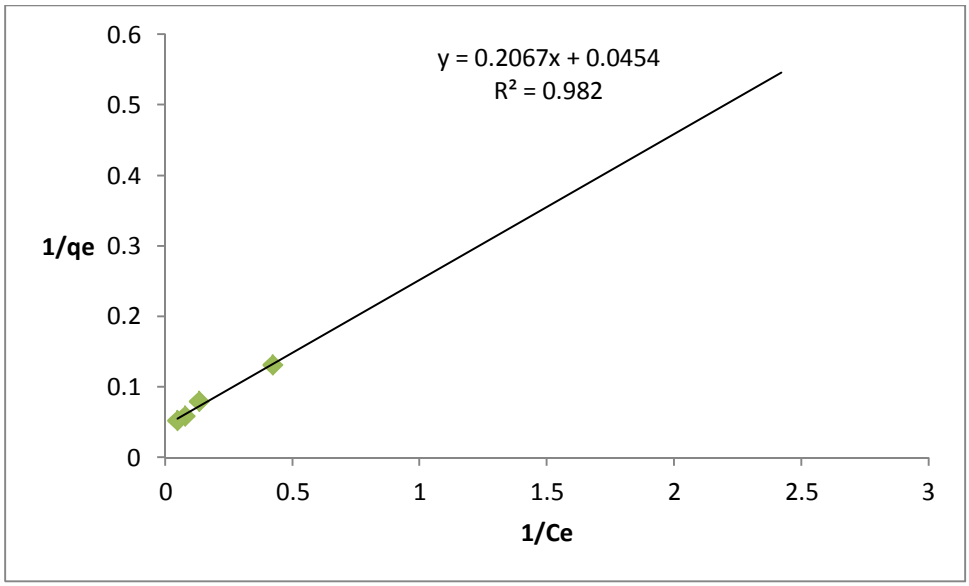


Figure 83: Langmuir isotherm of IG from aqueous $Pb(NO_3)_2$ and $Cd(NO_3)_2.4H_2O$ mixture onto PMAC

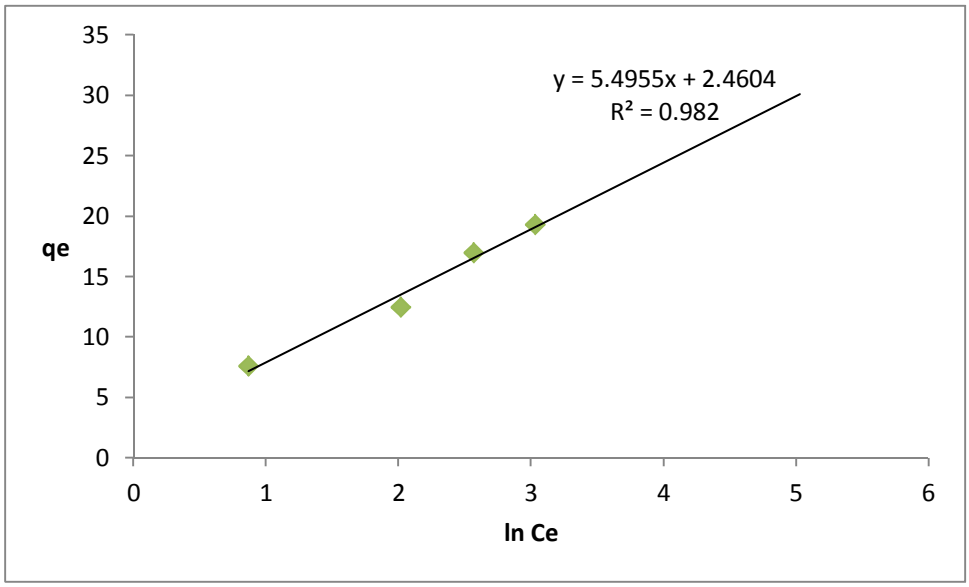


Figure 84: Temkin isotherm IG from aqueous $Pb(NO_3)_2$ and $Cd(NO_3)_2.4H_2O$ mixture onto PMAC

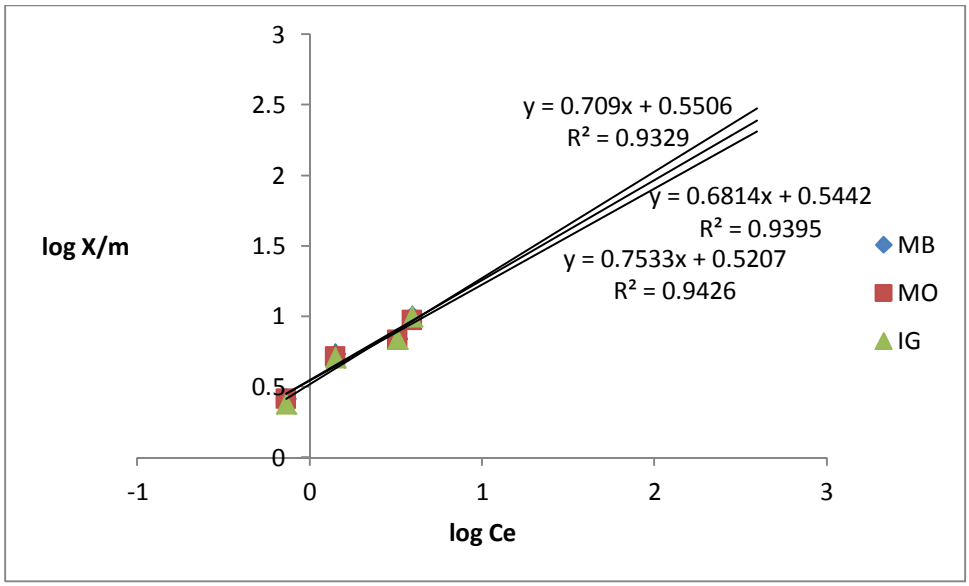


Figure 85: Freundlich isotherm of components of aqueous MBMOIG adsorbed onto UMAC

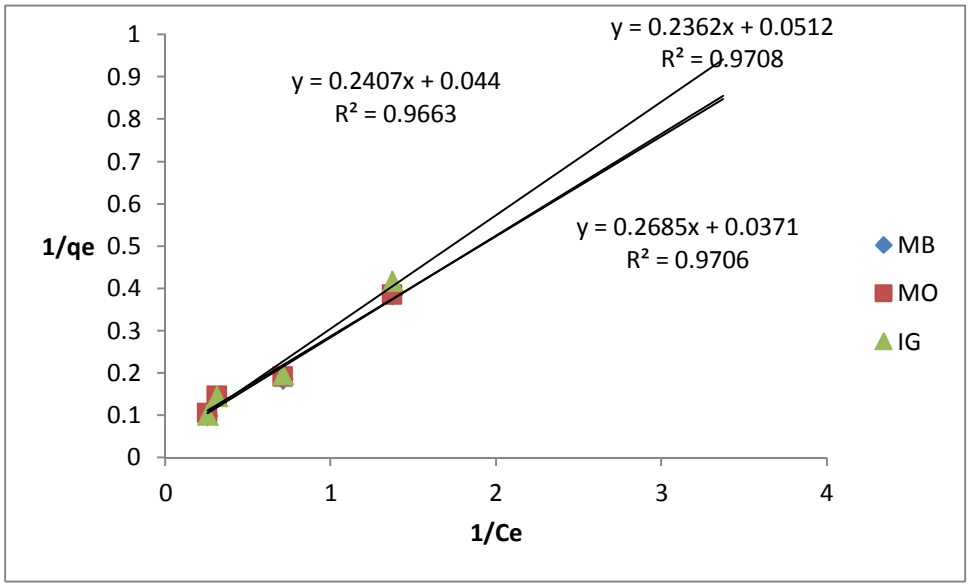


Figure 86: Langmuir isotherm of components of aqueous MBMOIG adsorbed onto UMAC

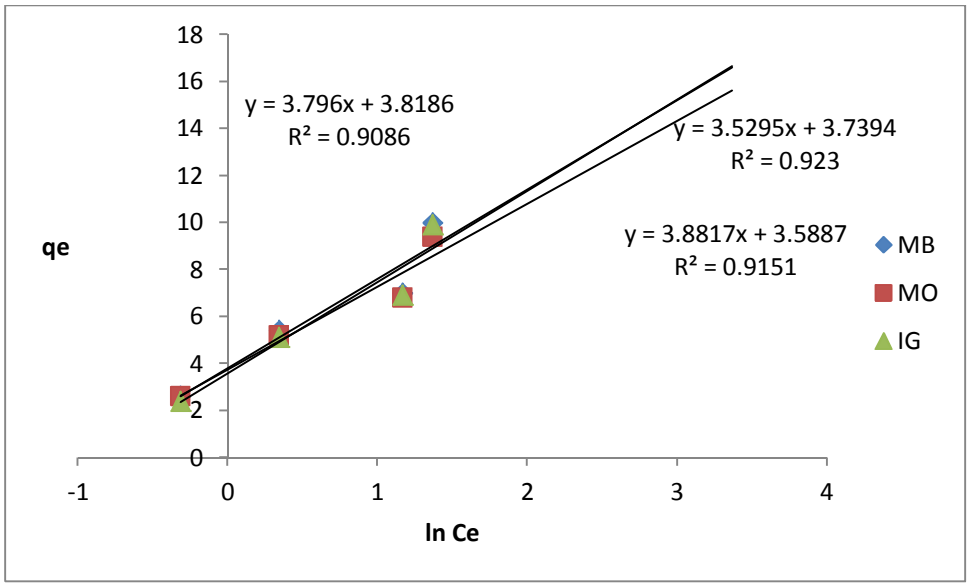


Figure 87: Temkin isotherm of components of Aqueous MBMOIG adsorbed onto UMAC

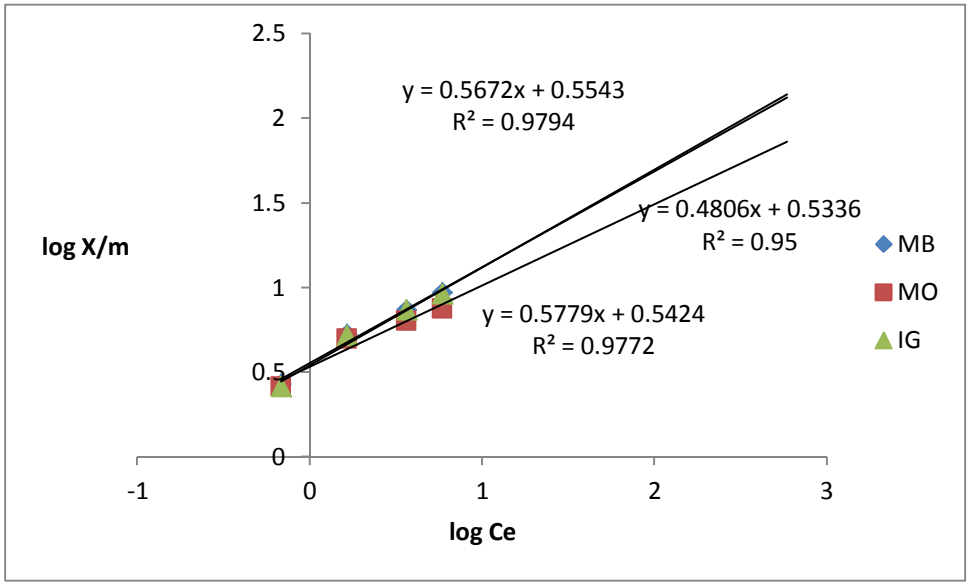


Figure 88: Freundlich isotherm of components of aqueous MBMOIG adsorbed onto CMAC

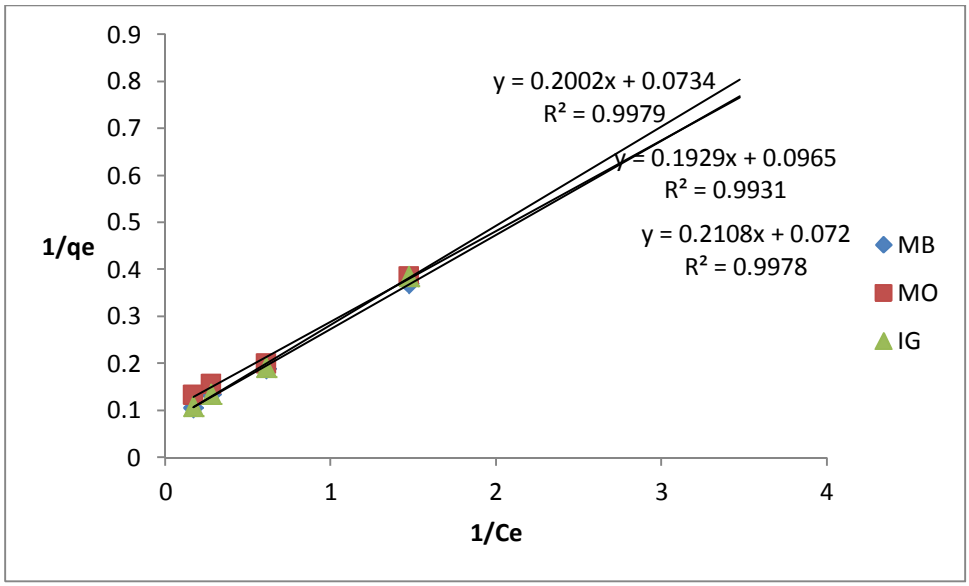


Figure 89: Langmuir isotherm of components of aqueous MBMOIG adsorbed onto CMAC

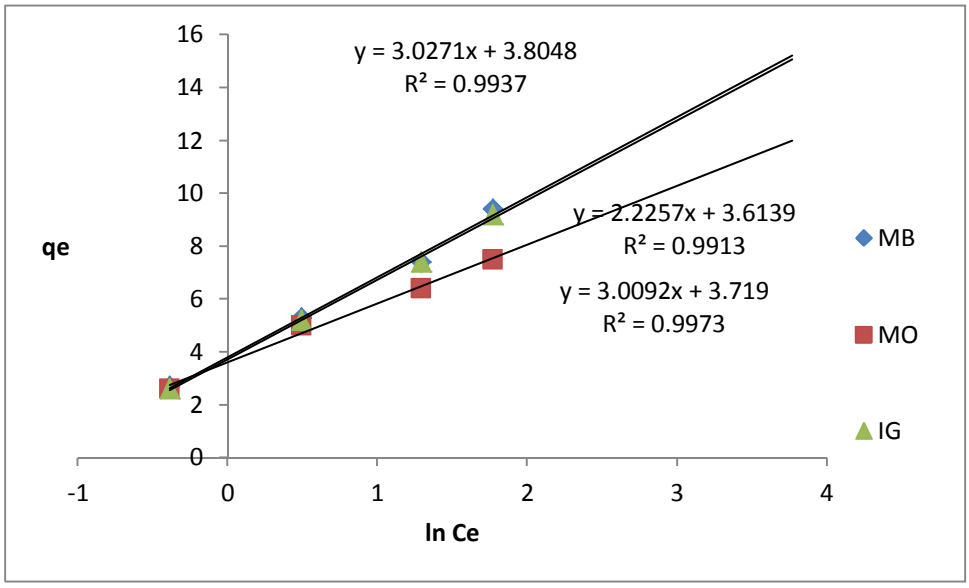


Figure 90: Temkin isotherm of components of aqueous MBMOIG adsorbed onto CMAC

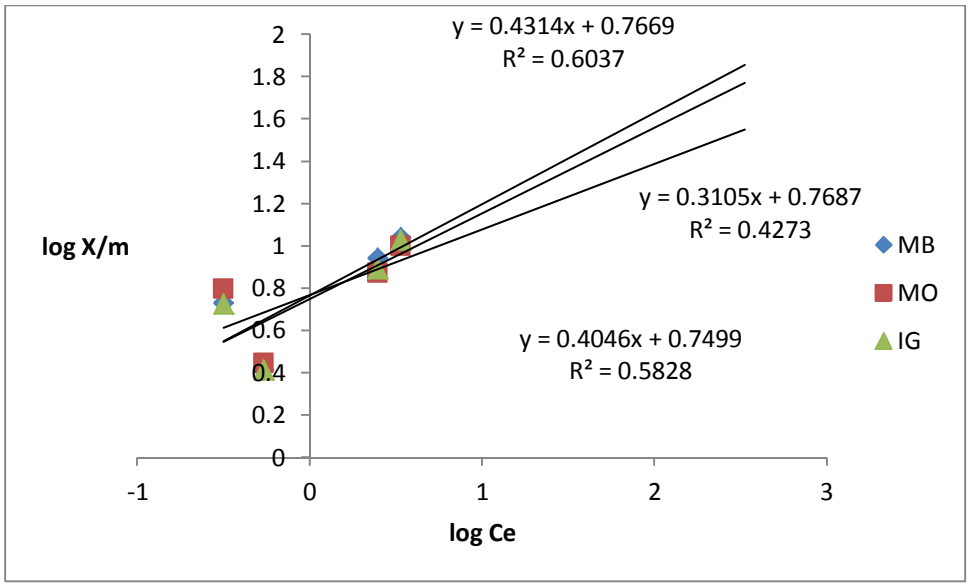


Figure 91: Freundlich isotherm of components of aqueous MBMOIG adsorbed onto PMAC

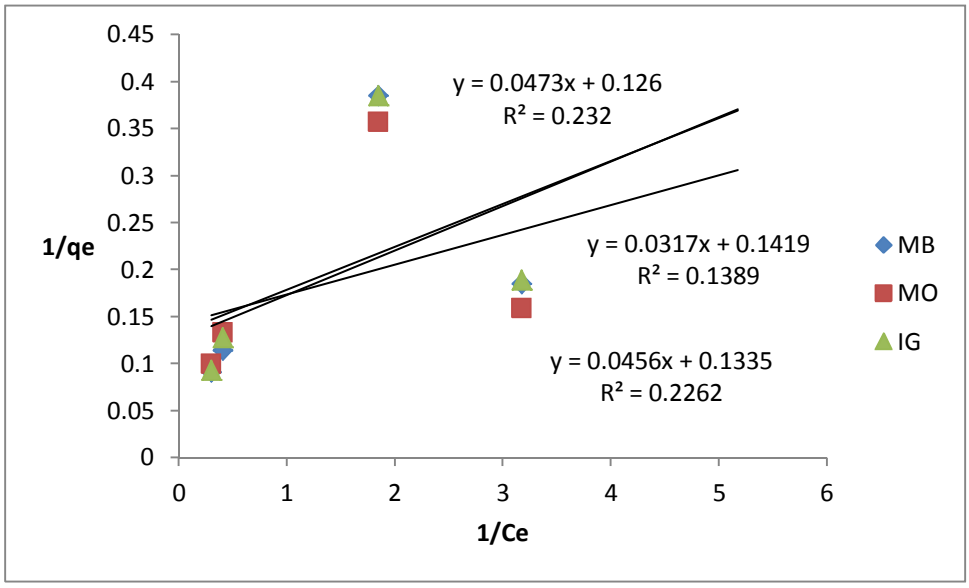


Figure 92: Langmuir isotherm of components of aqueous MBMOIG adsorbed onto PMAC

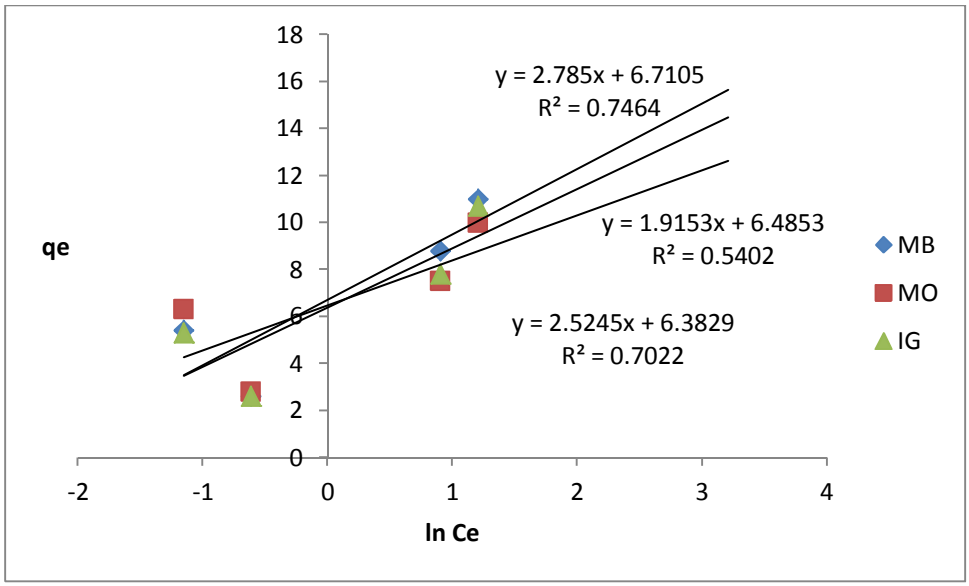


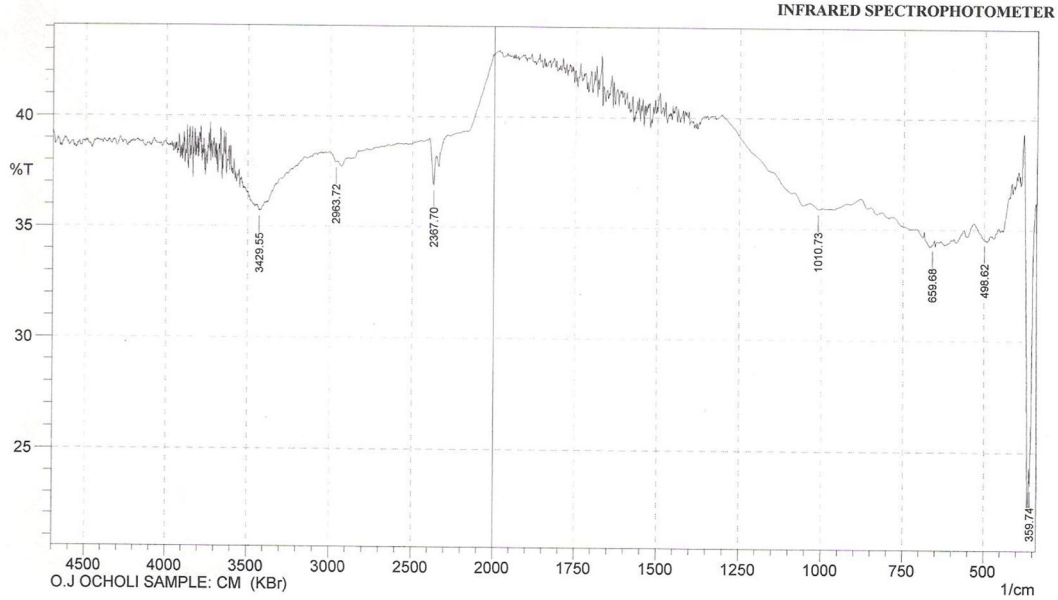
Figure 93: Temkin isotherm of components of aqueous MBMOIG adsorbed onto PMAC

Appendix XIV: FTIR analysis result (CM)

SHIMADZU

FTIR ANALYSIS RESULT NARICT,ZARIA

FTIR- 8400S FOURIER TRANSFORM
INFRARED SPECTROPHOTOMETER



	Peak	Intensity	Corr. Intensity	Base (H)	Base (L)	Area	Corr. Area
1	359.74	23.524	1.987	361.66	342.38	10.091	-0.084
2	498.62	34.525	0.103	531.41	495.72	16.323	0.024
3	659.68	34.319	0.034	660.64	652.93	3.575	0.003
4	1010.73	35.891	0.024	1034.84	1008.8	11.544	0
5	2367.7	36.904	1.598	2394.7	2353.23	17.48	0.344
6	2963.72	37.923	0.018	2966.62	2957.94	3.654	0.001
7	3429.55	35.699	0.089	3432.44	3427.62	2.154	0.003

Comment;
O.J OCHOLI SAMPLE: CM (KBr)

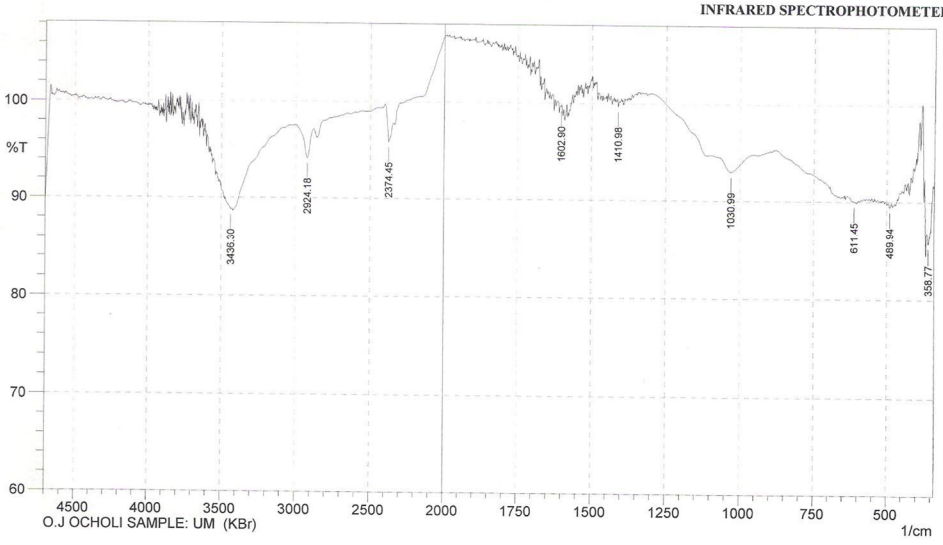
Apodization;
User; Administrator
No. of Scans;
Date/Time; 1/27/2012 3:25:19 PM

Appendix XV: Appendix XV : FTIR analysis result (UM)

SHIMADZU

FTIR ANALYSIS RESULT NARICT,ZARIA

FTIR- 8400S FOURIER TRANSFORM INFRARED SPECTROPHOTOMETER



	Peak	Intensity	Corr. Intensity	Base (H)	Base (L)	Area	Corr. Area
1	358.77	85.672	1.216	363.59	352.02	0.742	0.036
2	489.94	89.449	0.469	494.76	484.15	0.502	0.012
3	611.45	89.983	0.088	616.28	606.63	0.44	0.002
4	1030.99	92.971	0.027	1031.95	961.55	1.927	-0.005
5	1410.98	99.674	0.765	1412.9	1406.15	-0.003	0.008
6	1602.9	99.676	0.177	1606.76	1601.93	0.006	0.002
7	2374.45	95.847	0.892	2400.49	2369.63	0.283	0.006
8	2924.18	94.123	3.15	2995.55	2880.78	1.982	0.628
9	3436.3	88.838	0.106	3453.66	3433.41	1.02	0.005

Comment;
O.J OCHOLI SAMPLE: UM (KBr)

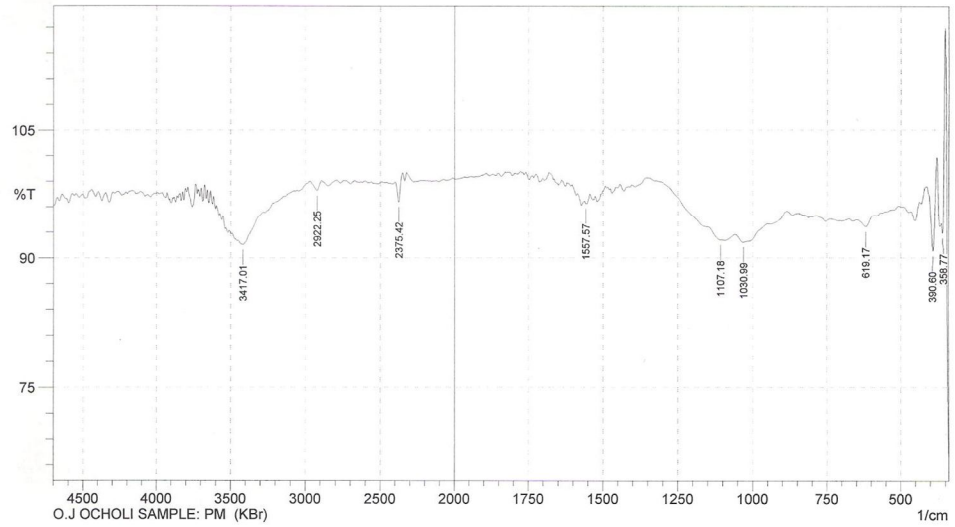
Apodization;
User; Administrator
No. of Scans;
Date/Time; 1/27/2012 3:10:56 PM

Appendix XVI: Appendix XVI : FTIR analysis result (PM)

SHIMADZU

FTIR ANALYSIS RESULT NARICT,ZARIA

FTIR- 8400S FOURIER TRANSFORM INFRARED SPECTROPHOTOMETER

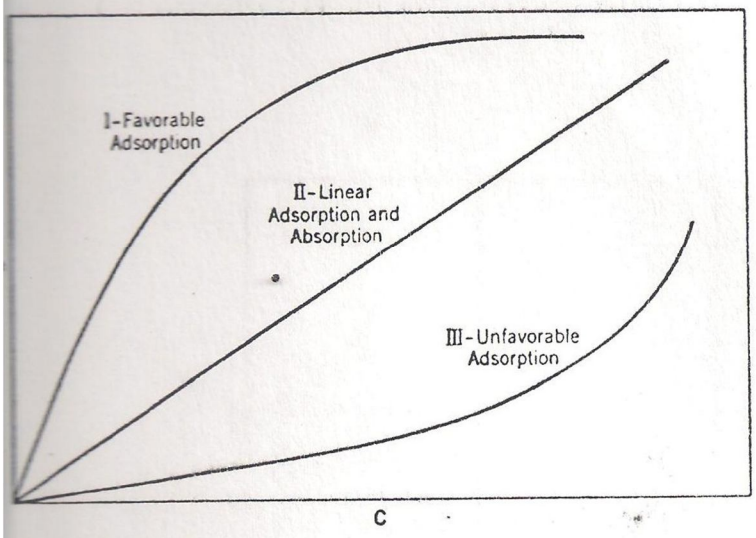


	Peak	Intensity	Corr. Intensity	Base (H)	Base (L)	Area	Corr. Area
1	358.77	92.863	10.696	363.59	352.02	0.016	0.254
2	390.6	90.774	9.911	414.71	379.02	0.675	0.685
3	619.17	93.617	1.094	653.89	591.2	1.618	0.131
4	1030.99	91.83	1.225	1059.92	949.97	3.662	0.375
5	1107.18	92.086	0.128	1152.51	1103.32	1.603	0.018
6	1557.57	96.363	0.056	1562.39	1556.61	0.09	0.001
7	2375.42	96.552	2.846	2399.53	2349.38	0.396	0.268
8	2922.25	97.88	1.142	2970.48	2892.36	0.521	0.186
9	3417.01	91.556	1.128	3449.8	3280.06	5.193	0.375

Comment;
O.J OCHOLI SAMPLE: PM (KBr)

Apodization;
User; Administrator
No. of Scans;
Date/Time; 1/27/2012 1:14:11 PM

Appendix XVII



GENERAL TYPES OF ADSORPTION ISOTHERMS
(Reproduced with permission from Physico-chemical Processes For Water Quality Control, W. J. Weber, Jr., Wiley Interscience, N. Y. 1972)

Appendix XVIII: Giles classification of isotherms for adsorption from solution

